A New Equation of State and Tables of Thermodynamic Properties for Methane Covering the Range from the Melting Line to 625 K at Pressures up to 1000 MPa[a]

U. Setzmann[b] and W. Wagner[c]

Institut für Thermo- und Fluiddynamik, Ruhr-Universität Bochum, D-4630 Bochum, Federal Republic of Germany

Received June 11, 1990; revised manuscript received May 29, 1991

This work reviews the data on thermodynamic properties of methane which were available up to the middle of 1991 and presents a new equation of state in the form of a fundamental equation explicit in the Helmholtz free energy. A new strategy for optimizing the structure of empirical thermodynamic correlation equations was used to determine the functional form of the equation. The Helmholtz function containing 40 fitted coefficients was fitted to selected experimental data of the following properties: (a) thermal properties of the single phase ($p\rho T$) and (b) of the liquid-vapor saturation curve ($p_s\rho'\rho''$) including the Maxwell criterion, (c) speed of sound w, (d) isochoric heat capacity c_v, (e) isobaric heat capacity c_p, (f) difference of enthalpy Δh, and (g) second virial coefficient B. Independent equations are also included for the vapor pressure, the saturated liquid and vapor densities, the isobaric ideal gas heat capacity and the melting pressure as functions of temperature. Tables for the thermodynamic properties of methane from 90 K to 620 K for pressures up to 1000 MPa are presented. For the density, uncertainties of ± 0.03% for pressures below 12 MPa and temperatures below 350 K and ± 0.03% to ± 0.15% for higher pressures and temperatures are estimated. For the speed of sound, the uncertainty ranges from ± 0.03% to ± 0.3% depending on temperature and pressure. Heat capacities may be generally calculated within an uncertainty of ± 1%. To verify the accuracy of the new formulation, the calculated property values are compared with selected experimental results and existing equations of state for methane.

The new equation of state corresponds to the new International Temperature Scale of 1990 (ITS–90) and is extrapolable up to pressures of 20000 MPa.

Key words: correlation; data evaluation; equation of state; fundamental equation; methane; melting line; vapor-liquid coexistence curve; property table; thermal and caloric properties; metastable states.

Contents

[a]Dedicated to Prof. Dr.-Ing. K. Stephan on occasion of his 60th birthday.
[b]Present address: Hüls AG, D–4370 Marl, Federal Republic of Germany.
[c]To whom correspondence should be addressed.

List of Tables

List of Figures

Nomenclature

Symbol Description

a	Adjustable coefficient
A	Specific Helmholtz energy
B	Second virial coefficient
C	Third virial coefficient
c	Adjustable coefficient
c_p	Specific isobaric heat capacity
c_v	Specific isochoric heat capacity
c_σ	Specific heat capacity along the saturated liquid line
g	Specific Gibbs energy
h	Specific enthalpy
Δh_v	Specific enthalpy of vaporization
i,j	Serial numbers
J	Maximum value for the serial number j
M	Number of data, Molar mass
m	Serial number
n	Adjustable coefficient
p	Pressure
s	Specific entropy
T	Absolute temperature
t	Adjustable coefficient
u	Specific internal energy, Adjustable coefficient ($u = \Theta_i/T$)
w	Speed of sound
x	Any thermodynamic property
z	Compression factor [$z = p/(\rho RT)$]

Greek

$\alpha,\beta,\gamma,\Delta$	Adjustable coefficients
γ^w	Precorrelated value for w data ($\gamma^w = c_p/c_v$)
Δ	Difference in a quantity
δ	Reduced density ($\delta = \rho/\rho_c$)
δ_t	Isothermal throttling coefficient
∂	Partial differential
ζ^p	Precorrelated value for c_p data
Θ	Adjustable coefficient
Θ^c	Converted coefficient ($\Theta^c = \Theta/T_c$)
ϑ	Transformed temperature ($\vartheta = 1 - T/T_c$)
μ	Joule-Thomson coefficient
ρ	Mass density
σ	Standard deviation
τ	Inverse reduced temperature ($\tau = T_c/T$)
Φ	Dimensionless Helmholtz energy [$\Phi = A/(RT)$]
χ^2	Weighted sum of squares

Superscripts

$^\circ$	Ideal gas property
^{r}	Residual
$'$	Saturated liquid state
$''$	Saturated vapor state
$^-$	Denotes a vector

Subscripts

b	At the boiling point
c	At the critical point
corr	Corrected
expt	Experimental
i,j	Indices
m	Denotes the melting pressure, Index for experimental data
nl	Nonlinear
$_\circ$	Reference state
oH	Initial state values for the Hugoniot curve measurements
opt	Optimated
orig	Original
s	Denotes the vapor pressure on the liquid-vapor saturation curve
t	At the triple point
σ	Along the saturation curve

Physical constants for methane

M	Molar mass M = (16.0428 ± 0.0013) g/mol, cf. Ref. 209
R_m	Molar gas constant R_m = (8.31451 ± 0.00021) J/(mol K), cf. Ref. 210
R	Specific gas constant $R = R_m/M$ = 0.5182705 kJ/(kg K)
T_c	Critical temperature T_c = 190.564 K
p_c	Critical pressure p_c = 4.5922 MPa
ρ_c	Critical density ρ_c = 162.66 kg/m^3
T_t	Triple point temperature T_t = 90.6941 K
p_t	Triple point pressure p_t = 0.011696 MPa
T_b	Normal boiling point temperature T_b = 111.668 K

T_o Reference temperature T_o = 298.15 K
p_o Reference pressure p_o = 0.101325 MPa
h_o° Reference enthalpy in the ideal gas state at T_o h_o° = 0 kJ/kg
s_o° Reference entropy in the ideal gas state at T_o and p_o s_o° = 0 kJ/(kg K)

1. Introduction

1.1. Background

Methane is the major component of natural gas. In this context knowledge of the thermodynamic properties of methane is required for the processes of liquefaction, separation, storage, pumping and transport of natural gas, etc. Moreover, methane serves as an important raw material for the production of hydrogen, alcohols and many other products of the chemical industry. Due to increasing efforts in the optimization of chemical plants, it is necessary to provide accurate thermodynamic properties of methane. Furthermore, since methane is the first compound of the group of the alkanes, it is often referred to as a reference fluid.

In 1978, the International Union of Pure and Applied Chemistry (IUPAC) published a monograph[1] which reviewed most of the experimental data available up to 1976 and presented extensive tables of the thermal and caloric properties of methane derived from an equation of state. Since 1976, many investigations of the thermodynamic properties of methane have been carried out. A comparison of the new experimental data[2-6] with existing equations of state[1,7-16] shows that none of these equations is able to represent the new measurements within their experimental uncertainties, cf. Sec. 6. In addition to the increasing amount of experimental data, the correlation techniques have been significantly improved during the last decade. Up to now, none of the existing equations of state for methane has been optimized with respect to its structure. This means that the terms in these equations have been determined subjectively by experience or by trial and error. In 1989, Setzmann and Wagner[18] presented a new strategy for optimizing the structure of empirical thermodynamic correlation equations. Based on a comprehensive functional expression for the considered physical dependence, which is called a 'bank of terms', the new procedure optimizes the structure and the length of the equation simultaneously. The application of this optimization procedure results in an equation which meets the quality desired for representing the experimental data with the lowest number of fitted coefficients. In combination with this optimization method we used several thermodynamic properties for the determination of the new fundamental equation. The use of more than one thermodynamic property is called 'multi-property fitting' which is the state-of-the-art procedure for establishing effective wide-range equations of state. This technique was extensively applied when establishing our new fundamental equation for methane.

1.2. Prior Correlations of Methane Properties and Need for a New Correlation

A comprehensive evaluation of methane data was reported by Angus *et al.*[1] in 1978. This IUPAC monograph reviewed the experimental data of methane which had been published prior to 1976. Since 1976, and especially during the last five years, many state-of-the-art experiments on the determination of the thermodynamic properties of methane have been carried out. The steadily increasing amount of data stimulated many authors to develop correlation equations for methane. Table 1 summarizes the equations of state for methane which have been developed since 1970. All of these wide-

TABLE 1. Available correlations for methane

Authors	Year	Temperature range/K	Pressure range/MPa	Structure of the equation	Number of coefficients	Data used in the correlation
Bender[7]	1970	90.66–623	0–50	Extended BWR[a]	20	$p\rho T$,$p_s\rho'\rho''$
Goodwin[8]	1974	90.68–500	0–50	Nonanalytic	23	$p\rho T$,$p_s\rho'\rho''$
McCarty[9]	1974	90.68–400	0–40	Extended BWR	32	$p\rho T$,$p_s\rho'\rho''$,c_v
Angus *et al.*[1] (IUPAC)	1978	90.68–625	0–1000	Extended BWR	32	$p\rho T$,$p_s\rho'\rho''$,c_v
Sytchev *et al.*[10]	1979	90.68–1000	0–100	Double power expansion in T and ρ	54	$p\rho T$,$p_s\rho'\rho''$, B,C,c_v
Ely & Hanley[11]	1981	90.68–500	0–260	Extended BWR	32	$p\rho T$,$p_s\rho'\rho''$,c_v
Sievers & Schulz[12]	1984	90.68–625	0–50	Extended BWR (Bender)	20	$p\rho T$,$p_s\rho'\rho''$,B
Erickson & Leland[13]	1986	90.68–500	0–260	Damping function for the critical region in combination with the Eq. of Ely and Hanley[11]	4+32	$p\rho T$,$p_s\rho'\rho''$, c_v,c_p,w
Younglove & Ely[14]	1987	90.68–600	0–200	Modified BWR	32	–[b]
Kurumov *et al.*[15]	1988	187–208	4.4–7	Revised and extended scaling law	12	$p\rho T$,w
Friend *et al.*[16]	1989	91–600	0–100	Developed for oxygen by Schmidt and Wagner[206]	32	$p\rho T$,$p_s\rho'\rho''$, c_v,c_p,w

[a]Benedict-Webb-Rubin.
[b]Details on selected data will be given by Ely (to be published).

range equations of state are based mainly on the $p\rho T$ data (pressure p, density ρ, temperature T) published by Goodwin and Prydz,[8,19] Douslin *et al.*,[20] and Cheng.[21] Recent experimental investigations of the $p\rho T$ properties of methane measured by Kleinrahm and Wagner,[2] Kleinrahm *et al.*,[3,4] Händel *et al.*,[5] Pieperbeck *et al.*,[22] and Achtermann *et al.*[23] indicate that the older experimental values of Goodwin[8,19] show systematic deviations - up to 0.2% in density - from the new state-of-the-art $p\rho T$ data. Therefore, all equations of state, which have been developed up to now, contain errors at least of up to ± 0.2% in density in a wide range of temperatures and pressures.

In 1988, Kurumov *et al.*[15] published a revised and extended scaling law equation which represents the thermodynamic properties of methane in the critical region. This nonanalytic function represents most of the experimental data in the critical region within the estimated experimental uncertainties. It gives correct limiting behavior at the critical point (weak divergence of the isochoric heat capacity c_v and the reciprocal speed of sound w^{-1}, etc.), but the scaled equation is valid only in a very small region around the critical point and the agreement with experimental data deteriorates very rapidly as soon as the equation is extrapolated outside the near-critical region. Because of its small range of validity and its mathematically complex structure, the scaled equation is not very convenient for engineering applications. For our correlation, we decided to retain a completely analytic form of the fundamental equation which guarantees a fast and convenient evaluation of the equation. It will be shown later that our new fundamental equation represents the experimental data in the critical region at least as well as the scaling law equation of Kurumov *et al.*,[15] although our equation cannot reproduce the limiting behavior when approaching the critical point.

The most recent equation of state for methane was developed by Friend *et al.*[16] in 1989.

Each of the existing equations of state for methane has several of the following disadvantages: (a) not able to represent the data within the experimental uncertainties, (b) only valid in a restricted temperature or pressure range, (c) not able to represent the properties in the enlarged critical region, (d) a rather complicated structure, (e) not corresponding to the current International Temperature Scale of 1990 (ITS-90).[24] Therefore, we developed a new equation of state which is capable of representing the thermodynamic surface of methane in the range from 90.69 K ≤ T ≤ 625 K at pressures up to 1000 MPa within the uncertainty of the available data.

1.3. Organization of the Paper

In Sec. 2, we discuss the available experimental information on the thermal and caloric properties of methane in the fluid region, on the melting line, and on the liquid-vapor saturation curve. The selected data which were used to develop the new fundamental equation, the auxiliary equations for the saturation line, and the melting pressure equation are discussed in this section. In addition to the fundamental equation, we developed supplementary equations for the vapor pressure p_s, the saturated liquid density ρ', the saturated vapor density ρ'', the melting pressure p_m, and the ideal gas heat capacity c_p° which are given in Sec. 3. Section 4 contains a description of the techniques used when developing the fundamental equation (multi-property-fitting, optimization procedure). The structure and the coefficients of the new Helmholtz function are presented in Sec. 5. Comparisons of properties calculated from the new equation of state for methane with the selected experimental data are given in Sec. 6. Finally, the uncertainties of the properties calculated with the new formulation are discussed and tables of the thermodynamic properties of methane are listed in the Appendix.

2. Experimental Results

All available experimental information on the thermal and caloric properties, the triple point, the critical point, the normal boiling point, and the melting pressure has been reviewed in order to determine the most accurate data set for methane. Throughout this paper the word 'data' is used to refer to experimental measurements.

The literature review was based mainly on earlier data compilations of Angus *et al.*,[1] Sytchev. *et al.*,[10] and Sievers and Schulz.[25] After our critical evaluation of all the data we concluded that the measurements before 1950 did not meet the present quality requirements. Therefore, this section includes all experimental investigations which have been carried out during the last 40 years or older works which are of essential importance for the characterization of the data situation of single properties. References of experimental results not mentioned can be found in Refs. 1, 10, 25 and in the work of Setzmann.[26]

To condense the description of the data situation, the characteristic information on the single data sets is summarized in the tables for the corresponding property. When the information could be found, these tables also contain values for the experimental uncertainties for such data which were used to establish the new equation of state or, at least, to check its quality by comparison with the corresponding data. Usually, these uncertainty values correspond to the values given by the experimentalists. Since we noticed, however, that a few authors had published overly optimistic estimations of their experimental uncertainties, we sometimes had to estimate more realistic values of the corresponding experimental uncertainties; these new uncertainty values which we ourselves changed are presented in parenthesis in the corresponding tables.

To simplify the evaluation process regarding the quality of the different data sets for the reader, for some properties the data have been classified into three groups. In these cases, the criterion for putting the single data sets into the corresponding group is clearly defined in these tables.

The new equation of state should correspond to the new International Temperature Scale of 1990 (ITS–90).[24] Therefore, all data which had been based on older temperature scales (including IPTS–68) and which had been considered to be relevant for the development of the new equation of state or for any comparisons were converted to ITS–90. This means that all temperature values in this paper[d] correspond to ITS–90. The conversion from IPTS–68 scale to ITS–90 scale was not carried out by interpolation within Table 6 of Ref. 24[e] but with a conversion equation given in Table 1.6 of the Supplementary Information for ITS–90.[24a] This conversion equation is accurate to within 1 mK above 273 K and 1.5 mK below 273 K. In spite of this uncertainty, in some cases it was necessary to add an additional decimal to the converted temperatures in order to ensure that any recalculation from ITS–90 temperatures to the original IPTS–68 temperatures produces the same figures as given in the original source after rounding to the same number of decimals.

2.1. Triple Point

The triple point temperature and the triple point pressure were measured by numerous workers. The most recent sources of triple point data are listed in Table 2. The agreement between the results of Blanke,[35] Bedford *et al.*,[36] Pavese *et al.*,[34,37] and Kleinrahm and Wagner[2] is excellent. Based on our assessment of these works we selected the following values for the temperature and pressure of the triple point:

$$T_t = (90.6941 \pm 0.0025)\ \text{K}$$
$$p_t = (116.96 \pm 0.02) \times 10^2\ \text{Pa}. \qquad (2.1)$$

The uncertainty given for T_t includes an uncertainty in the temperature conversion of ± 0.0015 K. When taking into account the phase equilibrium condition, the solution of the new fundamental equation, Eq. (5.1), at 90.6941 K yields a pressure of 116.96×10^2 Pa. The vapor pressure equation, Eq. (3.2), and the melting pressure equation, Eq. (3.7), have been constrained to the selected triple point parameters.

2.2. Two-Phase Regions

2.2.1. The Normal Boiling Point

The temperature at which methane boils under a pressure of 0.101325 MPa (1 atmosphere) has been measured extensively. Table 3 is a summary of reported experimental values for the boiling point temperature. The selected temperature from the work of Pavese *et al.*[30] and Kleinrahm and Wagner[2] is

$$T_b = (111.668 \pm 0.0025)\ \text{K}, \qquad (2.2)$$

where the uncertainty corresponds to the value given by Pavese *et al.*[30] (± 0.001 K) including the uncertainty of the temperature conversion (± 0.0015 K).

When taking into account the phase equilibrium condition, the solution of the new fundamental equation for 0.101325 MPa yields a temperature of 111.667 K. The vapor-pressure equation, Eq. (3.2), has been constrained to the selected temperature of the normal boiling point.

TABLE 2. Summary of the experimental values for the triple point of methane[a]

Source	Year	T/K	$p/(10^2$ Pa)
Lovejoy[27]	1963	90.6946	–
Calado *et al.*[28]	1974	90.6891	116.9
Kidnay *et al.*[29]	1975	90.6891	116.82
Pavese *et al.*[30]	1976	90.6952 ± 0.0005	116.96 ± 0.02
Bonhoure & Pello[31]	1978	90.6952[b]	–
Inaba & Mitsui[32]	1978	90.6941	–
Bonhoure & Pello[33]	1980	90.6947[b]	–
Pavese[34]	1981	90.6947[b]	116.96 ± 0.02
Blanke[35]	1983	90.6937 ± 0.00045[c]	–
Blanke[35]	1983	90.6945 ± 0.00045[b]	–
Bedford *et al.*[36]	1984	90.6945 ± 0.001[d]	–
Pavese *et al.*[37]	1984	90.69428 ± 0.00068[c]	–
Pavese *et al.*[37]	1984	90.69360 ± 0.00079[b]	–
Kleinrahm & Wagner[2]	1986	90.6941 ± 0.003	116.96 ± 0.20

[a]All temperatures were converted to ITS-90. In some cases it was necessary to give an additional figure when converting from IPTS-68 to ITS-90. The uncertainties in the temperature values taken from the corresponding papers were not increased due to the uncertainty in the temperature conversion to ITS-90.

[b]The temperature of the triple point was originally determined on the IPTS-68 scale using the triple point of argon as the reference.

[c]The measurement (IPTS-68 scale) of the triple point temperature of methane was based on the condensation point of oxygen. There is a systematic difference of 0.4 mK for measurements based on the the triple point of argon and those based upon the condensation point of oxygen. For details see Bedford *et al.*[36]

[d]No data; the value was selected by comparison of the existing measurements and taking into account the quality requirements of the IPTS-68.

TABLE 3. Summary of the experimental values for the normal boiling point of methane

Source	Year	T/K
Olszewski[38]	1885	109.2
Hunter[39]	1906	110.2
Henning & Stock[40]	1921	111.80
Keyes *et al.*[41]	1922	111.53
Young[42]	1928	111.5
Brickwedde & Scott[43]	1937	111.674 ± 0.01
Bloomer & Parent[45]	1953	111.71
Timrot & Pavlovich[46]	1959	111.77
Clusius *et al.*[47]	1960	111.680
Hestermann & White[48]	1961	111.43
Lovejoy[27]	1963	111.6653
Pavese *et al.*[30]	1976	111.6679 ± 0.001
Kleinrahm & Wagner[2]	1986	111.6675 ± 0.003

[d]The only exception are the ideal gas properties, obtained from statistical thermodynamics, which have been based on the universal thermodynamic temperature scale.

[e]In the temperature range considered here, the differences between ITS-90 and IPTS-68 ranges from +14 mK to −41 mK.

2.2.2. Critical Point

The results of recent determinations of the critical point parameters of methane are given in Table 4. Summaries of earlier investigations concerned with the critical temperature T_c, the critical density ρ_c, and the critical pressure p_c are given by Armstrong *et al.*[44] and Sytchev *et al.*[10] In 1984, Kleinrahm and Wagner[2,82] described the development and the construction of a new apparatus to obtain accurate measurements of the saturated liquid and vapor densities of pure fluids together with the vapor pressure along the whole coexistence curve. The authors presented new experimental results for the saturation densities and the vapor pressure of methane and extracted the critical point parameters given in Table 4 from their measurements. We took over their values with two exceptions. The uncertainty in T_c was enlarged due to the uncertainty in the temperature conversion to ITS-90. The enlargement of the uncertainty in ρ_c was based on our experience with the evaluation of our recent $p\rho T$ measurements on carbon dioxide,[57a,57b] where the parameters of the critical point were also extracted from the experimental densities of the saturated liquid and vapor.

$$\begin{aligned} T_c &= (190.564 \pm 0.012)\ \text{K} \\ p_c &= (4.5922 \pm 0.002)\ \text{MPa} \\ \rho_c &= (162.66 \pm 0.2)\ \text{kg/m}^3 \end{aligned} \qquad (2.3)$$

TABLE 4. Summary of the experimental values for the critical point of methane

Source	Year	T_c/K	p_c/MPa	ρ_c/(kg/m^3)
Bloomer & Parent[45]	1953	190.593	4.6072	162.50
Vennix[49,50,51]	1966	190.8	4.6265	162.50
Grigor & Steele[52]	1968	190.8	4.62	162.60
Ricci & Scafè[53]	1969	190.6	–	166.00
Jansoone *et al.*[54]	1970	190.563	4.5947	162.80
Goodwin[55]	1973	190.543	–	163.64
Gielen *et al.*[56]	1973	190.568	4.5955	159.59
Olson[57]	1975	–	–	163.0
Kleinrahm & Wagner[2]	1986	190.5640 ±0.01	4.5992 ±0.002	162.66 ±0.05

The values for the critical parameters given by Kleinrahm and Wagner[2] were confirmed by Kurumov *et al.*[15] in 1988. Kurumov et al. presented a revised and extended scaling law equation for methane. When determining the constants of their scaled equation of state, it was possible to treat the critical parameters as adjustable parameters. Since, however, a refit of the critical parameters led to values which were in very good agreement with the values given by Kleinrahm and Wagner.[2] Kurumov *et al.*[15] also accepted the critical parameters given in Eq. (2.3) for their equation.

2.2.3. Melting Curve

There are 11 sets of measurements of the pressure-temperature relationship along the melting curve. Table 5 summarizes the information on the available data sets which are classified into three groups. Group 1 covers the data having the smallest experimental uncertainty. Group 2 comprises data which do not differ by more than 3% from the values of Group 1. Group 3 includes data which have larger systematic deviations from Group 1 and Group 2 data which form the selected data. Table 6 reports the uncertainties of the selected data used to establish the melting pressure equation, Eq. (3.7).

TABLE 5. Summary of the experimental values for the melting pressures of methane

Source	Year	Number of data	Temperature range T/K	Group
Freeth & Verschoyle[58]	1931	7	90.7–91.9	3
Clusius & Weigand[59]	1940	18	90.7–94.6	1
Stryland *et al.*[60]	1960	8	110.5–146.4	3
Reeves *et al.*[61]	1964	1	262.5	3
Grace & Kennedy[62]	1967	7[a]	210–390	3
Nunes Da Ponte & Staveley[63]	1976	4	110–120	2
Cheng[21]	1972	7	111.2–261	1
Prydz & Goodwin[64]	1972	13	91–96	1
Cheng *et al.*[65]	1975	8[b]		
Hazen *et al.*[66]	1980	1	293.15	3
Wieldraaijer *et al.*[67]	1983	2[c]	342–367	2
Kortbeek *et al.*[68]	1986	5[c]	148–248	2

[a]Since the experimental results were only published in graphical form, it is difficult to classify the data.
[b]These data are identical with the data of Cheng; the additional point, the triple point pressure, is an extrapolated value.
[c]The experimental results were only published in graphical form. Their numerical values were communicated to us by Kortbeek.[69]

TABLE 6. Selected melting pressure data

Source	Year	Uncertainties $3\sigma_T$/mK	$3\sigma_p$
Clusius & Weigand[59]	1940	20	0.005–0.01 MPa
Nunes Da Ponte & Staveley[63]	1976	–	0.1 MPa
Cheng[21]	1972	–	0.5 MPa
Prydz & Goodwin[64]	1972	6	0.4×10^{-3}p
Wieldraaijer *et al.*[67]	1983	500	3×10^{-2}p[a]
Kortbeek *et al.*[68,69]	1986	30	10 MPa

[a]Estimated

2.2.4. Liquid-Vapor Saturation Curve

Based on a detailed investigation of existing data along the saturation curve we concluded that the measurements of Kleinrahm and Wagner[2] represent the phase boundary of methane more accurately than previous measurements. Thus, new correlation equations for the vapor pressure p_s, the saturated liquid density ρ', and the saturated vapor density ρ'', given in Sec. 3, have been established based only on the results of Kleinrahm and Wagner. Friend *et al.*[16] of the National Institute of Standards and Technology (NIST), who developed an equation of state for methane in 1989, came to the same conclusion. They strongly emphasized the use of the data of Kleinrahm and Wagner when establishing their correlation equations for the vapor-liquid phase boundary.

2.2.4.1. Vapor Pressure

The vapor pressure of methane has been measured extensively from the triple point to the critical point; within the last 100 years, more than 30 data sets have been published. The most recent determinations of the vapor pressure are given in Table 7. Since the residual part of the fundamental equation, Eq. (5.3), and the vapor pressure equation, Eq. (3.2), are based on the experimental vapor pressures of Kleinrahm and Wagner,[2] only this data set was assigned to form the Group 1 data. Group 2 data contain experimental results which do not differ by more than ± 0.3% in pressure from the values of Group 1. The third group includes data which differ considerably in a systematic way from the selected data. A detailed comparison of the selected data set for the phase boundary with measurements of other experimentalists was previously given by Kleinrahm and Wagner in Ref. 2. Figure 1 illustrates the percentage deviations of the Group 1 and Group 2 data from values calculated from the vapor pressure equation, Eq. (3.2). This comparison shows that the Group 2 data are clearly outside the total experimental uncertainties of Kleinrahm and Wagner's vapor pressures; the numerical values of these uncertainties are given in Ref. 2. Kleinrahm and Wagner[2] discussed that the effect of impurities on the vapor pressure may explain the disagreement between the data sets.

TABLE 7. Summary of the experimental values for the vapor pressure of methane

Source	Year	Number of data	Temperature range T/K	Group
Bloomer & Parent[45]	1953	20	105–190.5	3
Armstrong *et al.*[44]	1955	87[a]	90.6–112	2
Hestermans & White[48]	1961	18	109–190	3
Van Itterbeek *et al.*[70]	1963	22	123–189	3
Van Itterbeek *et al.*[71]	1964	38	112–189	3
Cutler & Morrison[72]	1965	15	93–108	3
Van Dael[73]	1965	13	140–188	3
Grigor[74]	1966	38	93–190	3
Vennix *et al.*[75]	1970	32	134–190.5	3
Jansoone *et al.*[54,56]	1970	7	189–190.5	2
DeVaney *et al.*[76]	1971	9	124–190	3
Liu & Miller[77]	1972	9	91–120	3
Pope[78]	1972	13	132–190.5	2
Prydz & Goodwin[64]	1972	105	91–190.5	2
Calado *et al.*[28]	1974	2	116–135	2
Douglas *et al.*[79]	1974	31	144–190	3
Olson[57]	1975	6	169–190	2
Gammon & Douslin[80]	1976	47	113–190.5	2
Calado & Soares[81]	1977	2	104–116	3
Kleinrahm & Wagner[2]	1986	161	90.7–190.5	1

[a]The reference only contains smoothed data; the original experimental values were published by Angus *et al.* in the IUPAC monograph on methane.[1]

2.2.4.2. Saturated Liquid Density

The saturated liquid density has been investigated extensively over the entire temperature range. Table 8 summarizes the information on these data sets. Since the experimental uncertainties of the saturated liquid densities of Kleinrahm and Wagner[2] are clearly less than the uncertainties of the ρ′ data of other authors, we decided to use only the 54 data points published by Kleinrahm and Wagner[2] for the establishment of our equation of state. These ρ′ values form the Group 1 data. All data sets which agree within the combined experimental uncertainties with the data of Kleinrahm and Wagner are considered to belong to the Group 2 data. All the other available saturated liquid density data deviate systematically from the selected data and are placed in Group 3.

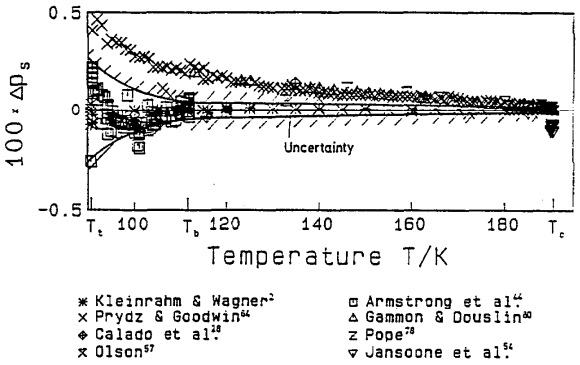

FIG. 1. Percentage deviation $\Delta p_s = (p_{s,expt} - p_{s,calc})/p_{s,expt}$ of experimental vapor pressure data from values calculated from the vapor pressure equation, Eq. (3.2). The plotted uncertainty range corresponds to the data of Kleinrahm and Wagner.[2]

TABLE 8. Summary of the experimental values for saturated liquid density of methane

Source	Year	Number of data	Temperature range T/K	Group
Cardoso[83]	1915	8	165–189	3
Keyes *et al.*[41]	1922	46	101–191	3
Bloomer & Parent[45]	1952	12	124–191	3
Fuks *et al.*[85]	1965	16	98–112	3
Vennix[49]	1965	12	139–191	3
Davenport *et al.*[86]	1966	20	115–154	3
Grigor[52,74]	1966	24	95–190	3
Sinor & Kurata[87]	1966	6	93–188	3
Klosek & McKinley[88]	1968	8	94–133	2
Shana'a & Canfield[89]	1968	1	108	3
Jensen & Kurata[90]	1969	5	93–113	3
Ricci & Scafè[53]	1969	6	185–190	3
Terry *et al.*[91]	1969	25	92–151	3
Jansoone *et al.*[54,56]	1970	12	187–191	3
Vennix *et al.*[75]	1970	15	139–190	3
Goodwin & Prydz[19]	1972	19	93–175	2
Lui & Miller[77]	1972	9	91–120	3
Verbeke[84]	1973	5	190–191	3
Rodosevich & Miller[92]	1973	4	91–115	2
Goodwin[8]	1974	18	130–188	2
Orrit & Olives[93]	1974	20	99–159	2–3
Olson[57]	1975	31	90–191	2
McClune[94]	1976	12	93–123	2
Orrit & Laupretre[95]	1976	10	99–159	2–3
Haynes & Hiza[96]	1977	11	105–160	2
Kleinrahm & Wagner[2]	1986	54	60–191	1

Figure 2 illustrates the deviation of the data sets of Group 2 from the experimental values of Kleinrahm and Wagner.[2] This comparison shows that the Group 2 data are clearly outside the total experimental uncertainties of Kleinrahm and Wagner's saturated liquid densities; the numerical values of these uncertainties are given in Ref. 2.

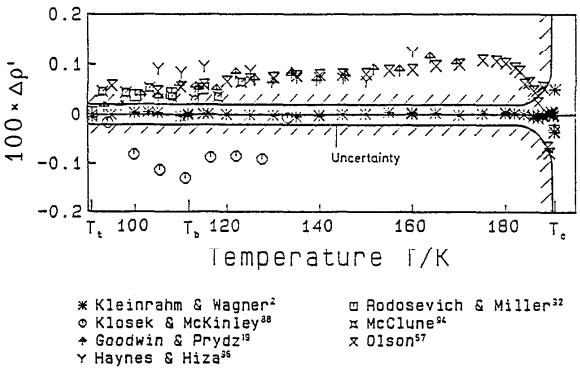

FIG. 2. Percentage deviation $\Delta\rho' = (\rho'_{expt} - \rho'_{calc})/\rho'_{expt}$ of experimental saturated liquid density data from values calculated from the saturated liquid density equation, Eq. (3.4). The plotted uncertainty range corresponds to the data of Kleinrahm and Wagner.[2]

2.2.4.3. Saturated Vapor Density

Because of experimental difficulties, especially in the low density region, measurements of the saturated vapor density of methane are, with the exception of the data of Kleinrahm and Wagner,[2] generally poor. Since the available data were extensively discussed by Kleinrahm and Wagner in different papers,[2,82] Table 9 presents only a summary of the information on the data sets of the saturated vapor density for methane. Thus, we considered using only the Kleinrahm and Wagner ρ'' values, which form the Group 1 data, for the development of the new equation of state. All the other ρ'' data which are far outside the experimental uncertainty of Kleinrahm and Wagner's data (see Fig. 4 in Ref. 2) are considered to belong to Group 2–3 and Group 3, respectively.

TABLE 9. Summary of the experimental values for saturated vapor density of methane

Source	Year	Number of data	Temperature range T/K	Group
Cardoso[83]	1915	8	165–189	3
Bloomer & Parent[45]	1953	13	124–165	2–3
Ricci & Scafè[53]	1969	6	185–190	2–3
Jansoone *et al.*[54,56]	1970	6	189–191	2–3
Verbeke[84]	1973	5	190–191	2–3
Goodwin[8]	1974	42	169–189	2–3
Olson[57]	1975	14	160–191	2–3
Kleinrahm & Wagner[2]	1986	65	91–191	1

To take into account the phase equilibrium condition [Maxwell criterion, see Eqs. (4.9) to (4.11)] for fitting the new fundamental equation, a set of vapor pressures p_s, saturated liquid densities ρ', and saturated vapor densities ρ'' must be available covering the whole saturation curve with temperature steps not greater than 1 K. Since the experimental p_s, ρ', and ρ'' data are not measured in such small steps, the required data have to be calculated for temperatures from the triple point to the critical point using independent equations for the vapor pressure and the saturation densities. At the beginning of the development of the new fundamental equation for methane we used the correlation equations for these properties given by Kleinrahm and Wagner.[2] Later calculations, however, have shown that it was impossible to produce 'reasonable' plots of the various thermodynamic properties in the homogeneous gas region for temperatures $T \leq 120$ K with an equation of state developed with ρ'' values calculated from Eq. (13) of Ref. 2. The uncertainty of the experimental ρ'' data and, consequently, the uncertainty of the derived correlation equation published by Kleinrahm and Wagner increases to about ± 0.8% at the triple point. Therefore, small inconsistencies between the data in the triple point region were not unexpected. For the purpose of checking the values calculated from the saturated vapor density equation of Kleinrahm and Wagner, we calculated second virial coefficients from their saturated vapor density and vapor pressure equations. The compressibility factor z [$z = p/(\rho RT)$] of a gas can be expressed by a power series in density. The gas density of methane at temperatures below 120 K can be represented using the following truncated virial equation

$$z = p/(\rho RT) = 1 + B(T)\rho. \tag{2.4}$$

By rearranging Eq. (2.4) we get

$$B = p/(\rho^2 RT) - 1/\rho. \tag{2.5}$$

By introducing values for the saturated vapor density ρ'' and the vapor pressure p_s calculated from the equations given by Kleinrahm and Wagner,[2] one obtains second virial coefficients B for given temperatures T. Figure 3 shows that the second virial coefficient, calculated using the procedure desribed above, behaves in a physically absurd way (increasing second virial coefficients for decreasing temperatures) in the triple point region. The additional values of the second virial coefficients in Fig. 3, which were calculated by using the experimental saturated vapor densities, indicate that the uncertainties (up to ± 0.8%) of the ρ'' data do not allow the calculation of reliable second virial coefficients at temperatures below 120 K. In an iterative process [(a) optimization of the fundamental equation using saturated vapor densities from a preliminary correlation equation for ρ'', (b) calculation of the saturated vapor densities from the fundamental equation using the phase equilibrium condition, (c) establishment of a new correlation equation for ρ'' using the values calculated from the fundamental equation]

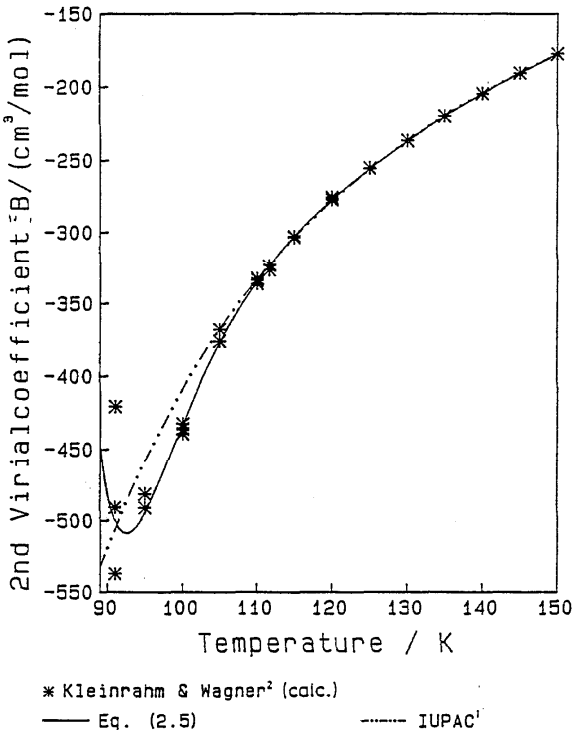

FIG. 3. Second virial coefficients of methane calculated from Eq. (2.5) when the vapor pressure and the saturated vapor density equation published by Kleinrahm and Wagner[2] is used. The B values calculated from the IUPAC equation[1] are plotted for comparison.

we obtained saturated vapor densities which are considered to be much more reliable than those calculated from the original saturated vapor density equation of Kleinrahm and Wagner.[2] The final values for the saturated vapor densities at temperatures below 120 K are given in Table 10. These revised ρ'' values are clearly within the experimental uncertainty given for the originally measured saturated vapor densities; see Fig. 4. Table 11 presents the uncertainties estimated for the original saturated vapor densities of Kleinrahm and Wagner for $T > 120$ K and for the saturated vapor densities calculated by using the procedure desribed above for $T \leq 120$ K. The uncertainties given for the revised ρ'' values correspond to maximum shifts of ρ'' which would not

TABLE 10. Calculated saturated vapor densities ρ'' for temperatures $T \leq 120$ K

T/K	ρ''/(kg/m³)	T/K	ρ''/(kg/m³)
90.6941	0.25074	91	0.25996
92	0.29197	93	0.32702
94	0.36530	95	0.40702
96	0.45238	97	0.50159
98	0.55488	99	0.61246
100	0.67457	101	0.74143
102	0.81329	103	0.89039
104	0.97298	105	1.06130
106	1.15562	107	1.25621
108	1.36332	109	1.47722
110	1.59821	111	1.72655
112	1.86254	113	2.00646
114	2.15862	115	2.31931
116	2.48885	117	2.66755
118	2.85573	119	3.05372
120	3.26185		

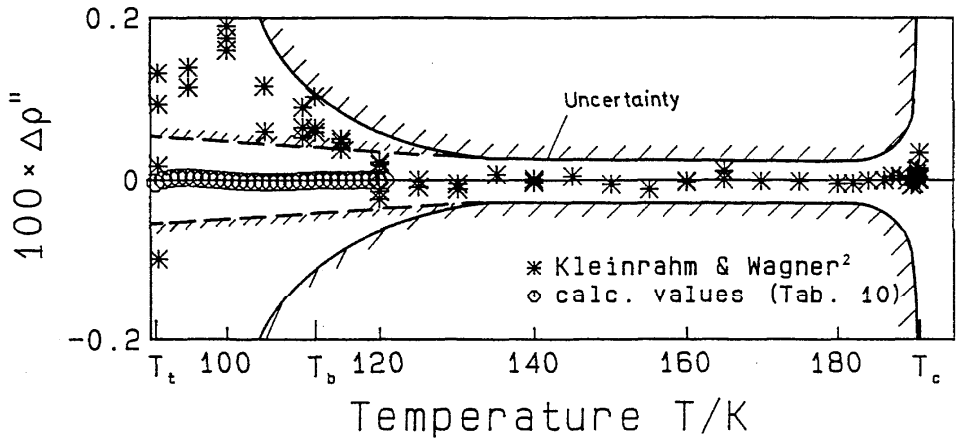

FIG. 4. Percentage deviation $\Delta\rho'' = (\rho''_{expt} - \rho''_{calc})/\rho''_{expt}$ of experimental saturated vapor density data of Kleinrahm and Wagner[2] and of the data listed in Table 10 from values calculated from the saturated vapor density equation, Eq. (3.5). The uncertainty range plotted by solid lines corresponds to the original values of Kleinrahm and Wagner.[2] The uncertainty range plotted by dotted lines corresponds to the uncertainties estimated for the calculated values of Table 10.

TABLE 11. Total experimental uncertainties of the saturated vapor densities ($T > 120$ K) published by Kleinrahm and Wagner[2] and of the calculated densities ($T \leq 120$ K, see text)

Temperature T/K	Uncertainty $(2\sigma_\rho/\rho) \times 100$
90.694	0.050
100.000	0.045
120.000	0.033
140.000	0.025
160.000	0.024
180.000	0.027
189.000	0.062
190.000	0.130
190.313	0.313
190.543	1.91

quite produce an absurd behavior of the equation of state in the gas region for $T \leq 120$ K when these shifted ρ'' values were used for establishing the equation. The uncertainties estimated for the revised ρ'' values are also shown in Fig. 4.

The physically incorrect behavior of the second virial coefficient calculated from the original equations for the saturated vapor density and the vapor pressure is caused by the correlation equation for ρ'' and not by the vapor pressure equation. The vapor pressure equation was constrained at the triple point and the normal boiling point which means that two of the four fitted coefficients were fixed. Since the remaining two coefficients were determined by fitting the equation to the whole vapor pressure curve, this equation does not have the degree of freedom to produce a basically wrong course between the triple point and the normal boiling point. Thus, there is no reason why the vapor pressure equation might be so incorrect as to produce these wrong B values.

As a result of our detailed investigation of the saturated vapor densities we have developed a new correlation equation for this property, see Sec. 3.3.

2.2.4.4. Enthalpy of Vaporization

There are only four sets of data of the enthalpy of vaporization. The data of Hestermans and White[48] depend on the knowledge of values for the saturated liquid and vapor density. The authors used values for these quantities which were published by Bloomer and Parent[45] and Matthews and Hurd.[48a] These data sets are not consistent with the data published by Kleinrahm and Wagner[2] for the saturation densities. Therefore, the values of Hestermans and White[48] have to be considered to be less reliable. Jones *et al.*[98] used methane with a purity of the sample of only 99.45 mol%. The characteristics of the four data sets, which were not used to establish the new equation of state, are summarized in Table 12.

2.2.4.5. Heat Capacity

There are only a few laboratories which have published experimental measurements of heat capacities in the saturation state. The experimental data of the heat capacity along the saturated liquid curve c_σ and of the heat capacity c_p' are summarized in Table 13. However, these data were not used for the development of the new equation of state.

2.2.4.6. Speed of Sound

A list of experimental studies concerned with the speed of sound of the saturated liquid and vapor is given in Table 14. The data sets which were used for the development of the new fundamental equation are characterized by a number which differs from zero in the column 'selected data points' of Table 14. The difference between the number of data points of a data set and the number of selected data points of this data set is based on the fact that we either rejected abundant data or that there were obviously misprints in the publication. The speed of sound measurements of Gammon and Douslin[80] were performed close to the phase boundary. All data points of their publication for which the measured pressure differs by more than 0.002 MPa from the vapor pressure [calculated from Eq. (3.2)] at the measured temperature were not included in Table 14.

2.3. Single-Phase Region

2.3.1. Thermal Properties

The temperature and pressure dependence of the density of methane has been investigated in more than 50 papers. A detailed description of the quality of the available

TABLE 12. Summary of the experimental data for the enthalpy of vaporization

Source	Year	Number of data	Temperature range T/K	Uncertainty	Purity of sample
Frank & Clusius[97]	1939	1	99.54	$3\sigma_{\Delta h_v}$ = 0.5 J/g	–
Hestermans & White[48]	1961	10	111–185	–	99.96 mol%
Jones *et al.*[98]	1963	20	99–189	–	99.45 mol%
Colwell *et al.*[99]	1964	1	100	$3\sigma_{\Delta h_v}$ = 1.3 J/g	99.98 mol%

TABLE 13. Summary of the experimental data for the heat capacity on the saturated liquid line

Source	Year	Number of data	Temperature range T/K	Property
Eucken & Karwat[100]	1924	7	96–109	c'_p
Clusius[101]	1929	6	95–105	c_σ
Wiebe & Brevoort[102]	1930	20	97–188	c_σ
Hestermans und White[48]	1961	9	115–188	c_σ
Cutler and Morrison[72]	1965	5	94–107	c'_p
Younglove[103]	1974	66	95–187	c_σ
Roder[104]	1976	3	116–122	c_σ

data was presented by Angus *et al.*,[1] Sytchev *et al.*,[10] Tester,[110] as well as by Sievers and Schulz.[25] As a result of recent experimental investigations of Kleinrahm *et al.*,[3,4] Achtermann *et al.*,[23,109] and Morris,[114,115] we had to revise the assessment of the data situation given in the prior investigations mentioned above; details were discussed by Setzmann.[26]

One of the most important results of our investigations for assembling a selected $p\rho T$ data set was the fact that Goodwin's $p\rho T$ data[8,19] were not consistent with the experimental saturated liquid densities ρ' of Kleinrahm and Wagner.[2] If we had used these two data sets together in the selected data, it would not have been possible to establish an equation of state which showed a smooth behavior of the derivatives near the saturated liquid line. On the other hand, we had to use Goodwin's data for the development of the new equation of state because these values had been the only good $p\rho T$ data in the liquid region up to that time (1988). Therefore, we tried to find the reason for the assumed errors in Goodwin's data but we could not find any hint in the corresponding papers.[8,19] Based on the order of the difference between the ρ' data of Ref. 2 and the ρ' values extrapolated from Goodwin's $p\rho T$ data for $\rho < \rho_c$ it was unlikely that the reason for the difference was an error in the temperature or pressure measurement. Consequently, we assumed an error in the density values. Thus, we concluded to 'correct' Goodwin's densities by the same correction for all values on the same isochore but by different corrections from isochore to isochore. For $\rho > \rho_c$, the corrections $\Delta\rho$ were determined by comparison of the ρ' values extrapolated from Goodwin's isochoric $p\rho T$ values[8,19] with Kleinrahm and Wagner's[2] ρ' values and, for $\rho < \rho_c$, by the comparison of Goodwin's $p\rho T$ data[8,19] with the very reliable $p\rho T$ data of Kleinrahm *et al.*[4], Schamp *et al.*[111] and Roe.[112] The numerical values of these corrections are listed in Table 15 for the most characteristic isochores; the maximum correction obtained in this way amounts to 0.14%.

Since we had, of course, our doubts as to whether these corrections were objectively reasonable we initiated new $p\rho T$ measurements in our group carried out by Händel *et al.*[5] for pressures up to 8 MPa (pressure limit of the apparatus) with the densitometer based on our 'Two-Sinker' buoyancy method.[2] Figure 5 shows the comparison of Goodwin's original and corrected data with the new $p\rho T$ measurements of Händel *et al.*[5] and, for the 300 K isotherm, with recent data of other authors as well. These comparisons illustrate that Goodwin's corrected data agree well with recent experiments. This fact confirms that the corrections of Goodwin's $p\rho T$ data were not unreasonable. Thus, Goodwin's original $p\rho T$ data[8,19] probably contain systematic errors of up to 0.2% in density which is about two times greater than the uncertainty estimated by Goodwin himself.

In the course of the development of the new equation of state it became apparent again that Goodwin's corrected data are the only acceptable $p\rho T$ data set for the liquid region at higher pressures. Only the use of these corrected data allows a good representation of the caloric

TABLE 15. Density corrections $\Delta\rho$ ($\rho_{corr} = \rho_{orig} - \Delta\rho$) for selected pseudo-isochores published by Goodwin[8,19]

Isochore ρ/(kg/m^3)	Correction $\Delta\rho$
480	$0.4\times10^{-3}\rho_{orig}$
433	$0.5\times10^{-3}\rho_{orig}$
393	$0.7\times10^{-3}\rho_{orig}$
340	$0.9\times10^{-3}\rho_{orig}$
290	$0.9\times10^{-3}\rho_{orig}$
160	$1.2\times10^{-3}\rho_{orig}$
93	$1.4\times10^{-3}\rho_{orig}$
47	$0.6\times10^{-3}\rho_{orig}$

TABLE 14. Summary of the experimental data for the speed of sound on the saturated liquid and vapor line

Source	Year	Number of data total	Number of data selected	Property	Uncertainty
Van Itterbeek & Verhagen[105]	1949	6	–	w'	$3\sigma_w = 1.0\times10^{-2}w$
Van Dael *et al.*[73]	1965	28	26	w'	$3\sigma_w = 0.1\times10^{-2}w$
Blagoi *et al.*[106]	1967	26	–	w'	$3\sigma_w = 3-5$ m/s
Straty[107]	1974	30	28	w'	$3\sigma_w = 0.1\times10^{-2}w$ $3\sigma_T = 5-30$ mK
Straty[108]	1975	3	3	w'	$3\sigma_w = 0.5\times10^{-2}w$
Straty[108]	1975	3	–	w''	$3\sigma_w = 0.5\times10^{-2}w$
Gammon & Douslin[80]	1976	28	25	w'	$3\sigma_w = (0.01-1)\times10^{-2}w$ $3\sigma_T = 1$ mK
Gammon & Douslin[80]	1976	27	16	w''	$3\sigma_w = (0.01-1)\times10^{-2}w$ $3\sigma_T = 1$ mK

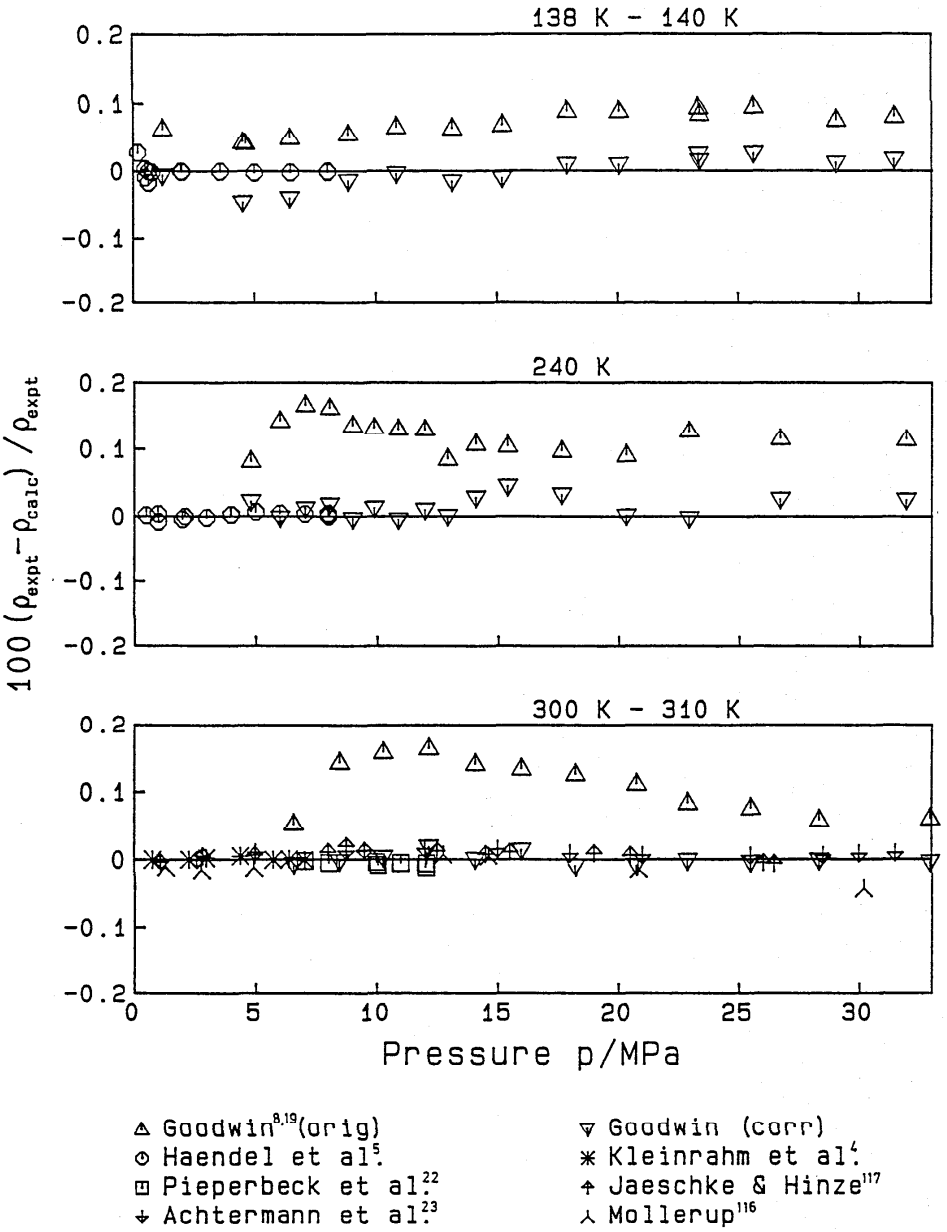

FIG. 5. Percentage deviation of the original and the corrected $p\rho T$ data of Goodwin[8,19] from values calculated from the fundamental equation, Eq. (5.3). For the experimental uncertainties see Table 16.

data, especially the speed of sound measurements, in this region. Since, however, all equations of state which have been developed during the last 16 years were fitted to Goodwin's original data, they have to differ substantially from our new equation of state, see Sec. 6.

The selected $p\rho T$ data sets which correspond to Group 1 data to which the new equation of state has been fitted are summarized in Table 16. Figure 6 shows the distribution of the selected data in a pT diagram. Not all of the selected data points are presented in Figure 6 because the representation of all data points in the critical region and in regions where several data sets overlap each other would have made the plot too crowded.

All experiments not mentioned in Table 16 are presented and classified in Table 17. Group 2 contains $p\rho T$ data which differ from the Group 1 data by more than their uncertainty given in Table 16. All the other available data deviate considerably from the Group 1 date and are only of historical interest.

Table 16. Summary of selected $p\rho T$ data for methane (Group 1 data)

Source	Year	Number of data total	Number of data selected	Temperature range T/K	Pressure range p/MPa	Purity of sample/mol%	$3\sigma_T$/mK	Uncertainty[a] $3\sigma_p$	$3\sigma_\rho$
Schamp *et al.*[111]	1958	118	118	273–423	1.8–26	99.99	10	$3\times10^{-5}p$	$(2\times10^{-4}\rho)$
Douslin *et al.*[20]	1964	374	220	273–623	1.6–38	99.994	1	$3\times10^{-4}p$	$(3-20)\times10^{-4}\rho$
Pope[78]	1972	140	134	126–191	0.1–4.7	99.995	10	$1\times10^{-4}p$	$(3-6)\times10^{-4}\rho$
Roe[112]	1972	82	70	155–291	0.3–10	99.99	5	$8\times10^{-4}p$	$((2-5)\times10^{-4}\rho)$
Goodwin[8,19]	1972	554	232	91–300	0.3–35	99.97	–	–	$((5-30)\times10^{-4}\rho)$
Trappeniers *et al.*[113]	1979	472	468	273–423	2–260	99.995	3	$1\times10^{-4}p$	$(5\times10^{-4}\rho)$
Morris[114,115]	1984	235	235	253–423	130–690	99.99	–	–	$(5\times10^{-4}\rho)$
Mollerup[116]	1985	51	51	310	0.2–72	99.995	30	–	$1\times10^{-3}\rho$
Achtermann *et al.*[109]	1986	35	35	323.14	1.1–29	–	–	–	$(2\times10^{-4}\rho)$
Kleinrahm *et al.*[3]	1986	206	206	180–193	3.2–6.7	99.9995	3	$7\times10^{-5}p$	$2\times10^{-4}\rho$
Jaeschke & Hinze[117]	1991	605	304	269–353	0.3–30	–	–	–	$5\times10^{-4}\rho$
Kleinrahm *et al.*[4]	1988	169	169	273–323	0.1–8	99.9995	3	$7\times10^{-5}p$	$2\times10^{-4}\rho$
Achtermann *et al.*[23]	1991	654	218[b]	273–373	1–34	–	–	–	$4\times10^{-4}\rho$
Händel *et al.*[5]	1991	270	270	100–260	0.1–8	99.9995	3	$7\times10^{-5}p$	$2\times10^{-4}\rho$
Kortbeek & Schouten[118]	1989	18	18	298.15	150–1000	–	–	–	$(1\times10^{-3}\rho)$
Pieperbeck *et al.*[22]	1990	175	175	273–323	0.1–12	99.9995	5	$7\times10^{-5}p$	$2\times10^{-4}\rho$

[a]Uncertainty values given in brackets were estimated by ourselves.
[b]To have a reasonable relation to the data of other authors in this region, only every third $p\rho T$ data was used.

2.3.2. Virial Coefficients

There are many reported values for the second virial coefficient in the literature. Figure 7 shows the comparison between values predicted by the new fundamental equation, Eq. (5.3), and experimental results for the second virial coefficient. Table 18 lists the temperature range, the number of data, and the uncertainty of the experimental values of the selected second virial coefficients. These selected data agree closely with each other and form the Group 1 data which were used to establish the new equation of state. All selected virial coefficients were derived from $p\rho T$ measurements except for those of Lemming[151] which originated from speed of sound measurements. In contrast to the selected data, all the other second virial coefficients show significant deviations from the Group 1 data and are placed in Group 2 and 3 of Table 19. The Group 2 data consist of virial coefficients which differ from the Group 1 data by more than their uncertainty given in Table 18. All the other data which clearly deviate from the Group 1 data are put into Group 3.

2.3.3. Difference of Enthalpy

The literature sources which deal with enthalpy measurements are summarized in Table 20. The data sets of measurements of enthalpy differences $\Delta h = h(T_1,p_1) - h(T_2,p_2)$ which were used to establish the new equation of state are marked as selected data in Table 20. The values given by Ayber[167] and Dawe and Snowdon[169] were derived from their measurements of the integral Joule-Thomson coefficient. Jones *et al.*[98] measured isobaric heat capacities and presented the results as smoothed and interpolated isobaric heat capacities. The authors included a table of enthalpy values in their publication. Instead of using the enthalpy data given by Jones *et al.*,[98] we decided to fit our equation directly to the isobaric heat capacities. The additional inclusion of the enthalpy data did not improve the representation of this data set. It should be stressed that Jones *et al.*[98] used methane containing 0.45 mol% impurities.

2.3.4. Isobaric Heat Capacity

Isobaric heat capacity data have been measured by six laboratories. Figure 8 shows the distribution of the selected data on pT coordinates. The available experimental data sets are summarized in Table 21. Since we could not find any uncertainty estimation in these papers we estimated the uncertainty of these data to be about ± 2%. This estimation is based on our critical review of the isobaric heat capacity data and consistency tests with other thermodynamic properties. The selected data were used to develop the new equation of state.

2.3.5. Isochoric Heat Capacity

There are three sets of experimental isochoric heat capacity measurements which are summarized in Table 22. Most of the data points were published by Younglove[103] in 1974. In 1976, Roder[104] repeated some of Younglove's c_v measurements on methane using the same apparatus as Younglove did. He found differences of up to 1% in comparison to the data published by Younglove. Roder's experimental data[104] and the values calculated from the fundamental equation of state agree within ± 0.5%. Hence we have to conclude that the uncertainty of ± 0.5%, which Younglove estimated for the majority of

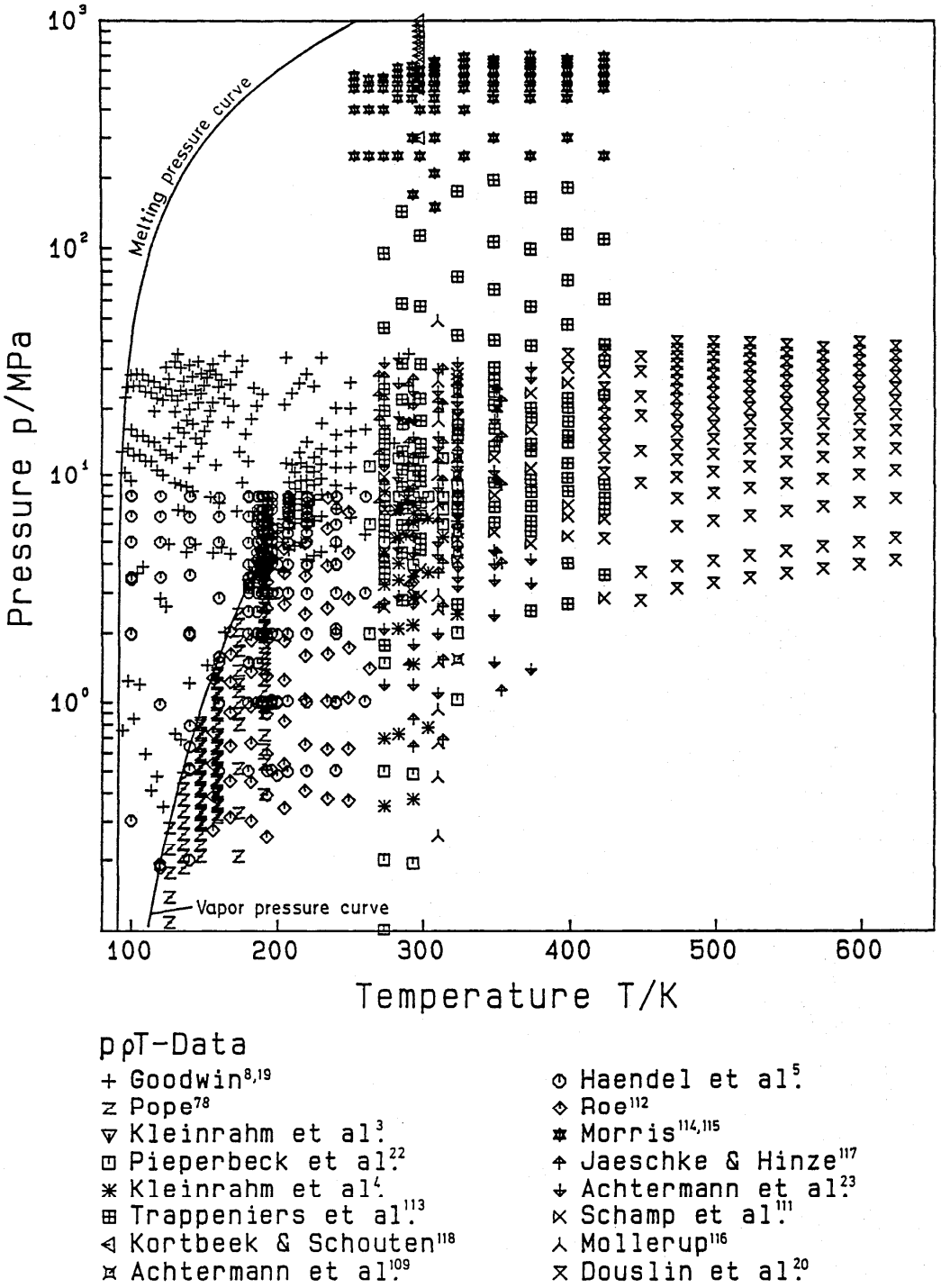

FIG. 6. Distribution of the $p\rho T$ data used in establishing the residual part of the fundamental equation, Eq. (5.3), in a pT diagram.

Table 17. Summary of experimental $pρT$ data for methane

Source	Year	Number of data	Temperature range T/K	Pressure range p/MPa	Group
Amagat[119]	1881	70	288–373	4–30	3
Keyes *et al.*[41]	1922	40	273–473	3.6–32	3
Keyes & Burks[120]	1927	40	273–473	3.2–26	3
Freeth & Verschoyle[121]	1931	27	273–293	1.7–22	3
Kvalnes & Gaddy[122]	1931	166	203–473	0.1–100	3
Michels & Nederbragt[123]	1935	56	273–423	1.8–8.2	2
Michels & Nederbragt[124]	1936	119	273–423	1.8–39	2
Olds *et al.*[125]	1943	294	294–511	1.3–67	3
Kazarnovskii & Levchenko[126]	1944	25	473–573	15–140	3
Pavlovich & Timrot[127]	1958	357	103–333	1–19.6	3
Date & Kobuya[128]	1961	196	273–373	3–104	3
Mueller *et al.*[129]	1961	75	144–283	1.4–48	3
Van Itterbeek *et al.*[130]	1963	162	115–188	0.7–32	3
Deffet *et al.*[131]	1964	228	324–425	1–30	3
Dobrovolskij *et al.*[132]	1964	52	110–193	1–50	3
Wallace *et al.*[133]	1964	20	248–348	0.1–0.2	3
Grigor *et al.*[52,74]	1966	78	95–190	0.1–5.7	3
Hoover[134]	1966	77	132–273	0.2–4.1	3
Huang[135]	1966	12	133–193	0.5–7	3
Mamedov & Mamedov[136]	1969	68	294–497	1.5–21	3
McMath & Edmister[137]	1969	32	266–298	1.8–15	3
Robertson & Babb[138]	1969	108	308–473	150–1000	3
Epperly[139]	1970	150	458–610	0.4–7	2
Jansoone *et al.*[54,56]	1970	62	189–194	4.5–5	3
Sorokin & Blagoy[140]	1970	41	95–129	0.02–49	3
Vennix *et al.*[75]	1970	260	150–273	1.5–69	3
Tsiklis *et al.*[141]	1971	70	323–673	203–861	3
Cheng[21]	1972	312	111–309	22–1000	2–3
Rodosevich & Miller[142]	1973	11	91–115	0.04–0.15	1–2
Bazaev & Skripka[143]	1974	19	523–673	29–98	3
Gammon & Douslin[80]	1976	262	114–323	0.1–24.5	2–3
Mihara *et al.*[144]	1977	47	298–348	1.8–9	3
Francesconi[145]	1978	454	291–723	14–270	3
Nunes Da Ponte *et al.*[146]	1978	63	110–120	5.5–128	3
Achtermann *et al.*[147]	1982	71	273–293	0.1–7.7	2
Achtermann *et al.*[148]	1982	68	273–293	0.1–8.5	2
Amer[149]	1986	40	323–398	0.4–6.3	3
Kortbeek *et al.*[68]	1986	19	298.15	100–1000	2
Sivaraman & Gammon[6]	1986	104	193–423	1.4–27.5	3
Machado *et al.*[150]	1988	79	130–160	25–111	3
Baidakov & Gurina[150a]	1989	165	143–185	0.15–5.2	3
McElroy *et al.*[70]	1989	22	313,323	0.8–12.6	3

TABLE 18. Summary of selected second virial coefficients for methane (Group 1 data)

Source	Year	Number of data	Temperature range T/K	Uncertainty $3\sigma_B$/(cm³/mol)
Douslin[20]	1964	16	273–623	0.2
Roe[112]	1972	10	156–291	0.1–0.6
Kleinrahm *et al.*[4]	1988	6	273–323	0.15
Lemming[151]	1989	7	232–350	0.7

his measurements, was too optimistic. The distribution of the selected c_v data in pT coordinates is shown in Fig. 9. These selected data were used to develop the new equation of state.

2.3.6. Joule-Thomson Coefficient

There are only two data sets of the Joule-Thomson coefficient which are listed in Table 23. The data measured by Ayber[167] are integral Joule-Thomson coefficients which could not be used in the fitting process of the new equation of state. As already stated by Angus *et al.*,[1] the data set published by Budenholzer *et al.*[165] does not seem to be very reliable. The inclusion of the data set of Budenholzer *et al.*[165] into the fitting process did not improve the representation of the Joule-Thomson data, and we decided not to use these measurements for establishing the new equation of state; see Sec. 6.2.7.

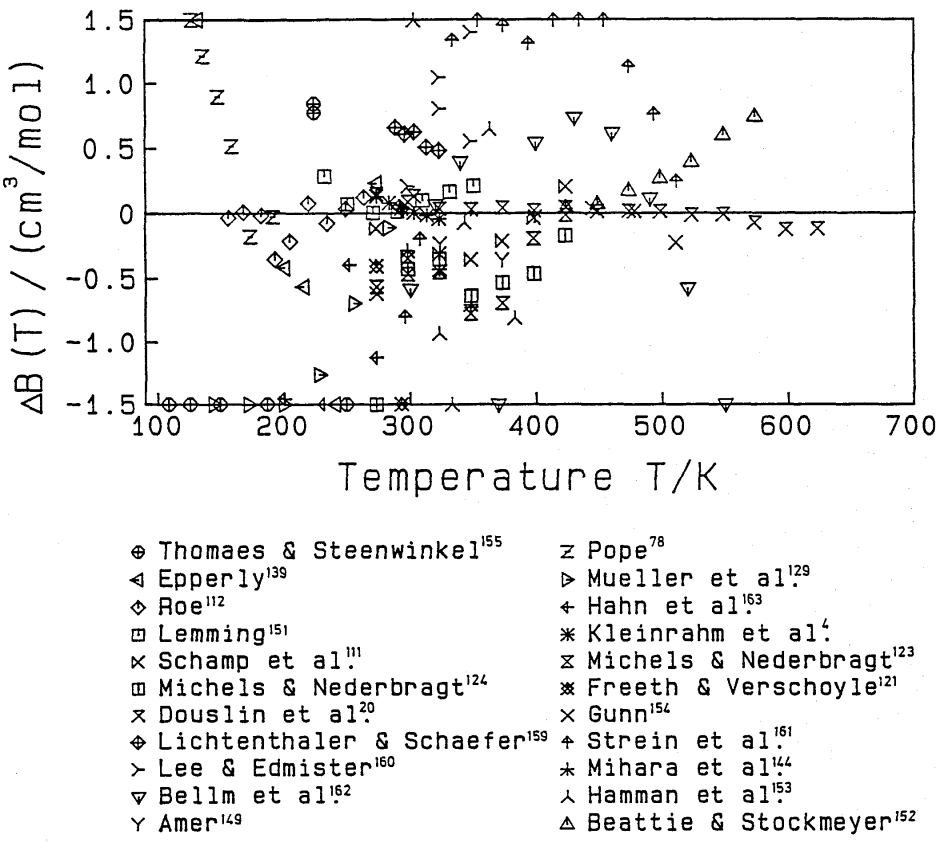

FIG. 7. Absolute deviation $\Delta B = (B_{expt} - B_{calc})$ of experimental second virial coefficients from values calculated from Eq. (5.3). All data with deviations of more than ± 1.5 cm³/mol are plotted on the limit of the deviation scale.

2.3.7. Isothermal Throttling Coefficient

In the literature only the paper of Eucken and Berger,[175] published in 1934, could be found which deals with integral isothermal throttling experiments. The authors published 75 data in the temperature range between 165 K and 293 K at pressures up to 11 MPa without giving any uncertainty value for their measurements. These data were not used to fit the new equation of state.

2.3.8. Speed of Sound

There are extensive measurements of the speed of sound for methane. The overwhelming majority of these measurements has been performed during the last 20 years. The information on these data is summarized in Table 24. Figure 10 shows the distribution of the selected data on pT coordinates. The speed of sound data cover the temperature range from 100 K to 450 K at pressures up to 1000 MPa and, due to the scarcity of information on the heat capacities of methane, the selected speed of sound data were extensively used to develop the new fundamental equation. These selected data are marked in Table 24 in the column 'Number of data sel.'.

2.4. Ideal Gas Properties

2.4.1. Isobaric Heat Capacity

The ideal gas heat capacity can be derived from statistical mechanical models based on spectroscopic data. In 1963, McDowell and Kruse[188] presented calculated values of c_p° for the temperature range from 60 K to 5000 K. These calculations were based on a rigid-rotator harmonic oscillator model which was modified to take into account the low-temperature quantum effects, anharmonicity, centrifugal distortion, and vibration-rotation interactions. Although the values of McDowell and Kruse were published nearly 30 years ago, they still represent the most accurate data for the isobaric heat capacity c_p° in

TABLE 19. Summary of second virial coefficients not belonging to Group 1 data and third virial coefficients for methane

Source	Year	Property	Number of data	Temperature range T/K	Group (only B)
Freeth & Verschoyle[121]	1931	B,C	2,1	273–293	2
Michels & Nederbragt[123]	1935	B,C	7,7	273–423	2
Michels & Nederbragt[124]	1936	B,C	7,7	273–423	2
Beattie & Stockmeyer[152]	1942	B	7	423–573	2
Hamman *et al.*[153]	1955	B	6	303–383	3
Gunn[154]	1958	B	4	273–511	3
Schamp *et al.*[111]	1958	B,C	7,7	273–423	2
Thomaes & Steenwinkel[155]	1960	B	12	108–249	3
Mueller *et al.*[129]	1961	B	6	144–283	3
Hoover *et al.*[134]	1966	C	1	132	–
Brewer[156]	1967	B	5	123–223	3
Byrne *et al.*[157]	1968	B	14	111–273	3
Hoover *et al.*[158]	1968	B,C	6,6	132–273	2
Lichtenthaler & Schäfer[159]	1969	B	5	288–323	3
McMath & Edmister[137]	1969	B,C	3,3	266–289	3
Epperly[139]	1970	B,C	6,6	458–610	3
Lee & Edmister[160]	1970	B,C	6,6	298–348	3
Strein *et al.*[161]	1971	B	12	296–511	3
Pope[78]	1972	B,C	6,6	127–191	2
Bellm *et al.*[162]	1974	B	10	300–550	3
Hahn *et al.*[163]	1974	B	4	200–273	3
Mihara *et al.*[144]	1977	B,C	3,3	298–348	2
Kerl & Häusler[164]	1984	B	5	299–366	3
Amer[149]	1986	B,C	4,4	323–398	3
McElroy *et al.*[70]	1989	B,C	6,6	303–323	3

TABLE 20. Summary of experimental data for the enthalpy of methane

Source	Year	Number of data total	Number of data selected	Temperature range T/K	Pressure range p/MPa	Uncertainty $3\sigma_{\Delta h}$
Budenholzer *et al.*[165]	1939	18	–	294–378	0.1–10.3	–
Jones *et al.*[98]	1963	796	–	100–283	0.3–14	$10^{-2}\Delta h$
Sahgal *et al.*[166]	1964	27	–	134–223	0.3–10	$6\times10^{-3}\Delta h$[a]
Ayber[167]	1965	21	–	188–311	0.1–8	–
Dillard *et al.*[168]	1968	4	–	338	1.8–14	$<3\times10^{-2}\Delta h$
Dawe & Snowdon[169]	1974	56	54	224–367	0.1–10	5J/mol
Kasteren & Zeldenrust[170]	1979	25	25	120–255	3.2–5	$10^{-2}\Delta h$

[a]Since the methane used for the measurements had a purity of only 98 mol%, the total uncertainty of these data is clearly greater than given by the authors.

the ideal gas state of methane, and they were used to determine our c_p° equation; see Sec. 3.5. Table 25 summarizes recent determinations of the ideal gas heat capacity. With the exception of Lemming's[151] and Goodwin's[187] data, who derived c_p° values from speed of sound measurements, all data sets were calculated from spectroscopic data.

2.4.2. Reference Value for the Entropy

For the calculation of the entropy in the property tables of the Appendix, the state at which the entropy was assumed to be zero was that of the ideal gas at 298.15 K and 0.101325 MPa. If the entropy of the crystalline solid methane at 0 K is to be taken as zero, then the difference of the entropy between this state and that of the ideal gas at 298.15 K and 0.101325 MPa has to be added to the values of the entropy given in the tables. The recommended value for this entropy difference is given by McDowell and Kruse[188] as 11.611 kJ/(kg K).

2.4.3. Reference Value for the Enthalpy

For calculations of the enthalpy, there are three different states in common use at which the enthalpy may be taken as zero. The first state is that of the ideal gas at 298.15 K, and this is the reference state used for the enthalpy values given in the property tables of the Appendix. The second commonly used state is that of the enthalpy of the ideal gas at 0 K. The enthalpy difference between the ideal gas at 0 K and at 298.15 K is given as 624.39 kJ/kg by McDowell and Kruse.[188] As discussed by

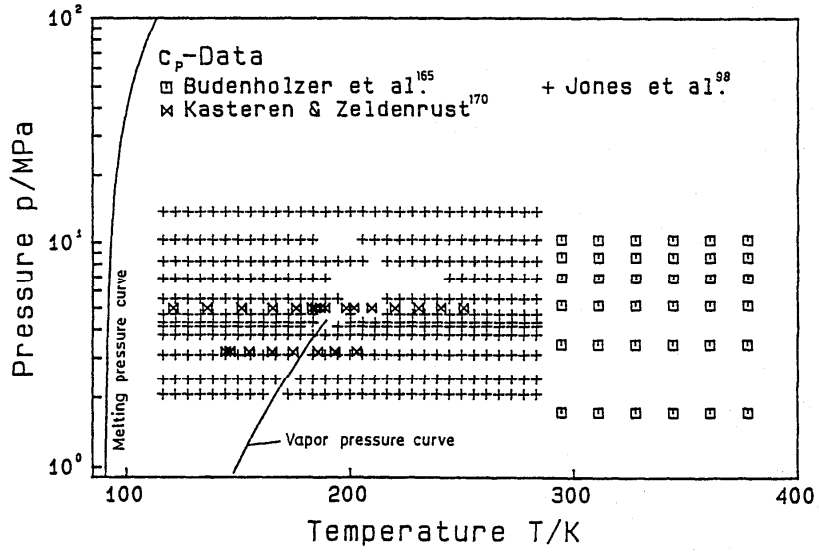

FIG. 8. Distribution of the isobaric heat capacity data used in the establishment of the residual part of the fundamental equation, Eq. (5.3), in a pT diagram.

TABLE 21. Summary of isobaric heat capacities for methane

Source	Year	Number of data total	Number of data selected	Temperature range T/K	Pressure range p/MPa
Heuse[171]	1919	8	–	193–290	0.1
Millar[172]	1923	13	–	139–278	0.1
Eucken & von Lüde[173]	1929	3	–	298–481	0.1
Budenholzer *et al.*[165]	1939	42	42	294–378	0.1–10.3
Jones *et al.*[98]	1963	400	345	116–283	1–14
Kasteren & Zeldenrust[170]	1979	58	50	121–251	3.2–5

TABLE 22. Summary of isochoric heat capacities for methane

Source	Year	Number of data total	Number of data selected	Temperature range T/K	Pressure range p/MPa	Uncertainty[a] $3\sigma_{c_v}$
Giacomini[174]	1925	4	–	83–288	0.001–0.1	–
Younglove[103]	1974	283	282	91–300	3.4–33	$((1-5)\times10^{-2}c_v)$
Roder[104]	1976	29	28	147–218	4.5–23.5	$(2-5)\times10^{-2}c_v$

[a]Uncertainty values given in brackets were estimated by ourselves.

TABLE 23. Summary of Joule-Thomson coefficients for methane

Source	Year	Number of data	Temperature range T/K	Pressure range p/MPa
Budenholzer *et al.*[165]	1939	42	294–378	0.1–10.3
Ayber[167]	1965	21	249–311	0.1–8

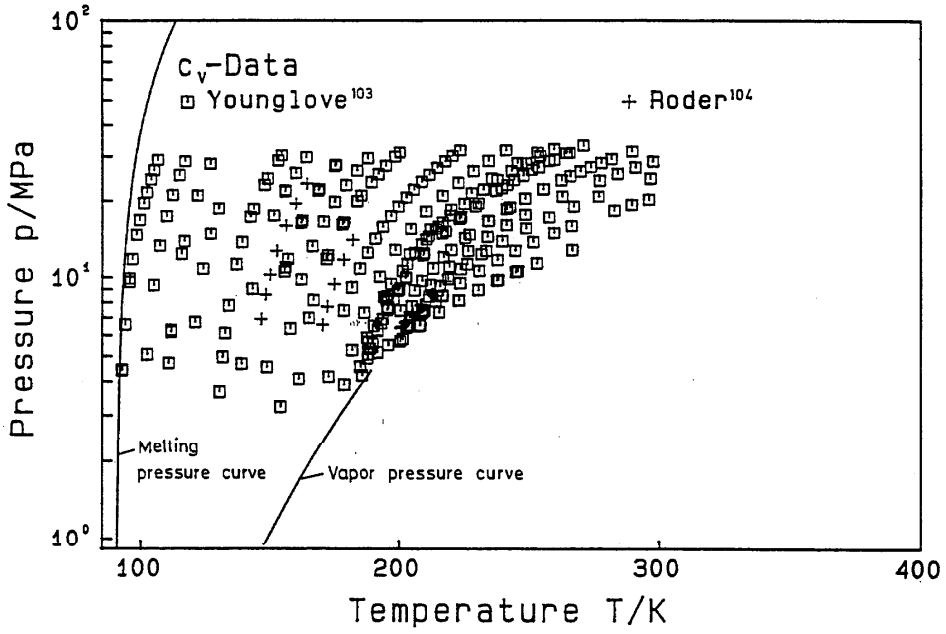

FIG. 9. Distribution of the isochoric heat capacity data used in the establishment of the residual part of the fundamental equation, Eq. (5.3), in a pT diagram.

TABLE 24. Summary of speed of sound data for methane

Source	Year	Number of data total	Number of data selected	Temperature range T/K	Pressure range p/MPa	Uncertainty[a] $3\sigma_w$
Dixon *et al.*[176]	1921	7	–	273–873	0.1	–
Quingley[177]	1945	19	–	116–253	0.1	$(10^{-2}w)$
Van Itterbeek & Verhagen[105]	1949	6	–	95–112	0.02–0.1	$((2-5)\times10^{-2}w)$
Lacam[178]	1956	68	–	298–473	10–100	$10^{-2}w$
Terres *et al.*[179]	1957	91	26	293–448	0.01–12	0.7 m/s
Blagoi *et al.*[106]	1967	25	–	91–178	0.01–3.2	(3–5) m/s
Van Itterbeek *et al.*[180]	1967	98	92	111–190	0.1–18	$10^{-3}w$
Singer[181]	1969	22	–	94–145	0.2–9	$5\times10^{-3}w$
Cardamone *et al.*[182]	1970	16	–	299	1.3–10.3	$(6\times10^{-2}w)$
Pitaevskaya & Bilevich[183]	1972	175	–	298–473	60–450	$((1-2)\times10^{-2}w)$
Dregulyas[184]	1973	145	–	298–473	0.02–16	$((1-2)\times10^{-2}w)$
Straty[107]	1974	61	59	100–300	1.7–35	$(0.5-2)\times10^{-3}w$
Straty[108]	1975	24	20	210–300	1.8–18	$5\times10^{-3}w$
Gammon & Douslin[80]	1976	197	173	113–323	0.1–24	$(0.1-10)\times10^{-3}w$
Baidakov *et al.*[185]	1982	119	119	150–183	1–4	$((1-3)\times10^{-3}w)$
Kortbeek *et al.*[68,186]	1986	130	–	148–298	100–1000	$(5\times10^{-3}w)$
Sivaraman & Gammon[6]	1986	95	91	193–423	1.4–27.5	$((0.1-10)\times10^{-3}w)$
Goodwin[187]	1988	108	108	250–350	0.2–7	$(1\times10^{-4}w)$
Lemming[151]	1989	62	62	230–350	0.1–0.5	$1\times10^{-4}w$
Kortbeek & Schouten[118]	1989	155	155	148–298	100–1000	$((1-5)\times10^{-3}w)$

[a] Uncertainty values given in brackets were estimated by ourselves.

TABLE 25. Ideal gas heat capacity values for methane

Source	Year	Number of data	Temperature range T/K
McDowell & Kruse[188]	1963	65[a]	60–5000
Bahro[189]	1965	17[a]	200–1000
Glushko[190]	1979	61[a]	100–6000
TRC-Tables[191]	1982	18[a]	50–1500
TRC-Tables[191a]	1987	54[a]	100–675
Goodwin[187]	1989	4[b]	255–350
Lemming[151]	1989	7[b]	232–350

[a] These data were calculated on the basis of spectroscopic data.
[b] Derived from speed of sound measurements.

Angus *et al.*,[1] it is not possible to give an exact value for the difference between the crystalline solid at zero temperature, which might be the third reference state, and the ideal gas at 298.15 K.

3. Auxiliary Equations for Methane

New correlation equations for liquid-vapor and solid-liquid coexistence properties, consistent with the ITS–90, have been developed. To obtain very effective equations for these properties, their functional structure was optimized using our new optimization procedure.[18] A brief description of the strategy for the development of effective correlation equations is given in Sec. 4.

It is to be pointed out that the correlation equations for the densities of the saturated liquid and vapor, Eq. (3.4) and (3.5), replace the corresponding equations given in Ref. 2 whereas the new vapor pressure equation (3.2) is only a conversion to the ITS–90; for details see the next subsections.

3.1. The Vapor Pressure Equation

The first step when establishing the new vapor pressure equation was to formulate a comprehensive bank of terms from which the optimization procedure selects the most effective combination of terms for the representation of the data set. For this purpose, the following general bank of terms has proven to be very effective:[192–197]

$$\ln(p_s/p_c) = (T_c/T) \sum_{i=1}^{21} n_i (1-T/T_c)^{i/2}, \qquad (3.1)$$

where p_s is the vapor pressure, T is the temperature and p_c and T_c are the critical temperature and pressure, respectively. This general functional form was used to represent the vapor pressure data of Kleinrahm and Wagner[2] as discussed in Sec. 2.2.4.1. As a result of applying the optimization procedure,[18] the final vapor pressure equation for methane has the following form:

$$\ln(p_s/p_c) = (T_c/T) [n_1\vartheta + n_2\vartheta^{1.5} + n_3\vartheta^2 + n_4\vartheta^{4.5}] \qquad (3.2)$$

with $\vartheta = (1-T/T_c)$, $T_c = 190.564$ K and $p_c = 4.5992$ MPa. The coefficients for this vapor pressure equation corresponding to the ITS–90 temperature scale are given in Table 26. A comparison of this equation with the vapor pressure data of Kleinrahm and Wagner[2] is given in Fig. 1 and with the vapor pressures calculated from the new fundamental equation, Eq. (5.3), is given in the upper diagram of Fig. 13. This simple four-coefficient equation represents the data along the whole saturation curve from the triple point temperature to the critical temperature without any systematic deviation. Eq. (3.2) was constrained to pass through the triple and the normal boiling point defined by Eqs. (2.1) and (2.2). Eq. (3.2) corresponds to the vapor pressure equation given in Ref. 2 which is, however, in the IPTS–68 temperature scale.

3.2. The Saturated Liquid Density Equation

To determine the equation for the saturated liquid density ρ', the following functional form was investigated:

$$\ln(\rho'/\rho_c) = \sum_{i=1}^{10} n_i (1-T/T_c)^{0.35+i/1000} + \sum_{j=1}^{60} n_j (1-T/T_c)^{j/6}, \qquad (3.3)$$

where ρ_c is the critical density. The most effective combination of terms out of the 70 terms of Eq. (3.3) has been determined using our new optimization procedure.[18] The equation for the representation of the selected liquid density data has the following form:

$$\ln(\rho'/\rho_c) = n_1\vartheta^{0.354} + n_2\vartheta^{1/2} + n_3\vartheta^{5/2} \qquad (3.4)$$

with $\vartheta = (1-T/T_c)$, $T_c = 190.564$ K and $\rho_c = 162.66$ kg/m^3. The coefficients for the saturated liquid density equation are given in Table 26. Figure 2 shows the very good representation of the selected experimental densities by Eq. (3.4) although the equation contains only three terms; see also the middle diagram of Fig. 13. Eq. (3.4) has a different form in comparison with the corresponding equation in Ref. 2 which consists of four terms. The reason why we could reduce the number of terms and maintain the same quality of representing the data was due to the inclusion of the exponent 0.354 instead of 1/3.

If we had used in Eq. (3.4) a value of the exponent 0.325 corresponding to the 3-dimensional Ising model instead of 0.354, the quality in representing the experimental saturated liquid densities in the critical region would have been much worse.

3.3. The Saturated Vapor Density Equation

When the new optimization procedure was applied to Eq. (3.3) in connection with the selected saturated vapor densities ρ'' (see Sec. 2.2.4.3.), we have found the following equation to be best:

$$\ln(\rho''/\rho_c) = n_1\vartheta^{0.354} + n_2\vartheta^{5/6} + n_3\vartheta^{3/2} + n_4\vartheta^{5/2} + n_5\vartheta^{25/6} + n_6\vartheta^{47/6} \qquad (3.5)$$

with $\vartheta = (1-T/T_c)$, $T_c = 190.564$ K and $\rho_c = 162.66$ kg/m^3; the coefficients n_i are listed in Table 26. Figure 4

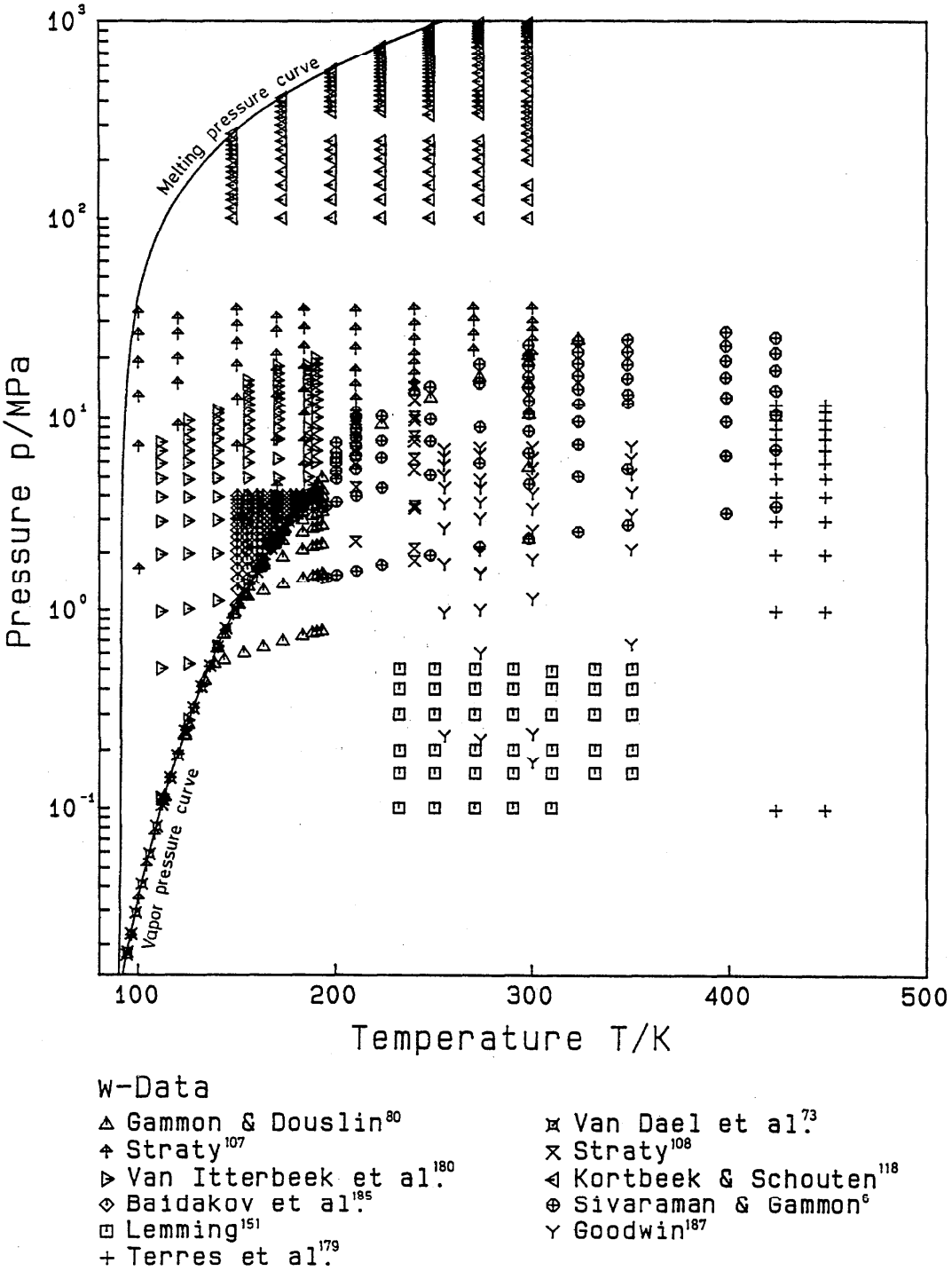

FIG. 10. Distribution of the speed of sound data used in the establishment of the residual part of the fundamental equation, Eq. (5.3), in a pT diagram.

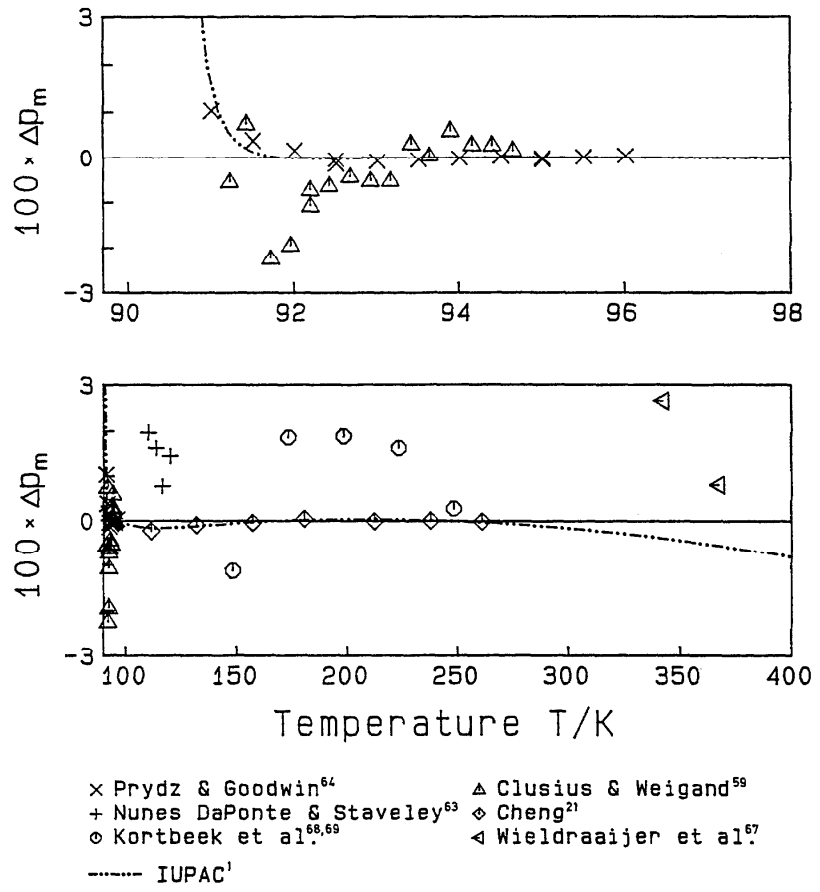

FIG. 11. Percentage deviation $\Delta p_m = (p_{m,expt} - p_{m,calc})/p_{m,expt}$ of experimental melting pressure data from values calculated from the melting pressure equation, Eq. (3.7). For the experimental uncertainties see Table 6.

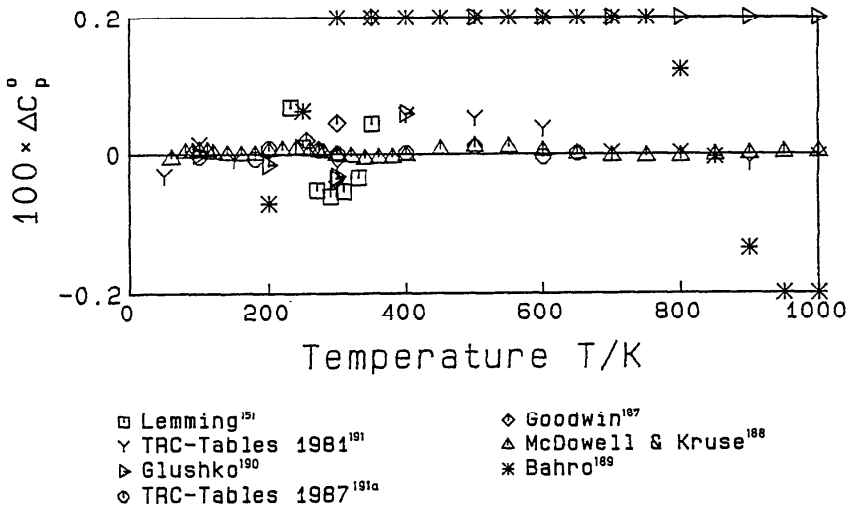

FIG. 12. Percentage deviation $\Delta c_p^\circ = (c_{p,expt}^\circ - c_{p,calc}^\circ)/c_{p,expt}^\circ$ of experimental ideal gas isobaric heat capacity data from values calculated from the ideal gas heat capacity equation, Eq. (3.8). All data with deviations of more than ± 0.2% are plotted on the limit of the deviation scale.

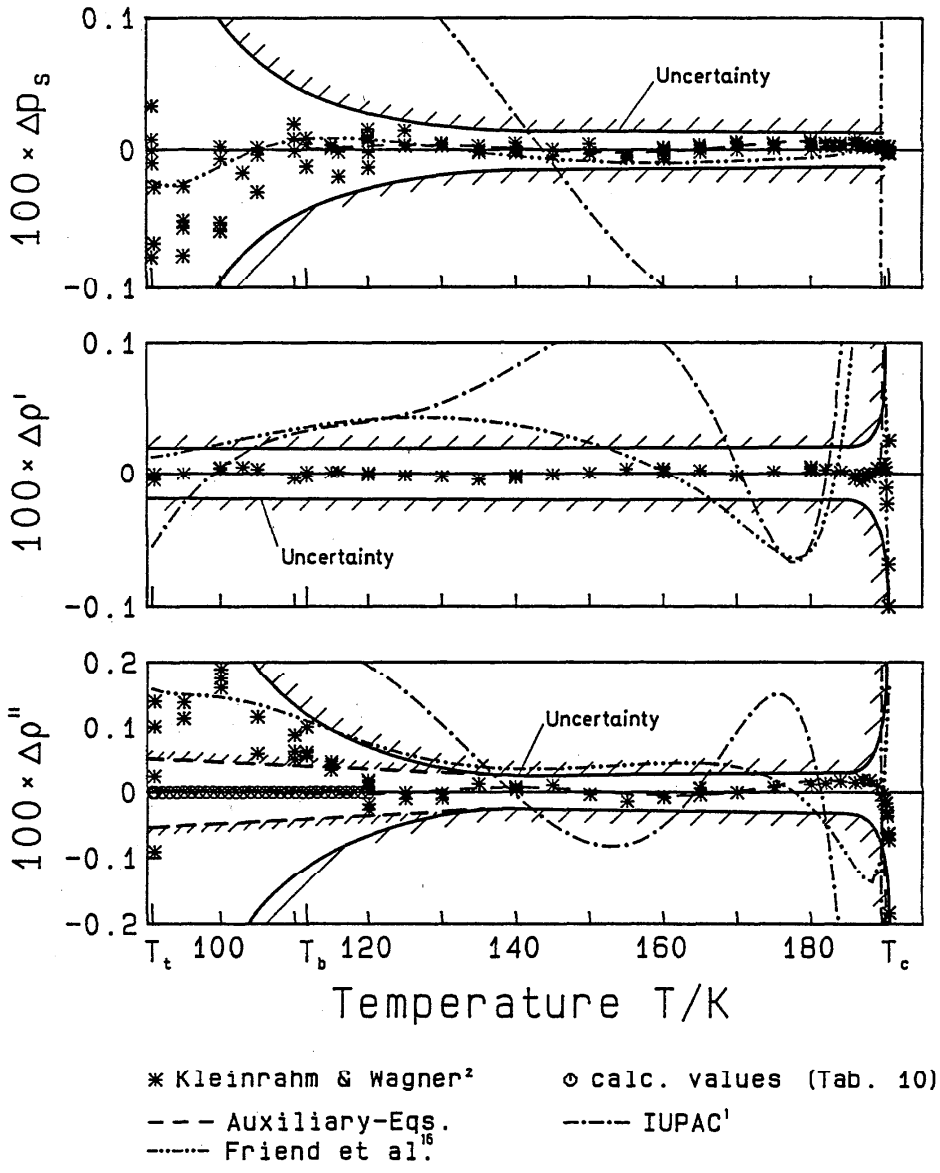

FIG. 13. Percentage deviation $\Delta y = (y_{expt} - y_{calc})/y_{expt}$ ($y = p_s$, ρ', ρ'') of experimental data on the vapor-liquid saturation line from values calculated from Eq. (5.3). The uncertainty range plotted by solid lines corresponds to the original values of Kleinrahm and Wagner.[2] The uncertainty range plotted by dotted lines corresponds to the uncertainties estimated for the calculated values of Table 10. The values calculated from the auxiliary equations [Eqs. (3.2), (3.4), and (3.5)] are plotted by dotted lines which are very close to the zero line.

shows that Eq. (3.5) represents the selected experimental density data for temperatures above 120 K within their very small scatter; see also the lowest diagram of Fig. 13. At temperatures below 120 K, the saturated vapor densities calculated from the new equation of state, Eq. (5.3), are represented within 0.005% by Eq. (3.5). Eq. (3.5) has a different form in comparison with the corresponding equation in Ref. 2 because the data set used to fit the new ρ'' equation was different for $T \leq 120$ K; see the discussion in Sec. 2.2.4.3.

TABLE 26. Coefficients of the auxiliary equations for the thermal properties p_s, ρ', and ρ'' along the vapor-liquid coexistence curve of methane

Vapor pressure equation (3.2)	
T_c = 190.564 K	p_c = 4.5992 MPa
n_1 = −6.036219	n_2 = 1.409353
n_3 = −0.4945199	n_4 = −1.443048
Saturated liquid density equation (3.4)	
T_c = 190.564 K	ρ_c = 162.66 kg/m³
n_1 = 1.9906389	n_2 = −0.78756197
n_3 = 0.036976723	
Saturated vapor density equation (3.5)	
T_c = 190.564 K	ρ_c = 162.66 kg/m³
n_1 = −1.8802840	n_2 = −2.8526531
n_3 = −3.0006480	n_4 = −5.2511690
n_5 = −13.191859	n_6 = −37.553961

3.4. The Melting Pressure Equation

A melting pressure equation has been developed to identify the properties of the coexisting liquid and solid phase. The following bank of terms, based on a functional form proposed by Simon, was investigated:

$$p_m/p_t = 1 + \sum_{i=1}^{40} n_i [(T/T_t)^{1+i/20} - 1], \quad (3.6)$$

where p_t is the triple point pressure and T_t is the triple point temperature. As a result of applying the optimization procedure,[18] the final melting pressure equation for methane is as follows:

$$p_m/p_t = 1 + n_1[(T/T_t)^{1.85} - 1] + n_2[(T/T_t)^{2.1} - 1] \quad (3.7)$$

with p_t = 0.011696 MPa, T_t = 90.6941 K, n_1 = 2.47568×10^4 and $n_2 = -7.36602 \times 10^3$. Comparisons of the melting pressures calculated from Eq. (3.7) with selected data and with the melting line equation of the IUPAC[1] are given in Fig. 11. The agreement between Eq. (3.7) and the results of Prydz and Goodwin[64] and of Cheng[21] is within ± 0.2% in pressure, except in the triple point region. Since the IUPAC equation was established based on triple point parameters (p_t = 0.011719 MPa and T_t = 90.6891 K) which differ significantly from the parameters used in this work [Eq. (2.1)], the disagreement between the two equations in the triple point region is not surprising.

3.5. The Equation for the Ideal Gas Heat Capacity

The equation

$$c_p^\circ/R = n_0 + \sum_{i=1}^{5} n_i \frac{(\Theta_i/T)^2 e^{\Theta_i/T}}{(e^{\Theta_i/T} - 1)^2} \quad (3.8)$$

was fitted to the ideal gas isobaric heat capacities of McDowell and Kruse[188] (see Table 25) of which, however, only the 56 data between 60 K and 3000 K were used. The coefficients n_i and values for Θ_i are given in Table 27. In the entire range of validity of Eq. (3.8) from 60 K to 3000 K, the differences between the c_p° data of McDowell and Kruse and the values calculated from this equation do not exceed ± 0.015%. A comparison of c_p° values up to 1000 K is shown in Fig. 12. The data reported by Lemming[151] and Goodwin,[187] which are based on speed of sound measurements, are in close agreement with the data of McDowell and Kruse; the deviations do not exceed ± 0.07%.

TABLE 27. Coefficients for the ideal gas heat capacity equation (3.8)

i	n_i	Θ_i
0	4.0016	–
1	0.008449	648 K
2	4.6942	1957 K
3	3.4865	3895 K
4	1.6572	5705 K
5	1.4115	15080 K

4. Development of the Fundamental Equation for Methane

The new equation of state developed for the representation of the thermodynamic properties of methane is a fundamental equation explicit in the Helmholtz energy. Since the application of optimization procedures and the multi-property-fitting technique used in the development of such fundamental equations was extensively discussed by Setzmann and Wagner[18] as well as by Saul and Wagner[198] in recent papers, we have restricted ourselves here to the main features of our strategy for the development of wide-range equations of state.

4.1. The Helmholtz Function

The fundamental equation is expressed in form of the Helmholtz energy A with the two independent variables, density ρ and temperature T. The dimensionless Helmholtz energy $\Phi = A/(RT)$ is commonly split into a

part depending on the ideal gas behavior Φ° and a part which takes into account the residual fluid behavior Φ^r, namely

$$\Phi(\delta,\tau) = \Phi^\circ(\delta,\tau) + \Phi^r(\delta,\tau), \quad (4.1)$$

where $\delta = \rho/\rho_c$ is the reduced density and $\tau = T_c/T$ is the inverse reduced temperature with ρ_c and T_c as the critical density and temperature, respectively. The equation for $\Phi^\circ(\delta,\tau)$ can be obtained from a correlation equation for the isobaric heat capacity in the ideal gas state.

4.1.1. The Helmholtz Energy for the Ideal Gas

The Helmholtz energy for the ideal gas is given by

$$A^\circ(\rho,T) = h^\circ(T) - RT - Ts^\circ(\rho,T). \quad (4.2)$$

The enthalpy of the ideal gas is a function of temperature only, and the entropy of the ideal gas depends on temperature and density. Both properties can be calculated if an equation for the ideal gas heat capacity c_p° is available. When c_p° is inserted into the expressions for $h^\circ(T)$ and $s^\circ(\rho,T)$ in Eq. (4.2), the following equation for $A^\circ(\rho,T)$ is obtained:

$$A^\circ(\rho,T) = \int_{T_\circ}^{T} c_p^\circ\, dT + h_\circ^\circ - RT - T\int_{T_\circ}^{T} \frac{c_p^\circ - R}{T}\, dT - RT[\ln(\rho/\rho_\circ)] - Ts_\circ^\circ, \quad (4.3)$$

where $\rho_\circ = p_\circ/(RT_\circ)$ is a reference density. Furthermore, arbitrary reference values for the temperature $T_\circ$, the pressure $p_\circ$, the entropy $s_\circ^\circ$, and the enthalpy $h_\circ^\circ$ have to be selected. For our fundamental equation, the reference enthalpy $h_\circ^\circ$ has been taken to be zero at $T_\circ = 298.15$ K, and the reference entropy $s_\circ^\circ$ has been taken to be zero at $T_\circ = 298.15$ K and $p_\circ = 0.101325$ MPa. The final equation for $\Phi^\circ = A^\circ/(RT)$ is given as Eq. (5.2) in Sec. 5.

4.1.2. Fitting and Optimizing the Residual Part of the Fundamental Equation

In this subsection, the procedure to determine the functional form of the residual part of the dimensionless Helmholtz energy $\Phi^r(\delta,\tau,\bar{n})$, where $\bar{n}$ represents the vector of the coefficients to be fitted, is summarized.

The basic tools are the 'multiproperty fit' to determine the coefficients n_i of the vector $\bar{n}$ for a fixed form of $\Phi^r(\delta,\tau,\bar{n})$ and the 'optimization' of the final functional form of the equation for Φ^r.

Since the Helmholtz energy is not accessible to direct measurements, it is necessary to determine the unknown structure and the unknown coefficients n_i of the residual part of the dimensionless Helmholtz energy from properties which are experimentally available. Some examples of relations of the Helmholtz function to different thermodynamic properties are given in Table 28.

During the optimization process for determining the best structure for Φ^r, a lot of different forms of Φ^r equations have to be fitted to the experimental data. Therefore, at first, this fitting process is explained using the general relationship $z = z(x,y)$, where x, y, and z denote general thermodynamic variables. In our case z might be $p, u, h, c_v, \ldots$ and x and y are δ and τ, respectively; see Table 28. This means that we have the experimental data $z_{exp}(x_{exp}, y_{exp})$ and the relationship to any correlation equation for Φ as $z = z(\Phi,\delta,\tau,\bar{n})$; for the example of $c_v = c_v(\delta,\tau)$ the equation $z = z(\Phi,\delta,\tau,\bar{n})$ corresponds to the sixth equation in Table 28 with $\Phi = \Phi^\circ + \Phi^r$ according to Eq. (4.1). With a known expression for $\Phi^\circ(\delta,\tau)$, see Eq. (5.2), $\Phi^r(\delta,\tau,\bar{n})$ is fitted to the experimental data in such a way that the weighted sum of squares

$$\chi_j^2 = \sum_{m=1}^{M_j} \left[\frac{[z_{exp} - z(\Phi, x_{exp}, y_{exp}, \bar{n})]^2}{\sigma_{exp}^2}\right]_{j,m} = \sum_{m=1}^{M_j} \frac{\Delta z_{j,m}^2}{\sigma_{j,m}^2} \quad (4.4)$$

is minimized, the index j denotes one particular property that is being considered. In Eq. (4.4), the weighting factor corresponds to $1/\sigma_j^2$ with σ as the total uncertainty of the experimental data according to the Gaussian error propagation formula given in this case by

$$\sigma_{j,m}^2 = \left[\left[\frac{\partial \Delta z}{\partial x}\right]_{y,z}^2 \sigma_x^2 + \left[\frac{\partial \Delta z}{\partial y}\right]_{x,z}^2 \sigma_y^2 + \left[\frac{\partial \Delta z}{\partial z}\right]_{x,y}^2 \sigma_z^2\right]_{j,m}, \quad (4.5)$$

where σ_x, σ_y, and σ_z are the uncertainties with respect to the single variable x,y, and z; the partial derivatives $(\partial \Delta z/\partial x)_{y,z}$, ... can be calculated from a preliminary equation of state. When Φ^r is fitted to more than one property, it is called a simultanious or multiproperty fit and the resulting sum of squares

$$\chi^2 = \sum_{j=1}^{J} \chi_j^2 \quad (4.6)$$

is to be minimized. Table 29 lists the different expressions for the sum of squares χ_j^2 corresponding to the single properties; for details see below.

The structures of most of the existing correlations for the residual part Φ^r of the Helmholtz energy have been determined subjectively based on the experience of the correlator or by trial and error. To improve this situation, Wagner and co-workers developed different optimization strategies.[18,192,193,200,201] For the optimization of formulations describing two-dimensional problems like vapor pressure equations, Wagner[192,193] developed a special version of a stepwise regression analysis, which has been adapted by de Reuck and Armstrong[199] for the development of equations of state. Based on the knowledge that the regression analysis does not provide sufficient variability to optimize complex problems like the determination of wide-range fundamental equations of state, Ewers and Wagner[200,201] developed the evolutionary optimization method (EOM), a random search strategy which uses some principles from biological evolution. The optimization method used in this work has recently been developed by Setzmann and Wagner.[18] This new method

combines both the reliability of the EOM and the high speed of convergence of the regression analysis of Wagner.

The development of the functional form for $\Phi^r(\delta,\tau)$ is split into three steps.

The first step is the formulation of a general expression for the equation which functions as a 'bank of terms'. For methane, this bank of terms of the residual part of the dimensionless Helmholtz energy was formulated as

$$\begin{aligned}\Phi^r = &\sum_{i=1}^{10}\sum_{j=-1}^{9} n_i\,\delta^i\,\tau^{j/2} + e^{-\delta}\sum_{i=1}^{6}\sum_{j=0}^{5} n_i\,\delta^i\,\tau^j \\ &+ e^{-\delta^2}\sum_{i=1}^{7}\sum_{j=0}^{10} n_i\,\delta^i\,\tau^j + e^{-\delta^3}\sum_{i=1}^{8}\sum_{j=0}^{6} n_i\,\delta^i\,\tau^{2j} \\ &+ e^{-\delta^4}\sum_{i=1}^{6}\sum_{j=5}^{11} n_i\,\delta^i\,\tau^{2j} + e^{-\delta^5}\sum_{i=1}^{3}\sum_{j=7}^{13} n_i\,\delta^i\,\tau^j \\ &+ (e^{-0.4\delta^6} - e^{-2\delta^6})\sum_{i=3}^{6}\sum_{j=10}^{15} n_i\,\delta^i\,\tau^{2j} \\ &+ \sum_{i=1}^{27} n_i\,\delta^{d_i}\,\tau^{t_i}\,e^{-\alpha_i(\delta-\Delta_i)^2-\beta_i(\tau-\gamma_i)^2}. \qquad (4.7)\end{aligned}$$

The last sum of Eq. (4.7), a two-dimensional Gaussian curve in combination with a polynomial of δ and τ, was introduced to improve the behavior of the equation in the vicinity of the critical point. The parameters d_i, t_i, α_i, β_i, Δ_i and γ_i of these terms are given in Table 30. The values for the parameters β_i and γ_i differ substantially from values used by other correlators.[200-202]

In the second step, after selecting a suitable bank of terms, we used our new optimization strategy,[18] which is based on a mathematical and statistical analysis, to determine the most effective equation for Φ^r. This equation consists of the particular combination of the 393 terms of Eq. (4.7) which yields the best representation of selected data discussed in Sec. 2.

In the entire optimization process different forms of equations $\Phi^r = \Phi^r(\delta,\tau,\bar{n})$ were fitted to the experimental data of different kinds of thermodynamic properties by minimizing χ^2 according to Eqs. (4.4) and (4.6). The problem of simultaneously minimizing the sum of squares of

TABLE 28. Relations of thermodynamic properties to the dimensionless Helmholtz function Φ consisting of Φ^o and Φ^r, see Eq. (4.1)

Property		Relation[a]
Pressure	$\frac{p(\delta,\tau)}{\rho RT}$	$= 1 + \delta\Phi^r_\delta$
Internal energy	$\frac{u(\delta,\tau)}{RT}$	$= \tau(\Phi^o_\tau + \Phi^r_\tau)$
Enthalpy	$\frac{h(\delta,\tau)}{RT}$	$= 1 + \tau(\Phi^o_\tau + \Phi^r_\tau) + \delta\Phi^r_\delta$
Entropy	$\frac{s(\delta,\tau)}{R}$	$= \tau(\Phi^o_\tau + \Phi^r_\tau) - \Phi^o - \Phi^r$
Gibbs energy	$\frac{g(\delta,\tau)}{RT}$	$= 1 + \delta\Phi^r_\delta + \Phi^o + \Phi^r$
Isochoric heat capacity	$\frac{c_v(\delta,\tau)}{R}$	$= -\tau^2(\Phi^o_{\tau\tau} + \Phi^r_{\tau\tau})$
Isobaric heat capacity	$\frac{c_p(\delta,\tau)}{R}$	$= -\tau^2(\Phi^o_{\tau\tau} + \Phi^r_{\tau\tau}) + \frac{(1+\delta\Phi^r_\delta - \delta\tau\Phi^r_{\delta\tau})^2}{1+2\delta\Phi^r_\delta + \delta^2\Phi^r_{\delta\delta}}$
Saturated liquid heat capacity	$\frac{c_\sigma(\tau)}{R}$	$= -\tau^2(\Phi^o_{\tau\tau} + \Phi^r_{\tau\tau}) + \frac{1 + \delta'\Phi^r_\delta - \delta'\tau\Phi^r_{\delta\tau}}{1 + 2\delta'\Phi^r_\delta - \delta'^2\Phi^r_{\delta\delta}} \cdot\left[(1 + \delta'\Phi^r_\delta - \delta'\tau\Phi^r_{\delta\tau}) - \frac{1}{R\rho'}\frac{dp_s}{dT}\right]$
Speed of sound	$\frac{w^2(\delta,\tau)}{RT}$	$= 1 + 2\delta\Phi^r_\delta + \delta^2\Phi^r_{\delta\delta} - \frac{(1+\delta\Phi^r_\delta - \delta\tau\Phi^r_{\delta\tau})^2}{\tau^2(\Phi^o_{\tau\tau} + \Phi^r_{\tau\tau})}$
Joule-Thomson coefficient	$\mu(\delta,\tau)R\rho$	$= \frac{-(\delta\Phi^r_\delta + \delta^2\Phi^r_{\delta\delta} + \delta\tau\Phi^r_{\delta\tau})}{(1+\delta\Phi^r_\delta - \delta\tau\Phi^r_{\delta\tau})^2 - \tau^2(\Phi^o_{\tau\tau} + \Phi^r_{\tau\tau})(1+2\delta\Phi^r_\delta + \delta^2\Phi^r_{\delta\delta})}$
Isothermal throttling coefficient	$\delta_T(\delta,\tau)\rho$	$= 1 - \frac{1+\delta\Phi^r_\delta - \delta\tau\Phi^r_{\delta\tau}}{1+2\delta\Phi^r_\delta + \delta^2\Phi^r_{\delta\delta}}$
Second virial coefficient	$B(\tau)\rho_c$	$= \lim_{\delta\to 0}\Phi^r_\delta(\delta,\tau)$
Third virial coefficient	$C(\tau)\rho_c^2$	$= \lim_{\delta\to 0}\Phi^r_{\delta\delta}(\delta,\tau)$

[a] $\Phi_\delta = \left[\frac{\partial\Phi}{\partial\delta}\right]_\tau$, $\Phi_{\delta\delta} = \left[\frac{\partial^2\Phi}{\partial\delta^2}\right]$, $\Phi_\tau = \left[\frac{\partial\Phi}{\partial\tau}\right]_\delta$, $\Phi_{\tau\tau} = \left[\frac{\partial^2\Phi}{\partial\tau^2}\right]$ and $\Phi_{\delta\tau} = \left[\frac{\partial^2\Phi}{\partial\delta\partial\tau}\right]$.

Table 29. Contributions of properties to the sum of squares for the optimization and fitting process

j	Data (measured)	Data[a] (precalculated)	Data (fitted to)	Sum of squares	
			Linear data		
1	$p(\rho,T)$	–	$p(\rho,T)$	$\chi_1^2 = \sum_{m=1}^{M} \left[\frac{p-\rho RT}{\rho^2 RT} - \rho_c^{-1}\Phi_\delta^r\right]_m^2 \sigma_m^{-2}$	(4.9)
2	$c_v(\rho,T)$	–	$c_v(\rho,T)$	$\chi_2^2 = \sum_{m=1}^{M} \left[\frac{c_v}{R} + \tau^2(\Phi_{\tau\tau}^o + \Phi_{\tau\tau}^r)\right]_m^2 \sigma_m^{-2}$	(4.10)
3	$u_1(\rho_1,T_1)$ $u_2(\rho_2,T_2)$	–	$u_1(\rho_1,T_1)$ $u_2(\rho_2,T_2)$	$\chi_3^2 = \sum_{m=1}^{M} \left[\frac{u_2}{RT_c} - \frac{u_1}{RT_c} - (\Phi_\tau^o+\Phi_\tau^r)_2 + (\Phi_\tau^o+\Phi_\tau^r)_1\right]_m^2 \sigma_m^{-2}$	(4.11)
4	$B(T)$	–	$B(T)$	$\chi_4^2 = \sum_{m=1}^{M} \left[B\rho_c - \Phi_\delta^r\ (\delta\to 0,\tau)\right]_m^2 \sigma_m^{-2}$	(4.12)
			Phase equilibrium condition		
5	$p_s(T_1)$ $\rho'(T_2),\rho''(T_3)$	$p_s(T)$ $\rho'(T),\rho''(T)$	$p_s(\rho',T)$	$\chi_5^2 = \sum_{m=1}^{M} \left[\frac{p_s-\rho' RT}{(\rho')^2 RT} - \rho_c^{-1}\Phi_\delta^r(\delta',\tau)\right]_m^2 \sigma_m^{-2}$	(4.13)
6			$p_s(\rho'',T)$	$\chi_6^2 = \sum_{m=1}^{M} \left[\frac{p_s-\rho'' RT}{(\rho'')^2 RT} - \rho_c^{-1}\Phi_\delta^r(\delta'',\tau)\right]_m^2 \sigma_m^{-2}$	(4.14)
7		Maxwell criterion		$\chi_7^2 = \sum_{m=1}^{M} \left[\frac{p_s}{RT_m}\left[\frac{1}{\rho''} - \frac{1}{\rho'}\right] - \ln\left[\frac{\delta'}{\delta''}\right] - \Phi^r(\delta',\tau) + \Phi^r(\delta'',\tau)\right]_m^2 \sigma_m^{-2}$	(4.15)
			Linearized data		
8	$w(T,p)$ $w'(T)$ $w''(T)$	$\gamma^w = c_p/c_v\ ;\ \rho(T,p)$ $\gamma^w = c_p/c_v\ ;\ \rho'(T,p)$ $\gamma^w = c_p/c_v\ ;\ \rho''(T,p)$	$w(\rho,T)$ $w(\rho')$ $w(\rho'')$	$\chi_8^2 = \sum_{m=1}^{M} \left[\frac{w^2}{RT} - \gamma^w(1 + 2\delta\Phi_\delta^r + \delta^2\Phi_{\delta\delta}^r)\right]_m^2 \sigma_m^{-2}$	(4.16)
9	$c_p(T,p)$	$\zeta^p = \frac{(1+\delta\Phi_\delta^r-\delta\tau\Phi_{\delta\tau}^r)^2}{1+2\delta\Phi_\delta^r+\delta^2\Phi_{\delta\delta}^r};\ \rho(T,p)$	$c_p(\rho,T)$	$\chi_9^2 = \sum_{m=1}^{M} \left[\frac{c_p}{R} - \zeta^p + \tau^2(\Phi_{\tau\tau}^o + \Phi_{\tau\tau}^r)\right]_m^2 \sigma_m^{-2}$	(4.17)
10	$h_1(T_1,p_1)$ $h_2(T_2,p_2)$	$\rho_1(T_1,p_1)\ ;\ \rho_2(T_2,p_2)$	$h_1(\rho_1,T_1)$ $h_2(\rho_2,T_2)$	$\chi_{10}^2 = \sum_{m=1}^{M} \left[\frac{h_2}{RT_c} - \frac{h_1}{RT_c} - \left[\Phi_\tau^o+\Phi_\tau^r+\tau^{-1}(1+\delta\Phi_\delta^r)\right]_2 + \left[\Phi_\tau^o+\Phi_\tau^r+\tau^{-1}(1+\delta\Phi_\delta^r)\right]_1\right]_m^2 \sigma_m^{-2}$	(4.18)
			Nonlinear data[b]		
11	$w(T,p)$ $w'(T)$ $w''(T)$	– $p_s(T)$ $p_s(T)$	$w(T,p)$ $w'(T,p_s)$ $w''(T,p_s)$	$\chi_{11}^2 = \sum_{m=1}^{M} \left[\frac{w^2}{RT} - 1 - 2\delta\Phi_\delta^r - \delta^2\Phi_{\delta\delta}^r + \frac{(1+\delta\Phi_\delta^r-\delta\tau\Phi_{\delta\tau}^r)^2}{\tau^2(\Phi_{\tau\tau}^o+\Phi_{\tau\tau}^r)}\right]_m^2 \sigma_m^{-2}$	(4.19)
12	$c_p(T,p)$	–	$c_p(T,p)$	$\chi_{12}^2 = \sum_{m=1}^{M} \left[\frac{c_p}{R} + \tau^2(\Phi_{\tau\tau}^o+\Phi_{\tau\tau}^r) - \frac{(1+\delta\Phi_\delta^r-\delta\tau\Phi_{\delta\tau}^r)^2}{1+2\delta\Phi_\delta^r+\delta^2\Phi_{\delta\delta}^r}\right]_m^2 \sigma_m^{-2}$	(4.20)
13	$h_1(T_1,p_1)$ $h_2(T_2,p_2)$	–	$h_1(T_1,p_1)$ $h_2(T_2,p_2)$	$\chi_{13}^2 = \sum_{m=1}^{M} \left[\frac{h_2}{RT_c} - \frac{h_1}{RT_c} - \left[\Phi_\tau^o+\Phi_\tau^r+\tau^{-1}(1+\delta\Phi_\delta^r)\right]_2 + \left[\Phi_\tau^o+\Phi_\tau^r+\tau^{-1}(1+\delta\Phi_\delta^r)\right]_1\right]_m^2 \sigma_m^{-2}$	(4.21)

[a]Values which have to be calculated from a preliminary equation of state.
[b]The coupling condition $p = \rho RT(1 + \delta\Phi_\delta^r)$ has to be taken into account.

different thermodynamic properties becomes a problem of solving a system of normal equations with regard to the unknown coefficients n_i. Depending on the properties to which the equation is fitted, the system of equations becomes linear or nonlinear. The optimization procedure of Setzmann and Wagner[18] is, however, restricted to those properties which lead to a system of normal equations that are linear in the coefficients n_i. If the relation $z = z(\Phi,\delta,\tau,\bar{n})$ between any property and the Helmholtz function is a linear combination of Φ^r and/or its derivatives, then the basic requirement for a system of linear equations is met. This is true for the pressure $p(\rho,T)$, the isochoric heat capacity $c_v(\rho,T)$, the internal energy $u(\rho,T)$, the second virial coefficient $B(T)$, and the indirect application of the phase equilibrium condition. However, many thermodynamic properties are measured as a function of pressure p and temperature T and not as a function of density ρ and temperature T which are the independent variables of the Helmholtz function A. This yields an implicit relation between the measured state variables p and T and the independent variables of the Helmholtz function and leads to a system of nonlinear equations for the determination of the coefficients n_i, even if the relation between the property (depending on T and ρ) and the Helmholtz function is linear, e.g. the enthalpy h. Several methods have been proposed which allow for the linearization of certain 'nonlinear' properties [$h(T,p)$, $c_p(T,p)$, $w(T,p)$], so that these linearized data can also be included in an optimization process. This means that the functional structure of the resulting best Φ^r equation was optimized (opt) by minimizing the following sum of squares:

$$\chi^2_{opt} = \sum_{j=1}^{10} \chi^2_j, \tag{4.8}$$

where the definitions of the single χ^2_j (j = 1, 2, ..., 10), corresponding to the linear and linearized data, are given as Eqs. (4.9) to (4.18) in Table 29.

However, to take into account the original experimental information of all selected data (linear and nonlinear data), in the third step, the final determination of the coefficients n_i of the optimized Φ^r equation was performed in a nonlinear fitting process. This nonlinear fit (nl) was realized by minimizing the following sum of squares:

$$\chi^2_{nl} = \sum_{j=1}^{7} \chi^2_j + \sum_{j=11}^{13} \chi^2_j, \tag{4.22}$$

where the relations between the nonlinear weighted sum of squares χ^2_{i1}, χ^2_{i2}, and χ^2_{i3} and the dimensionless Helmholtz energy Φ° and Φ^r are given as Eqs. (4.19) to (4.21) in Table 29. To solve this nonlinear minimization problem, a modified Marquardt method, presented by Fletcher,[203] was used.

Then, the optimized equation with the values of the coefficients n_i obtained from the nonlinear fit [Eq. (4.22)] was used to recalculate the 'precalculated data' (see Table 29) for the fit of the linearized data; see Eqs. (4.16) to (4.18) in Table 29. Based on these new values, the steps 'optimization' by taking into account the linear and linearized data [Eq. (4.8)] and the step 'nonlinear fit' of the optimized equation to the linear and nonlinear data [Eq. (4.22)] were repeated. This entire cycle (optimization, nonlinear fit, recalculation of the 'precalculated data' for the linearized least square sums) was repeated until convergence was achieved. The convergence criterion is met if the values of the nonlinear data calculated from the optimized equation before and after the nonlinear fit have differences which are at least one order of magnitude less than the estimated experimental uncertainties of these data. In this case, the final form of the Φ^r equation is determined.

At this stage we would emphasize that the entire iteration cycle described in the previous paragraph including the 'creation' of linearized data was only carried out to make the nonlinear data available for the linear optimization procedure. Comparisons (see Sec. 6) were always made with respect to the original linear and nonlinear data.

More details on the process of the determination of a fundamental equation of state using optimization procedures and multi-property fitting techniques are given by Saul and Wagner,[198] Setzmann,[26] and Marx;[204] the optimization procedure is described in detail by Setzmann and Wagner.[18]

TABLE 30. Values for the parameters of the modified two-dimensional Gaussian terms in the last sum of Eq. (4.7)

i	d_i	t_i	α_i	β_i	γ_i	Δ_i
1	0	0	20	200	1.07	1
2	0	1	20	200	1.07	1
3	0	2	20	200	1.07	1
4	1	0	20	200	1.07	1
5	1	1	20	200	1.07	1
6	1	2	20	200	1.07	1
7	2	0	20	200	1.07	1
8	2	1	20	200	1.07	1
9	2	2	20	200	1.07	1
10	3	0	20	200	1.07	1
11	3	1	20	200	1.07	1
12	3	2	20	200	1.07	1
13	0	0	30	200	1.13	1
14	0	1	30	200	1.13	1
15	0	2	30	200	1.13	1
16	1	0	30	200	1.13	1
17	1	1	30	200	1.13	1
18	1	2	30	200	1.13	1
19	2	0	30	200	1.13	1
20	2	1	30	200	1.13	1
21	2	2	30	200	1.13	1
22	3	0	30	200	1.13	1
23	3	1	30	200	1.13	1
24	3	2	30	200	1.13	1
25	0	0	40	250	1.11	1
26	0	1	40	250	1.11	1
27	0	2	40	250	1.11	1

4.2. The Data Set for the Optimization and the Fitting Procedure

In this subsection, we will give a survey of the selected data which were used for the optimization process and for the nonlinear fitting of the optimized equation to the experimental data.

To take into account the phase equilibrium condition when fitting a wide-range equation of state to data, we needed a set of vapor pressures p_s, saturated liquid densities ρ', and saturated vapor densities ρ'' in rather narrow temperature steps along the whole saturation curve. Therefore, the required data had to be calculated for temperatures from the triple point to the critical point with the help of independent equations for the vapor pressure and the saturation densities; these correlation equations are given in Sec. 3. Table 31 defines the calculated data set for the phase equilibrium condition, and Table 32 summarizes the experimental data which were used for the determination of the new fundamental equation.

TABLE 31. Calculated p_s, ρ', and ρ'' data for taking into account the phase equilibrium condition when developing the residual part Φ^r of the fundamental equation, Eq. (5.3)

Number of data	Temperature range	Step width
9	$90.6941 \leq T \leq 94.6941$	0.5 K
86	$95.1941 \leq T \leq 180.1941$	1 K
20	$180.6941 \leq T \leq 190.1941$	0.5 K
36	$190.2041 \leq T \leq 190.5541$	0.01 K

TABLE 32. Summary of the data used for the linear optimization procedure and for the nonlinear fit

Data	Sum of squares according to	Details of the data set are given in table	Number of data optimizing	fitting nonlinearly
p,ρ,T	Eq. (4.9)	16	2891	2891
B,T	Eq. (4.12)	18	39	39
p_s,ρ',T	Eq. (4.13)	31	151	151
p_s,ρ'',T	Eq. (4.14)	31	151	151
p_s,ρ',ρ'',T	Eq. (4.15)	31	151	151
c_v,ρ,T	Eq. (4.10)	22	310	310
$c_p,\rho,[p,T]$	Eq. (4.17)	21	437	–
c_p,p,T	Eq. (4.20)	21	–	437
w',ρ,γ^w,T	Eq. (4.16)	14	74	–
w'',ρ,γ^w,T	Eq. (4.16)	14	16	–
w,ρ,γ^w,T	Eq. (4.16)	24	905	–
w',p_s,T	Eq. (4.19)	14	– 74	
w'',p_s,T	Eq. (4.19)	14	– 16	
w,p,T	Eq. (4.19)	24	–	905
h_1,ρ_1,T_1 h_2,ρ_2,T_2	Eq. (4.18)	20	79	–
h_1,p_1,T_1 h_2,p_2,T_2	Eq. (4.21)	20	–	79

5. The New Fundamental Equation

As discussed in Sec. 4.1, the fundamental equation is expressed with the dimensionless Helmholtz energy $\Phi = A/(RT)$ as the ideal gas part and the residual part:

$$A(\delta,\tau)/(RT) = \Phi(\delta,\tau) = \Phi^\circ(\delta,\tau) + \Phi^r(\delta,\tau) \quad (5.1)$$

with $\delta = \rho/\rho_c$ and $\tau = T_c/T$; see also Eq. (4.1).

The ideal gas part of the Helmholtz function was obtained according to Eq. (4.3) when the c_p° equation given in Sec. 3.5 is used:

$$\Phi^\circ(\delta,\tau) = \ln(\delta) + a_1 + a_2\tau + a_3 \ln(\tau) + \sum_{i=4}^{8} a_i \ln(1 - e^{-\Theta_i^c \tau}), \quad (5.2)$$

where $\delta = \rho/\rho_c$, $\tau = T_c/T$, $T_c = 190.564$ K, and $\rho_c = 162.66$ kg/m^3. The values of the coefficients a_i and $\Theta_i^c = \Theta_i/T_c$ are given in Table 33. Equation (5.2) is valid in the temperature region 60 K $\leq T \leq$ 3000 K. The constants a_1 and a_2 were adjusted to give zero for the ideal gas enthalpy at $T_\circ = 298.15$ K and for the ideal gas entropy at $T_\circ = 298.15$ K and $p_\circ = 0.101325$ MPa. In Table 34, all required derivatives of the ideal gas part Φ° with respect to δ and τ are explicitly given.

TABLE 33. Numerical values of the coeffients of the ideal gas part of the dimensionless Helmholtz function, Eq.(5.2)

i	a_i	Θ_i^c	i	a_i	Θ_i^c
1	9.91243972	–	5	4.6942	10.26951575
2	−6.33270087	–	6	3.4865	20.43932747
3	3.0016	–	7	1.6572	29.93744884
4	0.008449	3.40043240	8	1.4115	79.13351945

Based on the bank of terms defined by Eq. (4.7) and the selected data (see Tables 31 and 32), the following residual part of the dimensionless Helmholtz function $\Phi^r = A^r(\delta,\tau)/(RT)$ was determined with the help of the procedure described in Sec. 4.1.2:

$$\Phi^r = \sum_{i=1}^{13} n_i \delta^{d_i} \tau^{t_i} + \sum_{i=14}^{36} n_i \delta^{d_i} \tau^{t_i} e^{-\delta^{c_i}} + \sum_{i=37}^{40} n_i \delta^{d_i} \tau^{t_i} e^{-\alpha_i(\delta-\Delta_i)^2 - \beta_i(\tau-\gamma_i)^2}, \quad (5.3)$$

where $\delta = \rho/\rho_c$ and $\tau = T_c/T$. The coefficients and the parameters of this equation of state are listed in Table 35. The entire Helmholtz equation, Eqs. (5.1) to (5.3), has been developed on the basis of data which cover the region

$$90.6941 \text{ K} \leq T < 625 \text{ K}$$

$$0.011696 \text{ MPa} \leq p \leq 1000 \text{ MPa (or melting pressure)}.$$

TABLE 34. The ideal gas part of the dimensionless Helmholtz energy Φ° and its derivatives

Φ°	=	$\ln\delta$	+	a_1	+	$a_2\tau$	+	$a_3\ln(\tau)$	+	$\sum_{i=4}^{8} a_i \ln(1 - e^{-\Theta_i^c \tau})$
Φ°_δ	=	$1/\delta$	+	0	+	0	+	0	+	0
$\Phi^\circ_{\delta\delta}$	=	$-1/\delta^2$	+	0	+	0	+	0	+	0
$\Phi^\circ_{\delta\tau}$	=	0	+	0	+	0	+	0	+	0
Φ°_τ	=	0	+	0	+	a_2	+	a_3/τ	+	$\sum_{i=4}^{8} a_i\Theta_i^c \left[\left[1 - e^{-\Theta_i^c \tau}\right]^{-1} - 1\right]$
$\Phi^\circ_{\tau\tau}$	=	0	+	0	+	0	−	a_3/τ^2	−	$\sum_{i=4}^{8} a_i(\Theta_i^c)^2 \, e^{-\Theta_i^c \tau}\left[1 - e^{-\Theta_i^c \tau}\right]^{-2}$

TABLE 35. Coefficients and exponents of Eq. (5.3)

i	c_i	n_i	d_i	t_i
1		$0.4367901028\times10^{-1}$	1	−0.5
2		0.6709236199	1	0.5
3		$-0.1765577859\times10^{1}$	1	1.0
4		0.8582330241	2	0.5
5		$-0.1206513052\times10^{1}$	2	1.0
6		0.5120467220	2	1.5
7		$-0.4000010791\times10^{-3}$	2	4.5
8		$-0.1247842423\times10^{-1}$	3	0.0
9		$0.3100269701\times10^{-1}$	4	1.0
10		$0.1754748522\times10^{-2}$	4	3.0
11		$-0.3171921605\times10^{-5}$	8	1.0
12		$-0.2240346840\times10^{-5}$	9	3.0
13		$0.2947056156\times10^{-6}$	10	3.0
14	1	0.1830487909	1	0.0
15	1	0.1511883679	1	1.0
16	1	−0.4289363877	1	2.0
17	1	$0.6894002446\times10^{-1}$	2	0.0
18	1	$-0.1408313996\times10^{-1}$	4	0.0
19	1	$-0.3063054830\times10^{-1}$	5	2.0
20	1	$-0.2969906708\times10^{-1}$	6	2.0
21	2	$-0.1932040831\times10^{-1}$	1	5.0
22	2	−0.1105739959	2	5.0
23	2	$0.9952548995\times10^{-1}$	3	5.0
24	2	$0.8548437825\times10^{-2}$	4	2.0
25	2	$-0.6150555662\times10^{-1}$	4	4.0
26	3	$-0.4291792423\times10^{-1}$	3	12.0
27	3	$-0.1813207290\times10^{-1}$	5	8.0
28	3	$0.3445904760\times10^{-1}$	5	10.0
29	3	$-0.2385919450\times10^{-2}$	8	10.0
30	4	$-0.1159094939\times10^{-1}$	2	10.0
31	4	$0.6641693602\times10^{-1}$	3	14.0
32	4	$-0.2371549590\times10^{-1}$	4	12.0
33	4	$-0.3961624905\times10^{-1}$	4	18.0
34	4	$-0.1387292044\times10^{-1}$	4	22.0
35	4	$0.3389489599\times10^{-1}$	5	18.0
36	4	$-0.2927378753\times10^{-2}$	6	14.0

i	n_i	d_i	t_i	α_i	β_i	γ_i	Δ_i
37	$0.9324799946\times10^{-4}$	2	2.0	20	200	1.07	1
38	$-0.6287171518\times10^{1}$	0	0.0	40	250	1.11	1
39	0.1271069467×10^{2}	0	1.0	40	250	1.11	1
40	$-0.6423953466\times10^{1}$	0	2.0	40	250	1.11	1

T_c = 190.564 K ρ_c = 162.66 kg/m³ R = 0.5182705 kJ/(kg K)

In this entire region, the new fundamental equation, Eq. (5.1), represents the selected data within the estimated experimental uncertainties.

Equation (5.3) has been constrained to the critical parameters given in Eq. (2.3) (T_c = 190.564 K, p_c = 4.5992 MPa, ρ_c = 162.66 kg/m³) and to the first and second partial derivative of pressure with respect to density being zero at the critical point. In Table 36 all required derivatives of the residual part Φ^r of the dimensionless Helmholtz function with respect to δ and τ are explicitly given.

6. Comparisons of the New Fundamental Equation with Experimental Data and Other Equations of State

In the following subsections, the quality of the new fundamental equation is discussed based on comparisons with experimental data. Most figures also show comparisons with the IUPAC equation of state,[1] the correlation published by Friend *et al.*,[16] and, especially in the enlarged critical region, with the revised and extended scaling law equation of Kurumov *et al.*[15] To avoid exceptionally long discussions, the comparisons given below are representative rather than exhaustive; a more detailed discussion can be found in Ref. 26, where, however, both the equation and the comparisons are based on the IPTS–68 temperature scale.

In all deviation plots, the zero-line represents our new fundamental equation. For caloric properties, the entire fundamental equation, Eq. (5.1), is necessary but for thermal properties only Eq. (5.3) is needed because the ideal gas part for the thermal properties is already incorporated in the corresponding relations between the single properties and the dimensionless Helmholtz energy Φ consisting of Φ° and Φ^r; see Table 28. The new equation and the data presented in the figures below correspond to the new temperature scale ITS–90. To compare our equation with those equations corresponding to the IPTS–68, we first converted the ITS–90 temperatures, used in the figures, into IPTS–68 values. This conversion

Table 36. The residual part Φ^r of the dimensionless Helmholtz energy and its derivatives

$$\Phi^r = \sum_{i=1}^{13} n_i \delta^{d_i}\tau^{t_i} + \sum_{i=14}^{36} e^{-\delta^{c_i}} n_i \delta^{d_i}\tau^{t_i} + \sum_{i=37}^{40} n_i \delta^{d_i}\tau^{t_i}\, e^{-\alpha_i(\delta-\Delta_i)^2-\beta_i(\tau-\gamma_i)^2}$$

$$\Phi^r_\delta = \sum_{i=1}^{13} n_i d_i \delta^{d_i-1}\tau^{t_i} + \sum_{i=14}^{36} e^{-\delta^{c_i}}[n_i\tau^{t_i}\delta^{d_i-1}(d_i - c_i\delta^{c_i})] + \sum_{i=37}^{40} n_i\delta^{d_i}\tau^{t_i} e^{-\alpha_i(\delta-\Delta_i)^2-\beta_i(\tau-\gamma_i)^2}[d_i/\delta - 2\alpha_i(\delta-\Delta_i)]$$

$$\Phi^r_{\delta\delta} = \sum_{i=1}^{13} n_i d_i(d_i-1)\delta^{d_i-2}\tau^{t_i} + \sum_{i=14}^{36} e^{-\delta^{c_i}}[n_i\tau^{t_i}\delta^{d_i-2}((d_i - c_i\delta^{c_i})(d_i - 1 - c_i\delta^{c_i}) - c_i^2\delta^{c_i})]$$
$$+ \sum_{i=37}^{40} n_i\tau^{t_i} e^{-\alpha_i(\delta-\Delta_i)^2-\beta_i(\tau-\gamma_i)^2}[-2\alpha_i\delta^{d_i} + 4\alpha_i^2\delta^{d_i}(\delta-\Delta_i)^2 - 4d_i\alpha_i\delta^{d_i-1}(\delta-\Delta_i) + d_i(d_i-1)\delta^{d_i-2}]$$

$$\Phi^r_\tau = \sum_{i=1}^{13} n_i t_i \delta^{d_i}\tau^{t_i-1} + \sum_{i=14}^{36} n_i e^{-\delta^{c_i}}\delta^{d_i} t_i\tau^{t_i-1} + \sum_{i=37}^{40} n_i\delta^{d_i}\tau^{t_i} e^{-\alpha_i(\delta-\Delta_i)^2-\beta_i(\tau-\gamma_i)^2}[t_i/\tau - 2\beta_i(\tau-\gamma_i)]$$

$$\Phi^r_{\tau\tau} = \sum_{i=1}^{13} n_i\,\delta^{d_i} t_i(t_i-1)\tau^{t_i-2} + \sum_{i=14}^{36} n_i e^{-\delta^{c_i}}\delta^{d_i} t_i(t_i-1)\tau^{t_i-2}$$
$$+ \sum_{i=37}^{40} n_i\delta^{d_i}\tau^{t_i} e^{-\alpha_i(\delta-\Delta_i)^2-\beta_i(\tau-\gamma_i)^2}[[t_i/\tau - \beta_i(\tau-\gamma_i)]^2 - t_i/\tau^2 - 2\beta_i]$$

$$\Phi^r_{\delta\tau} = \sum_{i=1}^{13} n_i d_i \delta^{d_i-1} t_i\tau^{t_i-1} + \sum_{i=14}^{36} n_i e^{-\delta^{c_i}} t_i\tau^{t_i-1}\delta^{d_i-1}(d_i - c_i\delta^{c_i})$$
$$+ \sum_{i=37}^{40} n_i\delta^{d_i}\tau^{t_i} e^{-\alpha_i(\delta-\Delta_i)^2-\beta_i(\tau-\gamma_i)^2}[d_i/\delta - 2\alpha_i(\delta-\Delta_i)][t_i/\tau - 2\beta_i(\tau-\gamma_i)]$$

from ITS–90 to IPTS–68 was carried out with the equation given in Table 1.6 of Ref. 24[a] which we also used to convert any IPTS–68 temperature of the experimental data to ITS–90; see the introduction to Sec. 2. In most regions, with the exception of the critical region, it is not at all necessary to apply the conversion procedure because the differences are so small that they are not recognizable in the figures.

6.1. Liquid-Vapor Boundary

6.1.1. Thermal Properties on the Coexistence Curve

Figure 13 shows the deviations between experimental and calculated values with respect to the vapor pressure, to the saturated liquid and saturated vapor density. For a given temperature the equation of state yields these properties when the phase equilibrium condition

$$T' = T'', \; p' = p'', \text{ and } g' = g'', \qquad (6.1)$$

is applied, which means that it is not necessary to use any auxiliary equation. The agreement between the new fundamental equation, Eq. (5.3), and the experimental p_s, ρ', and ρ'' data of Kleinrahm and Wagner[2] is excellent. All data points are reproduced within the claimed small uncertainty of the data. Figure 13 demonstrates that neither the IUPAC equation[1] nor the equation of Friend *et al.*,[16] both evaluated by applying the phase equilibrium condition, are able to represent the data within their uncertainty. As was stated in Sec. 2.2.4.3, for temperatures below 120 K the saturated vapor densities had to be calculated by an iterative procedure because the evaluation of the saturated vapor density equation given by Kleinrahm and Wagner[2] yields data which are not consistent with the various thermodynamic properties of the homogeneous gas region. Friend *et al.*[16] probably overfitted their equation to the saturated vapor density data of Kleinrahm and Wagner in the triple point region. Their equation represents these data within ± 0.1% although the uncertainty given in Ref. 2 is between ± 0.3% to ± 0.8% at the triple point temperature.

6.1.2. Speed of Sound on the Coexistence Curve

Figure 14 illustrates the comparison between the experimental data of speeds of sound and heat capacities and the corresponding values calculated from Eq. (5.1). The saturated liquid speed of sound data of van Dael *et al.*,[73] Straty,[107,108] and Gammon and Douslin[80] are in agreement with the speed of sound values calculated from Eq. (5.1) within ± 0.2%, except for the critical region, where the new equation of state fails to reproduce the limiting value $w = 0$ m/s when approaching the critical point; at the critical point Eq. (5.1) yields $w'' = w' = 205.95$ m/s, see also Table 38. Although the data of Straty[108] and Gammon and Douslin[80] agree quite well with each other for saturated liquid speeds of sound, the saturated vapor speed of sound values of these two data sets deviate systematically from each other. Bearing in mind that Gammon and Douslin measured the speed of sound at pressures which were slightly below the vapor pressure at the temperature being considered and taking into account that the pressure dependence of the speed of sound $(\partial w/\partial p)_{p=p_s,\rho=\rho'}$ at a temperature $T = 165$ K is about -50 (m/s)/MPa, the w'' values calculated from

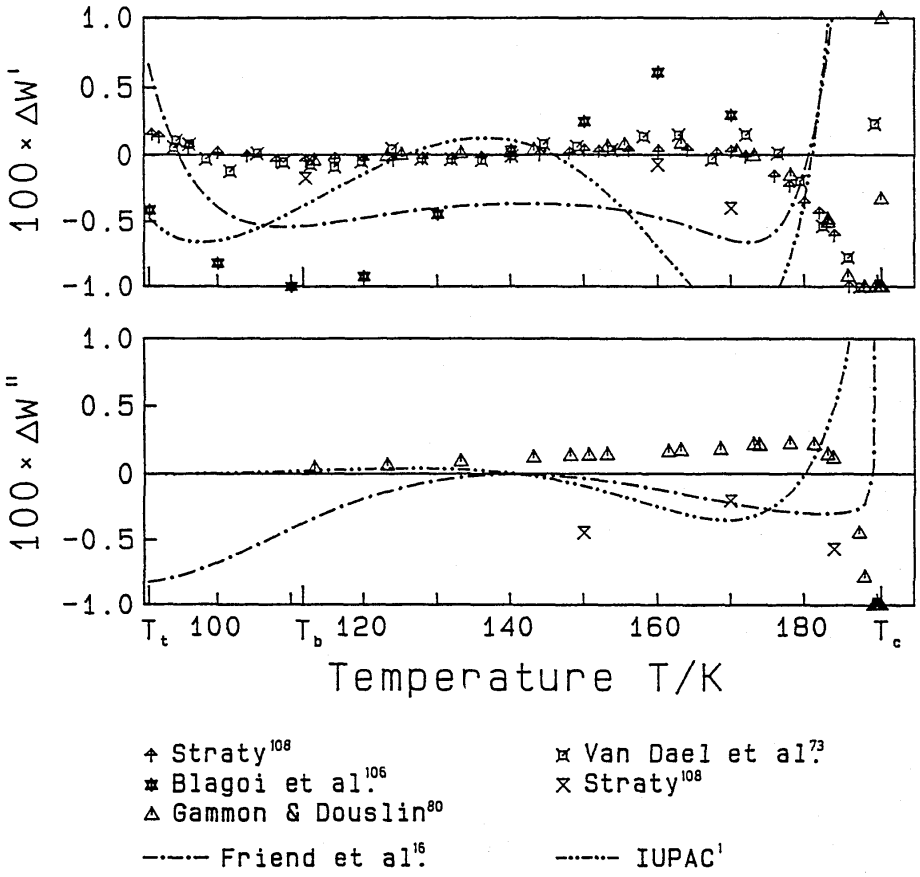

FIG. 14. Percentage deviation $\Delta y = (y_{expt} - y_{calc})/y_{expt}$ ($y = w', w''$) of experimental speed of sound data on the vapor-liquid saturation line from values calculated from Eq. (5.1). For the experimental uncertainties see Table 14.

TABLE 37. Values for the critical exponent β of the saturation densities ρ′ and ρ″ calculated from Eq. (5.3) in the region very close to the critical point

Temperature difference to the critical temperature	$(T_c-T)/m$K							
	50	40	30	20	10	1	0.1	0
Critical exponent β	0.354	0.356	0.361	0.370	0.391	0.470	0.483	0.5

TABLE 38. Values for the isochoric heat capacity and the speed of sound on the critical isochore calculated from Eq. (5.1) and the scaled equation of Kurumov[15] in the immediate vicinity of the critical point

Property compared		$(T-T_c)$/K					
		1	10^{-1}	10^{-2}	10^{-3}	10^{-4}	0
Eq. (5.1)	$\frac{w}{m/s}$	223.10	207.58	205.95	205.78	205.77	205.77
Scaled equation[15]	$\frac{w}{m/s}$	222.92	183.09	154.45	132.00	113.76	–
Eq. (5.1)	$\frac{c_v}{kJ/(kgK)}$	3.1290	3.5313	3.5794	3.5843	3.5848	3.5848
Scaled equation[15]	$\frac{c_v}{kJ/(kgK)}$	3.1241	4.4969	6.2936	8.6114	11.592	–

Eq. (5.1) agree well with the values of Gammon and Douslin. Based on these facts it is logical that the data of Gammon and Douslin show a positive deviation of up to several 0.1% from the w'' values calculated from our equation of state.

For the saturated vapor speeds of sound, the equation of Friend *et al.*[16] shows systematic deviations from Eq. (5.1) and from the IUPAC equation[1] in the temperature region below 130 K. The reason for this probable misbehavior might be the overfitting of the ρ'' values of Kleinrahm and Wagner[2] for temperatures below 120 K; see the end of the preceeding section. Friend *et al.*[16] adopted the structure of their methane equation from the oxygen equation of state developed by Schmidt and Wagner[205,206] which forms the basis of the IUPAC monograph on oxygen.[207] Friend *et al.*[16] determined the adjustable parameters of their methane version of the oxygen equation by fitting the parameters to selected data of the following properties of methane: $p\rho T$ data, $p_s\rho'\rho''$ data for the liquid-vapor coexistence curve (mainly the $p_s\rho'\rho''$ data of Kleinrahm and Wagner[2]), second virial coefficients, c_v data, and linearized c_p, c_σ and w data. A detailed investigation of their correlation shows that for temperatures below 120 K calculated c_p and c_v values of the saturated vapor rise to a maximum, whereas a monotonic decrease with falling temperature would be expected (This is at least the experience from corresponding investigations of other well measured substances, e. g. oxygen, water, and carbon dioxide.). Such an incorrect representation of the heat capacities also influences the representation of the speed of sound values because the calculation of this property from a fundamental equation implies the calculation of c_v and c_p values, see Table 28.

6.1.3. Heat Capacity on the Coexistence Curve

Figure 15 shows comparisons between experimental c_p' and c_σ data and the corresponding values calculated from Eq. (5.1). The data of Clusius,[101] Younglove,[103] Roder,[104] and Cutler and Morrison[72] are represented within their experimental uncertainties, which are between ± 0.5% at low temperatures and ± 5% near the critical point for Younglove's data, for example. Although these data were not included in the simultaneous nonlinear fit, their representation is fairly good.

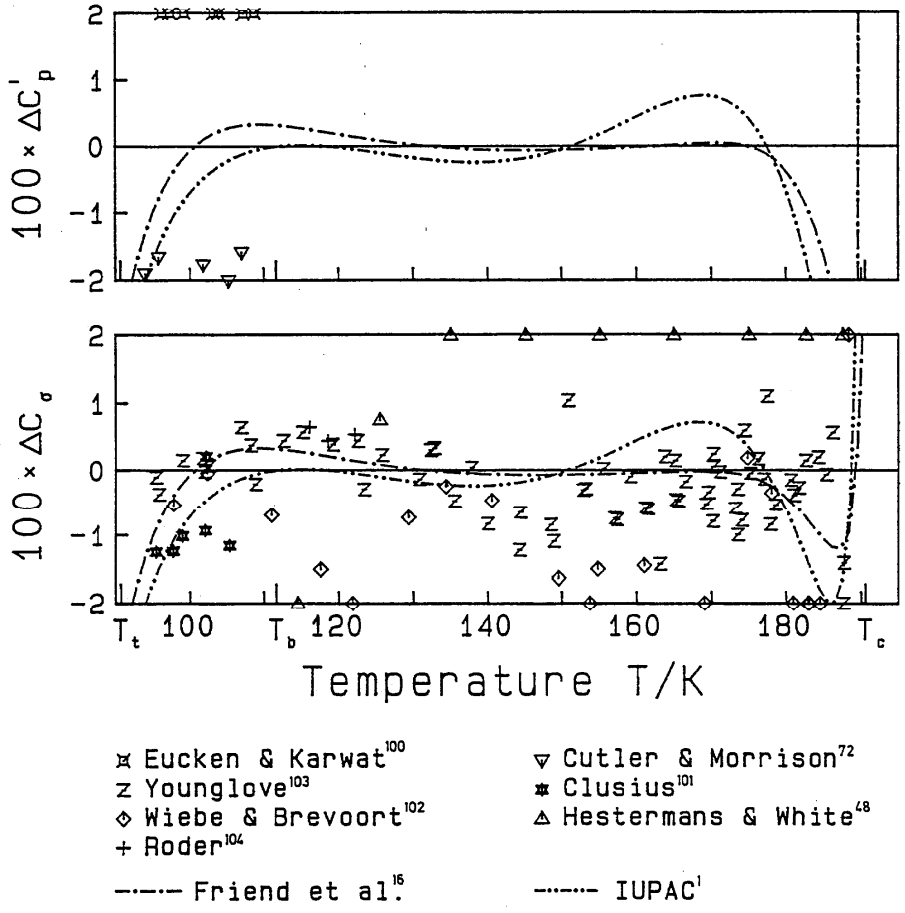

FIG. 15. Percentage deviation $\Delta y = (y_{expt} - y_{calc})/y_{expt}$ ($y = c_p', c_\sigma$) of experimental heat capacity data on or along the saturated liquid line from values calculated from Eq. (5.1). All data with deviations of more than ± 2% are plotted on the limit of the deviation scale.

6.1.4. Enthalpy of Vaporization

The deviation of experimental data of the enthalpy of vaporization Δh_v from values calculated from Eq. (5.3) is shown in Fig. 16. In addition to the experimental Δh_v data, Fig. 16 also contains Δh_v values calculated from the Clausius-Clapeyron equation

$$\frac{dp_s}{dT} = \frac{1}{T}\frac{\Delta h_v}{(1/\rho'') - (1/\rho')}, \qquad (6.2)$$

where the quantities dp_s/dT, ρ' and ρ'' were determined from Eqs. (3.2), (3.4), and (3.5). The agreement between these data and the Δh_v values calculated from Eq. (5.3) shows that, also for this combination of the thermal properties of the saturation curve, the consistency between the auxiliary equations for p_s, ρ', and ρ'' and Eq. (5.3) is very good. With the exception of the two data of Frank and Clusius[97] and Colwell *et al.*,[99] the other Δh_v data are less reliable because of impurities in the sample (Jones *et al.*[98]) or the use of older ρ' and ρ'' values for the evaluation of the measurements (Hestermans and White[48]).

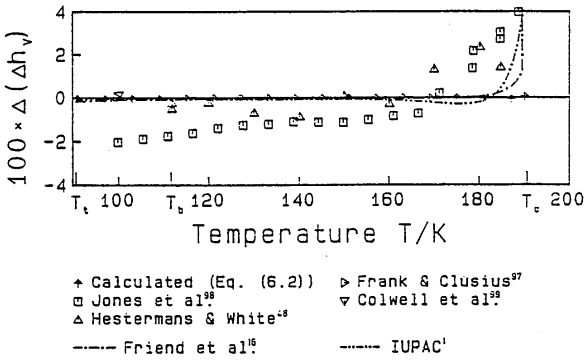

FIG. 16. Percentage deviation $\Delta(\Delta h_v) = (\Delta h_{v,expt} - \Delta h_{v,calc})/\Delta h_{v,expt}$ of experimental enthalpy of vaporization data from values calculated from Eq. (5.3).

6.2. Single Phase Region

Since this section only gives a compressed survey of the overall quality of the new fundamental equation, we will show a representative sample from the data set that we used for establishing our equation. The deviation plots do not contain any information on the uncertainty of the experimental data because such error bars would have made the figures overcrowded. In general, however, for these selected data the uncertainty is represented by the scatter of the data. Details with regard to the uncertainties of properties calculated from our new formulation are given in Sec. 7. Most figures also show comparisons with the IUPAC equation of state[1] and the correlation of Friend *et al.*[16] All the other equations of state for methane, which are summarized in Table 1, represent the properties of methane more unfavorably than the equations of the IUPAC and of Friend *et al.* do. Since the stated validity of the equation of Friend *et al.* is restricted to pressures below 100 MPa, comparisons of our equation of state with this equation are given only for pressures below 100 MPa. The IUPAC equation and the new fundamental equation are valid for pressures up to 1000 MPa.

6.2.1 Thermal Properties

Figures 17 and 18 show the percentage density deviation of the selected experimental $p\rho T$ data from the data calculated from Eq. (5.3). The estimated experimental uncertainties of these data and further information can be taken from Table 16. We chose the low resolution of $\Delta\rho/\rho = \pm 0.2\%$ for the density deviation, because otherwise it would not have been possible to compare our equation with the IUPAC equation[1] and the one of Friend *et al.*[16] The high resolution of the deviation scale in the additional Figs. 19 and 20 were selected to illustrate the quality of our new fundamental equation in two regions: $p\rho T$ data for $p \leq 12$ MPa and $T \leq 450$ K, and $p\rho T$ data for $p > 12$ MPa and $T \leq 450$ K. The quality of the representation of $p\rho T$ data for $T > 450$ K is discussed together with Fig. 18. The critical region will be discussed in detail in Sec. 6.3.

Figures 17 and 18 show that the new equation of state, Eq. (5.3), represents the selected experimental $p\rho T$ data significantly better than all the other equations available for methane do. The systematic deviations between the IUPAC equation[1] and the equation of Friend *et al.*[16] and our equation are based on the fact that both correlators relied too much on the data of Goodwin *et al.*[8,19] As discussed in Sec. 2.3.1, we used Goodwin's corrected data only for the development of the new equation of state but the deviation plots contain the original (uncorrected) data of Goodwin *et al.* It has already been mentioned that the data of Goodwin deviate by up to 0.2% in density from recent state-of-the-art measurements.

$p\rho T$ data for $p \leq 12$ MPa and $T \leq 450$ K

Figures 19 and 20 show comparisons of data from state-of-the-art $p\rho T$ experiments with density values calculated from Eq. (5.3). The new equation agrees within $\pm 0.02\%$ in density with the $p\rho T$ data of Kleinrahm *et al.*,[3,4] Pieperbeck *et al.*,[22] Achtermann *et al.*,[23,109] and Händel *et al.*[5] All $p\rho T$ data sets are represented within their experimental uncertainties; see Table 16.

$p\rho T$ data for $p > 12$ MPa and $T \leq 450$ K

Figures 19 and 20 illustrate that, also at higher pressures, Eq. (5.3) gives a good representation of the $p\rho T$ data of Morris[114,115], Achtermann *et al.*,[23,109] Jaeschke,[117] Trappeniers *et al.*,[113] and Kortbeek and Schouten.[118] The experimental and calculated densities generally agree within $\pm 0.05\%$. The range from 30 MPa to the melting pressure at temperatures below 250 K is not covered by reliable data. Nevertheless, we estimate that the uncertainty of density values calculated from Eq. (5.3) in this

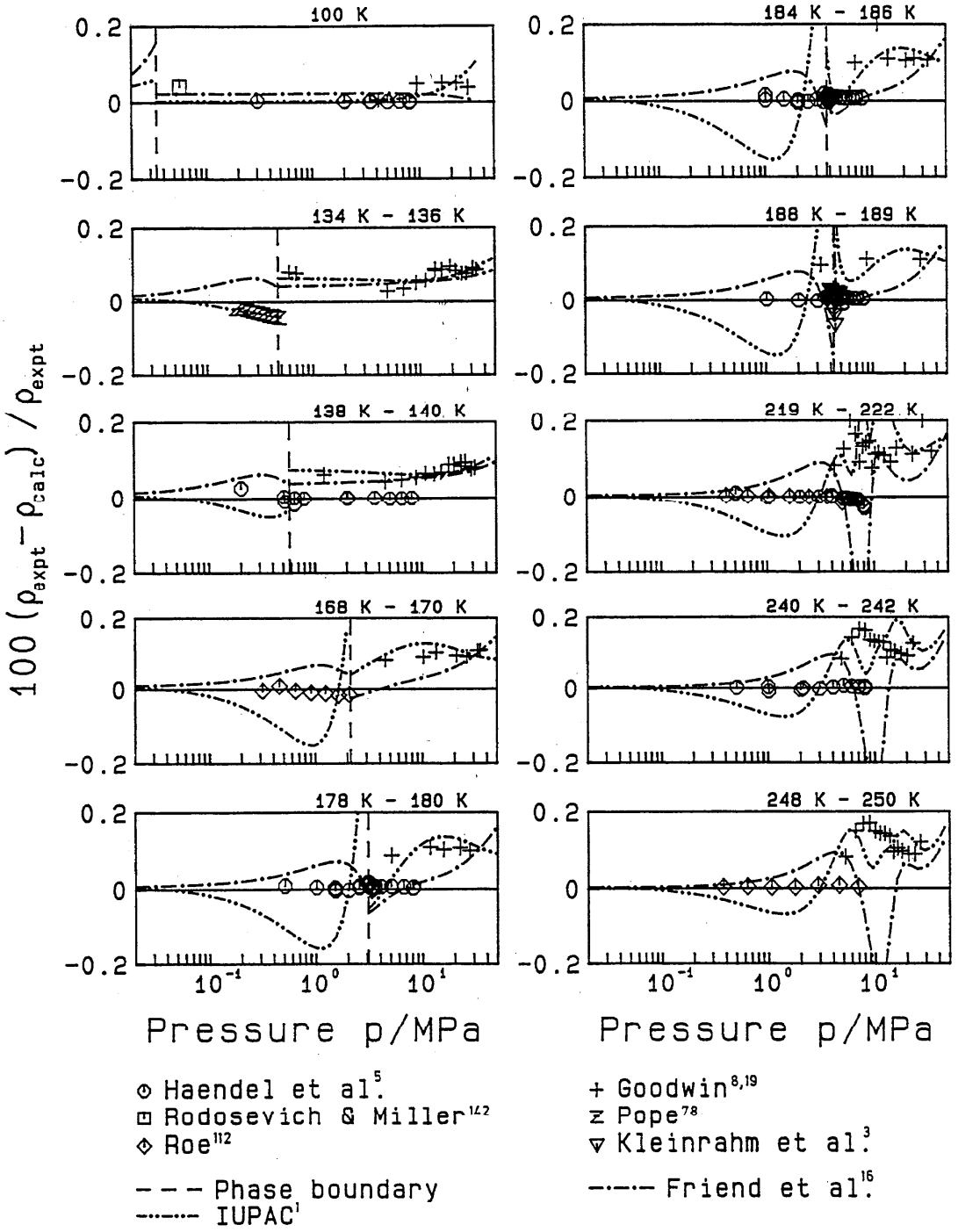

FIG. 17. Percentage density deviation of the experimental $p\rho T$ data from values calculated from Eq. (5.3). For the experimental uncertainties see Table 16.

region is less than ± 0.15%. This quality is achieved because the fitting and optimization process included speed of sound measurements which cover the range mentioned above.

$p\rho T$ data for $T >$ 450 K

There is only one set of Group 1 measurements which covers temperatures above 450 K (see Fig. 6). Douslin *et al.*[20] published 374 measurements of the compression factor z in the temperature range between 273 K and 623 K at pressures up to 37.5 MPa. The total uncertainty in z claimed for their measurements increases to about

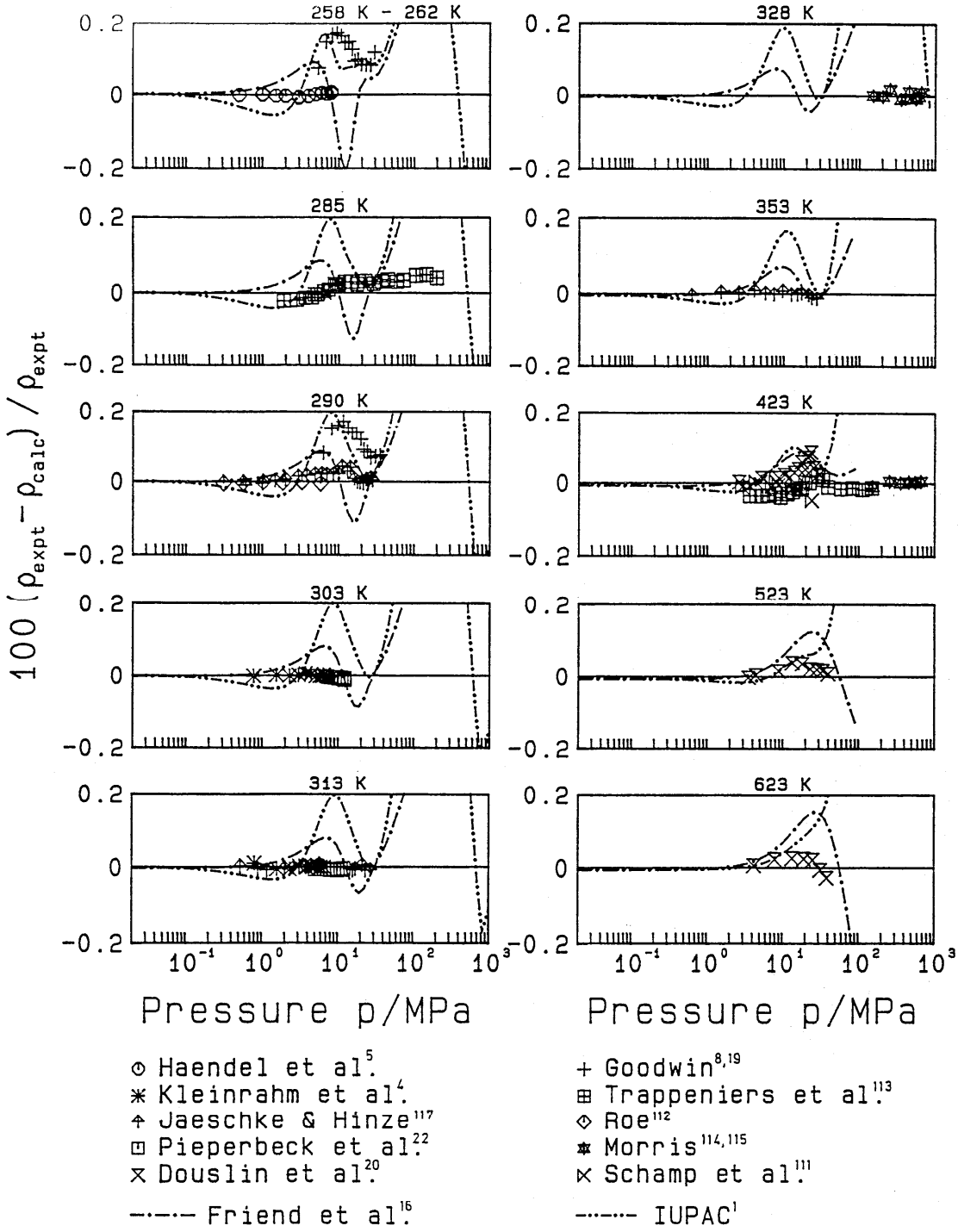

FIG. 18. Percentage density deviation of the experimental $p\rho T$ data from values calculated from Eq. (5.3). For the experimental uncertainties see Table 16.

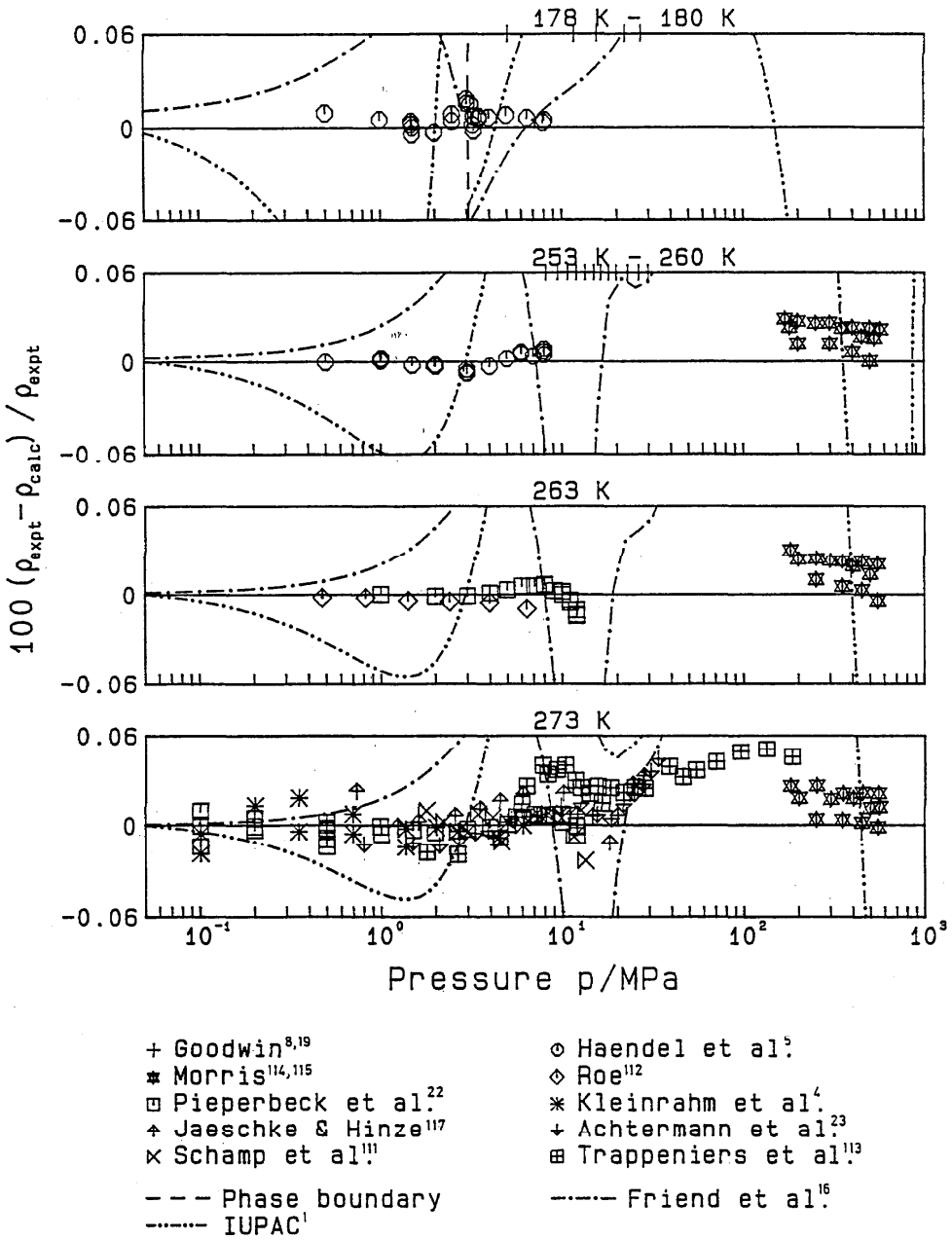

FIG. 19. Percentage density deviation of the experimental $p\rho T$ data from values calculated from Eq. (5.3) in a high resolution with respect to density. For the experimental uncertainties see Table 16.

± 0.3% at the highest temperature and pressure. The data are well reproduced by Eq. (5.3) within this error limit. Unfortunately, these data already show a systematic deviation from our primary $p\rho T$ data at temperatures below 450 K. Therefore, we estimate the uncertainty of density values calculated from Eq. (5.3) to be ± 0.07% to ± 0.15% for temperatures above 450 K at pressures of 30 MPa.

6.2.2. The Second Virial Coefficient

Figure 21 illustrates comparisons between selected experimental data of the second virial coefficient and B values calculated from Eq. (5.3). The calculated second virial coefficients are in good agreement with the data of Kleinrahm *et al.*,[4] Roe,[112] and Douslin *et al.*[20]

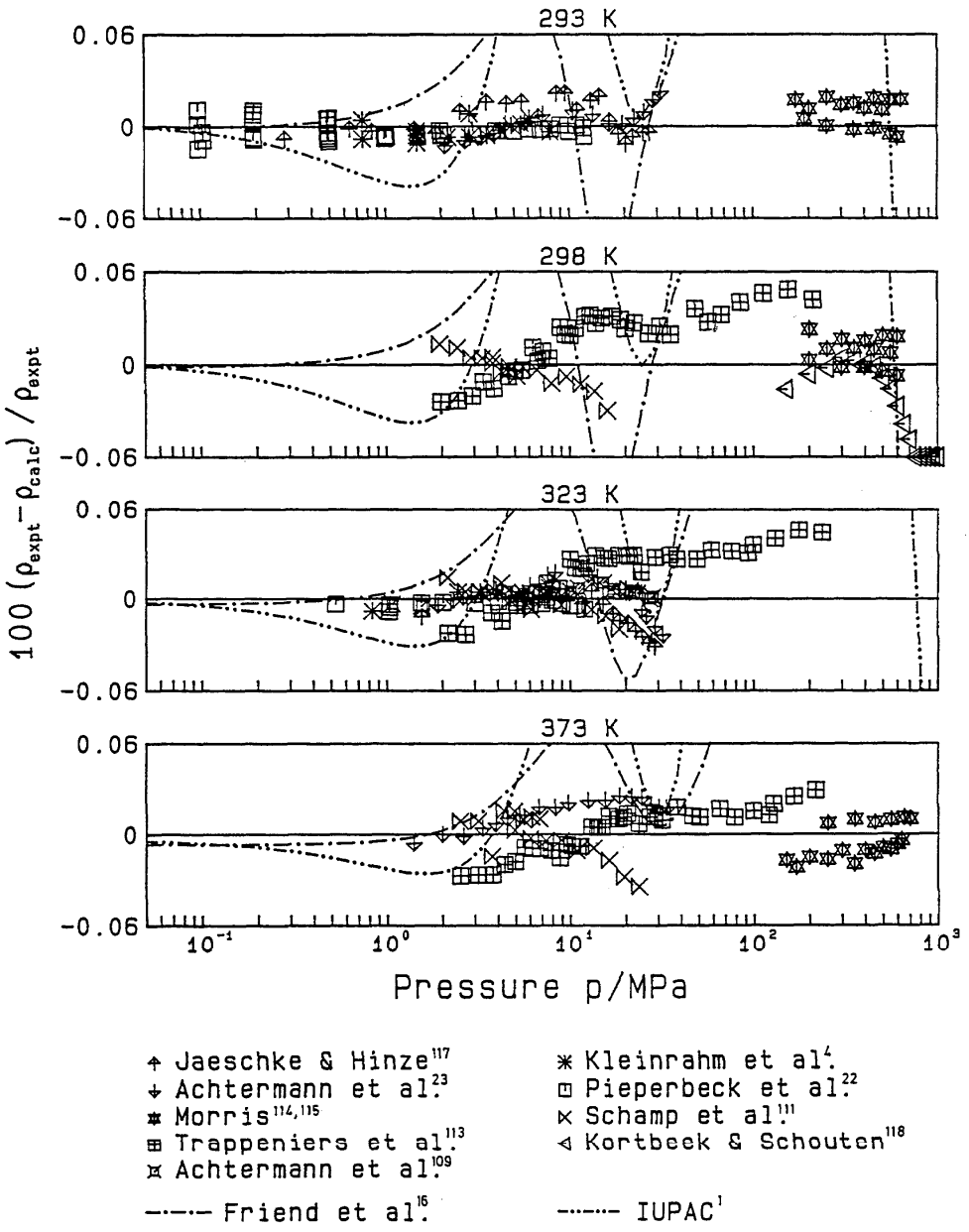

FIG. 20. Percentage density deviation of the experimental $p\rho T$ data from values calculated from Eq. (5.3) in a high resolution with respect to density. For the experimental uncertainties see Table 16.

6.2.3. Speed of Sound

Figure 22 shows the percentage speed of sound deviations along several isotherms plotted against pressure. The high quality of the selected data representation at all temperatures and pressures characterizes the new fundamental equation, Eq. (5.1). Neither the IUPAC equation[1] nor the equation of Friend *et al.*[16] is able to represent the speed of sound in the liquid region and in the high pressure region within the uncertainty of these data. However, many measurements of the properties of methane have been carried out in the last few years so that these data had not been available to most of the previous correlators.

In 1986, Kortbeek *et al.*[68,186] published $p\rho T$ and speed of sound data for methane. At that time we had already started with the development of our fundamental equation. Our preliminary equation of state was not able to reproduce the w data of Kortbeek although the data were included in the fitting and the optimization process. In 1989, Kortbeek and Schouten[118] repeated their measurements. The new set of data on the speed of sound differs

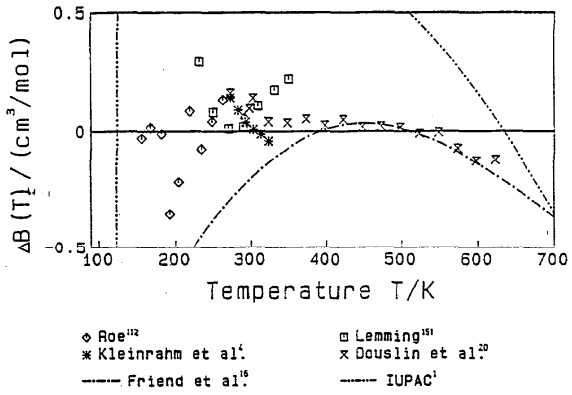

FIG. 21. Absolute deviation $\Delta B = (B_{expt} - B_{calc})/B_{expt}$ of experimental second virial coefficients from values calculated from Eq. (5.3). For the experimental uncertainties see Table 18.

up to − 0.7% from their first measurements. Although the data now agree much better with our equation of state, we believe that the maximum uncertainty of ± 0.12%, claimed by Kortbeek *et al.* for their new speed of sound data, might still be a little bit too optimistic.

6.2.4. The Isochoric Heat Capacity

Figure 23 shows the percentage deviations of c_v data from our new equation of state, while Figure 24 shows an absolute plot of c_v in the liquid region close to the saturated liquid line. Figure 23 illustrates that Eq. (5.1) can represent the data of Roder[104] better than the data of Younglove[103] although both experiments were performed with the same equipment. Figure 24 shows that the IUPAC equation[1] as well as the equation of Friend *et al.*[16] probably exhibit a physically incorrect behavior in the liquid region at lower temperatures. The values of the isochoric heat capacity on an isochore are expected to increase with decreasing temperature when approaching the saturated liquid line, and the heat capacity on the saturated liquid line is not expected to have a maximum at low temperatures. This is at least the experience from corresponding investigations of other well-measured fluids, e. g. O_2, H_2O, and CO_2.

6.2.5. The Isobaric Heat Capacity

Figure 25 gives an impression of the percentage deviations of the c_p data from values calculated from the equation of state, Eq. (5.1). With the exception of the low temperature region and the critical region, all investigated equations of state show very similar deviations from the experimental data. Except near the critical point, the maximum deviation between the data and the values calculated from our equation of state is about ± 2% which corresponds to the estimated experimental uncertainty; see Sec. 2.3.4.

6.2.6. Difference of Enthalpy

The absolute deviations between experimentally determined differences of enthalpy by Ayber,[167] Kasteren and Zeldenrust,[170] Dawe and Snowdon,[169] and Dillard *et al.*[168] and Δh values calculated from Eq. (5.1) are presented in Fig. 26. The main part of the enthalpy differences published by Dawe and Snowdon ($\Delta h_{expt,max}$ = 124.7 J/g) is reproduced within its stated uncertainty of 0.3 J/g. Ayber investigated the integral Joule-Thomson effect (ΔT_{max} = 60 K, Δp_{max} = 8 MPa, Δh = 0 kJ/kg) so that the maximum deviation of 1 J/g is acceptable, especially when bearing in mind that Ayber used methane which had contained 1.3 mol% impurities.

6.2.7. Joule-Thomson Coefficient

Figure 27 shows the Joule-Thomson coefficient calculated from three equations of state and the experimental coefficients of Budenholzer *et al.*[165] on six isotherms. The equations, which all agree in this region, indicate that the experimental Joule-Thomson coefficients of Budenholzer *et al.*[165] are not consistent with the other reliable experimental data which the IUPAC equation,[1] the equation of state of Friend *et al.*[16] and Eq. (5.1) are able to represent.

6.3. Critical Region

The opinion has been widely held that analytic equations of state covering the whole fluid region are not able to represent the properties in the critical region. In this context, we define the enlarged critical region of methane by a temperature region between 187 K and 205 K ($T_c \approx 190.6$ K) and densities from 90 to 230 kg/m³ ($\rho_c \approx 162.7$ kg/m³). We will show that our new equation is able to represent the existing experimental information on the thermodynamic properties of methane in the critical region at least as well as the revised and extended scaling model of Kurumov *et al.*[15] The validity range of the Kurumov equation corresponds to the region defined above.

Comparisons of the calculated and measured vapor pressure, saturated liquid and vapor densities for temperatures close to the critical temperature are given in Fig. 28. The scaling law equation has difficulties in representing the saturated liquid and vapor densities in the critical region. Our new fundamental equation, however, reproduces all experimental $p_s\rho'\rho''$ data of Kleinrahm and Wagner[2] within the experimental uncertainty.

It should be mentioned that the new fundamental equation, Eq. (5.3), is not consistent with Eqs. (3.4) for ρ' and (3.5) for ρ'' with regard to the critical exponent β. The critical exponent of Eqs. (3.4) and (3.5) is $\beta = 0.354$ whereas the critical exponent β of Eq. (5.3) is 0.5 (for $T \to T_c$ like for any analytical equation of state). However, as Table 37 shows, this inconsistency exists only for $(T_c - T) \leq$ (20 to 30)mK, and for $(T_c - T) \geq 50$ mK the three equations completely agree with respect to β. On the other hand, the β value has very little to do with the

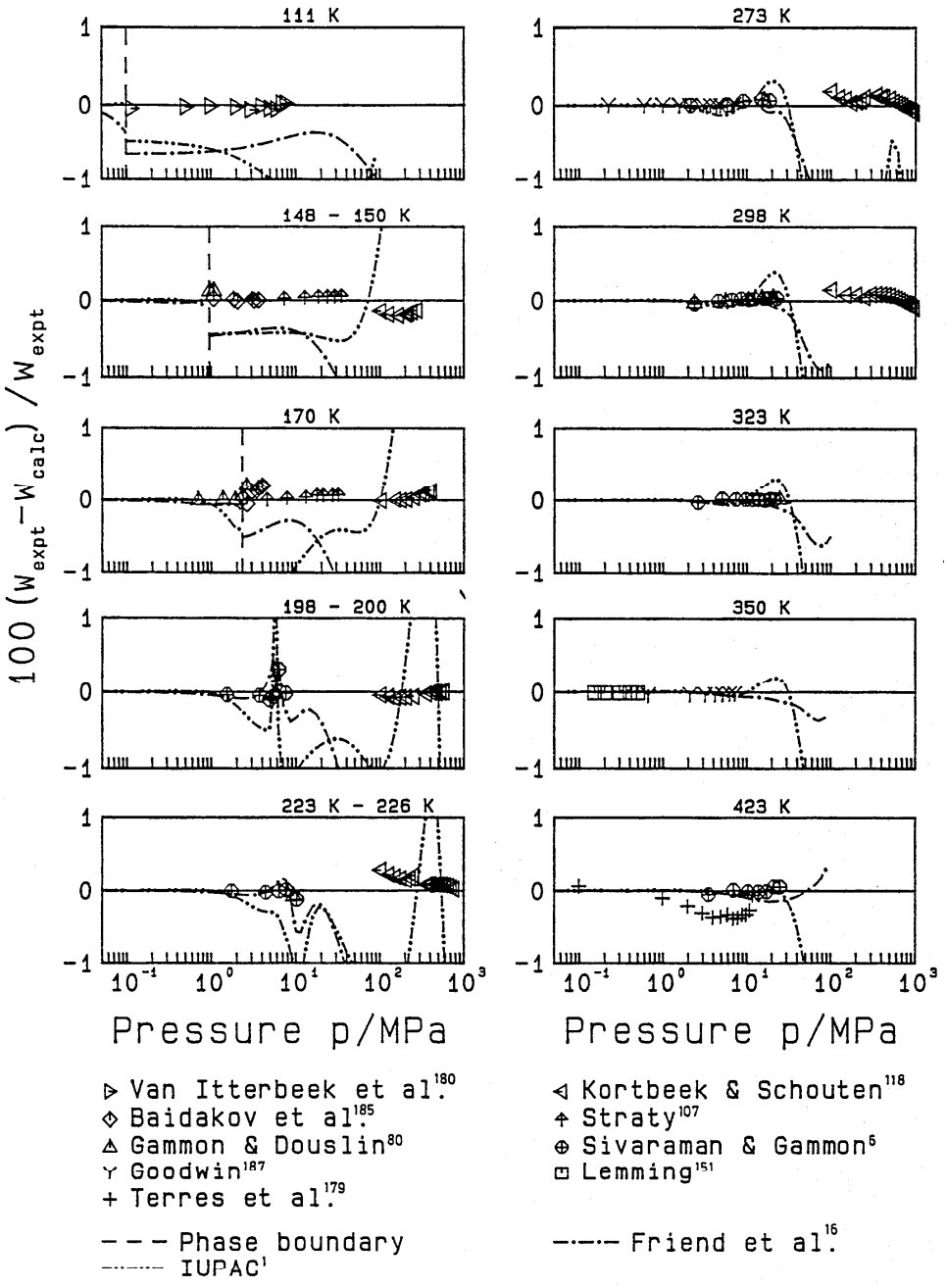

FIG. 22. Percentage deviation of the experimental speed of sound data from values calculated from Eq. (5.1). For the experimental uncertainties see Table 24.

quality of any correlation equation. Although the Kurumov equation[15] contains the so-called "true" value $\beta = 0.325$ corresponding to the universality hypothesis of the renormalization group theory, this equation is just not able to represent the saturation densities of the critical region within their experimental uncertainties.

A comparison of Eq. (5.3), the scaled equation of state of Kurumov *et al.*,[15] the equation of Friend *et al.*,[16] and the IUPAC equation[1] with the $p\rho T$ data of Kleinrahm *et al.*[3] and Händel *et al.*[5] is presented in Fig. 29. Again, only Eq. (5.3) is able to represent the data within the experimental uncertainty.

Up to now, the anomalous behavior of caloric properties of methane in the critical region could not have been properly modelled by analytical equations of state. With the help of special terms (modified two-dimensional Gaussian terms) in our equation, we are now able to represent the caloric properties speed of sound and heat ca-

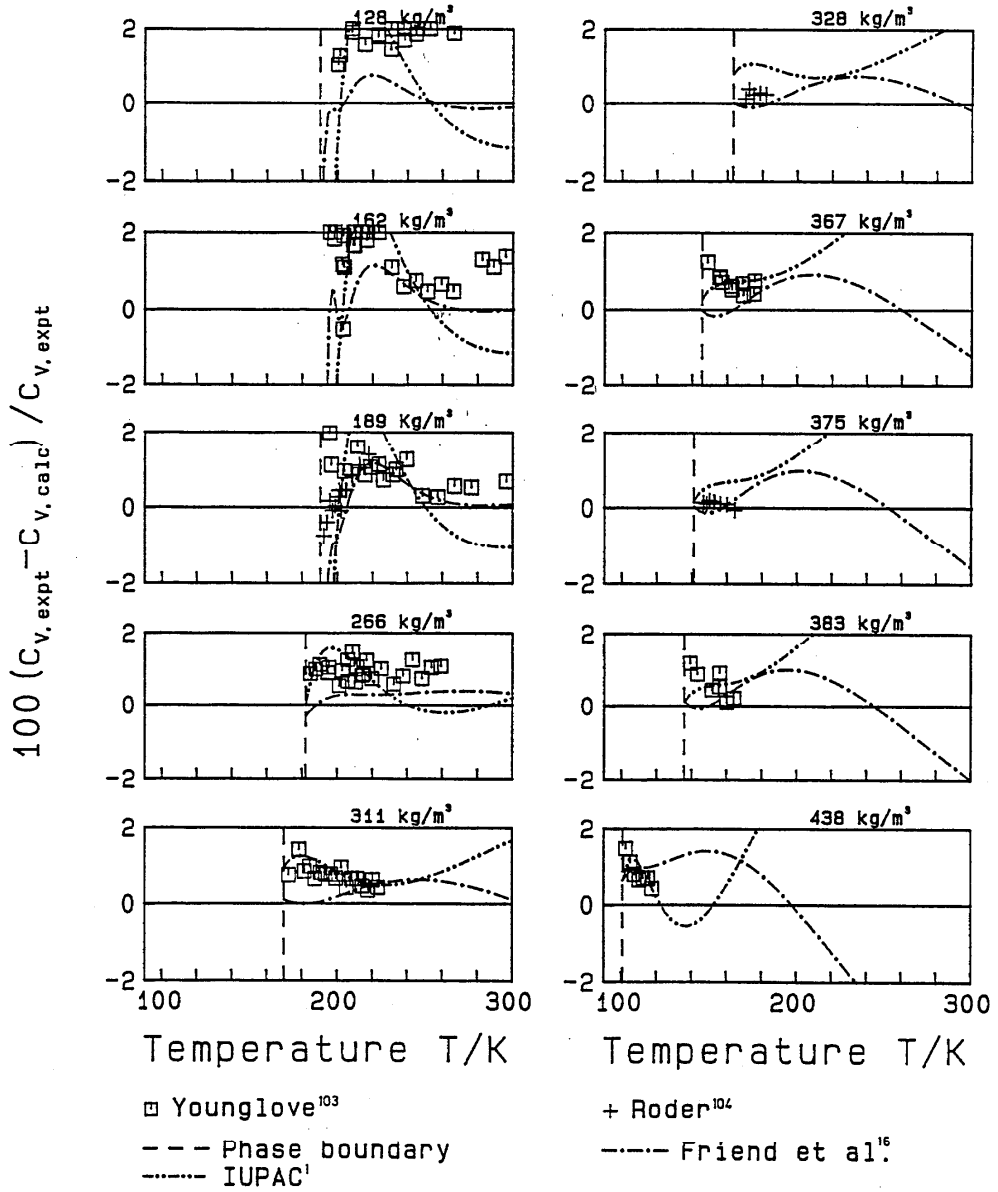

FIG. 23. Percentage deviation of the experimental isochoric heat capacity data from values calculated from Eq. (5.1). For the experimental uncertainties see Table 22.

pacity in a wide range of temperatures and densities as well as the scaled equation of state of Kurumov *et al.*[15] Although, of course, the new fundamental equation does not reproduce the *limiting* properties when approaching the critical point, which is however, not of importance for 'normal' engineering applications, it is possible to represent caloric properties much better than all the other existing equations of state for methane do. A comparison between the new fundamental equation, Eq. (5.1), the scaled equation of Kurumov *et al.*,[15] the equation of Friend *et al.*,[16] and the experimental speeds of sound of Gammon *et al.*[6,80] is presented in Fig. 30. Eq. (5.1) yields the best overall representation of the w data of Gammon *et al.* For temperatures $(T - T_c) \geq 1$ K, Eq. (5.1) represents the data within their experimental uncertainty of ± 1%. Closer to the critical point (within T_c + 0.5 K), the scaled equation is superior to our equation but it is obvious that its agreement with the experimental data deteriorates very rapidly as soon as the scaled equation is extrapolated outside its very small range of validity. Directly at the critical point, Eq. (5.1) yields a speed of sound value of 205.95 m/s which is, of course, in conflict with the expected limiting value 0 m/s. Table 38 shows in more detail which values for w and c_v Eq. (5.1) and the scaled equation of Kurumov[15] yield in the immediate vicinity of the critical point.

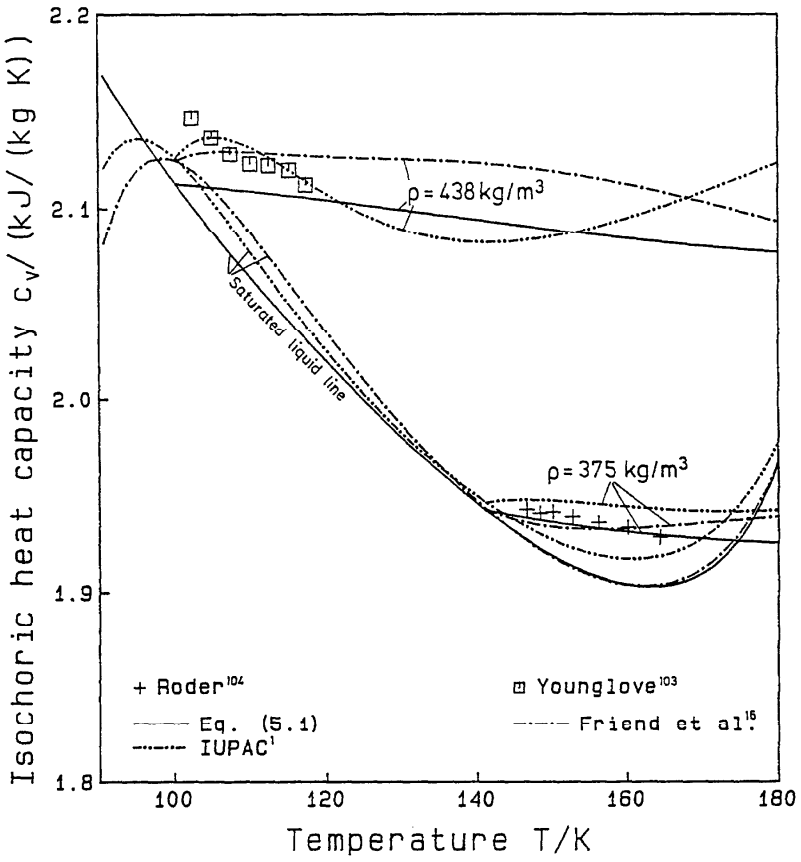

FIG. 24. Representation of the isochoric heat capacities in the liquid state below 180 K by Eq. (5.1) and by other equations.

The representation of the isochoric heat capacity data on a near critical isochore, $\rho = 163$ kg/m^3, and on the isochore $\rho = 189$ kg/m^3 by Eq. (5.1) is shown in Fig. 31. The comparison for the 189 kg/m^3 isochore shows that the c_v data of Younglove[103] are systematically higher than the more recent data of Roder[104] taken with the same apparatus which was also used by Younglove. With the exception of Roder's c_v value at $T = 190.97$ K and $\rho = 189$ kg/m^3 the scaled equation of Kurumov *et al.*[15] but also the new fundamental equation, Eq. (5.1), are able to represent all data within the experimental uncertainty estimated to be about ± 3% to ± 5% (see also Table 22). This is also valid for the critical isochore $\rho = 163$ kg/m^3 where, however, the data do not extend close enough to the critical temperature. The plot of the critical isochore also shows that Eq. (5.1) is in agreement with the scaled equation for temperatures $(T - T_c) \geq 1$ K but at $T = T_c$ Eq. (5.1) yields the finite value $c_v \approx 3.6$ kJ/(kg K), see also Table 38. The IUPAC equation[1] and the equation of Friend *et al.*[16] are not able to represent the isochoric heat capacities in the near critical region.

At the end of this critical region discussion, in Table 38, Eq. (5.1) and the scaled equation of Kurumov *et al.*[15] are compared with regard to their values for w and c_v very close to the critical point. Table 38 shows that the results calculated from the two equations deviate systematically for $(T - T_c) < 1$ K. When approaching T_c, the deviations between the two equations increase clearly. For $(T - T_c) < 10^{-1}$ K, however, the course of the two equations is only based on the mathematical model and not supported by experimental data. It is also interesting to note that for $(T - T_c) < 10^{-4}$ K the values calculated from the scaled equation for w are far away from zero and for c_v far away from infinite. However, this equation cannot be evaluated for $(T - T_c) < 10^{-4}$ K because this region is excluded from the application range due to numerical problems. When we switched off the temperature limit of 10^{-4} K in the program package of the Kurumov equation, at $(T - T_c) = 10^{-10}$ K we calculated with this equation $w \approx 50.6$ m/s and $c_v \approx 58.7$ kJ/(kg K).

6.4. Metastable States

Baidakov *et al.*[150a,185] published measurements of $p\rho T$ data (Ref. 150a) as well as speed of sound data (Ref. 185) in the metastable region. The $p\rho T$ experiments were only

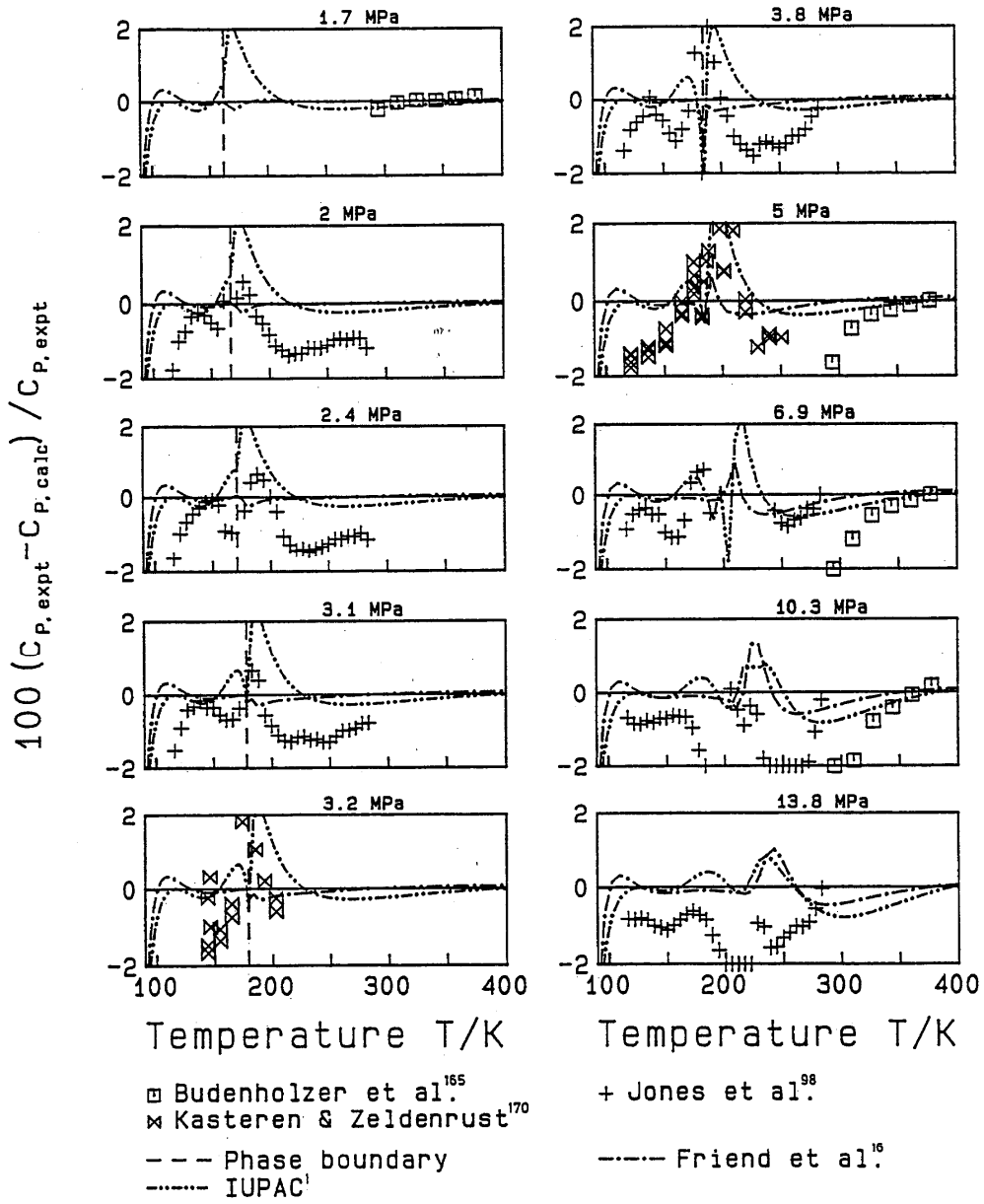

FIG. 25. Percentage deviation of the experimental isobaric heat capacity data from values calculated from Eq. (5.1).

relative measurements because Baidakov and Gurina[150a] determined their densities from density values on the saturated liquid line which had been given by Goodwin and Prydz[19] and McClune.[94] As discussed in Sec. 2.2.4.2., both data sets for the saturated liquid density used by Baidakov and Gurina deviate systematically from the state-of-the-art data of Kleinrahm and Wagner[2] and, necessarily, the $p\rho T$ data have to show systematic deviations from values calculated from Eq. (5.1). Fig. 32 shows the representation of the $p\rho T$ data on six isochores and we conclude that Eq. (5.1) is able to represent the properties in the metastable region as well as the properties in the homogeneous states. This statement is supported by Fig. 33, where the representation of the speed of sound data of Baidakov *et al.*[185] is shown. For both $p\rho T$ and speed of sound measurements Baidakov *et al.* used methane with a purity of only 99.9 mol%. It is commonly known that the effect of impurities becomes significant when the measurements approach near critical conditions.

6.5. Extrapolation Behavior of the New Fundamental Equation

To conclude the discussion of the new equation of state, its extrapolation capability is examined with the

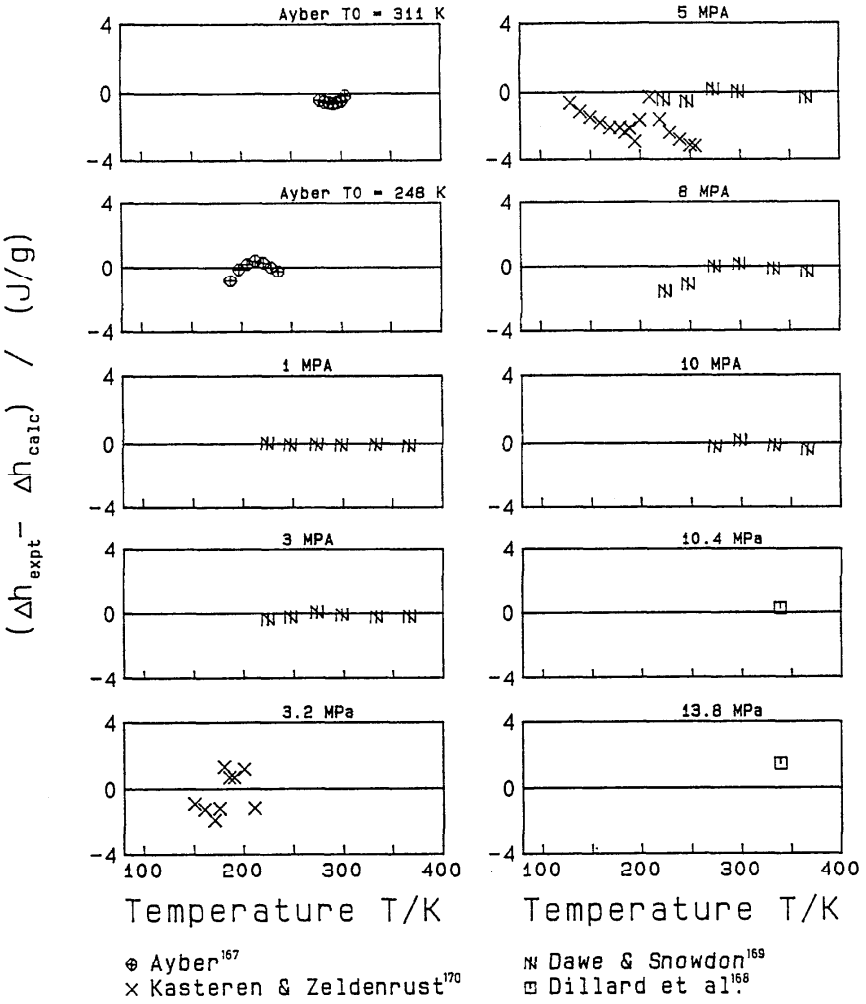

FIG. 26. Absolute deviation of experimental data of differences of enthalpy from values calculated from Eq. (5.1). For the experimental uncertainties see Table 20.

help of Fig. 34. In 1981, Nellis *et al.*[208] carried out shock wave measurements in methane. Based on the conservation relations for mass, momentum, and energy, they obtained data on the Hugoniot curve

$$h - h_{oH} = 0.5(p + p_{oH})(1/\rho_{oH} - 1/\rho), \qquad (6.3)$$

where h is the enthalpy, p the pressure and ρ the density after the shock wave experiment and h_{oH}, p_{oH}, and ρ_{oH} are the initial state values. The comparison of Eq. (5.1) to the experimental Hugoniot data, which were not used to fit the equation, is shown in Fig. 34. The agreement of the Hugoniot curve calculated with the help of Eqs. (5.1) and (6.3) with the data of Nellis *et al.*[208] is excellent. A safe extrapolation of Eq. (5.1) might be possible for pressures up to 20000 MPa.

7. Accuracy of the New Fundamental Equation

Estimates of the accuracy of the density, speed of sound, and enthalpy calculated from the new fundamental equation presented here have been made and are illustrated in the tolerance diagrams, Figs. 35, 36, and 37, respectively. The estimates were derived from comparisons of the various sets of experimental results and taking into account our own experience in judging experimental data.

The calculated values of heat capacity (c_p and c_v) are estimated to be accurate to within ± 1%. The estimates of the uncertainties of the enthalpy shown in Fig. 37 are considerably less certain than those of the density and speed of sound. Because of the scarcity of enthalpy data, the tolerances given are only rough estimates.

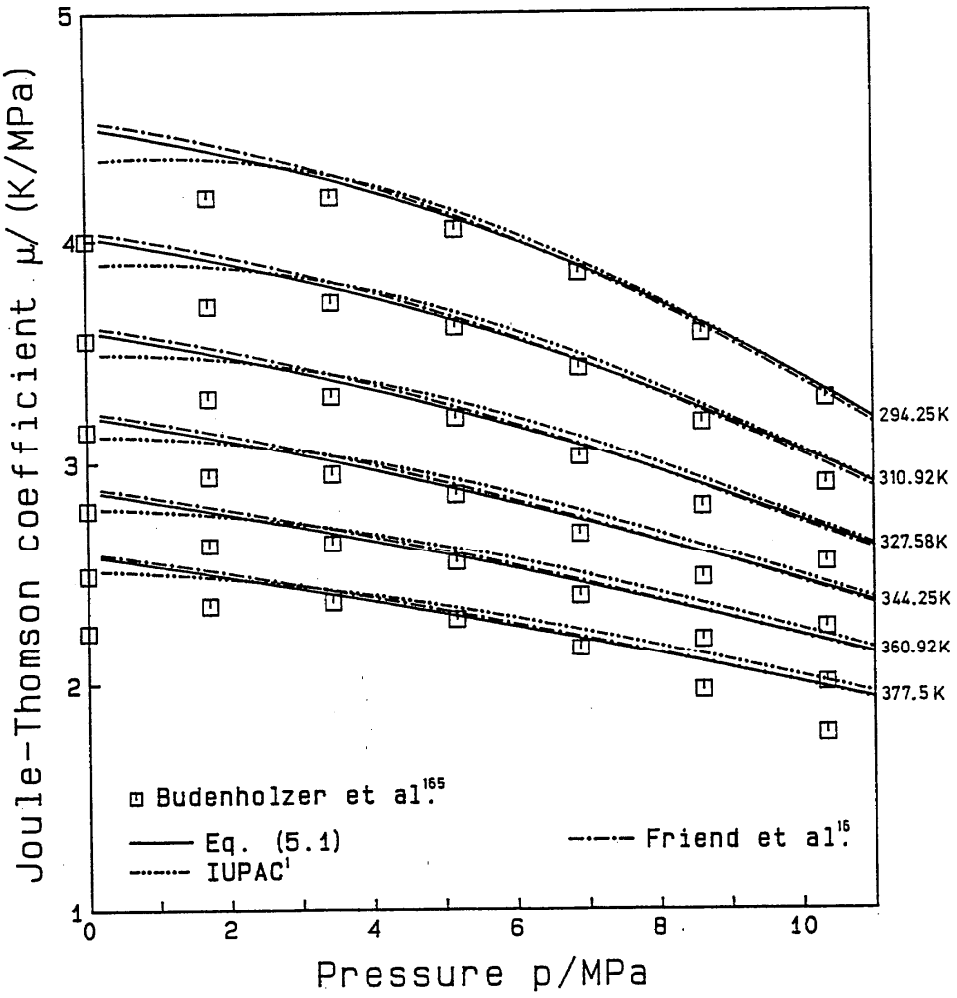

FIG. 27. The plot of the Joule-Thomson coefficient in the region below 11 MPa calculated from Eq. (5.1) and from other equations.

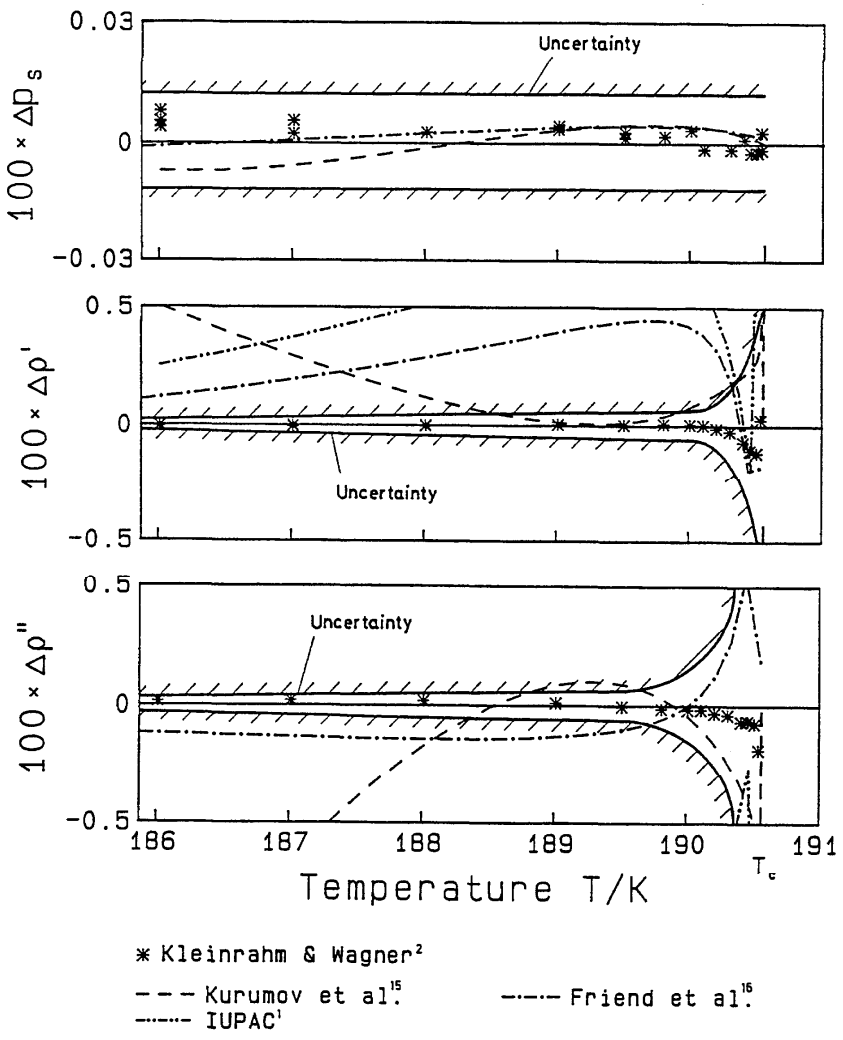

FIG. 28. Percentage deviation $\Delta y = (y_{expt} - y_{calc})/y_{expt}$ ($y = p_s$, ρ', ρ'') of selected experimental data on the vapor-liquid saturation line in the critical region from values calculated from Eq. (5.3). The uncertainty ranges of the experimental data are plotted as well. Since the Kurumov equation[15] is only valid for temperatures $T \geq 187$ K, the p_s and ρ' values calculated for $T < 187$ K correspond to extrapolated values.

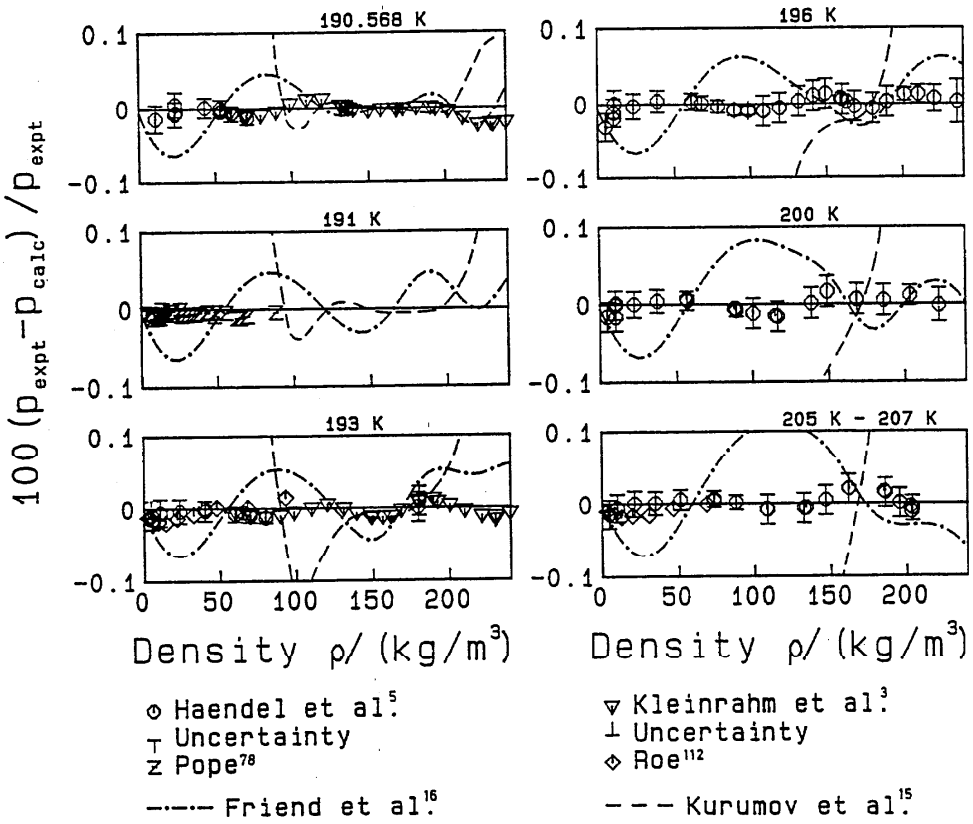

FIG. 29. Percentage pressure deviations of the experimental $p\rho T$ data from values calculated from Eq. (5.3) in the critical region. The plotted uncertainty range corresponds to the total uncertainty in pressure for the data of Kleinrahm *et al.*[3] and Händel *et al.*[5]

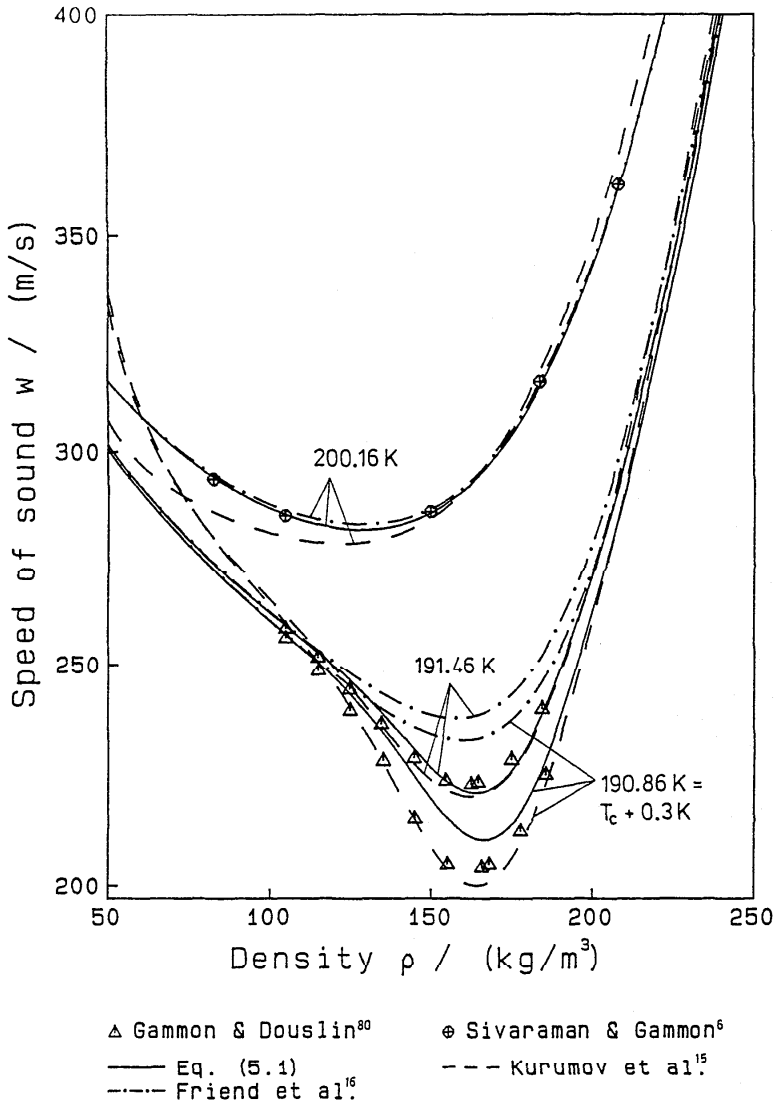

FIG. 30. Representation of the speed of sound in the critical region by Eq. (5.1) and by other equations. Since the Kurumov equation[15] is only valid for 90 kg/m^3 $\leq \rho \leq$ 230 kg/m^3, values calculated from this equation outside this region correspond to extrapolated values. The uncertainty of the data in this figure was estimated to be about ± 1% which corresponds roughly to the size of the symbols plotted.

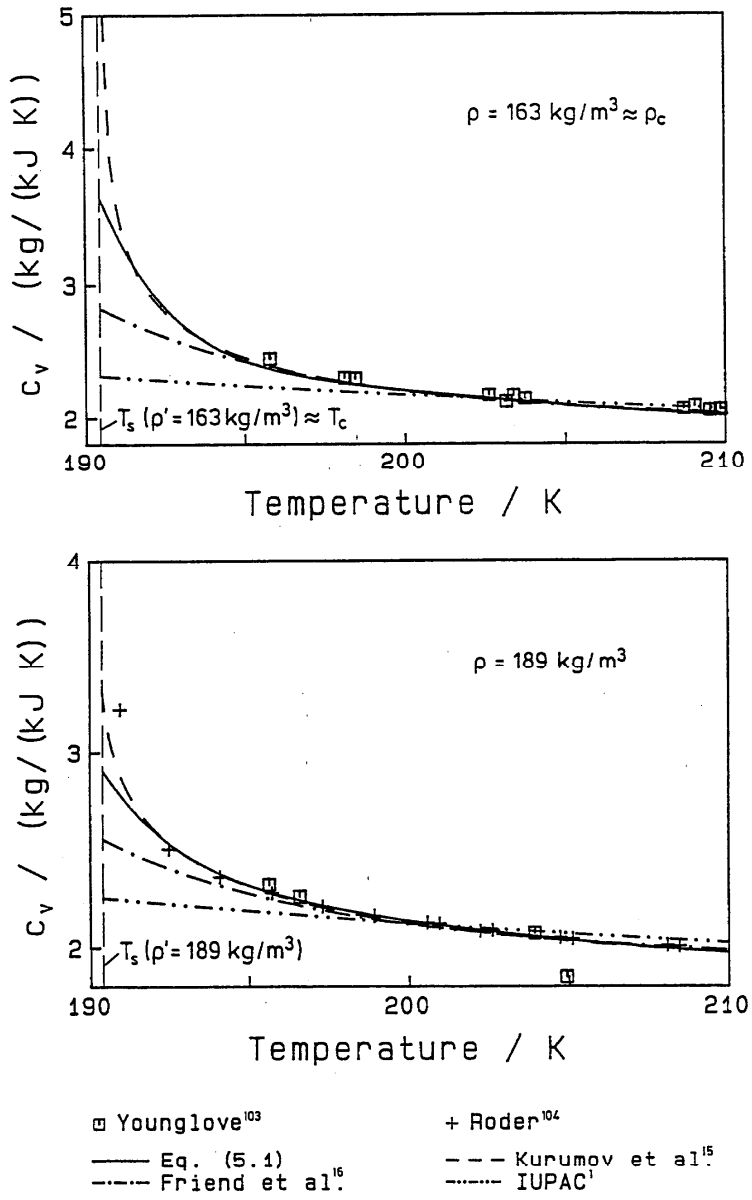

FIG. 31. Representation of the isochoric heat capacity in the critical region by Eq. (5.1) and by other equations. The uncertainty of the experimental data in this region corresponds roughly to the size of the symbols plotted.

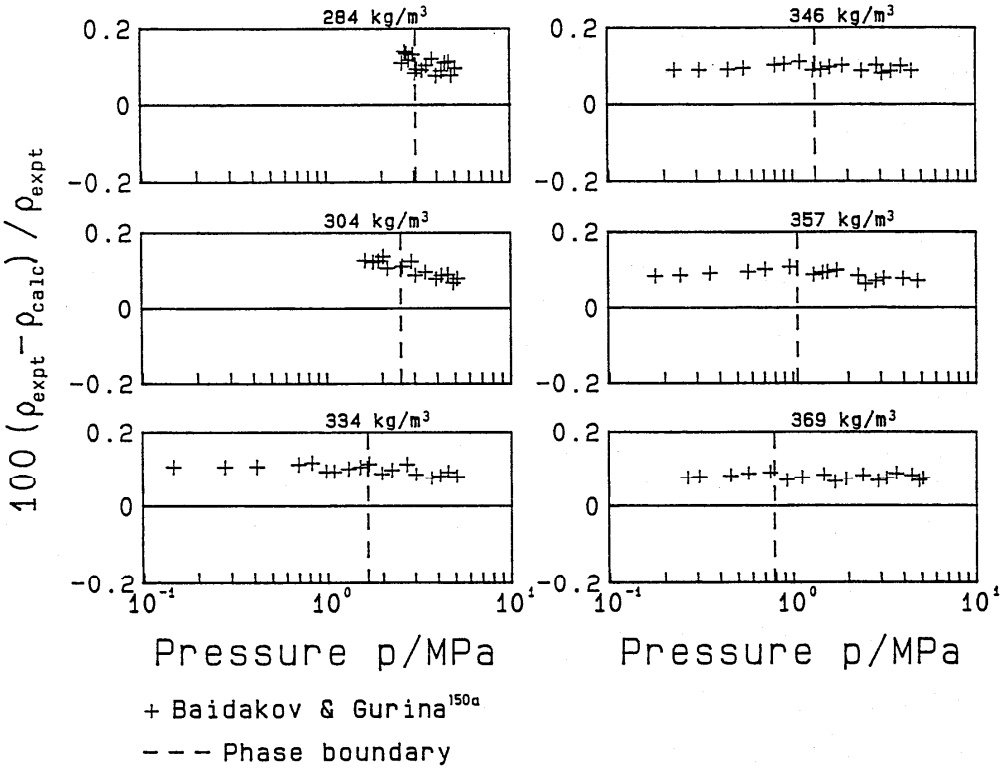

FIG. 32. Percentage density deviation of experimental $p\rho T$ data on six selected isochores in the metastable region from values calculated from Eq. (5.3).

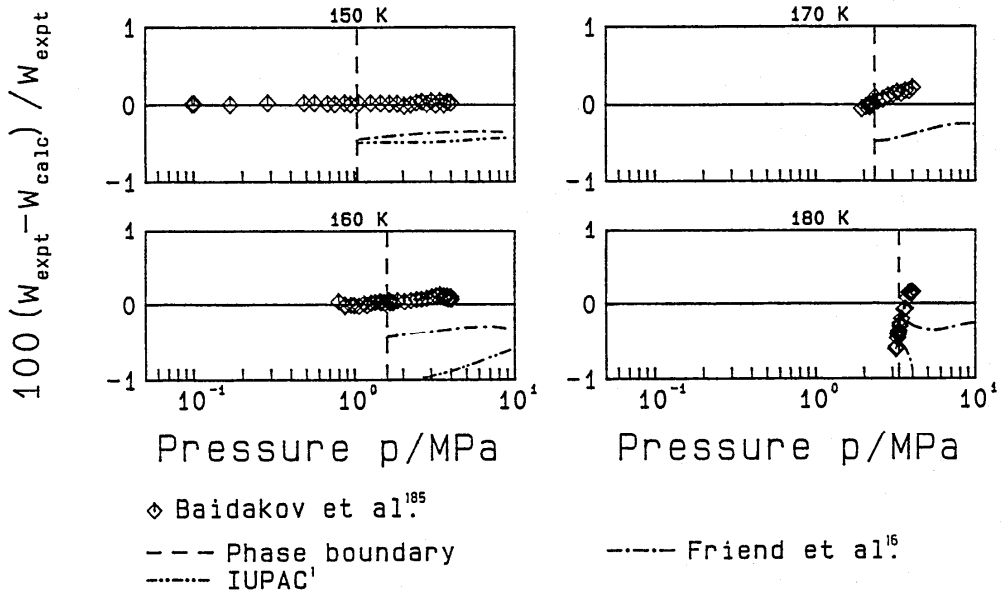

FIG. 33. Percentage deviation of the experimental speed of sound data in the metastable region from values calculated from Eq.(5.1).

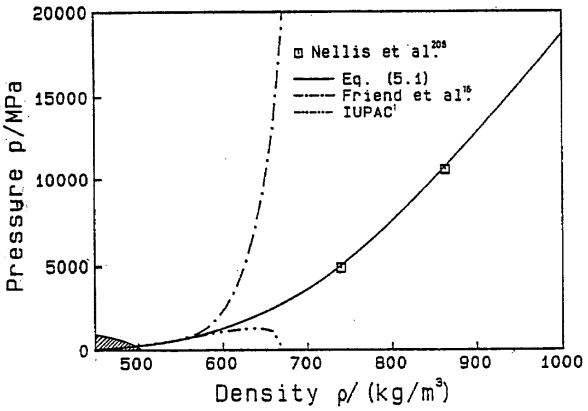

FIG. 34. The experimental Hugoniot data in comparison with corresponding values calculated from Eq. (5.1) and from other equations. The hatched area corresponds to the region where Eq. (5.1) has been fitted to experimental data.

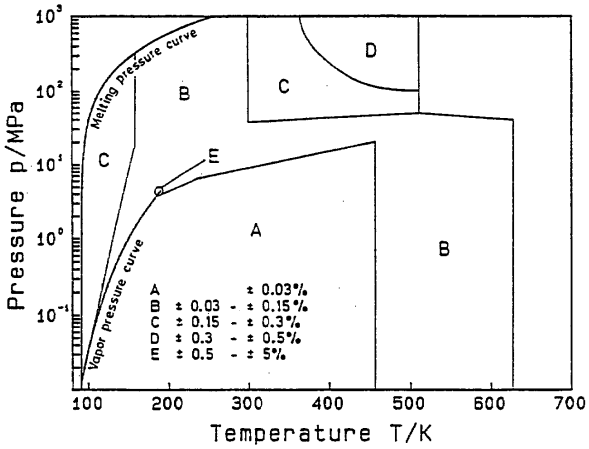

FIG. 36. Tolerance diagram for speed of sound. In the uncertainty statement for the region E, the temperature range $(T-T_c) <$ 0.3 K is excluded. The values for the uncertainties correspond to twice the standard deviation.

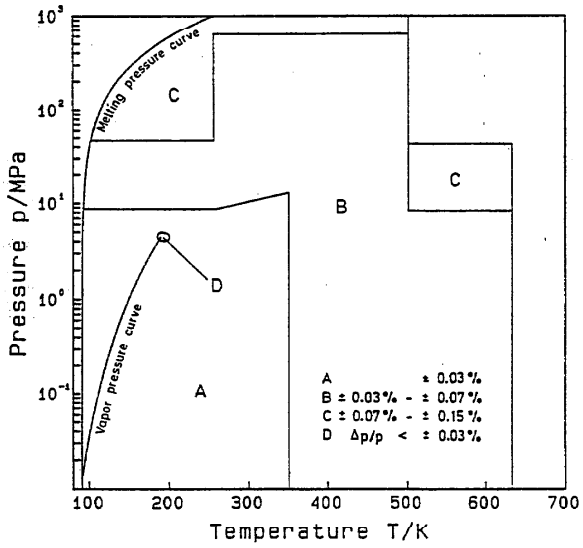

FIG. 35. Tolerance diagram for density (in region D the percentage pressure uncertainty is given). The values for the uncertainties correspond to twice the standard deviation.

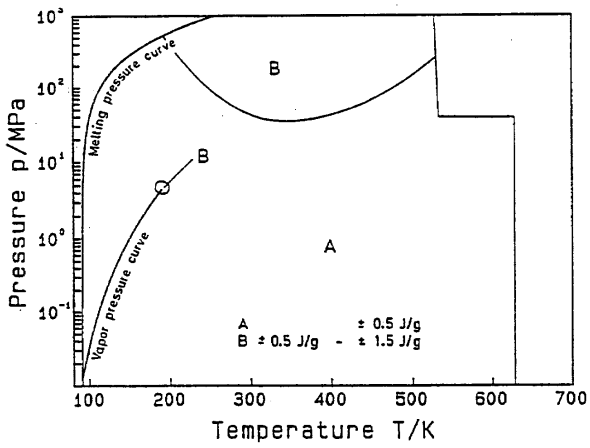

FIG. 37. Tolerance diagram for enthalpy. The values for the uncertainties correspond to twice the standard deviation.

8. Conclusions

Based on recent experimental data on the thermodynamic properties of methane, a new fundamental equation for the Helmholtz energy has been developed which covers the temperature range from 90 K to 625 K at pressures up to 1000 MPa. With the help of a new optimization procedure[18], we have established correlation equations which offer a state-of-the-art representation of the thermodynamic properties of methane.

The new equation of state, Eq. (5.1), which corresponds to the new temperature scale ITS–90, represents nearly all experimental thermal and caloric data, which are considered to be reliable, within the experimental uncertainty. This statement is not only valid for the homogeneous phases, but also for the vapor-liquid coexistence curve and even for the critical region. Furthermore, the equation allows a meaningful extrapolation for pressures up to 20000 MPa.

Based on the high overall accuracy, the ability of a reasonable representation of the critical region, and the extrapolation capability, the new formulation is a significant improvement in comparison to existing studies.

9. Acknowledgments

The authors are grateful to the Deutsche Forschungsgemeinschaft for their financial support of this project. We are indebted to P. J. Kortbeek, E. C. Morris, H. J. Achtermann, G. Magnus, G. Händel, and N. Pieperbeck for providing a copy of their experimental data prior to publication. We would also like to thank very much A. Pruss and H. Müller for their comprehensive help in converting all the equations to the ITS–90 temperature scale, for producing the figures on the computer and checking all the equations and tables.

10. References

[1]S. Angus, B. Armstrong, and K. M. de Reuck, *International Tables of the Fluid State - Methane*, International Union of Pure and Applied Chemistry (Pergamon Press, Oxford, 1978), Vol. 5.
[2]R. Kleinrahm and W. Wagner, J. Chem. Thermodyn. **18**, 739 (1986).
[3]R. Kleinrahm, W. Duschek, and W. Wagner, J. Chem. Thermodyn. **18**, 1103 (1986).
[4]R. Kleinrahm, W. Duschek, W. Wagner, and M. Jaeschke, J. Chem. Thermodyn. **20**, 621 (1988).
[5]G. Händel, R. Kleinrahm, and W. Wagner, *Measurement of the (pressure, density, temperature) relation of methane in the homogeneous gas and liquid region in the temperature range from 100 K to 260 K at pressures up to 8 MPa,* Submitted to J. Chem. Thermodyn. (1991).
[6]A. Sivaraman and B. E. Gammon, *"Speed-of-sound measurements in natural gas fluids,"* Gas Research Institute Report 86/0043, 1986.
[7]E. Bender, *Equation of state representing the phase behaviour of pure substances*, Proceedings of the 5th Symposium on Thermophysical Properties (American Society of Mechanical Engineers, New York, 1970), pp. 227–235.
[8]R. D. Goodwin, *The Thermophysical Properties of Methane, from 90 to 500 K at Pressures up to 700 bar*, Nat. Bur. Stand. (US), Tech. Note 653, 1974.
[9]R. D. McCarty, Cryogenics **14**, 276 (1974).
[10]V. V. Sytchev, A. A. Vasserman, V. A. Zagoruchenko, A. D. Kozlov, G. A. Spiridonov, and V. A. Tsymarny, *Thermodynamic Properties of Methane*, (Hemisphere Publishing Corporation, Washington, 1987), originally published by Standards Publishers, Moscow, 1979.
[11]J. F. Ely and H. J. M. Hanley, Ind. Engr. Chem. Fund. **3**, 323 (1981).
[12]U. Sievers and S. Schulz, VDI-Forschungsh. 622 (1984).
[13]D. D. Erickson and T. W. Leland, Int. J. Thermophys. **7**, 911 (1986).
[14]B. A. Younglove and J. F. Ely, J. Phys. Chem. Ref. Data **16**, 577 (1987).
[15]D. S. Kurumov, G. A. Olchowy, and J. V. Sengers, Int. J. Thermophys. **9**, 73 (1988).
[16]D. G. Friend, J. F. Ely, and H. Ingham, J. Phys. Chem. Ref. Data **18**, 583 (1989).
[17]M. Benedict, G. B. Webb, and L. C. Rubin, J. Chem. Phys. **8**, 334 (1940).
[18]U. Setzmann and W. Wagner, Int. J. Thermophys. **10**, 1103 (1989).
[19]R. D. Goodwin and R. Prydz, J. Res. Nat. Bur. Stand. Sec. A **76**, 81 (1972).
[20]D. R. Douslin, R. H. Harrison, R. T. Moore, and F. P. McCullough, J. Chem. Eng. Data **9**, 358 (1964).
[21]V. M. Cheng, Ph. D. Thesis, Princeton University, 1972.
[22]N. Pieperbeck, R. Kleinrahm, W. Wagner, and M. Jaeschke, J. Chem. Thermodyn. **23**, 175 (1991).
[23]H. J. Achtermann, J. Hong, W. Wagner, and A. Pruss, *Refractive Index and Density Isotherms for Methane from 273 K to 373 K and at Pressures to 34 MPa,* Submitted to J. Chem. Eng. Data (1991).
[24]H. Preston-Thomas, Metrologia **27**, 3 (1990).
[24a]*Supplementary Information for the ITS–90.* International Bureau of Weights and Measures: Pavillo Breteuil, F–92312 Sevres, France, 1990.
[25]U. Sievers and S. Schulz, Abstract: Chemie-Ing.-Techn. **53**, 741 (1981), Complete Text: Chemie-Ing.-Techn. MS 933/81.
[26]U. Setzmann, *Eine neue Methode zur Optimierung thermodynamischer Korrelationsgleichungen und ihre Anwendung zur Aufstellung einer Fundamentalgleichung für Methan.* Fort.-Ber. VDI-Z. Reihe 3, Heft 192 (1989).
[27]D. R. Lovejoy, Nature **197**, 353 (1963).
[28]J. C. G. Calado, G. A. Garcia, and L. A. Staveley, J. Chem. Soc., Faraday Trans. I **70**, 1445 (1974).
[29]A. J. Kidnay, K. L. Lewis, J. C. G. Calado, and L. A. K. Staveley, J. Chem. Thermodyn. **7**, 847 (1975).
[30]F. Pavese, G. Cagna, and D. Ferri, *The triple point of pure methane*, Proceedings of the 6th International Cryogenic Conference, IPC Science and Technology 1976, pp. 281–285.
[31]J. Bonhoure and R. Pello, Metrologia **14**, 175 (1978).
[32]A. Inaba and K. Mitsui, Jap. J. Appl. Phys. **17**, 1451 (1978).
[33]J. Bonhoure and R. Pello, Metrologia **16**, 95 (1980).
[34]F. Pavese, Metrologia **17**, 35 (1981).
[35]W. Blanke, PTB-Mitteilungen **93**, 230 (1983).
[36]R. E. Bedford, G. Bonnier, H. Maas, and F. Pavese, Metrologia **20**, 145 (1984).
[37]F. Pavese, J. Ancsin, D. N. Astrov, J. Bonhoure, G. Bonnier, G. T. Furukawa, R. C. Kemp, H. Maas, R. L. Rusby, H. Sakurai, and Ling Shan-Kang, Metrologia **10**, 127 (1984).
[38]K. Olszewski, Compt. Rend. Acad. Sci. **100**, 940 (1885).
[39]M. A. Hunter, J. Phys. Chem. **10**, 330 (1906).
[40]F. Henning and A. Stock, Z. Physik **4**, 226 (1921).
[41]F. G. Keyes, L. B. Smith, and D. B. Joubert, J. Math. Phys. **1**, 191 (1922).
[42]S. Young, Proc. Roy. Irish Acad. **38**, 65 (1928).
[43]F. G. Brickwedde and R. B. Scott, Data were published in Ref. 44.
[44]G. T. Armstrong, F. G. Brickwedde, and R. B. Scott, J. Res. Nat. Bur. Stand. **55**, 39 (1955).
[45]O. T. Bloomer and J. D. Parent, Chem. Eng. Prog. Symp. Ser. **49**, 11, (1953).
[46]D. L. Timrot and N. V. Pavlovich, *Thermodynamic properties of methane at low temperatures and high pressures*, In: Scientific reports of colleges Energetics, Sovetskaya Nauka Publishing House, Moscow, 137, (1959).
[47]K. Clusius, F. Endtinger, and K. Schleich, Helv. Chim. Acta **43**, 1267 (1960).
[48]P. Hestermans and D. White, J. Phys. Chem. **65**, 362 (1961).

[48a]C. S. Matthews and C. O. Hurd, Trans. Am. Inst. Chem. Engnrs. **42**, 55 (1946).
[48b]A. J. Vennix, Ph. D. Thesis, Rice University (1966).
[50]A. J. Vennix, T. W. Leyland, and R. Kobayashi, Advances in Cryogenic Engineering **12**, 700 (1966).
[51]A. J. Vennix and R. Kobayashi, A. I. Ch. E. J. **15**, 926 (1969).
[52]A. F. Grigor and W. A. Steele, J. Chem. Phys. **48**, 1032 (1968)
[53]F. P. Ricci and E. Scafè, Phys. Lett. **29A**, 650 (1969).
[54]V. Jansoone, H. Gielen, J. de Boelpaep, and O. Verbeke, Physica **46**, 213 (1970).
[55]R. D. Goodwin, *Dielectric constants and orthobaric densities of methane*, Appendix C, Survey of Current Information on LNG and Methane, NBSIR, 73–300, U. S. Dept. of Commerce (1973).
[56]H. Gielen, V. Jansoone, and O. Verbeke, J. Chem. Phys. *59, 5763* (1973).
[57]J. D. Olson, J. Chem. Phys. **63**, 474 (1975).
[57a]W. Duschek, R. Kleinrahm, and W. Wagner, J. Chem. Thermodyn. **22**,827 (1990).
[57b]W. Duschek, R. Kleinrahm, and W. Wagner, J. Chem. Thermodyn. **22**, 841 (1990).
[58]F. A. Freeth and T. T. H. Verschoyle, Proc. R. Soc. A **130**, 453 (1931).
[59]K. Clusius and K. Weigand, Z. Phys. Chemie **46B**, 1 (1940).
[60]J. C. Stryland, J. E. Crawford, and M. A. Mastoor, Can. J. Phys. **38**, 1546 (1960).
[61]L. E. Reeves, G. J. Scott, and S. E. Babb, J. Chem. Phys. *40, 3662* (1964).
[62]J. D. Grace and G. C. Kennedy, J. Phys. Chem. Solids **28**, 977 (1967).
[63]M. Nunes Da Ponte and L. A. K. Staveley, J. Chem. Thermodyn. **8**, 1109 (1976).
[64]R. Prydz and R. D. Goodwin, J. Chem. Thermodyn. **4**, 127 (1972).
[65]V. M. Cheng, W. B. Daniels, and R. K. Crawford, Phys. Rev. **B 11**, 3972 (1975).
[66]R. M. Hazen, H. K. Mao, L. W. Finger, and P. M. Bell, Appl. Phys. Lett. **37**, 288 (1980).
[67]H. Wieldraaijer, J. A. Schouten, and N. J. Trappeniers, High Temperature- High Pressure *15, 87 (1983)*.
[68]P. J. Kortbeek, S. N. Biswas, and N. J. Trappeniers, Physica **139&140B**, 109 (1986).
[69]P. J. Kortbeek, *Melting pressures of methane*, Private communication.
[70]P. J. McElroy, R. Battino, and M. K. Dowd, J. Chem. Thermodyn. **21**, 1287 (1989).
[71]A. Van Itterbeek, K. Staes, O. Verbeke, and F. Theeuwes, Physica **30**, 1896 (1964).
[72]A. J. Cutler and J. A. Morrison, Trans. Faraday Soc. **61**, 429 (1965).
[73]W. Van Dael, A. Van Itterbeek, J. Thoen, and A. Cops, Physica **31**, 1643 (1965).
[74]A. F. Grigor, P. D. Thesis, Dept. of Chem., Pennsylvania State Univ., 1966.
[75]A. J. Vennix, T. W. Leyland, and R. Kobayashi, J. Chem. Eng. Data **15**, 128 (1970).
[76]W. E. DeVaney, H. L. Rhodes, and P. C. Tully, J. Chem. Eng. Data **16**, 158 (1971).
[77]Y.-P. Liu and R. C. Miller, J. Chem. Thermodyn. **4**, 85 (1972).
[78]G. A. Pope, Ph. D. Thesis, Rice University (1972).
[79]G. E. Douglas, J. Chem. Eng. Data **19**, 71 (1974).
[80]B. E. Gammon and D. R. Douslin, J. Chem. Phys. **64**, 203 (1976).
[81]J. C. G. Calado and V. A. M. Soares, J. Chem. Soc. Faraday Trans. **I73**, 1271 (1977).
[82]R. Kleinrahm and W. Wagner, Fortschr.-Ber. VDI-Z. Reihe 3, Nr. 92 (1984).
[83]E. Cardoso, J. Chim. Phys. **13**, 312 (1915).
[84]O. B. Verbeke, *The dielectric constant of fluid methane in the vicinity of the critical point*, Unpublished manuscript, April 1973, Data were published in Ref. 8.
[85]S. Fuks, J. C. Legros, and A. Bellemans, Physica **31**, 606 (1965).
[86]A. J. Davenport, J. S. Rowlinson, and G. Saville, Trans. Faraday Soc. **62**, 322 (1966).
[87]J. E. Sinor and F. Kurata, J. Chem. Eng. Data **11**, 1 (1966).
[88]J. Klosek and C. McKinley, *Densities of LNG and of low molecular weight hydrocarbons*, Proc. First International Conference on LNG, Session 5, Paper 22, Chigaco 1968.
[89]M. J. Shana'a and F. B. Canfield, Trans. Faraday Soc. **64**, 2281 (1968).
[90]R. H. Jensen and F. Kurata, J. Petrol. Technol. **21**, 683 (1969).
[91]M. J. Terry, J. T. Lynch, M. Bunclark, K. R. Mansell, and L. A. K. Staveley, J. Chem. Thermodyn. **1**, 413 (1969).
[92]J. B. Rodosevich and R. C. Miller, A. I. Ch. E. J. **19**, 729 (1973).
[93]J. Orrit and J. Olives, *Density of liquefied natural gas and its components*, Distributed at the 4th International Conf. on LNG, Algeria, 1974.
[94]C. R. McClune, Cryogenics **16**, 289 (1976).
[95]J. E. Orrit and J. M. Laupretre, Adv. Cryog. Eng. **21**, 573 (1976).
[96]W. M. Haynes and M. J. Hiza, J. Chem. Thermodyn. **9**, 179 (1977).
[97]A. Frank and K. Clusius, Z. Phys. Chem. **B42**, 396 (1939).
[98]M. L. Jones, D. T. Mage, R. C. Faulkner, and D. L. Katz, Chem. Engng. Proc. Symp. Ser. **59**, 52 (1963).
[99]J. H. Colwell, E. K. Gill, and J. A. Morrison, J. Chem. Phys. **50**, 2041 (1964).
[100]A. Eucken and E. Karwat, Z. Phys. Chem. **112**, 467 (1924).
[101]K. Clusius, Z. Phys. Chemie **B3**, 41 (1929).
[102]R. Wiebe and M. J. Brevoort, J. Am. Chem. Soc. **52**, 622 (1930).
[103]B. A. Younglove, J. Res. NBS **78**, 401 (1974).
[104]H. M. Roder, J. Res. NBS **80A**, 739 (1976).
[105]A. Van Itterbeek and L. Verhagen, Proc. Phys. Soc. **62**, 800 (1949).
[106]Yu. P. Blagoi, A. E. Butko, S. A. Mikhailenko, and V. V. Yakuba, Russ. J. Phys. Chem. **41**, 908 (1967).
[107]G. C. Straty, Cryogenics **14**, 367 (1974).
[108]G. C. Straty, Cryogenics **15**, 729 (1975).
[109]H. J. Achtermann, T. K. Bose, H. Rögener, and J. M. St.-Arnaud, Int. J. Thermophys. **7**, 709 (1986).
[110]H. E. Tester, *Thermodynamic functions of gases, Vol. 3 Ethane, Methane and Nitrogen*, Editor: F. Din, Butterworths, London (1961).
[111]H. W. Schamp, E. A. Mason, A. C. B. Richardson, and A. Altman, Physics of Fluids **1**, 329 (1958).
[112]D. R. Roe, P. D. Thesis, Department of Chem. Eng. and Chem. Technology, Imperial College, London (1972).
[113]N. J. Trappeniers, R. Wassenaar, and J. C. Abels, Physica **98A**, 289 (1979). Erratum: Physica **100A**, 660 (1980).
[114]E. C. Morris, Int. J. Thermophys. **5**, 281 (1984).
[115]E. C. Morris, Private communication, 1987.
[116]J. Mollerup, J. Chem. Thermodyn. **17**, 489 (1985).
[117]M. Jaeschke and H. M. Hinze, *Ermittlung des Realgasverhaltens von Methan und Stickstoff und deren Gemischen im Temperaturbereich von 270 K bis* 350 K und Drücken *bis* 30 MPa. Fortschr.-Ber. VDI, Reihe 6, Nr. 262 (1991).
[118]P. J. Kortbeek and J. A. Schouten, Int. J. Thermophys. **11**, 455 (1990).
[119]E. H. Amagat, Annls. Chim. Phys. **22**, 353 (1881).
[120]F. G. Keyes and H. G. Burks, J. Am. Chem. Soc. **49**, 1403 (1927).
[121]F. A. Freeth and T. T. H. Verschoyle, Proc. R. Soc. **A130**, 453 (1931).
[122]H. M. Kvalnes and V. L. Gaddy, J. Am. Chem. Soc. **53**, 394 (1931).
[123]A. Michels and G. W. Nederbragt, Physica **2**, 1000 (1935).
[124]A. Michels and G. W. Nederbragt, Physica **3**, 369 (1936).
[125]R. H. Olds, H. H. Reamer, B. H. Sage, and W. N. Lacey, Ind. Eng. Chem. **35**, 992 (1943).
[126]Y. S. Kazarnovskii and G. T. Levchenko, Zurnal fiziceskoj chimii **18**, 380 (1944).
[127]N. V. Pavlovich and D. L. Timrot, Teploenergetika **5**, 69 (1958).
[128]K. Date and G. Kobuya, Bull. Chem. Res. Inst. Non Aqueous Solutions **10**, 67 (1961).
[129]W. H. Mueller, T. W. Leyland, and R. Kobayashi, A. I. Ch. E. J. **6**, 267 (1961).
[130]A. Van Itterbeek, O. Verbeke, and K. Staes, Physica **29**, 742 (1963).
[131]L. Deffet, L. Lialine, and F. Ficks, Industrie chim. belge **9**, 879 (1964).
[132]O. A. Dobrovolskij, T. N. Belyaeva, and I. F. Golubev, Gazovaja Promyslennost **9**, 47 (1964).
[133]C. B. Wallace, I. H. Silberberg, and J. J. McKetta, Hydrocarbon Processing **43**, 177 (1964).

[134]A. E. Hoover, Ph. D. Thesis, Rice University (1966).
[135]E. T. S. Huang, Ph. D. Thesis, University of Kansas (1966).
[136]A. M. Mamedov and A. R. Mamedov, Izvestiya Vysshikh nchebuytch zavedenii, Neft i gaz **12**, 71 (1969).
[137]H. H. Jr. McMath and W. C. Edmister, A. I. Ch. E. J. **15**, 370 (1969).
[138]S. L. Robertson and S. E. Babb, J. Chem. Phys. **51**, 1357 (1969).
[139]A. D. Epperly, Ph. D. Thesis, University of Missouri, Columbia (1970).
[140]V. A. Sorokin and Yu. P. Blagoy, in: Thermodinamiceskije i thermokhimiceskije konstanty, Editor: K. V. Astochov, Nauka Publishing House, Moscow, 97–101 (1970).
[141]D. S. Tsiklis, L. R. Linshits, and S. S. Tsimmerman, DAN SSSR **198**, 384 (1971).
[142]J. B. Rodosevich and R. C. Miller, A. I. Ch. E. J. **19**, 729 (1973).
[143]A. R. Bazaev and V. G. Skripka, Gazov. Prom.- st **12**, 44 (1974).
[144]S. Mihara, H. Sagara, Y. Arai, and S. Saito, J. Chem. Eng. Japan **19**, 395 (1977).
[145]A. Z. Francesconi, Ph. D. Thesis, Universität Fridericiana Karlsruhe (1978).
[146]M. Nunes Da Ponte, W. B. Streett, and L. A. K. Staveley, J. Chem. Thermodyn. **10**, 151 (1978).
[147]H. J. Achtermann, F. Klobasa, and H. Rögener, Brennst.-Wärme-Kraft **34**, 266 (1982).
[148]H. J. Achtermann, F. Klobasa, and H. Rögener, Brennst.-Wärme-Kraft **34**, 311 (1982).
[149]M. M. Amer, Ph. D. Thesis, University of Missouri (1986).
[150]J. R. S Machado, W. B. Streett, and U. Deiters, J. Chem. Eng. Data **33**, 148 (1988).
[150a]V. G. Baidakov and T. A. Gurina, J. Chem. Thermodyn. **21**, 1009 (1989).
[151]W. Lemming, Fortschr.-Ber. VDI-Z. Reihe 19, Nr. 32 (1989).
[152]J. A. Beattie and W. H. Stockmeyer, J. Chem. Phys. **10**, 473 (1942).
[153]S. D. Hamann, J. A. Lambert, and P. B. Thomas, Austr. J. Chem. **8**, 149 (1955).
[154]R. D. Gunn, M. S. Thesis, University of California, Berkley (1958). Data taken from: J. A. Huff and T. M. Reed, J. Chem. Engng. Data **8**, 306 (1963).
[155]G. Thomaes and R. van Steenwinkel, Nature **187**, 229 (1960).
[156]J. Brewer, *Determination of mixed virial coefficients*, US Air Force Report AFOSR No. 67–2795 (1967).
[157]M. A. Byrne, M. R. Jones, and L. A. K. Staveley, Trans. Faraday Soc. **64**, 1747 (1968).
[158]A. E. Hoover, I. Nagata, T. W. Jr. Leland, and R. Kobayashi, J. Chem. Phys. **48**, 2633 (1968).
[159]R. N. Lichtenthaler and K. Schäfer, Ber. Bunsenges. Phys. Chem. **73**, 42 (1969).
[160]R. C. Lee and W. C. Edmister, A. I. Ch. E. J. **16**, 1047 (1970).
[161]K. Strein, R. N. Lichtenthaler, B. Schramm, and K. Schäfer, Ber. Bunsenges. Phys. Chem. **75**, 1308 (1971).
[162]J. Bellm, W. Reinecke, K. Schäfer, and B. Schramm, Ber. Bunsenges. Phys. Chem. **78**, 282 (1974).
[163]R. Hahn, K. Schäfer, and B. Schramm, Ber. Bunsenges. Phys. Chem. **78**, 287 (1974).
[164]K. Kerl and H. Häusler, Ber. Bunsenges. Phys. Chem. **88**, 992 (1984).
[165]R. Budenholzer, B. Sage, and W. Lacey, Ind. Engng. Chem. **31**, 369 (1939).
[166]P. N. Sahgal, J. M. Geist, A. Jambhekar, and G. M. Wilson, Adv. Cry. Eng. **10**, 224 (1964).
[167]R. Ayber, VDI-Forsch.-Heft **511**, 1 (1965).
[168]D. D. Dillard, W. C. Edmister, J. H. Erbar, and R. L. Jr. Robinson, A. I. Ch. E. J. **14**, 923 (1968).
[169]R. A. Dawe and P. N. Snowdon, J. Chem. Eng. Data **19**, 220 (1974).
[170]P. H. G. Kasteren and H. Zeldenrust, Ind. Eng. Chem. Fundam. **18**, 333 (1979).
[171]W. Heuse, Ann. Physik **56**, 86 (1919).
[172]R. W. Millar, J. Am. Chem. Soc. **45**, 874 (1923).
[173]A. Eucken and K. von Lüde, Z. Phys. Chem. **B5**, 413 (1929).
[174]F. A. Giacomini, Phil. Mag. **50**, 146 (1925).
[175]A. Eucken and W. Berger, Z. Gesamte Kälte-Ind. **41**, 145 (1934).
[176]H. B. Dixon, C. Campball, and A. Parker, Proc. Roy. Soc., London **A100**, 1 (1921).
[177]T. H. Quingley, Phys. Rev. **67**, 298 (1945).
[178]A. Lacam, J. Rech. CNRS **35**, 26 (1956).
[179]E. Terres, W. Jahn, and H. Reissmann, Brennstoff-Chemie **38**, 129 (1957)
[180]A. Van Itterbeek, J. Thoen, A. Cops, and W. van Dael, Physica **35**, 162 (1967).
[181]J. R. Singer, J. Chem. Phys. **51**, 4729 (1969).
[182]M. J. Cardamone, T. T. Saito, D. P. R. Eastman, and D. H. Rank, J. Opt. Soc. Amer. **60**, 1264 (1970).
[183]L. L. Pitaevskaya and A. V. Bilevich, Russ. J. Phys. Chem. **46**, 1390 (1972).
[184]E. K. Dregulyas, Teplofiziceskie svojstva uglevodorodov ich smesej neftej i neftjanych frakcii, Nauc.-tech. sbornik **1**, 138 (1973).
[185]V. G. Baidakov, A. M. Kaverin, and V. P. Skripov, J. Chem. Thermodyn. **14**, 1003 (1982).
[186]P. J. Kortbeek, Private communication (1986).
[187]A. R. H. Goodwin, Ph. D. Thesis, University of London (1988).
[188]R. A. McDowell and F. H. Kruse, J. Chem. Engng. Data **7**, 547 (1963).
[189]W. Bahro, Kältetechnik **17**, 219 (1965).
[190]V. P. Glusko, (ed.), *Thermodynamic properties of individual substances,* Vol. 8, Moscow, Izdatel'stvo AN SSSR (1979).
[191]TRC Hydrocarbon Project, *Selected values of properties of hydrocarbons and related compounds*. TRC Table 23–2–(1. 200)–v^r (1982).
[191a]TRC Hydrocarbon Project, *Selected values of properties of hydrocarbons and related compounds*. TRC Table 23–2–(1. 2001)–JJ, page 8, (1987).
[192]W. Wagner, Fortschr.-Ber. VDI-Z. Reihe 3, Nr. 39 (1974).
[193]W. Wagner, Report PC/T15, IUPAC Thermodynamic Table Project Centre, Imperial College, London (1977).
[194]W. Wagner, Cryogenics **13**, 470 (1973).
[195]W. Wagner, J. Ewers, and W. Pentermann, J. Chem. Thermodyn. **8**, 1049 (1976).
[196]M. Jahangiri, R. T. Jacobsen, R. B. Stewart, and R. D. McCarty, J. Phys. Chem. Ref. Data. **15**, 593 (1986).
[197]M. Waxman and J. S. Gallagher, J. Chem. Eng. Data **28**, 224 (1983).
[198]A. Saul and W. Wagner, J. Phys. Chem. Ref. Data **18**, 1537 (1989).
[199]K. M. de Reuck and B. Armstrong, Cryogenics **19**, 505 (1979).
[200]J. Ewers and W. Wagner, VDI-Forsch.-Heft **609**, 27, 1982.
[201]J. Ewers and W. Wagner, *A method for optimizing the structure of equation of state and its application to an equation of state for oxygen.* In: Proceedings of the 8th Symposium on Thermophysical Properties, edited by J. V. Sengers, American Society of Mechanical Engineers, New York, pp. 78–87 (1982).
[202]L. Haar, J. S. Gallagher, and G. S. Kell, *The Anatomy of the thermodynamic Surface of water: the formulation and comparisons with data*, In: Proceedings of the 8th Symposium on Thermophysical Properties, edited by J. V. Sengers, American Society of Mechanical Engineers, New York, pp. 228–300 (1982).
[203]R. Fletcher, *A modified Marquardt subroutine for nonlinear least squares*, United Kingdom Atomic Authority Research Group Report AERE–R6799, Harwell (1971).
[204]V. Marx, Dissertation, Ruhr-Universität Bochum (1989).
[205]R. Schmidt, Dissertation, Ruhr-Universität Bochum (1983).
[206]R. Schmidt and W. Wagner, Fluid Phase Equilibria **19**, 175 (1985).
[207]W. Wagner and K. M. de Reuck, *International Thermodynamic Tables of the Fluid State - 9 Oxygen*, International Union of Pure and Applied Chemistry, Blackwell Scientific Publications, Oxford (1987).
[208]W. J. Nellis, F. M. Ree, M. van Thiel, and A. C. Mitchell, J. Chem. Phys. **75**, 3055 (1981).
[209]Pure Appl. Chem. **58**, 1677 (1986).
[210]E. R. Cohen and B. N. Taylor, *The 1986 Adjustment of the Fundamental Physical Constants.* CODATA Bulletin No. 63. Committee on Data for Science and Technology, Int. Council of Scientific Unions. Pergamon Press, Oxford (1986).

Appendix: Thermodynamic Properties of Methane

In order to preserve thermodynamic consistency, all values presented in Tables 39 and 40 were calculated only from the fundamental equation, Eq. (5.1). Ideally, each entry in these tables should be given to one more significant figure than the input data warrant, as an assurance of smoothness and a guard against inaccuracy in interpolation. A strict adherence to this principle is difficult, and a possible conflict has always been avoided by including more figures than are strictly necessary.

Table 39. Thermodynamic properties of saturated methane

Temperature K	Pressure MPa	Density kg/m³	Enthalpy kJ/kg	Entropy kJ/(kg K)	c_v kJ/(kg K)	c_p kJ/(kg K)	Speed of sound m/s
90.694[a]	0.011696	451.48	−982.76	−7.3868	2.1677	3.3678	1538.6
		0.25074	−438.50	−1.3857	1.5735	2.1100	249.13
92	0.013801	449.73	−978.36	−7.3386	2.1593	3.3723	1526.7
		0.29197	−435.95	−1.4429	1.5753	2.1141	250.76
94	0.017613	447.05	−971.60	−7.2661	2.1471	3.3801	1508.4
		0.36530	−432.08	−1.5265	1.5783	2.1209	253.20
96	0.022233	444.35	−964.82	−7.1948	2.1354	3.3888	1489.8
		0.45238	−428.25	−1.6055	1.5815	2.1284	255.57
98	0.027778	441.63	−958.03	−7.1249	2.1243	3.3982	1471.0
		0.55488	−424.46	−1.6804	1.5850	2.1367	257.87
100	0.034376	438.89	−951.21	−7.0562	2.1136	3.4084	1452.0
		0.67457	−420.73	−1.7514	1.5887	2.1458	260.09
102	0.042160	436.12	−944.37	−6.9887	2.1032	3.4193	1432.9
		0.81329	−417.04	−1.8188	1.5926	2.1558	262.24
104	0.051275	433.32	−937.51	−6.9222	2.0931	3.4308	1413.6
		0.97298	−413.42	−1.8829	1.5968	2.1667	264.31
106	0.061868	430.50	−930.62	−6.8568	2.0832	3.4429	1394.1
		1.1556	−409.85	−1.9440	1.6012	2.1785	266.29
108	0.074099	427.65	−923.70	−6.7925	2.0736	3.4557	1374.5
		1.3633	−406.35	−2.0022	1.6059	2.1914	268.20
110	0.088130	424.78	−916.75	−6.7290	2.0642	3.4692	1354.7
		1.5982	−402.92	−2.0578	1.6108	2.2053	270.01
112	0.10413	421.87	−909.78	−6.6665	2.0549	3.4835	1334.8
		1.8625	−399.56	−2.1110	1.6160	2.2203	271.75
114	0.12228	418.93	−902.77	−6.6049	2.0458	3.4986	1314.7
		2.1586	−396.28	−2.1620	1.6214	2.2364	273.39
116	0.14275	415.96	−895.73	−6.5441	2.0369	3.5145	1294.4
		2.4888	−393.07	−2.2108	1.6270	2.2539	274.94
118	0.16574	412.95	−888.65	−6.4841	2.0281	3.5314	1274.0
		2.8557	−389.95	−2.2578	1.6329	2.2727	276.40
120	0.19143	409.90	−881.54	−6.4248	2.0196	3.5493	1253.5
		3.2619	−386.93	−2.3030	1.6390	2.2930	277.76
122	0.22002	406.82	−874.38	−6.3662	2.0112	3.5683	1232.7
		3.7099	−383.99	−2.3466	1.6454	2.3148	279.03
124	0.25170	403.69	−867.18	−6.3084	2.0030	3.5886	1211.9
		4.2028	−381.15	−2.3888	1.6521	2.3384	280.21

Table 39. Thermodynamic properties of saturated methane — Continued

Temperature K	Pressure MPa	Density kg/m³	Enthalpy kJ/kg	Entropy kJ/(kg K)	c_v kJ/(kg K)	c_p kJ/(kg K)	Speed of sound m/s
126	0.28667	400.52	−859.94	−6.2511	1.9950	3.6102	1190.8
		4.7434	−378.42	−2.4295	1.6591	2.3638	281.28
128	0.32514	397.30	−852.65	−6.1945	1.9871	3.6333	1169.5
		5.3348	−375.79	−2.4690	1.6663	2.3912	282.25
130	0.36732	394.04	−845.31	−6.1384	1.9795	3.6580	1148.1
		5.9804	−373.28	−2.5074	1.6739	2.4208	283.13
132	0.41341	390.72	−837.92	−6.0829	1.9722	3.6845	1126.4
		6.6837	−370.88	−2.5447	1.6818	2.4528	283.90
134	0.46363	387.35	−830.47	−6.0278	1.9650	3.7130	1104.6
		7.4483	−368.61	−2.5811	1.6901	2.4875	284.57
136	0.51819	383.92	−822.96	−5.9732	1.9581	3.7437	1082.5
		8.2783	−366.47	−2.6167	1.6987	2.5252	285.13
138	0.57730	380.42	−815.38	−5.9191	1.9515	3.7769	1060.2
		9.1779	−364.46	−2.6515	1.7077	2.5662	285.58
140	0.64118	376.87	−807.74	−5.8653	1.9452	3.8129	1037.7
		10.152	−362.60	−2.6857	1.7172	2.6108	285.93
142	0.71006	373.24	−800.02	−5.8119	1.9391	3.8519	1014.9
		11.205	−360.89	−2.7194	1.7272	2.6596	286.16
144	0.78415	369.53	−792.22	−5.7587	1.9334	3.8944	991.81
		12.343	−359.33	−2.7525	1.7377	2.7131	286.29
146	0.86368	365.74	−784.34	−5.7059	1.9281	3.9407	968.46
		13.571	−357.95	−2.7853	1.7487	2.7718	286.30
148	0.94887	361.87	−776.37	−5.6532	1.9231	3.9916	944.81
		14.897	−356.74	−2.8179	1.7604	2.8366	286.19
150	1.0400	357.90	−768.30	−5.6007	1.9186	4.0474	920.85
		16.328	−355.71	−2.8502	1.7727	2.9083	285.97
152	1.1372	353.83	−760.12	−5.5484	1.9145	4.1091	896.54
		17.871	−354.89	−2.8824	1.7858	2.9880	285.63
154	1.2408	349.64	−751.83	−5.4961	1.9109	4.1775	871.87
		19.537	−354.28	−2.9146	1.7997	3.0771	285.16
156	1.3509	345.34	−743.41	−5.4438	1.9079	4.2537	846.82
		21.336	−353.89	−2.9470	1.8145	3.1772	284.57
158	1.4680	340.90	−734.85	−5.3915	1.9055	4.3391	821.35
		23.279	−353.75	−2.9795	1.8303	3.2903	283.86
160	1.5921	336.31	−726.14	−5.3391	1.9037	4.4354	795.43
		25.382	−353.87	−3.0124	1.8473	3.4189	283.01
162	1.7235	331.57	−717.27	−5.2864	1.9028	4.5448	769.03
		27.660	−354.28	−3.0457	1.8655	3.5665	282.03
164	1.8626	326.64	−708.21	−5.2334	1.9027	4.6702	742.10
		30.132	−355.01	−3.0797	1.8852	3.7374	280.91
166	2.0096	321.50	−698.95	−5.1800	1.9037	4.8154	714.59
		32.822	−356.07	−3.1145	1.9066	3.9373	279.65

Table 39. Thermodynamic properties of saturated methane — Continued

Temperature K	Pressure MPa	Density kg/m³	Enthalpy kJ/kg	Entropy kJ/(kg K)	c_v kJ/(kg K)	c_p kJ/(kg K)	Speed of sound m/s
168	2.1647	316.14	−689.46	−5.1261	1.9059	4.9854	686.42
		35.758	−357.52	−3.1503	1.9300	4.1740	278.23
170	2.3283	310.50	−679.70	−5.0715	1.9095	5.1872	657.52
		38.974	−359.40	−3.1874	1.9556	4.4585	276.66
172	2.5007	304.56	−669.64	−5.0159	1.9149	5.4311	627.77
		42.514	−361.77	−3.2260	1.9840	4.8066	274.93
174	2.6822	298.25	−659.22	−4.9591	1.9225	5.7318	597.05
		46.434	−364.71	−3.2666	2.0157	5.2416	273.02
176	2.8732	291.50	−648.37	−4.9009	1.9330	6.1124	565.18
		50.808	−368.31	−3.3096	2.0515	5.8000	270.92
178	3.0740	284.21	−637.01	−4.8406	1.9473	6.6105	531.94
		55.740	−372.71	−3.3558	2.0925	6.5421	268.60
180	3.2852	276.23	−625.00	−4.7778	1.9669	7.2923	497.01
		61.375	−378.11	−3.4062	2.1404	7.5740	266.04
182	3.5071	267.33	−612.14	−4.7112	1.9944	8.2863	459.94
		67.940	−384.81	−3.4621	2.1977	9.1030	263.17
184	3.7405	257.14	−598.08	−4.6393	2.0346	9.8808	420.00
		75.810	−393.29	−3.5262	2.2688	11.592	259.89
186	3.9860	244.93	−582.19	−4.5586	2.0978	12.883	375.88
		85.704	−404.47	−3.6032	2.3620	16.333	255.97
188	4.2448	228.93	−562.88	−4.4612	2.2130	20.738	324.57
		99.377	−420.58	−3.7044	2.5001	28.774	250.72
190	4.5186	200.78	−532.67	−4.3082	2.6022	94.012	250.31
		125.18	−451.91	−3.8831	2.8546	140.81	238.55
190.564[b]	4.5992	162.66	−495.35	−4.1144			

[a]Triple point.
[b]Critical point.

Table 40. Thermodynamic properties of methane

Temperature K	Density kg/m³	Internal Energy kJ/kg	Enthalpy kJ/kg	Entropy kJ/(kg K)	c_v kJ/(kg K)	c_p kJ/(kg K)	Speed of sound m/s
			0.025 MPa Isobar				
90.698[a]	451.48	−982.78	−982.73	−7.3868	2.1677	3.3677	1538.7
92	449.74	−978.39	−978.34	−7.3387	2.1593	3.3723	1526.8
94	447.06	−971.64	−971.59	−7.2661	2.1471	3.3801	1508.4
96	444.35	−964.87	−964.82	−7.1949	2.1354	3.3888	1489.8
97.042[b]	442.94	−961.34	−961.28	−7.1582	2.1296	3.3936	1480.0
97.042[b]	0.50377	−475.90	−426.27	−1.6450	1.5833	2.1326	256.78
98	0.49864	−474.37	−424.23	−1.6241	1.5817	2.1298	258.11
100	0.48827	−471.18	−419.97	−1.5811	1.5787	2.1244	260.86
105	0.46421	−463.23	−409.38	−1.4778	1.5732	2.1141	267.60
110	0.44250	−455.33	−398.83	−1.3796	1.5694	2.1067	274.14

Table 40. Thermodynamic properties of methane – Continued

Temperature K	Density kg/m³	Internal Energy kJ/kg	Enthalpy kJ/kg	Entropy kJ/(kg K)	c_v kJ/(kg K)	c_p kJ/(kg K)	Speed of sound m/s
			0.025 MPa Isobar				
115	0.42278	−447.44	−388.31	−1.2861	1.5667	2.1012	280.50
120	0.40478	−439.58	−377.81	−1.1967	1.5647	2.0970	286.70
125	0.38828	−431.72	−367.34	−1.1112	1.5633	2.0938	292.75
130	0.37310	−423.88	−356.88	−1.0291	1.5622	2.0913	298.67
135	0.35908	−416.05	−346.42	−0.95024	1.5615	2.0894	304.47
140	0.34608	−408.22	−335.98	−0.87428	1.5610	2.0879	310.15
145	0.33401	−400.39	−325.54	−0.80104	1.5607	2.0867	315.71
150	0.32275	−392.57	−315.11	−0.73031	1.5606	2.0859	321.18
155	0.31224	−384.75	−304.68	−0.66192	1.5607	2.0854	326.54
160	0.30240	−376.93	−294.26	−0.59572	1.5609	2.0851	331.81
165	0.29316	−369.11	−283.83	−0.53156	1.5614	2.0851	336.99
170	0.28447	−361.29	−273.41	−0.46931	1.5621	2.0853	342.09
175	0.27629	−353.47	−262.98	−0.40885	1.5630	2.0858	347.09
180	0.26856	−345.64	−252.55	−0.35008	1.5641	2.0867	352.02
185	0.26126	−337.80	−242.11	−0.29290	1.5655	2.0878	356.87
190	0.25435	−329.96	−231.67	−0.23720	1.5673	2.0892	361.64
195	0.24779	−322.11	−221.22	−0.18291	1.5693	2.0910	366.34
200	0.24157	−314.25	−210.76	−0.12994	1.5716	2.0931	370.96
210	0.23001	−298.49	−189.80	−0.02769	1.5775	2.0986	380.00
220	0.21952	−282.67	−168.78	0.07009	1.5849	2.1057	388.75
230	0.20994	−266.76	−147.68	0.16388	1.5941	2.1147	397.24
240	0.20117	−250.76	−126.48	0.25410	1.6052	2.1255	405.47
250	0.19310	−234.63	−105.17	0.34112	1.6182	2.1383	413.45
260	0.18566	−218.37	−83.711	0.42527	1.6331	2.1530	421.19
270	0.17877	−201.95	−62.098	0.50683	1.6500	2.1698	428.71
280	0.17237	−185.35	−40.308	0.58608	1.6689	2.1885	436.00
290	0.16642	−168.55	−18.321	0.66323	1.6896	2.2091	443.09
300	0.16086	−151.53	3.8805	0.73849	1.7121	2.2315	449.98
310	0.15566	−134.29	26.315	0.81206	1.7363	2.2557	456.69
320	0.15079	−116.79	49.000	0.88407	1.7622	2.2815	463.22
330	0.14622	−99.030	71.949	0.95469	1.7895	2.3087	469.60
340	0.14191	−80.987	95.179	1.0240	1.8182	2.3374	475.82
350	0.13785	−62.652	118.70	1.0922	1.8482	2.3673	481.91
360	0.13402	−44.011	142.53	1.1593	1.8794	2.3984	487.86
370	0.13039	−25.054	166.67	1.2255	1.9115	2.4305	493.70
380	0.12696	−5.7706	191.14	1.2907	1.9446	2.4635	499.42
390	0.12370	13.847	215.95	1.3552	1.9785	2.4974	505.04
400	0.12061	33.807	241.09	1.4188	2.0130	2.5319	510.57
410	0.11766	54.116	266.59	1.4818	2.0483	2.5671	516.01
420	0.11486	74.780	292.43	1.5441	2.0840	2.6028	521.36
430	0.11219	95.803	318.64	1.6057	2.1202	2.6390	526.64
440	0.10964	117.19	345.21	1.6668	2.1568	2.6755	531.84
450	0.10720	138.94	372.15	1.7274	2.1936	2.7123	536.98
460	0.10487	161.07	399.46	1.7874	2.2307	2.7494	542.05
470	0.10264	183.56	427.14	1.8469	2.2681	2.7867	547.06
480	0.10050	206.43	455.20	1.9060	2.3055	2.8242	552.02
490	0.09844	229.68	483.63	1.9646	2.3431	2.8617	556.92
500	0.09648	253.30	512.43	2.0228	2.3807	2.8993	561.77
520	0.09276	301.67	571.17	2.1380	2.4560	2.9746	571.32

Table 40. Thermodynamic properties of methane — Continued

Temperature K	Density kg/m³	Internal Energy kJ/kg	Enthalpy kJ/kg	Entropy kJ/(kg K)	c_v kJ/(kg K)	c_p kJ/(kg K)	Speed of sound m/s
			0.025 MPa Isobar				
540	0.08933	351.54	631.41	2.2516	2.5311	3.0497	580.70
560	0.08614	402.92	693.16	2.3639	2.6059	3.1244	589.92
580	0.08317	455.78	756.39	2.4748	2.6801	3.1986	598.98
600	0.08039	510.12	821.10	2.5845	2.7538	3.2723	607.90
620	0.07780	565.93	887.27	2.6930	2.8267	3.3451	616.69
			0.050 MPa Isobar				
90.704[a]	451.49	−982.78	−982.67	−7.3867	2.1677	3.3676	1538.8
92	449.76	−978.41	−978.30	−7.3389	2.1594	3.3721	1527.0
94	447.08	−971.66	−971.55	−7.2663	2.1471	3.3799	1508.6
96	444.37	−964.89	−964.78	−7.1950	2.1355	3.3886	1490.0
98	441.65	−958.11	−957.99	−7.1251	2.1244	3.3981	1471.2
100	438.90	−951.30	−951.19	−7.0563	2.1136	3.4083	1452.2
103.738[b]	433.69	−938.52	−938.41	−6.9309	2.0944	3.4292	1416.1
103.738[b]	0.95080	−466.48	−413.89	−1.8747	1.5962	2.1652	264.04
105	0.93858	−464.43	−411.16	−1.8486	1.5933	2.1597	265.79
110	0.89331	−456.38	−400.41	−1.7485	1.5843	2.1426	272.54
115	0.85246	−448.38	−389.73	−1.6535	1.5782	2.1303	279.09
120	0.81535	−440.42	−379.10	−1.5631	1.5738	2.1212	285.44
125	0.78147	−432.49	−368.51	−1.4766	1.5706	2.1142	291.62
130	0.75039	−424.59	−357.96	−1.3938	1.5682	2.1087	297.65
135	0.72176	−416.70	−347.42	−1.3143	1.5664	2.1044	303.54
140	0.69529	−408.82	−336.91	−1.2379	1.5651	2.1010	309.30
145	0.67073	−400.96	−326.41	−1.1642	1.5642	2.0983	314.94
150	0.64788	−393.10	−315.93	−1.0931	1.5636	2.0962	320.47
155	0.62657	−385.25	−305.45	−1.0244	1.5633	2.0946	325.89
160	0.60663	−377.40	−294.98	−0.95790	1.5632	2.0934	331.22
165	0.58795	−369.56	−284.51	−0.89350	1.5634	2.0926	336.44
170	0.57039	−361.71	−274.05	−0.83103	1.5638	2.0921	341.58
175	0.55387	−353.87	−263.59	−0.77039	1.5645	2.0921	346.62
180	0.53828	−346.02	−253.13	−0.71145	1.5655	2.0924	351.58
185	0.52356	−338.17	−242.67	−0.65411	1.5668	2.0930	356.47
190	0.50963	−330.31	−232.20	−0.59828	1.5684	2.0941	361.27
195	0.49643	−322.45	−221.73	−0.54387	1.5703	2.0955	365.99
200	0.48390	−314.57	−211.25	−0.49079	1.5726	2.0973	370.64
210	0.46066	−298.79	−190.25	−0.38835	1.5783	2.1022	379.71
220	0.43956	−282.94	−169.19	−0.29041	1.5856	2.1089	388.51
230	0.42032	−267.02	−148.06	−0.19648	1.5947	2.1175	397.03
240	0.40270	−251.00	−126.84	−0.10615	1.6057	2.1280	405.28
250	0.38651	−234.86	−105.50	−0.01903	1.6186	2.1405	413.29
260	0.37157	−218.58	−84.020	0.06520	1.6335	2.1551	421.05
270	0.35775	−202.15	−62.388	0.14684	1.6504	2.1717	428.58
280	0.34493	−185.54	−40.580	0.22615	1.6692	2.1902	435.89
290	0.33299	−168.73	−18.578	0.30336	1.6899	2.2107	443.00
300	0.32185	−151.71	3.6391	0.37867	1.7123	2.2330	449.90
310	0.31144	−134.46	26.088	0.45228	1.7366	2.2570	456.62
320	0.30168	−116.95	48.785	0.52433	1.7624	2.2827	463.17
330	0.29252	−99.183	71.746	0.59499	1.7897	2.3098	469.55
340	0.28390	−81.135	94.986	0.66437	1.8184	2.3384	475.78
350	0.27577	−62.793	118.52	0.73258	1.8484	2.3683	481.87
360	0.26809	−44.147	142.36	0.79973	1.8795	2.3993	487.84
370	0.26083	−25.185	166.51	0.86590	1.9116	2.4313	493.68

Table 40. Thermodynamic properties of methane – Continued

Temperature K	Density kg/m³	Internal Energy kJ/kg	Enthalpy kJ/kg	Entropy kJ/(kg K)	c_v kJ/(kg K)	c_p kJ/(kg K)	Speed of sound m/s
			0.050 MPa Isobar				
380	0.25396	−5.8969	190.99	0.93117	1.9447	2.4643	499.41
390	0.24744	13.725	215.80	0.99562	1.9786	2.4981	505.04
400	0.24124	33.689	240.95	1.0593	2.0132	2.5326	510.57
410	0.23535	54.002	266.45	1.1223	2.0484	2.5677	516.01
420	0.22974	74.669	292.31	1.1846	2.0841	2.6034	521.37
430	0.22439	95.696	318.52	1.2463	2.1203	2.6395	526.65
440	0.21929	117.09	345.10	1.3074	2.1568	2.6760	531.85
450	0.21441	138.84	372.04	1.3679	2.1937	2.7129	536.99
460	0.20974	160.97	399.36	1.4279	2.2308	2.7499	542.07
470	0.20528	183.47	427.04	1.4875	2.2681	2.7872	547.08
480	0.20100	206.34	455.10	1.5465	2.3056	2.8246	552.04
490	0.19689	229.59	483.53	1.6052	2.3431	2.8622	556.94
500	0.19295	253.21	512.34	1.6634	2.3808	2.8997	561.80
520	0.18553	301.59	571.09	1.7786	2.4560	2.9749	571.36
540	0.17865	351.46	631.34	1.8923	2.5311	3.0500	580.74
560	0.17227	402.84	693.09	2.0045	2.6059	3.1247	589.96
580	0.16632	455.71	756.33	2.1155	2.6802	3.1989	599.02
600	0.16078	510.05	821.04	2.2252	2.7538	3.2725	607.95
620	0.15559	565.86	887.22	2.3337	2.8267	3.3454	616.74
			0.075 MPa Isobar				
90.710[a]	451.50	−982.77	−982.60	−7.3866	2.1678	3.3675	1538.9
92	449.78	−978.43	−978.26	−7.3391	2.1595	3.3720	1527.2
94	447.09	−971.67	−971.51	−7.2665	2.1472	3.3798	1508.8
96	444.39	−964.91	−964.74	−7.1952	2.1356	3.3884	1490.2
98	441.67	−958.12	−957.95	−7.1252	2.1244	3.3979	1471.4
100	438.92	−951.32	−951.15	−7.0565	2.1137	3.4081	1452.4
105	431.93	−934.21	−934.04	−6.8895	2.0882	3.4366	1404.0
108.137[b]	427.46	−923.40	−923.23	−6.7881	2.0729	3.4566	1373.1
108.137[b]	1.3785	−460.52	−406.12	−2.0061	1.6062	2.1923	268.32
110	1.3530	−457.47	−402.04	−1.9687	1.6010	2.1823	270.90
115	1.2894	−449.35	−391.18	−1.8722	1.5906	2.1617	277.64
120	1.2320	−441.29	−380.41	−1.7805	1.5835	2.1469	284.15
125	1.1798	−433.28	−369.71	−1.6931	1.5783	2.1356	290.47
130	1.1320	−425.31	−359.05	−1.6095	1.5745	2.1269	296.61
135	1.0882	−417.36	−348.44	−1.5294	1.5716	2.1201	302.60
140	1.0477	−409.44	−337.85	−1.4524	1.5695	2.1146	308.45
145	1.0102	−401.53	−327.29	−1.3783	1.5679	2.1102	314.16
150	0.97544	−393.63	−316.75	−1.3068	1.5667	2.1067	319.76
155	0.94303	−385.75	−306.22	−1.2378	1.5660	2.1040	325.24
160	0.91275	−377.87	−295.71	−1.1710	1.5655	2.1018	330.61
165	0.88440	−370.00	−285.20	−1.1064	1.5654	2.1002	335.89
170	0.85779	−362.14	−274.70	−1.0437	1.5656	2.0991	341.06
175	0.83276	−354.27	−264.21	−0.98284	1.5661	2.0984	346.15
180	0.80918	−346.40	−253.72	−0.92373	1.5670	2.0982	351.15
185	0.78692	−338.54	−243.23	−0.86624	1.5681	2.0984	356.06
190	0.76586	−330.66	−232.73	−0.81028	1.5695	2.0990	360.89
195	0.74592	−322.78	−222.24	−0.75574	1.5714	2.1001	365.64
200	0.72700	−314.90	−211.73	−0.70255	1.5735	2.1016	370.31
210	0.69193	−299.09	−190.70	−0.59992	1.5791	2.1059	379.43
220	0.66012	−283.22	−169.61	−0.50182	1.5863	2.1122	388.26

Table 40. Thermodynamic properties of methane – Continued

Temperature K	Density kg/m³	Internal Energy kJ/kg	Enthalpy kJ/kg	Entropy kJ/(kg K)	c_v kJ/(kg K)	c_p kJ/(kg K)	Speed of sound m/s
			0.075 MPa Isobar				
230	0.63113	−267.28	−148.45	−0.40775	1.5953	2.1204	396.81
240	0.60460	−251.24	−127.19	−0.31730	1.6062	2.1306	405.10
250	0.58022	−235.09	−105.83	−0.23009	1.6190	2.1428	413.13
260	0.55775	−218.80	−84.330	−0.14577	1.6339	2.1572	420.91
270	0.53696	−202.35	−62.678	−0.06406	1.6507	2.1735	428.46
280	0.51767	−185.73	−40.853	0.01531	1.6695	2.1919	435.79
290	0.49972	−168.92	−18.834	0.09258	1.6901	2.2122	442.90
300	0.48299	−151.89	3.3977	0.16794	1.7126	2.2344	449.82
310	0.46734	−134.62	25.860	0.24160	1.7368	2.2583	456.55
320	0.45267	−117.11	48.569	0.31369	1.7626	2.2839	463.11
330	0.43891	−99.337	71.542	0.38438	1.7899	2.3110	469.50
340	0.42595	−81.282	94.793	0.45379	1.8186	2.3395	475.74
350	0.41375	−62.935	118.34	0.52203	1.8485	2.3692	481.84
360	0.40222	−44.283	142.18	0.58921	1.8796	2.4002	487.81
370	0.39132	−25.316	166.34	0.65540	1.9118	2.4322	493.66
380	0.38100	−6.0232	190.83	0.72070	1.9448	2.4651	499.40
390	0.37121	13.603	215.65	0.78517	1.9787	2.4988	505.03
400	0.36191	33.572	240.81	0.84887	2.0133	2.5333	510.56
410	0.35306	53.888	266.32	0.91185	2.0485	2.5684	516.01
420	0.34464	74.559	292.18	0.97417	2.0842	2.6040	521.37
430	0.33661	95.589	318.40	1.0359	2.1204	2.6401	526.65
440	0.32895	116.98	344.98	1.0970	2.1569	2.6766	531.87
450	0.32163	138.74	371.93	1.1575	2.1938	2.7134	537.01
460	0.31463	160.87	399.25	1.2176	2.2309	2.7504	542.09
470	0.30792	183.37	426.94	1.2771	2.2682	2.7877	547.10
480	0.30150	206.25	455.00	1.3362	2.3057	2.8251	552.07
490	0.29534	229.50	483.44	1.3948	2.3432	2.8626	556.97
500	0.28943	253.12	512.25	1.4531	2.3808	2.9001	561.83
520	0.27829	301.50	571.01	1.5683	2.4561	2.9753	571.39
540	0.26797	351.39	631.27	1.6820	2.5312	3.0503	580.78
560	0.25839	402.77	693.02	1.7943	2.6059	3.1250	590.00
580	0.24948	455.64	756.26	1.9052	2.6802	3.1992	599.07
600	0.24116	509.98	820.98	2.0149	2.7538	3.2728	607.99
620	0.23337	565.80	887.17	2.1234	2.8267	3.3456	616.78
			0.100 MPa Isobar				
90.717[a]	451.50	−982.76	−982.54	−7.3866	2.1678	3.3674	1539.0
92	449.79	−978.44	−978.22	−7.3392	2.1595	3.3718	1527.3
94	447.11	−971.69	−971.47	−7.2666	2.1473	3.3796	1509.0
96	444.41	−964.92	−964.70	−7.1954	2.1356	3.3883	1490.4
98	441.68	−958.14	−957.91	−7.1254	2.1245	3.3977	1471.6
100	438.94	−951.34	−951.11	−7.0567	2.1138	3.4079	1452.6
105	431.95	−934.23	−934.00	−6.8897	2.0883	3.4363	1404.2
110	424.79	−916.97	−916.74	−6.7291	2.0642	3.4691	1354.8
111.508[b]	422.59	−911.74	−911.50	−6.6818	2.0572	3.4799	1339.7
111.508[b]	1.7946	−456.10	−400.38	−2.0981	1.6147	2.2165	271.33
115	1.7341	−450.34	−392.68	−2.0301	1.6041	2.1957	276.16
120	1.6550	−442.18	−381.76	−1.9371	1.5937	2.1741	282.84
125	1.5834	−434.08	−370.93	−1.8487	1.5864	2.1582	289.30
130	1.5182	−426.04	−360.17	−1.7643	1.5810	2.1459	295.56
135	1.4584	−418.03	−349.46	−1.6835	1.5770	2.1363	301.65

Table 40. Thermodynamic properties of methane – Continued

Temperature K	Density kg/m³	Internal energy kJ/kg	Enthalpy kJ/kg	Entropy kJ/(kg K)	c_v kJ/(kg K)	c_p kJ/(kg K)	Speed of sound m/s
			0.100 MPa Isobar				
140	1.4034	−410.06	−338.80	−1.6060	1.5739	2.1287	307.59
145	1.3526	−402.11	−328.17	−1.5314	1.5716	2.1225	313.38
150	1.3055	−394.17	−317.57	−1.4595	1.5699	2.1176	319.04
155	1.2617	−386.26	−307.00	−1.3902	1.5687	2.1136	324.58
160	1.2208	−378.35	−296.44	−1.3231	1.5679	2.1105	330.01
165	1.1825	−370.45	−285.89	−1.2582	1.5675	2.1080	335.33
170	1.1467	−362.56	−275.36	−1.1953	1.5675	2.1061	340.55
175	1.1130	−354.68	−264.83	−1.1343	1.5678	2.1048	345.67
180	1.0813	−346.79	−254.31	−1.0750	1.5684	2.1040	350.71
185	1.0513	−338.90	−243.79	−1.0173	1.5694	2.1038	355.65
190	1.0230	−331.02	−233.27	−0.96123	1.5707	2.1040	360.51
195	0.99627	−323.12	−222.75	−0.90657	1.5724	2.1047	365.29
200	0.97088	−315.22	−212.22	−0.85328	1.5745	2.1058	369.98
210	0.92384	−299.39	−191.14	−0.75045	1.5799	2.1096	379.14
220	0.88121	−283.50	−170.02	−0.65218	1.5869	2.1154	388.01
230	0.84238	−267.54	−148.83	−0.55798	1.5959	2.1232	396.60
240	0.80686	−251.49	−127.55	−0.46742	1.6067	2.1331	404.91
250	0.77425	−235.32	−106.16	−0.38010	1.6195	2.1451	412.96
260	0.74418	−219.02	−84.640	−0.29570	1.6343	2.1592	420.77
270	0.71638	−202.56	−62.969	−0.21391	1.6510	2.1754	428.34
280	0.69060	−185.93	−41.126	−0.13448	1.6698	2.1936	435.68
290	0.66662	−169.10	−19.090	−0.05715	1.6904	2.2138	442.81
300	0.64425	−152.06	3.1561	0.01826	1.7128	2.2358	449.74
310	0.62335	−134.79	25.632	0.09196	1.7370	2.2596	456.48
320	0.60377	−117.27	48.354	0.16409	1.7628	2.2851	463.05
330	0.58538	−99.490	71.339	0.23482	1.7901	2.3121	469.45
340	0.56809	−81.429	94.600	0.30426	1.8188	2.3405	475.70
350	0.55179	−63.076	118.15	0.37253	1.8487	2.3702	481.81
360	0.53640	−44.419	142.01	0.43973	1.8798	2.4011	487.79
370	0.52185	−25.447	166.18	0.50595	1.9119	2.4330	493.64
380	0.50808	−6.1496	190.67	0.57127	1.9449	2.4659	499.38
390	0.49501	13.481	215.50	0.63576	1.9788	2.4996	505.02
400	0.48260	33.454	240.67	0.69947	2.0134	2.5340	510.56
410	0.47080	53.774	266.18	0.76247	2.0485	2.5690	516.01
420	0.45956	74.449	292.05	0.82481	2.0843	2.6046	521.38
430	0.44885	95.482	318.27	0.88652	2.1204	2.6407	526.66
440	0.43863	116.88	344.86	0.94764	2.1570	2.6771	531.88
450	0.42886	138.64	371.82	1.0082	2.1938	2.7139	537.03
460	0.41952	160.77	399.14	1.0683	2.2310	2.7509	542.11
470	0.41058	183.28	426.84	1.1278	2.2683	2.7881	547.13
480	0.40201	206.16	454.91	1.1869	2.3057	2.8255	552.09
490	0.39379	229.41	483.35	1.2456	2.3433	2.8630	557.00
500	0.38591	253.04	512.17	1.3038	2.3809	2.9005	561.86
520	0.37105	301.42	570.93	1.4190	2.4561	2.9757	571.43
540	0.35729	351.31	631.19	1.5327	2.5312	3.0507	580.82
560	0.34452	402.69	692.95	1.6450	2.6060	3.1253	590.04
580	0.33263	455.56	756.20	1.7560	2.6802	3.1995	599.11
600	0.32153	509.92	820.93	1.8657	2.7538	3.2730	608.04
620	0.31115	565.73	887.12	1.9742	2.8267	3.3459	616.83

Table 40. Thermodynamic properties of methane – Continued

Temperature K	Density kg/m³	Internal energy kJ/kg	Enthalpy kJ/kg	Entropy kJ/(kg K)	c_v kJ/(kg K)	c_p kJ/(kg K)	Speed of sound m/s
			0.101325 MPa Isobar				
90.717[a]	451.50	−982.76	−982.54	−7.3865	2.1678	3.3674	1539.0
92	449.79	−978.44	−978.22	−7.3392	2.1595	3.3718	1527.3
94	447.11	−971.69	−971.46	−7.2666	2.1473	3.3796	1509.0
96	444.41	−964.93	−964.70	−7.1954	2.1356	3.3883	1490.4
98	441.68	−958.14	−957.91	−7.1254	2.1245	3.3977	1471.6
100	438.94	−951.34	−951.11	−7.0567	2.1138	3.4079	1452.6
105	431.95	−934.23	−934.00	−6.8897	2.0883	3.4363	1404.3
110	424.79	−916.97	−916.74	−6.7291	2.0642	3.4691	1354.8
111.667[b]	422.36	−911.18	−910.94	−6.6769	2.0564	3.4811	1338.1
111.667[b]	1.8164	−455.90	−400.11	−2.1023	1.6151	2.2177	271.46
115	1.7579	−450.40	−392.76	−2.0374	1.6049	2.1976	276.08
120	1.6776	−442.23	−381.83	−1.9444	1.5943	2.1756	282.77
125	1.6050	−434.12	−370.99	−1.8559	1.5868	2.1594	289.24
130	1.5388	−426.08	−360.23	−1.7715	1.5814	2.1470	295.50
135	1.4781	−418.07	−349.52	−1.6906	1.5773	2.1372	301.60
140	1.4223	−410.09	−338.85	−1.6130	1.5741	2.1294	307.54
145	1.3708	−402.14	−328.22	−1.5384	1.5718	2.1232	313.34
150	1.3230	−394.20	−317.62	−1.4665	1.5701	2.1182	319.00
155	1.2786	−386.28	−307.04	−1.3972	1.5688	2.1141	324.55
160	1.2372	−378.38	−296.48	−1.3301	1.5680	2.1109	329.98
165	1.1984	−370.48	−285.93	−1.2652	1.5676	2.1084	335.30
170	1.1620	−362.59	−275.39	−1.2023	1.5676	2.1065	340.52
175	1.1279	−354.70	−264.86	−1.1412	1.5678	2.1052	345.65
180	1.0957	−346.81	−254.34	−1.0819	1.5685	2.1044	350.68
185	1.0654	−338.92	−243.82	−1.0243	1.5694	2.1041	355.63
200	0.98382	−315.24	−212.25	−0.86018	1.5745	2.1061	369.96
210	0.93615	−299.40	−191.17	−0.75735	1.5799	2.1098	379.13
220	0.89294	−283.52	−170.04	−0.65907	1.5870	2.1156	388.00
230	0.85359	−267.55	−148.85	−0.56486	1.5959	2.1234	396.58
240	0.81760	−251.50	−127.57	−0.47429	1.6067	2.1333	404.90
250	0.78454	−235.33	−106.18	−0.38697	1.6195	2.1452	412.95
260	0.75407	−219.03	−84.657	−0.30257	1.6343	2.1593	420.76
270	0.72590	−202.57	−62.984	−0.22078	1.6511	2.1755	428.33
280	0.69977	−185.94	−41.140	−0.14134	1.6698	2.1937	435.67
290	0.67547	−169.11	−19.104	−0.06401	1.6904	2.2139	442.81
300	0.65281	−152.07	3.1433	0.01141	1.7129	2.2359	449.74
310	0.63162	−134.80	25.620	0.08511	1.7370	2.2597	456.48
320	0.61178	−117.28	48.343	0.15725	1.7628	2.2851	463.05
330	0.59315	−99.499	71.328	0.22797	1.7901	2.3121	469.45
340	0.57562	−81.437	94.590	0.29742	1.8188	2.3406	475.70
350	0.55911	−63.084	118.14	0.36569	1.8487	2.3703	481.81
360	0.54351	−44.426	142.00	0.43289	1.8798	2.4011	487.79
370	0.52877	−25.454	166.17	0.49911	1.9119	2.4331	493.64
380	0.51481	−6.1563	190.66	0.56443	1.9449	2.4659	499.38
390	0.50157	13.475	215.49	0.62892	1.9788	2.4996	505.02
400	0.48900	33.448	240.66	0.69264	2.0134	2.5340	510.56
410	0.47704	53.768	266.17	0.75564	2.0486	2.5691	516.01
420	0.46565	74.443	292.04	0.81797	2.0843	2.6047	521.38
430	0.45480	95.477	318.27	0.87968	2.1204	2.6407	526.67
440	0.44444	116.87	344.86	0.94081	2.1570	2.6772	531.88

Table 40. Thermodynamic properties of methane – Continued

Temperature K	Density kg/m³	Internal energy kJ/kg	Enthalpy kJ/kg	Entropy kJ/(kg K)	c_v kJ/(kg K)	c_p kJ/(kg K)	Speed of sound m/s
			0.101325 MPa Isobar				
450	0.43454	138.64	371.81	1.0014	2.1939	2.7139	537.03
460	0.42508	160.77	399.14	1.0614	2.2310	2.7510	542.11
470	0.41602	183.27	426.83	1.1210	2.2683	2.7882	547.13
480	0.40734	206.15	454.90	1.1801	2.3057	2.8255	552.09
490	0.39901	229.40	483.34	1.2387	2.3433	2.8630	557.00
500	0.39102	253.03	512.16	1.2970	2.3809	2.9006	561.86
520	0.37596	301.42	570.92	1.4122	2.4561	2.9757	571.43
540	0.36202	351.30	631.19	1.5259	2.5312	3.0507	580.82
560	0.34908	402.69	692.95	1.6382	2.6060	3.1253	590.04
580	0.33703	455.56	756.20	1.7492	2.6802	3.1995	599.11
600	0.32579	509.91	820.93	1.8589	2.7539	3.2731	608.04
620	0.31527	565.73	887.12	1.9674	2.8267	3.3459	616.83
			0.150 MPa Isobar				
90.729[a]	451.52	−982.75	−982.42	−7.3864	2.1678	3.3671	1539.2
92	449.83	−978.47	−978.14	−7.3395	2.1596	3.3715	1527.7
94	447.15	−971.72	−971.39	−7.2670	2.1474	3.3793	1509.3
96	444.44	−964.96	−964.62	−7.1957	2.1358	3.3879	1490.7
98	441.72	−958.17	−957.83	−7.1258	2.1246	3.3974	1471.9
100	438.97	−951.37	−951.03	−7.0570	2.1139	3.4075	1453.0
105	431.99	−934.27	−933.92	−6.8901	2.0884	3.4359	1404.7
110	424.83	−917.02	−916.66	−6.7295	2.0643	3.4686	1355.3
115	417.47	−899.59	−899.23	−6.5745	2.0414	3.5062	1304.8
116.655[b]	414.98	−893.78	−893.41	−6.5243	2.0340	3.5199	1287.8
116.655[b]	2.6049	−449.63	−392.04	−2.2264	1.6289	2.2599	275.43
120	2.5215	−444.02	−384.53	−2.1629	1.6164	2.2343	280.12
125	2.4076	−435.73	−373.43	−2.0723	1.6037	2.2067	286.89
130	2.3046	−427.54	−362.45	−1.9862	1.5948	2.1864	293.41
135	2.2109	−419.40	−351.56	1.9040	1.5882	2.1707	299.71
140	2.1251	−411.32	−340.74	−1.8253	1.5832	2.1582	305.83
145	2.0462	−403.28	−329.97	−1.7497	1.5794	2.1482	311.78
150	1.9732	−395.27	−319.25	−1.6770	1.5765	2.1401	317.58
155	1.9056	−387.28	−308.57	−1.6070	1.5743	2.1336	323.25
160	1.8427	−379.32	−297.91	−1.5393	1.5728	2.1283	328.79
165	1.7840	−371.36	−287.28	−1.4739	1.5717	2.1240	334.20
170	1.7290	−363.43	−276.67	−1.4105	1.5712	2.1206	339.51
175	1.6775	−355.49	−266.08	−1.3491	1.5710	2.1180	344.72
180	1.6291	−347.57	−255.49	−1.2895	1.5713	2.1160	349.82
185	1.5834	−339.65	−244.91	−1.2315	1.5720	2.1148	354.83
190	1.5403	−331.72	−234.34	−1.1751	1.5730	2.1141	359.75
195	1.4996	−323.80	−223.77	−1.1202	1.5745	2.1140	364.58
200	1.4610	−315.87	−213.20	−1.0667	1.5764	2.1145	369.33
210	1.3896	−299.99	−192.05	−0.96346	1.5815	2.1171	378.58
220	1.3250	−284.06	−170.85	−0.86487	1.5883	2.1220	387.52
230	1.2662	−268.06	−149.60	−0.77039	1.5970	2.1290	396.17
240	1.2125	−251.98	−128.26	−0.67960	1.6077	2.1383	404.54
250	1.1632	−235.78	−106.83	−0.59208	1.6204	2.1497	412.64
260	1.1178	−219.45	−85.261	−0.50751	1.6350	2.1634	420.48
270	1.0759	−202.97	−63.550	−0.42557	1.6517	2.1792	428.09

Table 40. Thermodynamic properties of methane – Continued

Temperature K	Density kg/m³	Internal energy kJ/kg	Enthalpy kJ/kg	Entropy kJ/(kg K)	c_v kJ/(kg K)	c_p kJ/(kg K)	Speed of sound m/s
			0.150 MPa Isobar				
280	1.0370	−186.32	−41.671	−0.34601	1.6704	2.1970	435.47
290	1.0009	−169.47	−19.603	−0.26857	1.6909	2.2169	442.63
300	0.96720	−152.41	2.6729	−0.19305	1.7133	2.2387	449.58
310	0.93573	−135.13	25.176	−0.11927	1.7375	2.2622	456.35
320	0.90625	−117.59	47.923	−0.04705	1.7632	2.2875	462.94
330	0.87858	−99.798	70.931	0.02375	1.7904	2.3143	469.36
340	0.85257	−81.724	94.215	0.09325	1.8191	2.3426	475.62
350	0.82806	−63.359	117.79	0.16158	1.8490	2.3721	481.75
360	0.80493	−44.691	141.66	0.22884	1.8801	2.4029	487.74
370	0.78306	−25.709	165.85	0.29510	1.9122	2.4347	493.61
380	0.76235	−6.4023	190.36	0.36047	1.9452	2.4675	499.36
390	0.74271	13.238	215.20	0.42499	1.9790	2.5010	505.01
400	0.72407	33.218	240.38	0.48874	2.0136	2.5354	510.56
410	0.70634	53.547	265.91	0.55178	2.0487	2.5704	516.02
420	0.68946	74.228	291.79	0.61414	2.0844	2.6059	521.39
430	0.67337	95.269	318.03	0.67588	2.1206	2.6419	526.69
440	0.65802	116.67	344.63	0.73703	2.1571	2.6782	531.91
450	0.64335	138.44	371.60	0.79763	2.1940	2.7149	537.06
460	0.62933	160.58	398.93	0.85771	2.2311	2.7519	542.15
470	0.61590	183.09	426.63	0.91729	2.2684	2.7891	547.17
480	0.60304	205.97	454.71	0.97640	2.3058	2.8264	552.14
490	0.59071	229.23	483.16	1.0351	2.3434	2.8638	557.05
500	0.57887	252.86	511.99	1.0933	2.3810	2.9013	561.92
520	0.55656	301.25	570.77	1.2086	2.4562	2.9764	571.49
540	0.53591	351.15	631.04	1.3223	2.5313	3.0513	580.89
560	0.51675	402.54	692.82	1.4346	2.6061	3.1259	590.12
580	0.49890	455.42	756.08	1.5456	2.6803	3.2001	599.20
600	0.48225	509.78	820.82	1.6553	2.7539	3.2736	608.13
620	0.46668	565.60	887.02	1.7639	2.8268	3.3463	616.93
			0.200 MPa Isobar				
90.742[a]	451.53	−982.74	−982.29	−7.3863	2.1679	3.3669	1539.4
92	449.86	−978.50	−978.06	−7.3399	2.1598	3.3712	1528.0
94	447.18	−971.75	−971.31	−7.2673	2.1475	3.3790	1509.7
96	444.48	−964.99	−964.54	−7.1961	2.1359	3.3876	1491.1
98	441.76	−958.21	−957.76	−7.1261	2.1248	3.3970	1472.3
100	439.01	−951.41	−950.95	−7.0574	2.1140	3.4071	1453.3
105	432.04	−934.31	−933.85	−6.8905	2.0885	3.4354	1405.1
110	424.88	−917.06	−916.59	−6.7299	2.0645	3.4680	1355.8
115	417.52	−899.64	−899.16	−6.5750	2.0415	3.5055	1305.3
120	409.91	−882.01	−881.52	−6.4249	2.0196	3.5492	1253.6
120.622[b]	408.95	−879.80	−879.32	−6.4065	2.0169	3.5551	1247.0
120.622[b]	3.3966	−444.88	−386.00	−2.3168	1.6410	2.2996	278.17
125	3.2560	−437.45	−376.02	−2.2355	1.6229	2.2611	284.39
130	3.1112	−429.08	−364.80	−2.1475	1.6095	2.2304	291.19
135	2.9803	−420.81	−353.71	−2.0637	1.6000	2.2076	297.72
140	2.8611	−412.62	−342.72	−1.9838	1.5930	2.1897	304.04
145	2.7520	−404.48	−331.80	−1.9072	1.5875	2.1754	310.16
150	2.6516	−396.38	−320.96	−1.8337	1.5834	2.1639	316.11
155	2.5588	−388.32	−310.16	−1.7629	1.5802	2.1545	321.90
160	2.4727	−380.29	−299.41	−1.6946	1.5778	2.1468	327.55

Table 40. Thermodynamic properties of methane – Continued

Temperature K	Density kg/m³	Internal energy kJ/kg	Enthalpy kJ/kg	Entropy kJ/(kg K)	c_v kJ/(kg K)	c_p kJ/(kg K)	Speed of sound m/s
			0.200 MPa Isobar				
165	2.3925	−372.29	−288.69	−1.6286	1.5761	2.1406	333.07
170	2.3176	−364.30	−278.00	−1.5648	1.5750	2.1355	338.47
175	2.2475	−356.32	−267.33	−1.5030	1.5744	2.1315	343.75
180	2.1818	−348.35	−256.69	−1.4430	1.5743	2.1283	348.93
185	2.1199	−340.40	−246.05	−1.3847	1.5746	2.1260	354.00
190	2.0615	−332.44	−235.42	−1.3280	1.5754	2.1244	358.98
195	2.0064	−324.48	−224.80	−1.2728	1.5767	2.1235	363.87
200	1.9543	−316.53	−214.19	−1.2191	1.5784	2.1233	368.67
210	1.8579	−300.60	−192.95	−1.1154	1.5831	2.1248	378.01
220	1.7709	−284.62	−171.68	−1.0165	1.5897	2.1286	387.02
230	1.6918	−268.59	−150.37	−0.92177	1.5982	2.1349	395.74
240	1.6196	−252.47	−128.98	−0.83074	1.6087	2.1435	404.16
250	1.5534	−236.24	−107.49	−0.74302	1.6212	2.1544	412.31
260	1.4925	−219.88	−85.883	−0.65828	1.6358	2.1676	420.20
270	1.4363	−203.38	−64.133	−0.57619	1.6524	2.1829	427.85
280	1.3842	−186.71	−42.218	−0.49649	1.6710	2.2005	435.26
290	1.3358	−169.84	−20.117	−0.41894	1.6915	2.2200	442.44
300	1.2907	−152.77	2.1893	−0.34332	1.7138	2.2415	449.43
310	1.2486	−135.46	24.720	−0.26945	1.7379	2.2649	456.22
320	1.2091	−117.92	47.493	−0.19715	1.7636	2.2899	462.82
330	1.1721	−100.11	70.524	−0.12628	1.7908	2.3166	469.26
340	1.1373	−82.019	93.829	−0.05671	1.8194	2.3447	475.55
350	1.1046	−63.643	117.42	0.01168	1.8493	2.3741	481.69
360	1.0737	−44.964	141.31	0.07898	1.8804	2.4047	487.69
370	1.0444	−25.971	165.52	0.14530	1.9124	2.4364	493.57
380	1.0168	−6.6551	190.05	0.21070	1.9454	2.4690	499.34
390	0.99055	12.994	214.90	0.27527	1.9792	2.5025	504.99
400	0.96564	32.983	240.10	0.33906	2.0138	2.5368	510.55
410	0.94197	53.319	265.64	0.40213	2.0489	2.5717	516.02
420	0.91943	74.008	291.53	0.46452	2.0846	2.6071	521.40
430	0.89795	95.055	317.78	0.52629	2.1208	2.6430	526.71
440	0.87746	116.46	344.40	0.58747	2.1573	2.6793	531.93
450	0.85788	138.24	371.37	0.64809	2.1941	2.7160	537.09
460	0.83917	160.38	398.72	0.70819	2.2312	2.7529	542.19
470	0.82125	182.90	426.43	0.76779	2.2685	2.7900	547.22
480	0.80409	205.79	454.52	0.82692	2.3060	2.8273	552.19
490	0.78763	229.05	482.98	0.88560	2.3435	2.8647	557.11
500	0.77183	252.69	511.81	0.94385	2.3811	2.9022	561.98
520	0.74207	301.09	570.60	1.0591	2.4563	2.9771	571.56
540	0.71453	350.99	630.90	1.1729	2.5314	3.0520	580.97
560	0.68896	402.39	692.68	1.2852	2.6061	3.1266	590.20
580	0.66516	455.28	755.96	1.3963	2.6804	3.2006	599.28
600	0.64295	509.64	820.70	1.5060	2.7540	3.2741	608.22
620	0.62219	565.47	886.91	1.6145	2.8269	3.3468	617.02
			0.250 MPa Isobar				
90.755[a]	451.55	−982.72	−982.17	−7.3861	2.1679	3.3667	1539.7
92	449.89	−978.53	−977.98	−7.3402	2.1599	3.3709	1528.4
94	447.21	−971.79	−971.23	−7.2676	2.1477	3.3787	1510.0
96	444.52	−965.02	−964.46	−7.1964	2.1360	3.3873	1491.5
98	441.79	−958.24	−957.68	−7.1265	2.1249	3.3966	1472.7

Table 40. Thermodynamic properties of methane – Continued

Temperature K	Density kg/m³	Internal energy kJ/kg	Enthalpy kJ/kg	Entropy kJ/(kg K)	c_v kJ/(kg K)	c_p kJ/(kg K)	Speed of sound m/s
			0.250 MPa Isobar				
100	439.05	−951.44	−950.87	−7.0578	2.1142	3.4068	1453.7
105	432.08	−934.35	−933.77	−6.8909	2.0887	3.4350	1405.5
110	424.93	−917.11	−916.52	−6.7303	2.0646	3.4674	1356.2
115	417.57	−899.69	−899.09	−6.5754	2.0417	3.5049	1305.8
120	409.97	−882.07	−881.46	−6.4253	2.0197	3.5483	1254.1
123.898[b]	403.85	−868.17	−867.55	−6.3113	2.0034	3.5875	1212.9
123.898[b]	4.1765	−441.15	−381.29	−2.3866	1.6518	2.3371	280.15
125	4.1311	−439.24	−378.73	−2.3660	1.6456	2.3240	281.77
130	3.9396	−430.69	−367.23	−2.2758	1.6256	2.2789	288.89
135	3.7678	−422.27	−355.92	−2.1904	1.6126	2.2473	295.68
140	3.6124	−413.95	−344.74	−2.1091	1.6032	2.2232	302.20
145	3.4709	−405.70	−333.68	−2.0315	1.5960	2.2041	308.50
150	3.3411	−397.52	−322.69	−1.9570	1.5905	2.1888	314.60
155	3.2216	−389.38	−311.78	−1.8854	1.5863	2.1763	320.53
160	3.1110	−381.29	−300.93	−1.8165	1.5830	2.1661	326.30
165	3.0083	−373.22	−290.12	−1.7500	1.5806	2.1578	331.92
170	2.9127	−365.18	−279.35	−1.6857	1.5789	2.1510	337.41
175	2.8233	−357.16	−268.61	−1.6234	1.5778	2.1454	342.78
180	2.7395	−349.15	−257.89	−1.5630	1.5773	2.1410	348.03
185	2.6608	−341.15	−247.19	−1.5044	1.5774	2.1376	353.17
190	2.5867	−333.16	−236.51	−1.4475	1.5779	2.1350	358.21
195	2.5168	−325.17	−225.84	−1.3920	1.5789	2.1333	363.16
200	2.4508	−317.19	−215.18	−1.3380	1.5803	2.1323	368.01
210	2.3289	−301.20	−193.86	−1.2340	1.5847	2.1325	377.44
220	2.2189	−285.19	−172.52	−1.1347	1.5911	2.1354	386.53
230	2.1192	−269.11	−151.14	−1.0397	1.5994	2.1408	395.31
240	2.0282	−252.96	−129.70	−0.94844	1.6097	2.1487	403.79
250	1.9449	−236.70	−108.16	−0.86052	1.6221	2.1591	411.99
260	1.8683	−220.32	−86.507	−0.77560	1.6366	2.1718	419.92
270	1.7976	−203.79	−64.716	−0.69337	1.6531	2.1867	427.60
280	1.7321	−187.10	−42.765	−0.61354	1.6716	2.2039	435.04
290	1.6713	−170.21	−20.631	−0.53587	1.6920	2.2232	442.26
300	1.6147	−153.12	1.7054	−0.46015	1.7143	2.2444	449.27
310	1.5619	−135.80	24.264	−0.38618	1.7383	2.2675	456.08
320	1.5124	−118.24	47.062	−0.31380	1.7640	2.2924	462.71
330	1.4660	−100.41	70.116	−0.24286	1.7912	2.3188	469.17
340	1.4224	−82.314	93.443	−0.17323	1.8198	2.3467	475.47
350	1.3814	−63.926	117.06	−0.10478	1.8496	2.3760	481.62
360	1.3426	−45.236	140.97	−0.03742	1.8806	2.4065	487.64
370	1.3060	−26.234	165.19	0.02894	1.9127	2.4381	493.54
380	1.2714	−6.9080	189.73	0.09439	1.9457	2.4706	499.31
390	1.2385	12.750	214.60	0.15900	1.9795	2.5040	504.98
400	1.2073	32.747	239.81	0.22282	2.0140	2.5382	510.55
410	1.1777	53.091	265.37	0.28592	2.0491	2.5730	516.03
420	1.1495	73.787	291.28	0.34835	2.0848	2.6083	521.42
430	1.1226	94.841	317.54	0.41014	2.1209	2.6442	526.73
440	1.0970	116.26	344.16	0.47135	2.1575	2.6804	531.96
450	1.0725	138.04	371.15	0.53199	2.1943	2.7170	537.13
460	1.0490	160.19	398.50	0.59211	2.2314	2.7539	542.23
470	1.0266	182.71	426.23	0.65174	2.2687	2.7910	547.26
480	1.0051	205.60	454.32	0.71089	2.3061	2.8282	552.24
490	0.98456	228.87	482.79	0.76959	2.3436	2.8655	557.17
500	0.96480	252.51	511.63	0.82785	2.3812	2.9030	562.04
520	0.92757	300.92	570.44	0.94317	2.4564	2.9779	571.63
540	0.89312	350.83	630.75	1.0570	2.5315	3.0527	581.04

Table 40. Thermodynamic properties of methane – Continued

Temperature K	Density kg/m³	Internal energy kJ/kg	Enthalpy kJ/kg	Entropy kJ/(kg K)	c_v kJ/(kg K)	c_p kJ/(kg K)	Speed of sound m/s
			0.250 MPa Isobar				
560	0.86115	402.24	692.55	1.1693	2.6062	3.1272	590.28
580	0.83139	455.13	755.83	1.2804	2.6804	3.2012	599.37
600	0.80363	509.50	820.59	1.3901	2.7540	3.2746	608.31
620	0.77766	565.33	886.81	1.4987	2.8269	3.3473	617.12
			0.300 MPa Isobar				
90.768[a]	451.57	−982.71	−982.05	−7.3860	2.1680	3.3664	1539.9
92	449.93	−978.56	−977.89	−7.3405	2.1600	3.3707	1528.7
94	447.25	−971.82	−971.15	−7.2680	2.1478	3.3783	1510.4
96	444.55	−965.06	−964.38	−7.1968	2.1362	3.3869	1491.8
98	441.83	−958.28	−957.60	−7.1268	2.1250	3.3963	1473.1
100	439.09	−951.48	−950.80	−7.0581	2.1143	3.4064	1454.1
105	432.12	−934.39	−933.69	−6.8912	2.0888	3.4345	1406.0
110	424.97	−917.15	−916.44	−6.7307	2.0648	3.4669	1356.7
115	417.62	−899.74	−899.02	−6.5758	2.0418	3.5042	1306.3
120	410.02	−882.12	−881.39	−6.4258	2.0199	3.5475	1254.7
125	402.15	−864.28	−863.53	−6.2800	1.9990	3.5986	1201.7
126.714[b]	399.38	−858.09	−857.34	−6.2308	1.9921	3.6182	1183.2
126.714[b]	4.9486	−438.09	−377.47	−2.4438	1.6616	2.3733	281.64
130	4.7917	−432.35	−369.74	−2.3835	1.6437	2.3333	286.51
135	4.5748	−423.76	−358.19	−2.2963	1.6260	2.2903	293.57
140	4.3799	−415.31	−346.82	−2.2136	1.6139	2.2590	300.32
145	4.2034	−406.96	−335.58	−2.1348	1.6048	2.2346	306.81
150	4.0422	−398.68	−324.46	−2.0594	1.5979	2.2150	313.07
155	3.8944	−390.46	−313.43	−1.9870	1.5925	2.1992	319.14
160	3.7580	−382.29	−302.46	−1.9174	1.5884	2.1863	325.03
165	3.6317	−374.17	−291.56	−1.8503	1.5852	2.1757	330.76
170	3.5143	−366.07	−280.71	−1.7855	1.5829	2.1669	336.35
175	3.4048	−358.00	−269.89	−1.7228	1.5814	2.1598	341.80
180	3.3024	−349.95	−259.11	−1.6620	1.5804	2.1540	347.13
185	3.2064	−341.91	−248.35	−1.6031	1.5801	2.1494	352.34
190	3.1160	−333.89	−237.61	−1.5458	1.5803	2.1458	357.44
195	3.0309	−325.87	−226.89	−1.4901	1.5811	2.1432	362.44
200	2.9506	−317.85	−216.18	−1.4359	1.5823	2.1415	367.34
210	2.8026	−301.82	−194.77	−1.3314	1.5864	2.1403	376.86
220	2.6692	−285.75	−173.36	−1.2318	1.5924	2.1422	386.03
230	2.5484	−269.64	−151.92	−1.1365	1.6006	2.1468	394.88
240	2.4383	−253.45	−130.41	−1.0450	1.6107	2.1540	403.42
250	2.3376	−237.16	−108.83	−0.95687	1.6230	2.1638	411.66
260	2.2451	−220.76	−87.131	−0.87177	1.6374	2.1760	419.64
270	2.1598	−204.20	−65.300	−0.78939	1.6538	2.1906	427.36
280	2.0808	−187.49	−43.312	−0.70942	1.6722	2.2074	434.83
290	2.0075	−170.58	−21.145	−0.63164	1.6926	2.2263	442.08
300	1.9393	−153.47	1.2212	−0.55581	1.7148	2.2473	449.12
310	1.8757	−136.14	23.807	−0.48176	1.7388	2.2702	455.95
320	1.8161	−118.56	46.631	−0.40930	1.7644	2.2948	462.60
330	1.7603	−100.72	69.709	−0.33829	1.7916	2.3211	469.08
340	1.7078	−82.610	93.057	−0.26859	1.8201	2.3488	475.40
350	1.6584	−64.210	116.69	−0.20008	1.8499	2.3780	481.56
360	1.6118	−45.509	140.62	−0.13267	1.8809	2.4083	487.60
370	1.5678	−26.496	164.86	−0.06626	1.9130	2.4398	493.50

Table 40. Thermodynamic properties of methane – Continued

Temperature K	Density kg/m³	Internal energy kJ/kg	Enthalpy kJ/kg	Entropy kJ/(kg K)	c_v kJ/(kg K)	c_p kJ/(kg K)	Speed of sound m/s
			0.300 MPa Isobar				
380	1.5261	−7.1609	189.42	−0.00076	1.9459	2.4722	499.29
390	1.4866	12.506	214.31	0.06388	1.9797	2.5055	504.97
400	1.4491	32.511	239.53	0.12774	2.0142	2.5396	510.55
410	1.4135	52.863	265.10	0.19088	2.0493	2.5743	516.03
420	1.3796	73.567	291.02	0.25333	2.0850	2.6096	521.43
430	1.3473	94.628	317.29	0.31516	2.1211	2.6454	526.75
440	1.3165	116.05	343.93	0.37638	2.1576	2.6816	531.99
450	1.2871	137.84	370.93	0.43706	2.1944	2.7181	537.16
460	1.2589	159.99	398.29	0.49720	2.2315	2.7549	542.27
470	1.2320	182.52	426.02	0.55684	2.2688	2.7919	547.31
480	1.2062	205.42	454.13	0.61601	2.3062	2.8291	552.29
490	1.1815	228.69	482.61	0.67473	2.3437	2.8664	557.22
500	1.1578	252.34	511.46	0.73301	2.3813	2.9038	562.10
520	1.1131	300.76	570.28	0.84836	2.4565	2.9786	571.70
540	1.0717	350.67	630.60	0.96218	2.5316	3.0534	581.12
560	1.0333	402.09	692.41	1.0746	2.6063	3.1278	590.37
580	0.99760	454.99	755.71	1.1856	2.6805	3.2018	599.46
600	0.96427	509.36	820.48	1.2954	2.7541	3.2751	608.41
620	0.93310	565.20	886.71	1.4040	2.8270	3.3478	617.22
			0.400 MPa Isobar				
90.793[a]	451.60	−982.68	−981.80	−7.3857	2.1680	3.3660	1540.3
92	449.99	−978.62	−977.73	−7.3412	2.1603	3.3701	1529.4
94	447.32	−971.88	−970.99	−7.2686	2.1480	3.3777	1511.1
96	444.62	−965.12	−964.22	−7.1974	2.1364	3.3863	1492.6
98	441.90	−958.35	−957.44	−7.1275	2.1253	3.3956	1473.9
100	439.16	−951.55	−950.64	−7.0588	2.1146	3.4056	1454.9
105	432.20	−934.47	−933.54	−6.8920	2.0891	3.4336	1406.8
110	425.06	−917.24	−916.30	−6.7315	2.0650	3.4658	1357.6
115	417.72	−899.83	−898.88	−6.5767	2.0421	3.5029	1307.3
120	410.14	−882.23	−881.26	−6.4267	2.0202	3.5459	1255.8
125	402.27	−864.40	−863.41	−6.2810	1.9993	3.5966	1203.0
130	394.08	−846.29	−845.28	−6.1388	1.9796	3.6571	1148.5
131.436[b]	391.66	−841.03	−840.01	−6.0985	1.9742	3.6768	1132.6
131.436[b]	6.4792	−433.28	−371.54	−2.5343	1.6795	2.4435	283.69
135	6.2534	−426.90	−362.94	−2.4696	1.6571	2.3904	289.15
140	5.9680	−418.15	−351.12	−2.3837	1.6372	2.3387	296.42
145	5.7126	−409.55	−339.53	−2.3023	1.6236	2.3010	303.32
150	5.4819	−401.06	−328.10	−2.2248	1.6135	2.2717	309.93
155	5.2718	−392.67	−316.80	−2.1507	1.6057	2.2482	316.29
160	5.0794	−384.36	−305.61	−2.0797	1.5996	2.2291	322.44
165	4.9022	−376.10	−294.50	−2.0113	1.5949	2.2134	328.40
170	4.7383	−367.89	−283.47	−1.9454	1.5913	2.2005	334.18
175	4.5861	−359.71	−272.49	−1.8818	1.5887	2.1898	339.81
180	4.4442	−351.57	−261.57	−1.8203	1.5869	2.1811	345.30
185	4.3116	−343.45	−250.68	−1.7606	1.5858	2.1739	350.66
190	4.1872	−335.35	−239.83	−1.7027	1.5854	2.1682	355.89
195	4.0704	−327.27	−229.00	−1.6464	1.5856	2.1637	361.00
200	3.9603	−319.19	−218.19	−1.5917	1.5864	2.1603	366.01
210	3.7580	−303.05	−196.61	−1.4864	1.5897	2.1564	375.72
220	3.5764	−286.89	−175.05	−1.3861	1.5953	2.1561	385.04

Table 40. Thermodynamic properties of methane -- Continued

Temperature K	Density kg/m³	Internal energy kJ/kg	Enthalpy kJ/kg	Entropy kJ/(kg K)	c_v kJ/(kg K)	c_p kJ/(kg K)	Speed of sound m/s
			0.400 MPa Isobar				
230	3.4122	−270.70	−153.47	−1.2902	1.6029	2.1590	394.02
240	3.2631	−254.44	−131.86	−1.1982	1.6128	2.1648	402.67
250	3.1268	−238.09	−110.17	−1.1097	1.6248	2.1733	411.02
260	3.0019	−221.63	−88.382	−1.0242	1.6389	2.1846	419.08
270	2.8868	−205.03	−66.470	−0.94155	1.6552	2.1983	426.87
280	2.7805	−188.27	−44.409	−0.86132	1.6734	2.2144	434.42
290	2.6819	−171.33	−22.176	−0.78330	1.6937	2.2327	441.72
300	2.5901	−154.18	0.25179	−0.70727	1.7158	2.2531	448.81
310	2.5046	−136.81	22.893	−0.63303	1.7397	2.2755	455.69
320	2.4247	−119.20	45.768	−0.56041	1.7652	2.2997	462.38
330	2.3497	−101.34	68.893	−0.48925	1.7923	2.3256	468.90
340	2.2794	−83.201	92.285	−0.41942	1.8208	2.3530	475.25
350	2.2132	−64.777	115.96	−0.35080	1.8505	2.3819	481.45
360	2.1508	−46.055	139.93	−0.28328	1.8815	2.4119	487.50
370	2.0918	−27.021	164.20	−0.21677	1.9135	2.4432	493.43
380	2.0360	−7.6670	188.79	−0.15119	1.9464	2.4754	499.25
390	1.9832	12.017	213.71	−0.08647	1.9801	2.5085	504.95
400	1.9331	32.040	238.97	−0.02253	2.0146	2.5423	510.54
410	1.8854	52.407	264.56	0.04067	2.0497	2.5769	516.05
420	1.8401	73.125	290.51	0.10319	2.0854	2.6121	521.46
430	1.7969	94.200	316.80	0.16507	2.1215	2.6477	526.79
440	1.7557	115.64	343.46	0.22635	2.1579	2.6838	532.05
450	1.7164	137.44	370.48	0.28707	2.1947	2.7202	537.23
460	1.6788	159.60	397.86	0.34725	2.2318	2.7569	542.35
470	1.6429	182.14	425.62	0.40694	2.2690	2.7938	547.41
480	1.6084	205.05	453.74	0.46615	2.3065	2.8309	552.40
490	1.5754	228.33	482.24	0.52490	2.3440	2.8681	557.34
500	1.5437	251.99	511.10	0.58322	2.3815	2.9054	562.22
520	1.4840	300.42	569.96	0.69863	2.4567	2.9801	571.84
540	1.4288	350.36	630.31	0.81249	2.5317	3.0547	581.27
560	1.3776	401.79	692.14	0.92493	2.6064	3.1290	590.53
580	1.3299	454.70	755.46	1.0360	2.6807	3.2029	599.64
600	1.2855	509.09	820.26	1.1458	2.7542	3.2762	608.59
620	1.2439	564.94	886.51	1.2545	2.8271	3.3488	617.41
			0.500 MPa Isobar				
90.819[a]	451.63	−982.66	−981.55	−7.3854	2.1681	3.3655	1540.8
92	450.06	−978.68	−977.57	−7.3419	2.1605	3.3695	1530.1
94	447.39	−971.94	−970.83	−7.2693	2.1483	3.3771	1511.8
96	444.69	−965.19	−964.06	−7.1981	2.1367	3.3856	1493.3
98	441.98	−958.41	−957.28	−7.1282	2.1256	3.3949	1474.6
100	439.24	−951.62	−950.48	−7.0595	2.1148	3.4048	1455.7
105	432.28	−934.55	−933.39	−6.8928	2.0894	3.4327	1407.7
110	425.15	−917.33	−916.15	−6.7323	2.0653	3.4647	1358.5
115	417.82	−899.93	−898.74	−6.5775	2.0424	3.5015	1308.3
120	410.25	−882.34	−881.12	−6.4276	2.0205	3.5443	1256.9
125	402.40	−864.52	−863.28	−6.2820	1.9996	3.5946	1204.2
130	394.22	−846.43	−845.16	−6.1398	1.9799	3.6546	1149.9
135	385.66	−828.01	−826.71	−6.0006	1.9616	3.7278	1093.7
135.351[b]	385.04	−826.70	−825.40	−5.9909	1.9603	3.7335	1089.7
135.351[b]	8.0016	−429.63	−367.15	−2.6052	1.6959	2.5127	284.96

Table 40. Thermodynamic properties of methane — Continued

Temperature K	Density kg/m³	Internal energy kJ/kg	Enthalpy kJ/kg	Entropy kJ/(kg K)	c_v kJ/(kg K)	c_p kJ/(kg K)	Speed of sound m/s
			0.500 MPa Isobar				
140	7.6355	−421.15	−355.66	−2.5218	1.6645	2.4334	292.28
145	7.2869	−412.26	−343.65	−2.4375	1.6442	2.3767	299.66
150	6.9757	−403.55	−331.87	−2.3576	1.6302	2.3348	306.66
155	6.6950	−394.97	−320.28	−2.2816	1.6196	2.3020	313.35
160	6.4398	−386.49	−308.84	−2.2090	1.6114	2.2756	319.78
165	6.2063	−378.08	−297.52	−2.1393	1.6050	2.2541	325.98
170	5.9914	−369.75	−286.30	−2.0723	1.6000	2.2364	331.98
175	5.7927	−361.47	−275.15	−2.0077	1.5963	2.2218	337.80
180	5.6083	−353.23	−264.07	−1.9452	1.5935	2.2097	343.45
185	5.4365	−345.02	−253.05	−1.8848	1.5917	2.1997	348.95
190	5.2758	−336.85	−242.07	−1.8263	1.5906	2.1916	354.32
195	5.1253	−328.69	−231.13	−1.7695	1.5903	2.1850	359.55
200	4.9837	−320.55	−220.22	−1.7142	1.5906	2.1798	364.67
210	4.7245	−304.29	−198.46	−1.6080	1.5932	2.1730	374.56
220	4.4925	−288.04	−176.75	−1.5070	1.5981	2.1704	384.05
230	4.2835	−271.77	−155.04	−1.4105	1.6054	2.1714	393.16
240	4.0940	−255.44	−133.31	−1.3180	1.6149	2.1757	401.93
250	3.9212	−239.03	−111.52	−1.2291	1.6266	2.1831	410.38
260	3.7630	−222.51	−89.638	−1.1433	1.6405	2.1932	418.52
270	3.6175	−205.86	−67.644	−1.0603	1.6565	2.2061	426.39
280	3.4832	−189.06	−45.508	−0.97977	1.6747	2.2214	434.00
290	3.3588	−172.07	−23.207	−0.90152	1.6948	2.2391	441.37
300	3.2432	−154.89	−0.71882	−0.82528	1.7168	2.2590	448.50
310	3.1355	−137.49	21.979	−0.75086	1.7406	2.2809	455.43
320	3.0348	−119.85	44.905	−0.67807	1.7660	2.3047	462.16
330	2.9406	−101.96	68.078	−0.60677	1.7930	2.3302	468.72
340	2.8521	−83.793	91.514	−0.53680	1.8214	2.3573	475.10
350	2.7690	−65.345	115.23	−0.46806	1.8512	2.3858	481.33
360	2.6906	−46.601	139.23	−0.40044	1.8821	2.4156	487.42
370	2.6166	−27.547	163.54	−0.33384	1.9140	2.4465	493.37
380	2.5466	−8.1733	188.17	−0.26817	1.9469	2.4785	499.20
390	2.4803	11.529	213.12	−0.20336	1.9806	2.5114	504.93
400	2.4174	31.568	238.40	−0.13936	2.0150	2.5451	510.54
410	2.3577	51.951	264.02	−0.07609	2.0501	2.5795	516.06
420	2.3009	72.684	289.99	−0.01351	2.0857	2.6145	521.49
430	2.2468	93.773	316.31	0.04843	2.1218	2.6500	526.84
440	2.1952	115.22	342.99	0.10976	2.1583	2.6860	532.11
450	2.1459	137.03	370.03	0.17053	2.1950	2.7223	537.31
460	2.0988	159.21	397.44	0.23076	2.2321	2.7588	542.44
470	2.0538	181.76	425.21	0.29049	2.2693	2.7957	547.50
480	2.0107	204.68	453.35	0.34973	2.3067	2.8327	552.51
490	1.9693	227.97	481.87	0.40852	2.3442	2.8698	557.45
500	1.9297	251.64	510.75	0.46687	2.3817	2.9070	562.35
520	1.8550	300.09	569.64	0.58234	2.4569	2.9816	571.98
540	1.7859	350.04	630.01	0.69626	2.5319	3.0560	581.43
560	1.7218	401.49	691.88	0.80875	2.6066	3.1303	590.70
580	1.6622	454.41	755.22	0.91988	2.6808	3.2040	599.81
600	1.6066	508.81	820.03	1.0297	2.7544	3.2772	608.78
620	1.5546	564.67	886.30	1.1384	2.8272	3.3497	617.61

Table 40. Thermodynamic properties of methane – Continued

Temperature K	Density kg/m³	Internal energy kJ/kg	Enthalpy kJ/kg	Entropy kJ/(kg K)	c_v kJ/(kg K)	c_p kJ/(kg K)	Speed of sound m/s
			0.800 MPa Isobar				
90.895[a]	451.72	−982.58	−980.80	−7.3845	2.1684	3.3641	1542.1
92	450.26	−978.86	−977.09	−7.3438	2.1613	3.3678	1532.2
94	447.59	−972.13	−970.34	−7.2713	2.1491	3.3753	1514.0
96	444.91	−965.38	−963.58	−7.2002	2.1375	3.3836	1495.5
98	442.20	−958.62	−956.81	−7.1303	2.1264	3.3927	1476.9
100	439.47	−951.83	−950.01	−7.0617	2.1157	3.4026	1458.1
105	432.53	−934.78	−932.93	−6.8950	2.0902	3.4299	1410.2
110	425.42	−917.59	−915.71	−6.7347	2.0662	3.4614	1361.3
115	418.12	−900.22	−898.31	−6.5801	2.0432	3.4976	1311.4
120	410.58	−882.67	−880.72	−6.4304	2.0213	3.5395	1260.2
125	402.77	−864.89	−862.90	−6.2849	2.0005	3.5886	1207.8
130	394.64	−846.85	−844.82	−6.1431	1.9808	3.6472	1153.9
135	386.13	−828.48	−826.41	−6.0041	1.9624	3.7183	1098.2
140	377.15	−809.73	−807.61	−5.8674	1.9455	3.8064	1040.4
144.410[b]	368.76	−792.78	−790.62	−5.7479	1.9323	3.9035	987.05
144.410[b]	12.587	−422.59	−359.03	−2.7593	1.7399	2.7246	286.30
145	12.503	−421.42	−357.43	−2.7482	1.7329	2.7052	287.37
150	11.852	−411.74	−344.24	−2.6588	1.6919	2.5824	295.97
155	11.289	−402.41	−331.54	−2.5755	1.6678	2.5021	303.89
160	10.791	−393.32	−319.18	−2.4970	1.6510	2.4432	311.32
165	10.347	−384.40	−307.09	−2.4225	1.6384	2.3973	318.36
170	9.9456	−375.63	−295.19	−2.3515	1.6286	2.3605	325.08
175	9.5806	−366.97	−283.47	−2.2836	1.6210	2.3306	331.52
180	9.2463	−358.40	−271.88	−2.2183	1.6150	2.3059	337.72
185	8.9384	−349.91	−260.40	−2.1554	1.6105	2.2855	343.71
190	8.6535	−341.47	−249.02	−2.0947	1.6072	2.2686	349.50
195	8.3887	−333.08	−237.71	−2.0359	1.6050	2.2546	355.12
200	8.1418	−324.73	−226.47	−1.9790	1.6038	2.2430	360.58
210	7.6939	−308.11	−204.13	−1.8700	1.6039	2.2260	371.08
220	7.2975	−291.56	−181.93	−1.7667	1.6070	2.2155	381.06
230	6.9433	−275.02	−159.80	−1.6684	1.6128	2.2104	390.59
240	6.6245	−258.47	−137.70	−1.5743	1.6212	2.2098	399.71
250	6.3357	−241.86	−115.59	−1.4840	1.6320	2.2131	408.46
260	6.0725	−225.17	−93.430	−1.3971	1.6453	2.2200	416.87
270	5.8315	−208.37	−71.183	−1.3132	1.6607	2.2300	424.97
280	5.6098	−191.43	−48.820	−1.2318	1.6784	2.2430	432.78
290	5.4051	−174.32	−26.313	−1.1529	1.6981	2.2587	440.32
300	5.2155	−157.03	−3.6380	−1.0760	1.7197	2.2768	447.61
310	5.0393	−139.52	19.230	−1.0010	1.7432	2.2972	454.68
320	4.8749	−121.79	42.313	−0.92771	1.7684	2.3196	461.53
330	4.7214	−103.81	65.629	−0.85597	1.7952	2.3440	468.20
340	4.5774	−85.573	89.198	−0.78561	1.8235	2.3700	474.68
350	4.4423	−67.053	113.03	0.71652	1.8530	2.3976	481.00
360	4.3151	−48.241	137.15	−0.64857	1.8837	2.4266	487.17
370	4.1952	−29.125	161.57	−0.58167	1.9156	2.4568	493.20
380	4.0819	−9.6937	186.29	−0.51574	1.9483	2.4881	499.10
390	3.9747	10.062	211.34	−0.45070	1.9819	2.5204	504.88
400	3.8731	30.152	236.70	−0.38647	2.0163	2.5536	510.55
410	3.7767	50.583	262.41	−0.32300	2.0513	2.5874	516.13
420	3.6850	71.360	288.46	−0.26024	2.0868	2.6220	521.60

Table 40. Thermodynamic properties of methane – Continued

Temperature K	Density kg/m³	Internal energy kJ/kg	Enthalpy kJ/kg	Entropy kJ/(kg K)	c_v kJ/(kg K)	c_p kJ/(kg K)	Speed of sound m/s
			0.800 MPa Isobar				
430	3.5978	92.491	314.85	−0.19813	2.1228	2.6570	527.00
440	3.5146	113.98	341.60	−0.13664	2.1592	2.6926	532.31
450	3.4353	135.83	368.70	−0.07573	2.1959	2.7285	537.54
460	3.3596	158.04	396.17	−0.01536	2.2329	2.7648	542.70
470	3.2871	180.62	424.00	0.04449	2.2701	2.8013	547.80
480	3.2178	203.58	452.20	0.10385	2.3074	2.8380	552.83
490	3.1513	226.90	480.76	0.16275	2.3449	2.8749	557.81
500	3.0876	250.59	509.69	0.22120	2.3824	2.9119	562.73
520	2.9676	299.10	568.67	0.33685	2.4575	2.9860	572.41
540	2.8568	349.10	629.13	0.45093	2.5324	3.0601	581.90
560	2.7540	400.58	691.07	0.56355	2.6071	3.1339	591.20
580	2.6584	453.55	754.49	0.67481	2.6812	3.2074	600.35
600	2.5692	507.99	819.37	0.78478	2.7547	3.2803	609.34
620	2.4859	563.88	885.70	0.89352	2.8275	3.3526	618.20
			1.000 MPa Isobar				
90.947[a]	451.79	−982.52	−980.31	−7.3839	2.1686	3.3632	1543.0
92	450.39	−978.98	−976.76	−7.3451	2.1618	3.3666	1533.5
94	447.73	−972.26	−970.02	−7.2727	2.1496	3.3740	1515.4
96	445.05	−965.51	−963.27	−7.2015	2.1380	3.3823	1497.0
98	442.34	−958.75	−956.49	−7.1317	2.1269	3.3913	1478.4
100	439.62	−951.97	−949.70	−7.0631	2.1162	3.4011	1459.6
105	432.70	−934.94	−932.63	−6.8965	2.0908	3.4282	1411.9
110	425.61	−917.76	−915.41	−6.7363	2.0667	3.4593	1363.2
115	418.32	−900.42	−898.03	−6.5818	2.0438	3.4950	1313.4
120	410.80	−882.89	−880.45	−6.4322	2.0219	3.5363	1262.4
125	403.01	−865.13	−862.65	−6.2869	2.0010	3.5848	1210.2
130	394.92	−847.12	−844.59	−6.1452	1.9813	3.6424	1156.6
135	386.44	−828.80	−826.21	−6.0065	1.9629	3.7122	1101.2
140	377.51	−810.09	−807.44	−5.8700	1.9460	3.7984	1043.7
145	368.02	−790.90	−788.19	−5.7348	1.9311	3.9075	983.57
149.139[b]	359.62	−774.57	−771.79	−5.6233	1.9205	4.0227	931.21
149.139[b]	15.698	−419.83	−356.13	−2.8363	1.7673	2.8765	286.08
150	15.536	−418.03	−353.67	−2.8198	1.7556	2.8402	287.76
155	14.690	−407.96	−339.88	−2.7294	1.7094	2.6869	296.87
160	13.965	−398.32	−326.71	−2.6458	1.6824	2.5878	305.18
165	13.332	−388.97	−313.96	−2.5673	1.6639	2.5159	312.91
170	12.769	−379.84	−301.53	−2.4930	1.6499	2.4604	320.20
175	12.265	−370.87	−289.34	−2.4224	1.6391	2.4162	327.13
180	11.807	−362.04	−277.35	−2.3548	1.6307	2.3803	333.74
185	11.390	−353.32	−265.52	−2.2900	1.6241	2.3508	340.09
190	11.007	−344.68	−253.83	−2.2277	1.6191	2.3264	346.20
195	10.654	−336.12	−242.25	−2.1675	1.6155	2.3062	352.10
200	10.326	−327.61	−230.77	−2.1093	1.6131	2.2895	357.81
210	9.7351	−310.73	−208.00	−1.9983	1.6113	2.2643	368.73
220	9.2166	−293.95	−185.45	−1.8934	1.6131	2.2477	379.06
230	8.7563	−277.23	−163.03	−1.7937	1.6179	2.2379	388.88
240	8.3440	−260.52	−140.67	−1.6985	1.6255	2.2336	398.24
250	7.9721	−243.78	−118.34	−1.6074	1.6358	2.2340	407.20
260	7.6344	−226.97	−95.980	−1.5197	1.6485	2.2385	415.79
270	7.3260	−210.06	−73.558	−1.4351	1.6635	2.2465	424.04

Table 40. Thermodynamic properties of methane – Continued

Temperature K	Density kg/m³	Internal energy kJ/kg	Enthalpy kJ/kg	Entropy kJ/(kg K)	c_v kJ/(kg K)	c_p kJ/(kg K)	Speed of sound m/s
			1.000 MPa Isobar				
280	7.0432	−193.02	−51.040	−1.3532	1.6809	2.2578	431.98
290	6.7826	−175.83	−28.393	−1.2737	1.7003	2.2720	439.64
300	6.5415	−158.46	−5.5903	−1.1964	1.7217	2.2889	447.04
310	6.3179	−140.89	17.393	−1.1210	1.7450	2.3082	454.19
320	6.1097	−123.09	40.582	−1.0474	1.7701	2.3298	461.13
330	5.9153	−105.06	63.995	−0.97537	1.7967	2.3533	467.87
340	5.7334	−86.763	87.653	−0.90474	1.8248	2.3786	474.42
350	5.5628	−68.194	111.57	−0.83541	1.8542	2.4056	480.80
360	5.4023	−49.337	135.77	−0.76725	1.8849	2.4340	487.02
370	5.2511	−30.179	160.26	−0.70016	1.9166	2.4637	493.09
380	5.1084	−10.709	185.05	−0.63405	1.9493	2.4945	499.04
390	4.9735	9.0840	210.15	−0.56884	1.9828	2.5264	504.86
400	4.8457	29.208	235.58	−0.50447	2.0171	2.5592	510.57
410	4.7244	49.670	261.34	−0.44086	2.0520	2.5927	516.18
420	4.6092	70.478	287.43	−0.37797	2.0875	2.6269	521.69
430	4.4996	91.636	313.88	−0.31575	2.1235	2.6617	527.11
440	4.3952	113.15	340.67	−0.25416	2.1598	2.6970	532.44
450	4.2957	135.03	367.82	−0.19315	2.1965	2.7327	537.70
460	4.2006	157.26	395.33	−0.13269	2.2334	2.7687	542.89
470	4.1097	179.87	423.19	−0.07276	2.2706	2.8051	548.01
480	4.0227	202.84	451.43	−0.01332	2.3079	2.8416	553.06
490	3.9394	226.18	480.03	0.04565	2.3453	2.8783	558.05
500	3.8595	249.90	508.99	0.10417	2.3828	2.9151	562.99
520	3.7092	298.44	568.03	0.21993	2.4579	2.9889	572.70
540	3.5704	348.47	628.55	0.33412	2.5328	3.0627	582.21
560	3.4416	399.98	690.54	0.44684	2.6074	3.1364	591.55
580	3.3220	452.98	754.00	0.55818	2.6815	3.2097	600.71
600	3.2104	507.44	818.92	0.66822	2.7550	3.2824	609.73
620	3.1062	563.36	885.30	0.77703	2.8278	3.3545	618.59
			1.500 MPa Isobar				
91.074[a]	451.94	−982.39	−979.07	−7.3824	2.1690	3.3608	1545.3
92	450.72	−979.28	−975.95	−7.3484	2.1631	3.3638	1537.0
94	448.07	−972.57	−969.22	−7.2760	2.1509	3.3710	1518.9
96	445.40	−965.84	−962.47	−7.2049	2.1393	3.3791	1500.6
98	442.71	−959.09	−955.70	−7.1352	2.1282	3.3879	1482.2
100	439.99	−952.33	−948.92	−7.0666	2.1175	3.3974	1463.5
105	433.11	−935.33	−931.86	−6.9002	2.0921	3.4237	1416.1
110	426.05	−918.19	−914.67	−6.7403	2.0681	3.4540	1367.7
115	418.81	−900.90	−897.32	−6.5860	2.0452	3.4887	1318.3
120	411.34	−883.42	−879.78	−6.4367	2.0233	3.5286	1267.9
125	403.62	−865.74	−862.02	−6.2917	2.0025	3.5753	1216.2
130	395.60	−847.80	−844.01	−6.1505	1.9827	3.6306	1163.2
135	387.21	−829.57	−825.70	−6.0122	1.9642	3.6973	1108.6
140	378.40	−810.98	−807.01	−5.8763	1.9472	3.7790	1052.0
145	369.05	−791.93	−787.87	−5.7420	1.9320	3.8817	993.01
150	359.03	−772.32	−768.14	−5.6083	1.9191	4.0146	930.89
155	348.11	−751.96	−747.65	−5.4739	1.9093	4.1936	864.64
158.528[b]	339.71	−736.98	−732.57	−5.3777	1.9049	4.3634	814.56
158.528[b]	23.818	−416.74	−353.76	−2.9881	1.8347	3.3226	283.65
160	23.327	−413.25	−348.95	−2.9579	1.8075	3.2135	287.05

Table 40. Thermodynamic properties of methane — Continued

Temperature K	Density kg/m³	Internal energy kJ/kg	Enthalpy kJ/kg	Entropy kJ/(kg K)	c_v kJ/(kg K)	c_p kJ/(kg K)	Speed of sound m/s
			1.500 MPa Isobar				
165	21.887	−402.10	−333.57	−2.8633	1.7487	2.9626	297.50
170	20.696	−391.64	−319.17	−2.7773	1.7150	2.8071	306.77
175	19.680	−381.64	−305.42	−2.6976	1.6922	2.6979	315.26
180	18.795	−371.95	−292.14	−2.6228	1.6753	2.6158	323.15
185	18.011	−362.51	−279.23	−2.5520	1.6623	2.5516	330.57
190	17.309	−353.27	−266.61	−2.4847	1.6521	2.5001	337.60
195	16.675	−344.17	−254.21	−2.4203	1.6443	2.4583	344.30
200	16.096	−335.20	−242.01	−2.3585	1.6384	2.4240	350.70
210	15.077	−317.54	−218.05	−2.2416	1.6313	2.3721	362.78
220	14.201	−300.14	−194.52	−2.1321	1.6292	2.3365	374.03
230	13.437	−282.91	−171.28	−2.0288	1.6312	2.3125	384.61
240	12.763	−265.77	−148.24	−1.9307	1.6367	2.2974	394.60
250	12.161	−248.65	−125.31	−1.8371	1.6452	2.2893	404.09
260	11.620	−231.52	−102.43	−1.7474	1.6567	2.2869	413.13
270	11.129	−214.34	−79.554	−1.6610	1.6707	2.2894	421.77
280	10.682	−197.05	−56.630	−1.5777	1.6871	2.2960	430.05
290	10.273	−179.64	−33.621	−1.4969	1.7059	2.3064	438.00
300	9.8958	−162.07	−10.492	−1.4185	1.7267	2.3200	445.66
310	9.5476	−144.32	12.788	−1.3422	1.7495	2.3365	453.05
320	9.2246	−126.36	36.246	−1.2677	1.7741	2.3556	460.19
330	8.9240	−108.18	59.907	−1.1949	1.8004	2.3769	467.10
340	8.6435	−89.749	83.792	−1.1236	1.8281	2.4004	473.82
350	8.3810	−71.056	107.92	−1.0537	1.8573	2.4257	480.34
360	8.1347	−52.083	132.31	−0.98496	1.8877	2.4526	486.69
370	7.9032	−32.819	156.98	−0.91738	1.9192	2.4810	492.89
380	7.6850	−13.250	181.94	−0.85082	1.9517	2.5107	498.94
390	7.4790	6.6351	207.20	−0.78521	1.9850	2.5415	504.86
400	7.2842	26.845	232.77	−0.72046	2.0191	2.5733	510.66
410	7.0997	47.387	258.66	−0.65652	2.0539	2.6060	516.35
420	6.9245	68.270	284.89	−0.59333	2.0893	2.6394	521.94
430	6.7581	89.500	311.46	−0.53082	2.1251	2.6735	527.43
440	6.5997	111.08	338.36	−0.46896	2.1614	2.7081	532.83
450	6.4488	133.02	365.62	−0.40771	2.1980	2.7432	538.15
460	6.3049	155.32	393.23	−0.34703	2.2348	2.7787	543.39
470	6.1673	177.98	421.19	−0.28689	2.2719	2.8144	548.56
480	6.0358	201.00	449.52	−0.22726	2.3091	2.8505	553.66
490	5.9099	224.39	478.20	−0.16811	2.3465	2.8867	558.70
500	5.7893	248.15	507.25	−0.10943	2.3839	2.9231	563.67
520	5.5625	296.78	566.45	0.00664	2.4588	2.9962	573.46
540	5.3532	346.90	627.10	0.12109	2.5336	3.0694	583.04
560	5.1593	398.48	689.22	0.23404	2.6082	3.1425	592.42
580	4.9792	451.54	752.80	0.34559	2.6822	3.2153	601.64
600	4.8114	506.07	817.83	0.45581	2.7556	3.2876	610.70
620	4.6547	562.04	884.30	0.56478	2.8283	3.3593	619.60
			2.000 MPa Isobar				
91.201[a]	452.10	−982.25	−977.83	−7.3809	2.1694	3.3586	1547.5
92	451.05	−979.58	−975.14	−7.3516	2.1644	3.3611	1540.4
94	448.41	−972.87	−968.41	−7.2793	2.1522	3.3681	1522.4
96	445.75	−966.16	−961.67	−7.2083	2.1406	3.3759	1504.3
98	443.07	−959.42	−954.91	−7.1386	2.1295	3.3845	1485.9
100	440.37	−952.67	−948.13	−7.0701	2.1188	3.3937	1467.4
105	433.51	−935.71	−931.10	−6.9039	2.0935	3.4194	1420.3
110	426.50	−918.62	−913.93	−6.7442	2.0695	3.4489	1372.3
115	419.30	−901.37	−896.60	−6.5902	2.0466	3.4825	1323.3
120	411.88	−883.95	−879.10	−6.4412	2.0248	3.5211	1273.3

Table 40. Thermodynamic properties of methane – Continued

Temperature K	Density kg/m³	Internal energy kJ/kg	Enthalpy kJ/kg	Entropy kJ/(kg K)	c_v kJ/(kg K)	c_p kJ/(kg K)	Speed of sound m/s
			2.000 MPa Isobar				
125	404.22	−866.33	−861.38	−6.2965	2.0039	3.5661	1222.1
130	396.27	−848.47	−843.42	−6.1557	1.9841	3.6193	1169.7
135	387.97	−830.33	−825.17	−6.0179	1.9656	3.6829	1115.8
140	379.27	−811.84	−806.57	−5.8826	1.9484	3.7606	1060.1
145	370.06	−792.94	−787.53	−5.7490	1.9330	3.8574	1002.2
150	360.21	−773.50	−767.95	−5.6163	1.9197	3.9813	941.45
155	349.55	−753.38	−747.65	−5.4832	1.9093	4.1456	877.06
160	337.78	−732.31	−726.39	−5.3481	1.9028	4.3754	807.65
165	324.40	−709.87	−703.71	−5.2086	1.9027	4.7243	730.83
165.873[b]	321.84	−705.76	−699.55	−5.1835	1.9036	4.8055	716.36
165.873[b]	32.644	−417.26	−355.99	−3.1123	1.9052	3.9235	279.73
170	30.533	−406.35	−340.84	−3.0220	1.8197	3.4665	290.52
175	28.530	−394.45	−324.34	−2.9263	1.7647	3.1600	301.59
180	26.904	−383.39	−309.06	−2.8402	1.7313	2.9678	311.34
185	25.535	−372.90	−294.57	−2.7608	1.7080	2.8331	320.21
190	24.354	−362.79	−280.67	−2.6867	1.6906	2.7325	328.40
195	23.316	−352.99	−267.21	−2.6167	1.6772	2.6544	336.07
200	22.392	−343.42	−254.10	−2.5503	1.6669	2.5923	343.30
210	20.805	−324.79	−228.66	−2.4262	1.6532	2.5009	356.70
220	19.480	−306.65	−203.98	−2.3114	1.6465	2.4390	368.98
230	18.348	−288.82	−179.82	−2.2040	1.6452	2.3965	380.37
240	17.364	−271.19	−156.01	−2.1026	1.6483	2.3678	391.03
250	16.497	−253.67	−132.43	−2.0064	1.6550	2.3493	401.07
260	15.724	−236.19	−109.00	−1.9145	1.6650	2.3388	410.57
270	15.030	−218.70	−85.632	−1.8263	1.6779	2.3348	419.61
280	14.402	−201.15	−62.281	−1.7414	1.6935	2.3363	428.22
290	13.830	−183.50	−38.892	−1.6593	1.7115	2.3423	436.47
300	13.307	−165.72	−15.422	−1.5797	1.7317	2.3522	444.38
310	12.825	−147.79	8.1642	−1.5024	1.7540	2.3656	452.00
320	12.379	−129.66	31.900	−1.4270	1.7781	2.3820	459.34
330	11.966	−111.32	55.814	−1.3535	1.8040	2.4011	466.43
340	11.582	−92.752	79.931	−1.2815	1.8315	2.4226	473.30
350	11.223	−73.930	104.27	−1.2109	1.8603	2.4461	479.96
360	10.887	−54.840	128.86	−1.1416	1.8905	2.4715	486.45
370	10.572	−35.466	153.71	−1.0736	1.9217	2.4986	492.76
380	10.276	−15.796	178.84	−1.0065	1.9540	2.5270	498.91
390	9.9964	4.1825	204.25	−0.94052	1.9872	2.5567	504.93
400	9.7326	24.479	229.97	−0.87541	2.0212	2.5875	510.82
410	9.4830	45.104	256.01	−0.81112	2.0558	2.6193	516.59
420	9.2464	66.063	282.36	−0.74762	2.0910	2.6519	522.24
430	9.0218	87.364	309.05	−0.68482	2.1268	2.6853	527.80
440	8.8083	109.01	336.07	−0.62270	2.1629	2.7192	533.26
450	8.6051	131.01	363.43	−0.56121	2.1994	2.7537	538.64
460	8.4113	153.37	391.15	−0.50031	2.2362	2.7886	543.93
470	8.2264	176.09	419.21	−0.43996	2.2732	2.8238	549.15
480	8.0497	199.17	447.62	−0.38014	2.3103	2.8594	554.30
490	7.8806	222.61	476.40	−0.32081	2.3476	2.8952	559.38
500	7.7187	246.42	505.53	−0.26196	2.3850	2.9312	564.39
520	7.4146	295.14	564.87	−0.14559	2.4598	3.0035	574.25
540	7.1342	345.33	625.67	−0.03087	2.5345	3.0761	583.89
560	6.8746	396.99	687.92	0.08231	2.6089	3.1486	593.33
580	6.6336	450.12	751.61	0.19406	2.6829	3.2209	602.59

Table 40. Thermodynamic properties of methane – Continued

Temperature K	Density kg/m³	Internal energy kJ/kg	Enthalpy kJ/kg	Entropy kJ/(kg K)	c_v kJ/(kg K)	c_p kJ/(kg K)	Speed of sound m/s
			2.000 MPa Isobar				
600	6.4093	504.70	816.75	0.30446	2.7562	3.2927	611.69
620	6.1999	560.73	883.32	0.41360	2.8289	3.3641	620.63
			2.500 MPa Isobar				
91.329[a]	452.26	−982.11	−976.58	−7.3795	2.1699	3.3563	1549.7
92	451.38	−979.87	−974.33	−7.3549	2.1656	3.3584	1543.8
94	448.75	−973.18	−967.61	−7.2826	2.1534	3.3652	1525.9
96	446.10	−966.47	−960.87	−7.2116	2.1419	3.3728	1507.9
98	443.43	−959.75	−954.12	−7.1420	2.1308	3.3812	1489.6
100	440.74	−953.02	−947.34	−7.0736	2.1202	3.3902	1471.2
105	433.92	−936.09	−930.33	−6.9076	2.0948	3.4152	1424.5
110	426.94	−919.04	−913.19	−6.7481	2.0709	3.4438	1376.8
115	419.78	−901.84	−895.89	−6.5943	2.0481	3.4764	1328.2
120	412.42	−884.48	−878.41	−6.4456	2.0262	3.5138	1278.6
125	404.81	−866.92	−860.74	−6.3013	2.0053	3.5572	1227.9
130	396.93	−849.13	−842.83	−6.1608	1.9855	3.6083	1176.1
135	388.72	−831.07	−824.64	−6.0235	1.9669	3.6692	1122.9
140	380.12	−812.69	−806.12	−5.8888	1.9497	3.7431	1068.0
145	371.04	−793.92	−787.18	−5.7559	1.9341	3.8345	1011.1
150	361.37	−774.65	−767.73	−5.6240	1.9205	3.9503	951.68
155	350.94	−754.74	−747.62	−5.4921	1.9095	4.1018	888.99
160	339.50	−733.98	−726.62	−5.3588	1.9020	4.3092	821.92
165	326.64	−712.02	−704.37	−5.2219	1.8999	4.6135	748.64
170	311.56	−688.19	−680.17	−5.0774	1.9072	5.1164	665.46
171.992[b]	304.58	−677.89	−669.68	−5.0161	1.9149	5.4300	627.90
171.992[c]	42.498	−420.59	−361.76	−3.2258	1.9839	4.8050	274.94
175	39.947	−410.99	−348.41	−3.1488	1.8915	4.1417	284.59
180	36.782	−397.25	−329.28	−3.0410	1.8108	3.5766	297.66
185	34.367	−384.98	−312.24	−2.9476	1.7661	3.2648	308.68
190	32.409	−373.59	−296.45	−2.8634	1.7366	3.0618	318.46
195	30.763	−362.79	−281.52	−2.7858	1.7152	2.9173	327.36
200	29.345	−352.41	−267.22	−2.7134	1.6990	2.8088	335.58
210	26.994	−332.56	−239.95	−2.5803	1.6771	2.6572	350.52
220	25.096	−313.52	−213.90	−2.4591	1.6651	2.5585	363.93
230	23.514	−294.99	−188.67	−2.3470	1.6601	2.4915	376.19
240	22.163	−276.80	−164.00	−2.2420	1.6604	2.4456	387.55
250	20.989	−258.82	−139.71	−2.1428	1.6652	2.4145	398.15
260	19.954	−240.96	−115.67	−2.0485	1.6736	2.3945	408.13
270	19.033	−223.14	−91.793	−1.9584	1.6853	2.3831	417.56
280	18.206	−205.31	−67.990	−1.8718	1.6999	2.3785	426.51
290	17.457	−187.41	−44.203	−1.7884	1.7171	2.3797	435.05
300	16.774	−169.42	−20.380	−1.7076	1.7367	2.3856	443.22
310	16.149	−151.28	3.523(	−1.6292	1.7584	2.3957	451.05
320	15.574	−132.98	27.545	−1.5530	1.7821	2.4092	458.58
330	15.042	−114.48	51.718	−1.4786	1.8076	2.4259	465.85
340	14.548	−95.770	76.072	−1.4059	1.8348	2.4452	472.87
350	14.089	−76.817	100.63	−1.3347	1.8633	2.4669	479.67
360	13.660	−57.605	125.42	−1.2649	1.8932	2.4907	486.28
370	13.258	−38.120	150.45	−1.1963	1.9243	2.5163	492.70
380	12.880	−18.347	175.75	−1.1288	1.9564	2.5435	498.96
390	12.525	1.7267	201.33	−1.0624	1.9894	2.5721	505.07
400	12.190	22.112	227.19	−0.99688	2.0232	2.6018	511.04
410	11.874	42.819	253.37	−0.93226	2.0577	2.6327	516.88
420	11.574	63.856	279.85	−0.86844	2.0928	2.6645	522.61

Table 40. Thermodynamic properties of methane – Continued

Temperature K	Density kg/m³	Internal energy kJ/kg	Enthalpy kJ/kg	Entropy kJ/(kg K)	c_v kJ/(kg K)	c_p kJ/(kg K)	Speed of sound m/s
			2.500 MPa Isobar				
430	11.290	85.230	306.66	−0.80536	2.1284	2.6971	528.23
440	11.021	106.95	333.79	−0.74298	2.1644	2.7303	533.75
450	10.764	129.01	361.27	−0.68124	2.2008	2.7641	539.18
460	10.520	151.43	389.08	−0.62011	2.2375	2.7985	544.52
470	10.287	174.20	417.24	−0.55956	2.2744	2.8332	549.79
480	10.064	197.33	445.74	−0.49954	2.3115	2.8683	554.98
490	9.8512	220.83	474.60	−0.44004	2.3487	2.9036	560.09
500	9.6476	244.68	503.82	−0.38102	2.3860	2.9392	565.15
520	9.2653	293.49	563.32	−0.26435	2.4607	3.0108	575.07
540	8.9131	343.76	624.25	−0.14937	2.5353	3.0827	584.77
560	8.5874	395.50	686.62	−0.03596	2.6097	3.1546	594.26
580	8.2853	448.69	750.43	0.07599	2.6836	3.2264	603.57
600	8.0042	503.34	815.68	0.18658	2.7569	3.2978	612.71
620	7.7419	559.43	882.35	0.29587	2.8295	3.3688	621.68
			3.000 MPa Isobar				
91.456[a]	452.41	−981.98	−975.34	−7.3780	2.1703	3.3541	1551.9
92	451.70	−980.16	−973.52	−7.3581	2.1669	3.3557	1547.1
94	449.08	−973.48	−966.80	−7.2858	2.1547	3.3623	1529.4
96	446.44	−966.79	−960.07	−7.2150	2.1431	3.3697	1511.4
98	443.78	−960.08	−953.32	−7.1454	2.1321	3.3779	1493.3
100	441.11	−953.36	−946.56	−7.0771	2.1215	3.3867	1475.0
105	434.32	−936.47	−929.56	−6.9113	2.0962	3.4110	1428.6
110	427.38	−919.46	−912.44	−6.7520	2.0723	3.4389	1381.2
115	420.26	−902.31	−895.17	−6.5984	2.0495	3.4705	1333.0
120	412.94	−884.99	−877.73	−6.4500	2.0276	3.5067	1283.8
125	405.40	−867.49	−860.09	−6.3060	2.0067	3.5486	1233.7
130	397.58	−849.78	−842.23	−6.1659	1.9869	3.5977	1182.4
135	389.45	−831.80	−824.10	−6.0290	1.9683	3.6560	1129.9
140	380.95	−813.52	−805.65	−5.8948	1.9509	3.7264	1075.8
145	372.00	−794.87	−786.81	−5.7626	1.9352	3.8128	1019.8
150	362.49	−775.76	−767.49	−5.6316	1.9213	3.9212	961.61
155	352.27	−756.06	−747.54	−5.5008	1.9098	4.0614	900.46
160	341.14	−735.59	−726.79	−5.3691	1.9015	4.2498	835.51
165	328.74	−714.04	−704.92	−5.2345	1.8978	4.5182	765.27
170	314.45	−690.90	−681.36	−5.0939	1.9016	4.9388	687.08
175	296.89	−665.05	−654.94	−4.9408	1.9211	5.7286	594.86
177.274[b]	286.93	−651.66	−641.20	−4.8628	1.9416	6.4129	544.18
177.274[b]	53.878	−426.69	−371.01	−3.3386	2.0769	6.2463	269.47
180	50.073	−415.81	−355.89	−3.2540	1.9568	5.0107	280.27
185	45.323	−399.82	−333.62	−3.1319	1.8499	4.0405	295.35
190	41.946	−386.22	−314.70	−3.0309	1.7951	3.5738	307.50
195	39.311	−373.90	−297.59	−2.9420	1.7603	3.2909	318.05
200	37.150	−362.40	−281.64	−2.8613	1.7357	3.0980	327.51
210	33.737	−340.94	−252.02	−2.7167	1.7034	2.8502	344.24
220	31.100	−320.79	−224.33	−2.5878	1.6850	2.6989	358.90
230	28.964	−301.44	−197.87	−2.4702	1.6757	2.5995	372.09
240	27.176	−282.62	−172.23	−2.3611	1.6730	2.5319	384.17
250	25.647	−264.13	−147.16	−2.2587	1.6756	2.4856	395.36
260	24.316	−245.85	−122.47	−2.1619	1.6824	2.4542	405.81
270	23.142	−227.67	−98.036	−2.0697	1.6928	2.4342	415.63

Table 40. Thermodynamic properties of methane — Continued

Temperature K	Density kg/m³	Internal energy kJ/kg	Enthalpy kJ/kg	Entropy kJ/(kg K)	c_v kJ/(kg K)	c_p kJ/(kg K)	Speed of sound m/s
			3.000 MPa Isobar				
280	22.095	−209.54	−73.757	−1.9814	1.7064	2.4229	424.92
290	21.153	−191.38	−49.554	−1.8964	1.7228	2.4187	433.75
300	20.300	−173.15	−25.364	−1.8144	1.7417	2.4202	442.16
310	19.521	−154.81	−1.1336	−1.7350	1.7629	2.4266	450.21
320	18.808	−136.33	23.182	−1.6578	1.7861	2.4371	457.93
330	18.150	−117.67	47.621	−1.5826	1.8113	2.4512	465.36
340	17.542	−98.804	72.215	−1.5091	1.8380	2.4683	472.53
350	16.977	−79.715	96.995	−1.4373	1.8663	2.4880	479.47
360	16.451	−60.379	121.98	−1.3669	1.8960	2.5101	486.19
370	15.959	−40.781	147.20	−1.2978	1.9268	2.5342	492.72
380	15.498	−20.903	172.67	−1.2299	1.9587	2.5601	499.07
390	15.065	−0.73177	198.41	−1.1631	1.9915	2.5875	505.27
400	14.657	19.744	224.43	−1.0972	2.0252	2.6162	511.32
410	14.272	40.535	250.74	−1.0322	2.0595	2.6462	517.23
420	13.908	61.650	277.35	−0.96808	2.0945	2.6771	523.03
430	13.563	83.096	304.28	−0.90472	2.1300	2.7089	528.71
440	13.236	104.88	331.53	−0.84207	2.1659	2.7414	534.29
450	12.925	127.01	359.11	−0.78009	2.2022	2.7746	539.77
460	12.629	149.49	387.03	−0.71874	2.2388	2.8084	545.16
470	12.347	172.32	415.28	−0.65798	2.2757	2.8426	550.47
480	12.078	195.50	443.88	−0.59777	2.3127	2.8771	555.70
490	11.821	219.05	472.83	−0.53809	2.3498	2.9120	560.85
500	11.575	242.96	502.12	−0.47890	2.3871	2.9472	565.94
520	11.114	291.85	561.77	−0.36193	2.4617	3.0180	575.93
540	10.690	342.21	622.85	−0.24670	2.5362	3.0893	585.68
560	10.298	394.01	685.35	−0.13306	2.6104	3.1607	595.22
580	9.9335	447.28	749.27	−0.02090	2.6842	3.2319	604.57
600	9.5958	501.98	814.62	0.08986	2.7575	3.3029	613.74
620	9.2805	558.13	881.39	0.19932	2.8300	3.3735	622.76
			3.500 MPa Isobar				
91.583[a]	452.57	−981.84	−974.10	−7.3765	2.1707	3.3518	1554.1
92	452.02	−980.45	−972.71	−7.3613	2.1681	3.3531	1550.5
94	449.41	−973.78	−965.99	−7.2891	2.1559	3.3595	1532.8
96	446.78	−967.10	−959.27	−7.2183	2.1444	3.3667	1515.0
98	444.14	−960.41	−952.53	−7.1488	2.1334	3.3747	1497.0
100	441.47	−953.70	−945.77	−7.0805	2.1228	3.3832	1478.8
105	434.71	−936.85	−928.79	−6.9149	2.0975	3.4070	1432.6
110	427.81	−919.87	−911.69	−6.7558	2.0736	3.4341	1385.6
115	420.73	−902.77	−894.45	−6.6025	2.0508	3.4648	1337.8
120	413.47	−885.50	−877.04	−6.4543	2.0290	3.4998	1289.0
125	405.97	−868.06	−859.44	−6.3106	2.0081	3.5403	1239.4
130	398.23	−850.41	−841.62	−6.1709	1.9883	3.5875	1188.6
135	390.18	−832.52	−823.55	−6.0345	1.9696	3.6433	1136.7
140	381.77	−814.34	−805.17	−5.9008	1.9522	3.7104	1083.4
145	372.93	−795.81	−786.42	−5.7692	1.9363	3.7922	1028.4
150	363.57	−776.84	−767.22	−5.6390	1.9222	3.8940	971.25
155	353.56	−757.34	−747.44	−5.5093	1.9102	4.0241	911.54
160	342.71	−737.12	−726.91	−5.3789	1.9012	4.1961	848.48
165	330.71	−715.95	−705.36	−5.2464	1.8962	4.4351	780.91
170	317.08	−693.40	−682.36	−5.1091	1.8974	4.7939	706.83

Table 40. Thermodynamic properties of methane – Continued

Temperature K	Density kg/m³	Internal energy kJ/kg	Enthalpy kJ/kg	Entropy kJ/(kg K)	c_v kJ/(kg K)	c_p kJ/(kg K)	Speed of sound m/s
			3.500 MPa Isobar				
175	300.81	−668.65	−657.01	−4.9621	1.9102	5.4107	622.17
180	279.24	−639.54	−627.00	−4.7932	1.9526	6.8456	515.91
181.937[b]	267.63	−625.63	−612.56	−4.7134	1.9934	8.2482	461.14
181.937[b]	67.716	−436.26	−384.58	−3.4603	2.1957	9.0439	263.27
185	60.619	−420.28	−362.54	−3.3401	2.0054	6.0072	278.29
190	53.919	−401.83	−336.92	−3.2034	1.8787	4.5064	295.00
195	49.467	−386.91	−316.15	−3.0954	1.8170	3.8698	307.98
200	46.109	−373.69	−297.78	−3.0024	1.7788	3.5052	319.06
210	41.163	−350.05	−265.02	−2.8425	1.7324	3.0936	337.90
220	37.554	−328.52	−235.32	−2.7043	1.7063	2.8656	353.93
230	34.731	−308.21	−207.43	−2.5803	1.6921	2.7228	368.11
240	32.423	−288.65	−180.71	−2.4665	1.6861	2.6278	380.94
250	30.483	−269.59	−154.77	−2.3607	1.6862	2.5629	392.71
260	28.815	−250.85	−129.38	−2.2611	1.6913	2.5183	403.63
270	27.358	−232.29	−104.36	−2.1666	1.7003	2.4883	413.85
280	26.070	−213.83	−79.580	−2.0765	1.7129	2.4695	423.47
290	24.919	−195.40	−54.942	−1.9900	1.7285	2.4593	432.58
300	23.882	−176.92	−30.371	−1.9067	1.7467	2.4560	441.23
310	22.940	−158.37	−5.8034	−1.8262	1.7673	2.4584	449.48
320	22.080	−139.70	18.813	−1.7480	1.7901	2.4657	457.39
330	21.291	−120.87	43.523	−1.6720	1.8148	2.4770	464.98
340	20.562	−101.85	68.364	−1.5978	1.8413	2.4917	472.29
350	19.887	−82.623	93.367	−1.5254	1.8693	2.5094	479.35
360	19.260	−63.162	118.56	−1.4544	1.8987	2.5297	486.19
370	18.675	−43.447	143.97	−1.3848	1.9293	2.5523	492.82
380	18.128	−23.462	169.61	−1.3164	1.9610	2.5768	499.26
390	17.614	−3.1925	195.51	−1.2491	1.9937	2.6030	505.54
400	17.131	17.374	221.68	−1.1829	2.0272	2.6307	511.66
410	16.676	38.250	248.13	−1.1176	2.0614	2.6596	517.65
420	16.246	59.444	274.88	−1.0531	2.0962	2.6897	523.51
430	15.840	80.965	301.93	−0.98945	2.1316	2.7207	529.24
440	15.454	102.82	329.29	−0.92654	2.1674	2.7526	534.87
450	15.088	125.01	356.98	−0.86432	2.2036	2.7851	540.40
460	14.740	147.55	385.00	−0.80275	2.2402	2.8183	545.84
470	14.409	170.44	413.35	−0.74178	2.2769	2.8519	551.19
480	14.093	193.68	442.04	−0.68138	2.3138	2.8860	556.46
490	13.791	217.28	471.07	−0.62152	2.3509	2.9204	561.65
500	13.502	241.23	500.45	−0.56217	2.3881	2.9551	566.77
520	12.961	290.22	560.25	−0.44490	2.4626	3.0252	576.82
540	12.464	340.65	621.46	−0.32940	2.5370	3.0958	586.62
560	12.005	392.53	684.08	−0.21554	2.6112	3.1666	596.21
580	11.579	445.86	748.12	−0.10318	2.6849	3.2374	605.60
600	11.184	500.63	813.58	0.00776	2.7581	3.3080	614.81
620	10.816	556.83	880.44	0.11738	2.8306	3.3782	623.85
			4.000 MPa Isobar				
91.710[a]	452.72	−981.70	−972.87	−7.3750	2.1711	3.3497	1556.3
92	452.34	−980.74	−971.89	−7.3644	2.1693	3.3505	1553.8
94	449.74	−974.08	−965.19	−7.2923	2.1572	3.3567	1536.3
96	447.13	−967.41	−958.46	−7.2216	2.1457	3.3638	1518.5
98	444.49	−960.73	−951.73	−7.1521	2.1347	3.3715	1500.6

Table 40. Thermodynamic properties of methane – Continued

Temperature K	Density kg/m³	Internal energy kJ/kg	Enthalpy kJ/kg	Entropy kJ/(kg K)	c_v kJ/(kg K)	c_p kJ/(kg K)	Speed of sound m/s
			4.000 MPa Isobar				
100	441.84	−954.03	−944.98	−7.0839	2.1240	3.3798	1482.5
105	435.11	−937.22	−928.02	−6.9185	2.0988	3.4030	1436.7
110	428.24	−920.28	−910.94	−6.7596	2.0750	3.4293	1390.0
115	421.20	−903.22	−893.72	−6.6065	2.0522	3.4592	1342.5
120	413.98	−886.01	−876.34	−6.4586	2.0304	3.4931	1294.2
125	406.55	−868.62	−858.78	−6.3152	2.0096	3.5322	1245.0
130	398.86	−851.04	−841.01	−6.1758	1.9897	3.5776	1194.8
135	390.89	−833.23	−822.99	−6.0398	1.9710	3.6311	1143.5
140	382.57	−815.14	−804.68	−5.9066	1.9535	3.6951	1090.8
145	373.85	−796.72	−786.02	−5.7757	1.9374	3.7726	1036.7
150	364.63	−777.90	−766.93	−5.6462	1.9231	3.8684	980.62
155	354.81	−758.57	−747.30	−5.5175	1.9108	3.9895	922.24
160	344.21	−738.59	−726.97	−5.3884	1.9011	4.1473	860.91
165	332.58	−717.76	−705.73	−5.2577	1.8950	4.3618	795.70
170	319.52	−695.71	−683.20	−5.1232	1.8942	4.6726	725.10
175	304.26	−671.84	−658.70	−4.9812	1.9022	5.1726	646.26
180	285.08	−644.73	−630.70	−4.8236	1.9295	6.1588	552.74
185	255.53	−609.25	−593.60	−4.6204	2.0305	9.7301	420.56
186.111[b]	244.17	−597.61	−581.23	−4.5538	2.1023	13.129	373.28
186.111[b]	86.337	−451.53	−405.20	−3.6080	2.3681	16.723	255.72
190	70.942	−423.54	−367.16	−3.4054	2.0278	6.8870	279.41
195	62.238	−402.92	−338.65	−3.2572	1.8951	4.9041	296.86
200	56.723	−386.83	−316.31	−3.1440	1.8314	4.1224	310.20
210	49.446	−360.06	−279.17	−2.9626	1.7645	3.4089	331.56
220	44.535	−336.78	−246.96	−2.8128	1.7291	3.0656	349.09
230	40.852	−315.31	−217.39	−2.6813	1.7093	2.8641	364.30
240	37.924	−294.92	−189.45	−2.5623	1.6996	2.7345	377.88
250	35.506	−275.22	−162.57	−2.4526	1.6971	2.6470	390.24
260	33.457	−255.97	−136.41	−2.3500	1.7003	2.5869	401.63
270	31.687	−237.00	−110.77	−2.2532	1.7080	2.5456	412.23
280	30.135	−218.19	−85.456	−2.1612	1.7194	2.5183	422.17
290	28.757	−199.46	−60.365	−2.0731	1.7341	2.5015	431.54
300	27.522	−180.74	−35.400	−1.9885	1.7517	2.4929	440.43
310	26.406	−161.96	−10.484	−1.9068	1.7718	2.4911	448.88
320	25.391	−143.09	14.442	−1.8276	1.7941	2.4949	456.96
330	24.463	−124.09	39.429	−1.7507	1.8184	2.5032	464.70
340	23.608	−104.91	64.519	−1.6758	1.8445	2.5155	472.15
350	22.819	−85.542	89.750	−1.6027	1.8722	2.5311	479.33
360	22.087	−65.951	115.15	−1.5312	1.9014	2.5496	486.27
370	21.406	−46.118	140.75	−1.4610	1.9318	2.5705	493.00
380	20.769	−26.024	166.57	−1.3922	1.9633	2.5937	499.53
390	20.173	−5.6548	192.63	−1.3245	1.9958	2.6186	505.88
400	19.613	15.005	218.95	−1.2578	2.0291	2.6452	512.08
410	19.087	35.966	245.54	−1.1922	2.0632	2.6732	518.13
420	18.590	57.240	272.41	−1.1274	2.0979	2.7023	524.04
430	18.120	78.835	299.59	−1.0635	2.1332	2.7326	529.84
440	17.675	100.76	327.07	−1.0003	2.1689	2.7637	535.52
450	17.253	123.02	354.86	−0.93784	2.2050	2.7956	541.09
460	16.852	145.62	382.98	−0.87604	2.2415	2.8281	546.57
470	16.470	168.56	411.43	−0.81486	2.2781	2.8612	551.96

Table 40. Thermodynamic properties of methane — Continued

Temperature K	Density kg/m³	Internal energy kJ/kg	Enthalpy kJ/kg	Entropy kJ/(kg K)	c_v kJ/(kg K)	c_p kJ/(kg K)	Speed of sound m/s
			4.000 MPa Isobar				
480	16.106	191.86	440.21	−0.75427	2.3150	2.8948	557.26
490	15.759	215.51	469.33	−0.69424	2.3520	2.9288	562.49
500	15.428	239.51	498.78	−0.63472	2.3891	2.9631	567.64
520	14.807	288.59	558.74	−0.51716	2.4635	3.0324	577.74
540	14.236	339.10	620.08	−0.40141	2.5378	3.1023	587.59
560	13.709	391.06	682.83	−0.28731	2.6119	3.1726	597.22
580	13.222	444.45	746.99	−0.17476	2.6856	3.2429	606.65
600	12.769	499.28	812.55	−0.06363	2.7587	3.3130	615.89
620	12.347	555.54	879.51	0.04614	2.8311	3.3828	624.96
			4.500 MPa Isobar				
91.836[a]	452.87	−981.56	−971.63	−7.3736	2.1716	3.3475	1558.5
92	452.66	−981.02	−971.08	−7.3676	2.1705	3.3480	1557.1
94	450.07	−974.37	−964.38	−7.2955	2.1584	3.3540	1539.7
96	447.46	−967.72	−957.66	−7.2248	2.1469	3.3609	1522.0
98	444.84	−961.05	−950.93	−7.1555	2.1359	3.3684	1504.2
100	442.20	−954.36	−944.19	−7.0873	2.1253	3.3765	1486.3
105	435.50	−937.58	−927.25	−6.9221	2.1001	3.3991	1440.7
110	428.66	−920.69	−910.19	−6.7634	2.0763	3.4247	1394.3
115	421.67	−903.67	−893.00	−6.6105	2.0536	3.4537	1347.2
120	414.49	−886.50	−875.65	−6.4628	2.0318	3.4866	1299.3
125	407.11	−869.18	−858.12	−6.3198	2.0110	3.5243	1250.5
130	399.49	−851.66	−840.40	−6.1807	1.9911	3.5680	1200.8
135	391.58	−833.92	−822.43	−6.0451	1.9723	3.6194	1150.1
140	383.36	−815.92	−804.19	−5.9124	1.9548	3.6804	1098.2
145	374.74	−797.61	−785.61	−5.7820	1.9386	3.7540	1044.8
150	365.67	−778.92	−766.62	−5.6533	1.9241	3.8443	989.75
155	356.02	−759.76	−747.12	−5.5255	1.9114	3.9573	932.60
160	345.65	−740.01	−726.99	−5.3976	1.9012	4.1027	872.85
165	334.35	−719.48	−706.02	−5.2686	1.8942	4.2965	809.75
170	321.78	−697.88	−683.90	−5.1365	1.8917	4.5690	742.13
175	307.35	−674.73	−660.09	−4.9985	1.8963	4.9854	667.96
180	289.86	−649.05	−633.53	−4.8489	1.9144	5.7217	583.19
185	266.01	−618.18	−601.26	−4.6722	1.9687	7.5262	477.08
189.868[b]	203.77	−557.77	−535.69	−4.3236	2.5406	74.902	257.35
189.868[b]	122.33	−485.23	−448.45	−3.8641	2.8030	112.21	240.30
190	115.69	−477.41	−438.51	−3.8118	2.6453	55.550	246.05
195	80.184	−424.74	−368.62	−3.4474	2.0217	7.3316	283.92
200	69.926	−402.76	−338.41	−3.2943	1.8996	5.1674	300.92
210	58.834	−371.21	−294.72	−3.0809	1.8003	3.8300	325.35
220	52.138	−345.65	−259.34	−2.9162	1.7533	3.3081	344.47
230	47.372	−322.78	−227.79	−2.7759	1.7272	3.0267	360.72
240	43.698	−301.43	−198.45	−2.6510	1.7135	2.8532	375.05
250	40.728	−281.02	−170.53	−2.5370	1.7083	2.7385	387.98
260	38.248	−261.22	−143.56	−2.4312	1.7095	2.6602	399.82
270	36.130	−241.80	−117.25	−2.3319	1.7157	2.6062	410.79
280	34.288	−222.62	−91.383	−2.2379	1.7260	2.5693	421.04
290	32.665	−203.58	−65.820	−2.1481	1.7398	2.5452	430.67
300	31.219	−184.59	−40.446	−2.0621	1.7567	2.5310	439.77
310	29.918	−165.58	−15.173	−1.9792	1.7762	2.5247	448.41
320	28.740	−146.51	10.069	−1.8991	1.7980	2.5247	456.65

Table 40. Thermodynamic properties of methane – Continued

Temperature K	Density kg/m³	Internal energy kJ/kg	Enthalpy kJ/kg	Entropy kJ/(kg K)	c_v kJ/(kg K)	c_p kJ/(kg K)	Speed of sound m/s
			4.500 MPa Isobar				
330	27.665	−127.32	35.338	−1.8214	1.8220	2.5300	464.54
340	26.679	−107.99	60.683	−1.7457	1.8477	2.5396	472.11
350	25.771	−88.470	86.144	−1.6719	1.8752	2.5530	479.40
360	24.931	−68.746	111.75	−1.5997	1.9040	.5696	486.44
370	24.150	−48.793	137.54	−1.5291	1.9342	.5889	493.26
380	23.422	−28.589	163.54	−1.4598	1.9655	2.6106	499.87
390	22.741	−8.1183	189.76	−1.3916	1.9979	2.6343	506.30
400	22.102	12.635	216.23	−1.3246	2.0311	2.6597	512.56
410	21.502	33.683	242.96	−1.2586	2.0650	2.6867	518.67
420	20.937	55.038	269.97	−1.1935	2.0996	2.7150	524.64
430	20.403	76.708	297.27	−1.1293	2.1348	2.7444	530.48
440	19.897	98.702	324.86	−1.0659	2.1704	2.7748	536.21
450	19.418	121.03	352.77	−1.0032	2.2064	2.8060	541.83
460	18.964	143.69	380.98	−0.94115	2.2427	2.8380	547.34
470	18.531	166.69	409.53	−0.87977	2.2793	2.8705	552.77
480	18.119	190.04	438.40	−0.81899	2.3161	2.9036	558.11
490	17.726	213.74	467.60	−0.75877	2.3531	2.9371	563.36
500	17.351	237.79	497.14	−0.69910	2.3901	2.9710	568.55
520	16.649	286.96	557.24	−0.58124	2.4644	3.0395	578.70
540	16.005	337.56	618.73	−0.46523	2.5387	3.1088	588.60
560	15.410	389.59	681.60	−0.35091	2.6127	3.1785	598.27
580	14.860	443.05	745.87	−0.23815	2.6863	3.2483	607.73
600	14.350	497.94	811.53	−0.12686	2.7593	3.3180	617.00
620	13.875	554.25	878.59	−0.01693	2.8317	3.3874	626.09
			5.000 MPa Isobar				
91.963[a]	453.03	−981.42	−970.39	−7.3721	2.1720	3.3454	1560.7
92	452.98	−981.30	−970.26	−7.3707	2.1717	3.3455	1560.4
94	450.40	−974.67	−963.57	−7.2987	2.1596	3.3514	1543.0
96	447.80	−968.02	−956.86	−7.2281	2.1482	3.3580	1525.5
98	445.19	−961.37	−950.13	−7.1588	2.1372	3.3654	1507.8
100	442.55	−954.69	−943.40	−7.0907	2.1266	3.3733	1490.0
105	435.89	−937.95	−926.48	−6.9256	2.1015	3.3953	1444.7
110	429.09	−921.09	−909.44	−6.7671	2.0777	3.4202	1398.6
115	422.13	−904.11	−892.27	−6.6145	2.0550	3.4483	1351.8
120	415.00	−887.00	−874.95	−6.4670	2.0332	3.4802	1304.3
125	407.67	−869.72	−857.46	−6.3243	2.0124	3.5166	1256.0
130	400.10	−852.27	−839.77	−6.1855	1.9925	3.5587	1206.8
135	392.27	−834.61	−821.86	−6.0503	1.9737	3.6080	1156.6
140	384.13	−816.69	−803.68	−5.9181	1.9561	3.6663	1105.3
145	375.62	−798.49	−785.18	−5.7883	1.9398	3.7363	1052.8
150	366.67	−779.93	−766.29	−5.6602	1.9251	3.8215	998.65
155	357.19	−760.93	−746.93	−5.5332	1.9122	3.9273	942.65
160	347.04	−741.38	−726.97	−5.4065	1.9015	4.0616	884.35
165	336.04	−721.12	−706.24	−5.2790	1.8937	4.2377	823.14
170	323.91	−699.92	−684.48	−5.1491	1.8898	4.4707	758.12
175	310.17	−677.39	−661.27	−5.0145	1.8917	4.8331	687.81
180	293.96	−652.80	−635.79	−4.8710	1.9037	5.4115	609.53
185	273.26	−624.53	−606.23	−4.7091	1.9376	6.5747	517.52
190	240.69	−586.68	−565.91	−4.4942	2.0517	10.712	393.44
195	114.94	−464.32	−420.82	−3.7424	2.3052	19.362	266.13

Table 40. Thermodynamic properties of methane – Continued

Temperature K	Density kg/m³	Internal energy kJ/kg	Enthalpy kJ/kg	Entropy kJ/(kg K)	c_v kJ/(kg K)	c_p kJ/(kg K)	Speed of sound m/s
			5.000 MPa Isobar				
200	87.764	−423.51	−366.54	−3.4670	1.9965	7.2726	291.29
210	69.687	−383.81	−312.06	−3.2007	1.8404	4.4121	319.48
220	60.479	−355.22	−272.55	−3.0167	1.7789	3.6049	340.20
230	54.337	−330.67	−238.65	−2.8660	1.7457	3.2141	357.45
240	49.769	−308.21	−207.74	−2.7344	1.7277	2.9851	372.50
250	46.159	−287.00	−178.68	−2.6157	1.7196	2.8379	385.97
260	43.193	−266.58	−150.83	−2.5065	1.7187	2.7385	398.24
270	40.689	−246.69	−123.80	−2.4045	1.7234	2.6699	409.56
280	38.532	−227.12	−97.357	−2.3083	1.7326	2.6226	420.08
290	36.644	−207.75	−71.303	−2.2169	1.7455	2.5906	429.95
300	34.972	−188.48	−45.507	−2.1294	1.7616	2.5703	439.25
310	33.475	−169.23	−19.867	−2.0453	1.7806	2.5590	448.07
320	32.124	−149.95	5.6982	−1.9642	1.8019	2.5551	456.47
330	30.897	−130.57	31.255	−1.8855	1.8255	2.5571	464.49
340	29.775	−111.07	56.857	−1.8091	1.8509	2.5641	472.18
350	28.743	−91.406	82.551	−1.7346	1.8780	2.5752	479.57
360	27.790	−71.548	108.37	−1.6619	1.9067	2.5898	486.71
370	26.907	−51.472	134.36	−1.5907	1.9366	2.6074	493.60
380	26.084	−31.156	160.53	−1.5209	1.9678	2.6276	500.29
390	25.317	−10.582	186.92	−1.4523	1.9999	2.6500	506.79
400	24.598	10.266	213.54	−1.3850	2.0330	2.6743	513.11
410	23.923	31.402	240.41	−1.3186	2.0668	2.7003	519.28
420	23.287	52.837	267.55	−1.2532	2.1013	2.7276	525.30
430	22.688	74.583	294.96	−1.1887	2.1363	2.7562	531.19
440	22.121	96.648	322.67	−1.1250	2.1718	2.7859	536.96
450	21.585	119.04	350.69	−1.0620	2.2078	2.8164	542.61
460	21.075	141.76	379.01	−0.99980	2.2440	2.8478	548.17
470	20.592	164.83	407.64	−0.93821	2.2806	2.8798	553.63
480	20.131	188.23	436.60	−0.87724	2.3173	2.9124	559.00
490	19.692	211.98	465.89	−0.81685	2.3542	2.9454	564.28
500	19.273	236.08	495.51	−0.75701	2.3912	2.9788	569.49
520	18.489	285.34	555.77	−0.63886	2.4653	3.0466	579.69
540	17.770	336.02	617.38	−0.52259	2.5395	3.1153	589.63
560	17.108	388.12	680.38	−0.40805	2.6134	3.1844	599.34
580	16.496	441.65	744.76	−0.29510	2.6869	3.2537	608.83
600	15.927	496.60	810.53	−0.18362	2.7599	3.3229	618.13
620	15.399	552.97	877.68	−0.07354	2.8322	3.3920	627.25
			8.000 MPa Isobar				
92.720[a]	453.94	−980.58	−962.96	−7.3633	2.1745	3.3330	1573.7
94	452.32	−976.38	−958.69	−7.3176	2.1668	3.3362	1563.0
96	449.78	−969.80	−952.01	−7.2473	2.1554	3.3419	1546.0
98	447.23	−963.21	−945.32	−7.1783	2.1446	3.3482	1528.9
100	444.66	−956.61	−938.62	−7.1106	2.1341	3.3549	1511.7
105	438.16	−940.06	−921.80	−6.9465	2.1091	3.3737	1468.0
110	431.55	−923.42	−904.88	−6.7891	2.0856	3.3950	1423.7
115	424.81	−906.68	−887.85	−6.6376	2.0630	3.4186	1378.8
120	417.93	−889.83	−870.69	−6.4916	2.0414	3.4450	1333.4
125	410.88	−872.86	−853.39	−6.3504	2.0206	3.4748	1287.4

Table 40. Thermodynamic properties of methane — Continued

Temperature K	Density kg/m³	Internal energy kJ/kg	Enthalpy kJ/kg	Entropy kJ/(kg K)	c_v kJ/(kg K)	c_p kJ/(kg K)	Speed of sound m/s
			8.000 MPa Isobar				
130	403.65	−855.75	−835.93	−6.2134	2.0007	3.5087	1240.9
135	396.20	−838.49	−818.30	−6.0803	1.9818	3.5476	1193.8
140	388.51	−821.04	−800.45	−5.9505	1.9640	3.5926	1146.0
145	380.55	−803.38	−782.36	−5.8235	1.9473	3.6452	1097.4
150	372.26	−785.47	−763.98	−5.6989	1.9318	3.7071	1048.0
155	363.60	−767.27	−745.27	−5.5762	1.9177	3.7808	997.54
160	354.49	−748.71	−726.15	−5.4548	1.9052	3.8697	946.00
165	344.85	−729.74	−706.54	−5.3341	1.8946	3.9781	893.16
170	334.57	−710.23	−686.32	−5.2135	1.8860	4.1129	838.83
175	323.47	−690.08	−665.35	−5.0919	1.8800	4.2840	782.74
180	311.36	−669.09	−643.40	−4.9682	1.8773	4.5073	724.60
185	297.89	−647.00	−620.15	−4.8408	1.8788	4.8093	664.04
190	282.59	−623.41	−595.10	−4.7072	1.8862	5.2371	600.74
195	264.64	−597.65	−567.42	−4.5635	1.9019	5.8777	534.76
200	242.77	−568.67	−535.72	−4.4030	1.9282	6.8799	467.60
210	183.43	−497.17	−453.55	−4.0026	1.9817	9.2012	360.94
220	133.25	−431.39	−371.35	−3.6198	1.9195	6.8234	341.61
230	108.01	−387.72	−313.65	−3.3630	1.8536	4.9604	353.14
240	93.382	−354.61	−268.94	−3.1726	1.8113	4.0803	367.87
250	83.511	−326.55	−230.75	−3.0166	1.7860	3.6004	382.13
260	76.211	−301.29	−196.32	−2.8815	1.7727	3.3073	395.41
270	70.493	−277.76	−164.27	−2.7606	1.7683	3.1149	407.72
280	65.834	−255.34	−133.82	−2.6498	1.7706	2.9830	419.16
290	61.931	−233.66	−104.49	−2.5468	1.7783	2.8902	429.85
300	58.589	−212.47	−75.930	−2.4500	1.7902	2.8246	439.89
310	55.682	−191.60	−47.929	−2.3582	1.8058	2.7784	449.35
320	53.119	−170.92	−20.313	−2.2705	1.8244	2.7469	458.32
330	50.834	−150.33	7.0469	−2.1863	1.8456	2.7267	466.86
340	48.780	−129.75	34.250	−2.1051	1.8691	2.7154	475.01
350	46.918	−109.13	61.378	−2.0265	1.8946	2.7112	482.82
360	45.220	−88.418	88.495	−1.9501	1.9218	2.7130	490.33
370	43.662	−67.570	115.65	−1.8757	1.9506	2.7197	497.57
380	42.226	−46.553	142.90	−1.8030	1.9806	2.7304	504.56
390	40.897	−25.339	170.27	−1.7319	2.0118	2.7446	511.33
400	39.662	−3.9038	197.80	−1.6622	2.0440	2.7617	517.91
410	38.509	17.773	225.52	−1.5938	2.0770	2.7812	524.31
420	37.431	39.709	253.43	−1.5265	2.1108	2.8030	530.54
430	36.420	61.918	281.58	−1.4603	2.1453	2.8265	536.63
440	35.468	84.415	309.97	−1.3950	2.1802	2.8517	542.58
450	34.571	107.21	338.62	−1.3306	2.2157	2.8781	548.40
460	33.723	130.31	367.54	−1.2671	2.2514	2.9058	554.11
470	32.920	153.73	396.74	−1.2043	2.2875	2.9344	559.71
480	32.159	177.46	426.23	−1.1422	2.3239	2.9640	565.21
490	31.435	201.53	456.02	−1.0808	2.3604	2.9942	570.62
500	30.746	225.92	486.12	−1.0200	2.3971	3.0251	575.94
520	29.463	275.72	547.25	−0.90010	2.4706	3.0883	586.35
540	28.292	326.89	609.66	−0.78233	2.5442	3.1531	596.46
560	27.216	379.43	673.38	−0.66648	2.6177	3.2188	606.32
580	26.225	433.36	738.41	−0.55237	2.6908	3.2852	615.95
600	25.308	488.68	804.79	−0.43987	2.7635	3.3519	625.37
620	24.457	545.39	872.49	−0.32887	2.8355	3.4186	634.59

Table 40. Thermodynamic properties of methane — Continued

Temperature K	Density kg/m³	Internal energy kJ/kg	Enthalpy kJ/kg	Entropy kJ/(kg K)	c_v kJ/(kg K)	c_p kJ/(kg K)	Speed of sound m/s
			10.000 MPa Isobar				
93.222[a]	454.54	−980.02	−958.02	−7.3575	2.1761	3.3251	1582.3
94	453.57	−977.48	−955.43	−7.3298	2.1715	3.3269	1575.9
96	451.06	−970.94	−948.77	−7.2598	2.1602	3.3320	1559.3
98	448.55	−964.40	−942.10	−7.1910	2.1493	3.3376	1542.5
100	446.02	−957.84	−935.42	−7.1235	2.1389	3.3437	1525.7
105	439.63	−941.41	−918.66	−6.9600	2.1141	3.3607	1483.0
110	433.13	−924.90	−901.81	−6.8032	2.0907	3.3797	1439.8
115	426.53	−908.30	−884.86	−6.6525	2.0683	3.4008	1396.1
120	419.79	−891.62	−867.80	−6.5073	2.0467	3.4243	1351.9
125	412.91	−874.83	−850.61	−6.3670	2.0260	3.4504	1307.3
130	405.87	−857.93	−833.29	−6.2311	2.0061	3.4799	1262.3
135	398.65	−840.89	−815.81	−6.0991	1.9872	3.5133	1216.9
140	391.22	−823.71	−798.15	−5.9707	1.9693	3.5516	1171.0
145	383.56	−806.35	−780.28	−5.8453	1.9524	3.5956	1124.6
150	375.63	−788.80	−762.18	−5.7226	1.9366	3.6467	1077.6
155	367.39	−771.02	−743.80	−5.6021	1.9221	3.7064	1030.1
160	358.81	−752.97	−725.10	−5.4833	1.9089	3.7765	981.80
165	349.81	−734.60	−706.01	−5.3659	1.8973	3.8596	932.79
170	340.33	−715.86	−686.47	−5.2492	1.8872	3.9590	882.98
175	330.29	−696.67	−666.39	−5.1328	1.8791	4.0791	832.32
180	319.56	−676.93	−645.64	−5.0159	1.8730	4.2262	780.76
185	308.00	−656.54	−624.07	−4.8977	1.8695	4.4085	728.32
190	295.43	−635.32	−601.48	−4.7772	1.8688	4.6379	675.09
195	281.59	−613.10	−577.59	−4.6531	1.8716	4.9300	621.38
200	266.19	−589.61	−552.04	−4.5238	1.8780	5.3036	567.92
210	229.53	−537.84	−494.27	−4.2421	1.8981	6.2783	469.31
220	187.59	−481.51	−428.20	−3.9348	1.9034	6.7130	404.38
230	152.24	−430.35	−364.66	−3.6522	1.8795	5.8612	382.48
240	128.40	−389.20	−311.32	−3.4251	1.8467	4.8533	383.61
250	112.43	−355.42	−266.47	−3.2419	1.8199	4.1685	392.22
260	101.01	−326.14	−227.14	−3.0876	1.8026	3.7301	402.84
270	92.361	−299.65	−191.38	−2.9526	1.7941	3.4407	413.78
280	85.507	−274.97	−158.02	−2.8312	1.7930	3.2424	424.47
290	79.893	−251.50	−126.34	−2.7200	1.7977	3.1025	434.73
300	75.175	−228.86	−95.840	−2.6166	1.8074	3.0023	444.53
310	71.133	−206.78	−66.199	−2.5194	1.8210	2.9299	453.87
320	67.614	−185.07	−37.174	−2.4273	1.8380	2.8780	462.78
330	64.511	−163.60	−8.5880	−2.3393	1.8579	2.8415	471.30
340	61.747	−142.26	19.696	−2.2549	1.8803	2.8170	479.45
350	59.261	−120.96	47.785	−2.1735	1.9048	2.8021	487.29
360	57.010	−99.645	75.764	−2.0946	1.9312	2.7948	494.83
370	54.957	−78.257	103.70	−2.0181	1.9592	2.7938	502.11
380	53.075	−56.754	131.66	−1.9435	1.9886	2.7980	509.14
390	51.341	−35.099	159.68	−1.8708	2.0192	2.8065	515.96
400	49.736	−13.262	187.80	−1.7996	2.0509	2.8187	522.58
410	48.244	8.7841	216.06	−1.7298	2.0835	2.8340	529.02
420	46.854	31.060	244.49	−1.6613	2.1168	2.8519	535.30
430	45.553	53.584	273.11	−1.5939	2.1509	2.8721	541.43
440	44.333	76.371	301.94	−1.5277	2.1855	2.8942	547.42
450	43.185	99.436	331.00	−1.4623	2.2206	2.9180	553.28

Table 40. Thermodynamic properties of methane — Continued

Temperature K	Density kg/m³	Internal energy kJ/kg	Enthalpy kJ/kg	Entropy kJ/(kg K)	c_v kJ/(kg K)	c_p kJ/(kg K)	Speed of sound m/s
			10.000 MPa Isobar				
460	42.103	122.79	360.30	−1.3979	2.2561	2.9432	559.03
470	41.080	146.44	389.87	−1.3344	2.2920	2.9697	564.66
480	40.112	170.40	419.70	−1.2716	2.3281	2.9972	570.20
490	39.194	194.67	449.81	−1.2095	2.3644	3.0256	575.64
500	38.322	219.27	480.21	−1.1480	2.4008	3.0548	580.99
520	36.700	269.43	541.91	−1.0271	2.4740	3.1150	591.45
540	35.222	320.92	604.83	−0.90834	2.5473	3.1773	601.62
560	33.869	373.75	669.01	−0.79165	2.6205	3.2409	611.52
580	32.624	427.95	734.47	−0.67680	2.6934	3.3053	621.18
600	31.474	483.51	801.23	−0.56365	2.7658	3.3704	630.63
620	30.409	540.43	869.29	−0.45207	2.8376	3.4357	639.88
			20.000 MPa Isobar				
95.705[a]	457.44	−977.10	−933.37	−7.3288	2.1838	3.2902	1623.8
96	457.09	−976.16	−932.40	−7.3186	2.1822	3.2906	1621.5
98	454.74	−969.80	−925.82	−7.2508	2.1717	3.2938	1606.4
100	452.37	−963.44	−919.23	−7.1842	2.1615	3.2973	1591.1
105	446.43	−947.52	−902.72	−7.0231	2.1374	3.3072	1552.6
110	440.43	−931.56	−886.15	−6.8690	2.1146	3.3182	1513.8
115	434.37	−915.58	−869.53	−6.7212	2.0928	3.3302	1474.8
120	428.24	−899.55	−852.85	−6.5792	2.0717	3.3430	1435.7
125	422.04	−883.49	−836.10	−6.4425	2.0514	3.3568	1396.5
130	415.75	−867.39	−819.28	−6.3105	2.0318	3.3718	1357.3
135	409.37	−851.24	−802.38	−6.1830	2.0130	3.3883	1318.2
140	402.88	−835.04	−785.39	−6.0594	1.9951	3.4063	1279.2
145	396.30	−818.78	−768.31	−5.9395	1.9779	3.4263	1240.2
150	389.59	−802.46	−751.13	−5.8230	1.9617	3.4484	1201.4
155	382.76	−786.08	−733.83	−5.7096	1.9464	3.4728	1162.8
160	375.79	−769.62	−716.40	−5.5989	1.9320	3.4998	1124.3
165	368.67	−753.07	−698.82	−5.4907	1.9185	3.5295	1086.1
170	361.40	−736.44	−681.10	−5.3849	1.9061	3.5622	1048.2
175	353.96	−719.70	−663.20	−5.2811	1.8947	3.5980	1010.7
180	346.34	−702.86	−645.11	−5.1792	1.8843	3.6371	973.55
185	338.53	−685.90	−626.82	−5.0790	1.8749	3.6794	936.96
190	330.53	−668.82	−608.31	−4.9803	1.8666	3.7249	901.01
195	322.32	−651.62	−589.57	−4.8829	1.8593	3.7733	865.83
200	313.91	−634.29	−570.57	−4.7867	1.8530	3.8242	831.58
210	296.49	−599.26	−531.81	−4.5976	1.8434	3.9299	766.53
220	278.37	−563.84	−491.99	−4.4124	1.8373	4.0315	707.42
230	259.79	−528.23	−451.25	−4.2313	1.8341	4.1119	655.86
240	241.22	−492.81	−409.89	−4.0553	1.8331	4.1496	613.27
250	223.23	−458.04	−368.45	−3.8861	1.8336	4.1293	580.44
260	206.41	−424.39	−327.49	−3.7255	1.8353	4.0536	556.92
270	191.14	−392.14	−287.50	−3.5746	1.8381	3.9395	541.27
280	177.57	−361.39	−248.76	−3.4336	1.8424	3.8069	531.72
290	165.67	−332.09	−211.37	−3.3024	1.8488	3.6726	526.67
300	155.28	−304.08	−175.28	−3.1800	1.8579	3.5478	524.86
310	146.20	−277.16	−140.36	−3.0655	1.8697	3.4383	525.31
320	138.23	−251.14	−106.46	−2.9579	1.8843	3.3457	527.32
330	131.21	−225.82	−73.394	−2.8561	1.9017	3.2696	530.41
340	124.98	−201.04	−41.016	−2.7595	1.9215	3.2083	534.23
350	119.41	−176.67	−9.1835	−2.6672	1.9435	3.1601	538.57
360	114.41	−152.59	22.224	−2.5787	1.9676	3.1232	543.24

Table 40. Thermodynamic properties of methane — Continued

Temperature K	Density kg/m³	Internal energy kJ/kg	Enthalpy kJ/kg	Entropy kJ/(kg K)	c_v kJ/(kg K)	c_p kJ/(kg K)	Speed of sound m/s
			20.000 MPa Isobar				
370	109.88	−128.71	53.312	−2.4935	1.9934	3.0957	548.14
380	105.76	−104.94	84.166	−2.4113	2.0208	3.0765	553.19
390	102.00	−81.216	114.86	−2.3315	2.0496	3.0641	558.33
400	98.543	−57.489	145.47	−2.2540	2.0795	3.0577	563.52
410	95.355	−33.707	176.04	−2.1786	2.1105	3.0564	568.73
420	92.404	−9.8301	206.61	−2.1049	2.1425	3.0594	573.95
430	89.662	14.175	237.24	−2.0328	2.1752	3.0662	579.15
440	87.105	38.337	267.95	−1.9622	2.2085	3.0762	584.33
450	84.715	62.682	298.77	−1.8930	2.2425	3.0890	589.48
460	82.473	87.230	329.73	−1.8249	2.2769	3.1042	594.60
470	80.366	112.00	360.86	−1.7580	2.3117	3.1216	599.67
480	78.381	137.01	392.17	−1.6920	2.3469	3.1408	604.70
490	76.506	162.26	423.68	−1.6271	2.3823	3.1616	609.69
500	74.731	187.78	455.41	−1.5630	2.4179	3.1838	614.64
520	71.452	239.65	519.55	−1.4372	2.4896	3.2316	624.40
540	68.485	292.66	584.70	−1.3143	2.5615	3.2832	633.98
560	65.783	346.87	650.90	−1.1939	2.6335	3.3375	643.38
580	63.311	402.31	718.21	−1.0758	2.7053	3.3940	652.62
600	61.038	459.00	786.67	−0.95975	2.7768	3.4520	661.70
620	58.939	516.97	856.30	−0.84560	2.8477	3.5111	670.62
			50.000 MPa Isobar				
102.890[a]	465.34	−967.69	−860.25	−7.2470	2.2052	3.2158	1737.1
105	463.20	−961.41	−853.46	−7.1817	2.1960	3.2156	1724.2
110	458.14	−946.52	−837.38	−7.0321	2.1748	3.2154	1693.5
115	453.08	−931.66	−821.31	−6.8892	2.1545	3.2152	1662.8
120	448.03	−916.83	−805.23	−6.7524	2.1348	3.2149	1632.3
125	442.97	−902.03	−789.16	−6.6212	2.1156	3.2144	1602.1
130	437.92	−887.26	−773.09	−6.4951	2.0971	3.2138	1572.1
135	432.87	−872.53	−757.02	−6.3738	2.0791	3.2132	1542.5
140	427.81	−857.83	−740.96	−6.2570	2.0617	3.2125	1513.3
145	422.75	−843.17	−724.90	−6.1443	2.0451	3.2119	1484.5
150	417.69	−828.54	−708.84	−6.0354	2.0291	3.2115	1456.1
155	412.62	−813.96	−692.78	−5.9301	2.0138	3.2112	1428.2
160	407.55	−799.41	−676.72	−5.8281	1.9993	3.2111	1400.7
165	402.47	−784.90	−660.67	−5.7293	1.9855	3.2112	1373.8
170	397.39	−770.43	−644.61	−5.6334	1.9725	3.2116	1347.4
175	392.31	−756.00	−628.55	−5.5403	1.9602	3.2122	1321.6
180	387.23	−741.61	−612.49	−5.4498	1.9488	3.2130	1296.3
185	382.15	−727.26	−596.42	−5.3618	1.9381	3.2140	1271.6
190	377.07	−712.95	−580.35	−5.2761	1.9283	3.2153	1247.4
195	371.99	−698.68	−564.27	−5.1925	1.9192	3.2167	1223.9
200	366.92	−684.45	−548.18	−5.1111	1.9110	3.2182	1201.0
210	356.80	−656.12	−515.98	−4.9540	1.8969	3.2217	1157.0
220	346.74	−627.95	−483.75	−4.8040	1.8860	3.2253	1115.6
230	336.75	−599.95	−451.48	−4.6606	1.8784	3.2288	1077.0
240	326.88	−572.14	−419.17	−4.5231	1.8739	3.2319	1041.0
250	317.15	−544.50	−386.84	−4.3911	1.8725	3.2342	1007.8
260	307.59	−517.05	−354.49	−4.2642	1.8741	3.2356	977.40
270	298.23	−489.79	−322.13	−4.1421	1.8786	3.2360	949.68
280	289.11	−462.72	−289.78	−4.0244	1.8858	3.2354	924.60
290	280.26	−435.84	−257.43	−3.9109	1.8956	3.2338	902.06

Table 40. Thermodynamic properties of methane — Continued

Temperature K	Density kg/m³	Internal energy kJ/kg	Enthalpy kJ/kg	Entropy kJ/(kg K)	c_v kJ/(kg K)	c_p kJ/(kg K)	Speed of sound m/s
			50.000 MPa Isobar				
300	271.69	−409.14	−225.10	−3.8013	1.9079	3.2314	881.94
310	263.42	−382.61	−192.80	−3.6954	1.9225	3.2286	864.08
320	255.47	−356.25	−160.53	−3.5930	1.9392	3.2255	848.34
330	247.85	−330.03	−128.29	−3.4937	1.9580	3.2226	834.54
340	240.55	−303.93	−96.079	−3.3976	1.9786	3.2200	822.53
350	233.59	−277.94	−63.888	−3.3043	2.0009	3.2182	812.13
360	226.95	−252.03	−31.711	−3.2136	2.0248	3.2174	803.20
370	220.62	−226.17	0.46389	−3.1255	2.0501	3.2178	795.59
380	214.60	−200.34	32.650	−3.0396	2.0767	3.2196	789.16
390	208.87	−174.52	64.860	−2.9560	2.1045	3.2228	783.79
400	203.43	−148.68	97.111	−2.8743	2.1333	3.2276	779.36
410	198.25	−122.79	129.42	−2.7945	2.1631	3.2341	775.76
420	193.32	−96.840	161.80	−2.7165	2.1937	3.2421	772.91
430	188.63	−70.798	194.27	−2.6401	2.2251	3.2517	770.71
440	184.17	−44.647	226.84	−2.5652	2.2571	3.2629	769.11
450	179.92	−18.368	259.53	−2.4918	2.2896	3.2755	768.02
460	175.87	8.0574	292.35	−2.4196	2.3227	3.2896	767.40
470	172.01	34.645	325.32	−2.3487	2.3561	3.3050	767.19
480	168.32	61.409	358.46	−2.2790	2.3899	3.3216	767.34
490	164.80	88.364	391.76	−2.2103	2.4240	3.3393	767.82
500	161.43	115.52	425.25	−2.1426	2.4583	3.3582	768.59
520	155.13	170.49	492.81	−2.0102	2.5275	3.3987	770.86
540	149.33	226.39	561.22	−1.8811	2.5972	3.4426	773.96
560	143.99	283.29	630.53	−1.7550	2.6670	3.4892	777.72
580	139.05	341.22	700.80	−1.6317	2.7367	3.5381	781.99
600	134.47	400.24	772.07	−1.5109	2.8062	3.5887	786.69
620	130.21	460.36	844.36	−1.3924	2.8754	3.6408	791.72
			100.000 MPa Isobar				
114.129[a]	476.63	−950.68	−740.87	−7.1249	2.2377	3.1449	1897.8
115	475.90	−948.26	−738.14	−7.1010	2.2345	3.1436	1893.7
120	471.72	−934.42	−722.44	−6.9674	2.2163	3.1364	1870.0
125	467.59	−920.64	−706.77	−6.8395	2.1985	3.1290	1846.6
130	463.48	−906.90	−691.15	−6.7169	2.1811	3.1214	1823.5
135	459.41	−893.23	−675.56	−6.5992	2.1641	3.1137	1800.8
140	455.37	−879.61	−660.01	−6.4861	2.1477	3.1059	1778.4
145	451.35	−866.05	−644.50	−6.3773	2.1317	3.0982	1756.3
150	447.37	−852.56	−629.03	−6.2724	2.1163	3.0904	1734.7
155	443.41	−839.12	−613.59	−6.1712	2.1014	3.0827	1713.5
160	439.48	−825.74	−598.20	−6.0734	2.0872	3.0752	1692.7
165	435.58	−812.42	−582.84	−5.9789	2.0737	3.0678	1672.3
170	431.70	−799.16	−567.52	−5.8874	2.0608	3.0607	1652.3
175	427.86	−785.96	−552.23	−5.7988	2.0486	3.0538	1632.7
180	424.04	−772.81	−536.98	−5.7129	2.0370	3.0472	1613.5
185	420.24	−759.72	−521.76	−5.6295	2.0262	3.0408	1594.8
190	416.48	−746.68	−506.57	−5.5485	2.0162	3.0348	1576.5
195	412.74	−733.70	−491.41	−5.4697	2.0068	3.0292	1558.5
200	409.03	−720.76	−476.28	−5.3931	1.9983	3.0239	1541.0
210	401.69	−695.04	−446.09	−5.2458	1.9834	3.0145	1507.1

Table 40. Thermodynamic properties of methane – Continued

Temperature K	Density kg/m³	Internal energy kJ/kg	Enthalpy kJ/kg	Entropy kJ/(kg K)	c_v kJ/(kg K)	c_p kJ/(kg K)	Speed of sound m/s
			100.000 MPa Isobar				
220	394.47	−669.49	−415.99	−5.1057	1.9715	3.0068	1474.8
230	387.36	−644.11	−385.95	−4.9722	1.9628	3.0008	1444.0
240	380.37	−618.86	−355.96	−4.8446	1.9571	2.9966	1414.6
250	373.51	−593.74	−326.01	−4.7223	1.9544	2.9943	1386.7
260	366,78	−568.72	−296.07	−4.6049	1.9548	2.9938	1360.2
270	360.17	−543.78	−266.13	−4.4919	1.9579	2.9951	1335.1
280	353.70	−518.89	−236.17	−4.3829	1.9639	2.9982	1311.3
290	347.36	−494.05	−206.16	−4.2776	1.9725	3.0030	1288.8
300	341.16	−469.22	−176.10	−4.1757	1.9836	3.0095	1267.5
310	335.10	−444.38	−145.96	−4.0769	1.9971	3.0176	1247.5
320	329.18	−419.53	−115.74	−3.9810	2.0127	3.0273	1228.7
330	323.40	−394.63	−85.415	−3.8876	2.0304	3.0383	1211.0
340	317.76	−369.67	−54.970	−3.7968	2.0500	3.0508	1194.4
350	312.26	−344.64	−24.395	−3.7081	2.0713	3.0645	1178.9
360	306.91	−319.51	6.3228	−3.6216	2.0942	3.0793	1164.4
370	301.69	−294.27	37.195	−3.5370	2.1185	3.0953	1150.9
380	296.61	−268.91	68.233	−3.4542	2.1441	3.1124	1138.3
390	291.67	−243.41	99.446	−3.3732	2.1709	3.1304	1126.7
400	286.86	−217.76	130.84	−3.2937	2.1987	3.1493	1115.8
410	282.18	−191.95	162.43	−3.2157	2.2274	3.1690	1105.8
420	277.63	−165.97	194.23	−3.1391	2.2570	3.1894	1096.5
430	273.21	−139.80	226.23	−3.0638	2.2872	3.2106	1087.9
440	268.91	−113.43	258.44	−2.9897	2.3181	3.2325	1080.1
450	264.73	−86.865	290.88	−2.9168	2.3496	3.2549	1072.8
460	260.67	−60.087	323.54	−2.8450	2.3815	3.2779	1066.2
470	256.72	−33.090	356.44	−2.7743	2.4139	3.3014	1060.1
480	252.88	−5.8672	389.57	−2.7045	2.4466	3.3254	1054.5
490	249.15	21.588	422.95	−2.6357	2.4795	3.3498	1049.4
500	245.53	49.283	456.57	−2.5678	2.5128	3.3746	1044.8
520	238.57	105.41	524.57	−2.4344	2.5797	3.4253	1036.9
540	232.00	162.55	593.59	−2.3042	2.6472	3.4772	1030.4
560	225.77	220.73	663.66	−2.1768	2.7149	3.5301	1025.3
580	219.87	279.98	734.80	−2.0520	2.7826	3.5837	1021.4
600	214.28	340.33	807.01	−1.9296	2.8501	3.6380	1018.4
620	208.97	401.78	880.32	−1.8094	2.9174	3.6927	1016.4
			200.000 MPa Isobar				
134.541[a]	495.07	−914.13	−510.15	−6.9233	2.2915	3.0768	2153.6
135	494.77	−912.96	−508.73	−6.9128	2.2900	3.0756	2152.1
140	491.58	−900.24	−493.39	−6.8012	2.2741	3.0635	2135.5
145	488.43	−887.58	−478.10	−6.6939	2.2586	3.0516	2119.1
150	485.31	−874.98	−462.87	−6.5906	2.2435	3.0400	2103.1
155	482.24	−862.43	−447.70	−6.4911	2.2289	3.0288	2087.3
160	479.19	−849.95	−432.58	−6.3951	2.2148	3.0179	2071.8
165	476.19	−837.52	−417.52	−6.3024	2.2013	3.0074	2056.6
170	473.21	−825.15	−402.51	−6.2128	2.1884	2.9972	2041.7
175	470.27	−812.83	−387.55	−6.1261	2.1761	2.9875	2027.0
180	467.36	−800.57	−372.63	−6.0420	2.1644	2.9782	2012.6
185	464.48	−788.35	−357.76	−5.9605	2.1534	2.9693	1998.5
190	461.63	−776.19	−342.94	−5.8815	2.1430	2.9610	1984.6
195	458.80	−764.07	−328.15	−5.8047	2.1334	2.9531	1971.0
200	456.01	−751.99	−313.41	−5.7300	2.1244	2.9458	1957.6

Table 40. Thermodynamic properties of methane — Continued

Temperature K	Density kg/m³	Internal energy kJ/kg	Enthalpy kJ/kg	Entropy kJ/(kg K)	c_v kJ/(kg K)	c_p kJ/(kg K)	Speed of sound m/s
			200.000 MPa Isobar				
210	450.51	−727.96	−284.02	−5.5866	2.1087	2.9327	1931.5
220	445.11	−704.07	−254.74	−5.4504	2.0958	2.9219	1906.3
230	439.82	−680.30	−225.57	−5.3207	2.0859	2.9134	1882.0
240	434.63	−656.63	−196.47	−5.1969	2.0791	2.9074	1858.5
250	429.55	−633.02	−167.41	−5.0783	2.0751	2.9038	1835.7
260	424.55	−609.47	−138.38	−4.9644	2.0741	2.9026	1813.6
270	419.66	−585.93	−109.35	−4.8549	2.0760	2.9038	1792.3
280	414.85	−562.39	−80.299	−4.7492	2.0805	2.9074	1771.7
290	410.14	−538.83	−51.198	−4.6471	2.0877	2.9132	1751.7
300	405.52	−515.22	−22.028	−4.5482	2.0974	2.9212	1732.4
310	400.99	−491.54	7.2324	−4.4522	2.1094	2.9311	1713.8
320	396.54	−467.76	36.602	−4.3590	2.1236	2.9431	1695.8
330	392.18	−443.88	66.100	−4.2682	2.1398	2.9568	1678.4
340	387.90	−419.86	95.743	−4.1797	2.1580	2.9721	1661.7
350	383.70	−395.70	125.55	−4.0933	2.1778	2.9890	1645.7
360	379.58	−371.37	155.53	−4.0089	2.1993	3.0074	1630.2
370	375.54	−346.87	185.70	−3.9262	2.2221	3.0270	1615.4
380	371.57	−322.18	216.07	−3.8452	2.2463	3.0477	1601.1
390	367.69	−297.28	246.66	−3.7658	2.2717	3.0696	1587.5
400	363.87	−272.18	277.47	−3.6878	2.2981	3.0924	1574.4
410	360.13	−246.85	308.51	−3.6111	2.3254	3.1160	1561.9
420	356.46	−221.29	339.79	−3.5357	2.3535	3.1404	1550.0
430	352.86	−195.48	371.32	−3.4616	2.3824	3.1655	1538.5
440	349.32	−169.44	403.10	−3.3885	2.4120	3.1912	1527.6
450	345.86	−143.13	435.14	−3.3165	2.4420	3.2174	1517.2
460	342.45	−116.57	467.45	−3.2455	2.4726	3.2441	1507.3
470	339.11	−89.743	500.03	−3.1754	2.5036	3.2713	1497.9
480	335.84	−62.647	532.88	−3.1063	2.5350	3.2987	1488.8
490	332.62	−35.278	566.00	−3.0380	2.5667	3.3265	1480.3
500	329.47	−7.6329	599.41	−2.9705	2.5986	3.3546	1472.1
520	323.33	48.500	667.07	−2.8378	2.6630	3.4114	1457.0
540	317.41	105.77	735.87	−2.7080	2.7280	3.4689	1443.3
560	311.70	164.19	805.82	−2.5808	2.7932	3.5268	1431.0
580	306.20	223.78	876.94	−2.4560	2.8585	3.5849	1419.9
600	300.89	284.53	949.22	−2.3335	2.9236	3.6432	1409.9
620	295.76	346.45	1022.67	−2.2131	2.9886	3.7014	1400.9
			500.000 MPa Isobar				
185.885[a]	535.12	−797.86	136.52	−6.5117	2.3897	3.0114	2689.7
190	533.45	−788.41	148.89	−6.4459	2.3799	3.0018	2682.2
195	531.44	−776.97	163.87	−6.3681	2.3687	2.9909	2673.1
200	529.46	−765.57	178.80	−6.2925	2.3582	2.9809	2664.2
210	525.56	−742.85	208.52	−6.1475	2.3396	2.9632	2646.5
220	521.75	−720.24	238.07	−6.0100	2.3240	2.9487	2629.2
230	518.02	−697.71	267.50	−5.8791	2.3116	2.9374	2612.2
240	514.37	−675.23	296.83	−5.7543	2.3022	2.9290	2595.5
250	510.80	−652.77	326.09	−5.6349	2.2959	2.9235	2579.0
260	507.29	−630.32	355.31	−5.5203	2.2925	2.9209	2562.8
270	503.85	−607.84	384.52	−5.4100	2.2920	2.9210	2546.8
280	500.47	−585.32	413.74	−5.3038	2.2943	2.9238	2531.0
290	497.16	−562.72	443.00	−5.2011	2.2993	2.9291	2515.4
300	493.90	−540.03	472.33	−5.1017	2.3067	2.9368	2500.0
310	490.69	−517.22	501.74	−5.0052	2.3165	2.9467	2484.8

Table 40. Thermodynamic properties of methane – Continued

Temperature K	Density kg/m³	Internal energy kJ/kg	Enthalpy kJ/kg	Entropy kJ/(kg K)	c_v kJ/(kg K)	c_p kJ/(kg K)	Speed of sound m/s
			500.000 MPa Isobar				
320	487.54	−494.28	531.27	−4.9115	2.3286	2.9586	2469.9
330	484.45	−471.18	560.92	−4.8202	2.3427	2.9726	2455.2
340	481.40	−447.90	590.73	−4.7313	2.3587	2.9883	2440.8
350	478.41	−424.44	620.69	−4.6444	2.3765	3.0057	2426.7
360	475.46	−400.77	650.85	−4.5594	2.3958	3.0246	2412.8
370	472.55	−376.89	681.19	−4.4763	2.4166	3.0448	2399.2
380	469.70	−352.77	711.75	−4.3948	2.4388	3.0663	2385.9
390	466.88	−328.42	742.52	−4.3149	2.4621	3.0889	2373.0
400	464.11	−303.81	773.53	−4.2364	2.4865	3.1125	2360.3
410	461.38	−278.94	804.77	−4.1592	2.5118	3.1370	2347.9
420	458.68	−253.81	836.27	−4.0833	2.5380	3.1623	2335.8
430	456.03	−228.40	868.02	−4.0086	2.5650	3.1882	2324.1
440	453.42	−202.70	900.04	−3.9350	2.5926	3.2148	2312.7
450	450.84	−176.73	932.32	−3.8625	2.6208	3.2420	2301.5
460	448.30	−150.46	964.88	−3.7909	2.6494	3.2696	2290.7
470	445.79	−123.89	997.71	−3.7203	2.6786	3.2976	2280.2
480	443.32	−97.033	1030.83	−3.6506	2.7081	3.3259	2269.9
490	440.88	−69.870	1064.23	−3.5817	2.7379	3.3546	2260.0
500	438.47	−42.403	1097.92	−3.5136	2.7680	3.3835	2250.3
520	433.75	13.448	1166.17	−3.3798	2.8288	3.4419	2231.9
540	429.16	70.532	1235.60	−3.2488	2.8903	3.5008	2214.5
560	424.68	128.85	1306.21	−3.1204	2.9520	3.5600	2198.1
580	420.31	188.42	1378.00	−2.9945	3.0139	3.6194	2182.6
600	416.06	249.22	1450.98	−2.8708	3.0758	3.6787	2168.1
620	411.90	311.26	1525.15	−2.7492	3.1375	3.7379	2154.4
			1000.00 MPa Isobar				
254.800[a]	580.88	−599.61	1121.92	−6.0955	2.5133	3.0321	3286.0
260	579.45	−588.10	1137.68	−6.0343	2.5100	3.0288	3279.8
270	576.73	−565.96	1167.95	−5.9200	2.5062	3.0251	3267.8
280	574.07	−543.76	1198.19	−5.8100	2.5056	3.0246	3255.7
290	571.46	−521.47	1228.45	−5.7039	2.5079	3.0271	3243.7
300	568.89	−499.07	1258.74	−5.6012	2.5128	3.0324	3231.7
310	566.37	−476.54	1289.10	−5.5016	2.5204	3.0402	3219.7
320	563.89	−453.86	1319.56	−5.4049	2.5302	3.0505	3207.7
330	561.44	−431.00	1350.12	−5.3109	2.5423	3.0628	3195.8
340	559.04	−407.96	1380.82	−5.2192	2.5564	3.0772	3183.9
350	556.67	−384.71	1411.67	−5.1298	2.5723	3.0934	3172.1
360	554.34	−361.24	1442.69	−5.0424	2.5899	3.1112	3160.5
370	552.05	−337.54	1473.90	−4.9569	2.6089	3.1305	3148.9
380	549.78	−313.59	1505.31	−4.8732	2.6294	3.1511	3137.4
390	547.55	−289.39	1536.93	−4.7910	2.6511	3.1730	3126.1
400	545.35	−264.92	1568.77	−4.7104	2.6739	3.1958	3115.0
410	543.18	−240.17	1600.85	−4.6312	2.6977	3.2197	3104.0
420	541.04	−215.14	1633.17	−4.5533	2.7223	3.2443	3093.2
430	538.92	−189.83	1665.74	−4.4767	2.7478	3.2697	3082.5
440	536.83	−164.22	1698.56	−4.4012	2.7739	3.2958	3072.1
450	534.77	−138.31	1731.65	−4.3269	2.8006	3.3224	3061.8
460	532.74	−112.09	1765.01	−4.2535	2.8279	3.3496	3051.7
470	530.72	−85.571	1798.65	−4.1812	2.8556	3.3771	3041.8
480	528.74	−58.740	1832.56	−4.1098	2.8837	3.4050	3032.1
490	526.77	−31.596	1866.75	−4.0393	2.9122	3.4332	3022.6

Table 40. Thermodynamic properties of methane – Continued

Temperature K	Density kg/m³	Internal energy kJ/kg	Enthalpy kJ/kg	Entropy kJ/(kg K)	c_v kJ/(kg K)	c_p kJ/(kg K)	Speed of sound m/s
			1000.000 MPa Isobar				
500	524.83	−4.1386	1901.22	−3.9697	2.9409	3.4617	3013.2
520	521.02	51.727	1971.03	−3.8328	2.9991	3.5193	2995.2
540	517.29	108.86	2042.00	−3.6989	3.0579	3.5775	2977.8
560	513.65	167.28	2114.13	−3.5677	3.1171	3.6360	2961.3
580	510.08	226.96	2187.44	−3.4391	3.1765	3.6946	2945.4
600	506.59	287.92	2261.92	−3.3129	3.2359	3.7531	2930.2
620	503.16	350.14	2337.56	−3.1888	3.2951	3.8115	2915.6

[a] Melting temperature.
[b] Saturation temperature.